

**Oligomeric Surfactants as Novel Type of Amphiphiles:
Structure – Property Relationships and Behaviour with Additives**

Dissertation

zur Erlangung des akademischen Grades
Doktor der Naturwissenschaften (Dr. rer. nat.)
in der Wissenschaftsdisziplin
Kolloid- und Polymerchemie

eingereicht an der Mathematisch-Naturwissenschaftlichen Fakultät
der Universität Potsdam

von

Laurent Wattebled

geboren am 16.06.1980 in Lesquin

Potsdam, im Dezember 2006

“Not in knowledge is happiness, but in the acquisition of knowledge”

Edgar Allan Poe, *The Power of Words* (1850)

ACKNOWLEDGEMENTS

I want to express my profound gratitude to the staffs of scientists and technicians and other persons directly or indirectly involved in the completion of this work. The findings within this dissertation would never have been so fruitful without the help of these people.

First of all, I would like to thank sincerely *Prof. André Laschewsky* (University of Potsdam and Fraunhofer Institute for Applied Polymer Research) for giving me the opportunity to carry out my PhD thesis under his supervision, on a research topic of colloid and polymer science. I enjoyed the multiple fields addressed within this PhD work, including surfactant chemistry (synthesis and analysis) and physics (characterization), as well as polymer science. I am indebted to him for his helpful guidance throughout these three years, especially when precise practical or theoretical problems arose. Furthermore, I am grateful for the real autonomy he gave me so that I could “explore” the topic by myself and fulfill my own ideas. I appreciated his availability for discussions, during which I definitely benefited from his great knowledge and experience in chemistry. Likewise, I thank him for his encouragement and trust, and for interesting conversations on open subjects. Finally I gratefully acknowledge him for giving me the opportunity to develop cooperations on the topic with other scientists and also for allowing me to present our results at international conferences.

I am grateful to *Dr. R. H. Rakotoaly* (Université Catholique de Louvain, Louvain-la-Neuve, Belgium) for the synthesis of the cationic oligomers, leaving enough material to start the first measurements of my work.

I would like to thank *Prof. J.-L. Habib-Jiwan* (UCL) for his hospitality during my stay in Louvain-la-Neuve and for allowing me to perform time-resolved fluorescence quenching measurements (TRFQ) with a first-rate Laser equipment. I greatly appreciated his comments on the use of an uncommon fluorescent probe for the determination of micellar aggregation numbers. Moreover, I am extremely grateful to *A. Moussa* for his valuable help with the TRFQ measurements and his involvement during my stay in Louvain-la-Neuve.

I am thankful to *Dr. K. Lunkenheimer* (Max Planck Institute of Colloids and Interfaces, Golm) for determination of the critical micellization concentrations of the cationic dimers and for interesting discussions about surface tension measurements. Likewise, I gratefully acknowledge *Dr. M. Arotçaréna* and *A. Baudoult* (UCL) for technical assistance with CMC determination via fluorescence, *Prof. J. Kötzt* and *Dr. S. Kosmella* (Universität Potsdam) for interesting discussions on colloid chemistry and for providing access to the surfactant selective electrodes, *C. Note* for help with phase diagram determination and turbidimetric measurements, *Dr. B. Tiersch* for the cryo-SEM

pictures, *Dr. M. Heydenreich* and *A. Krtitschka* for help with NMR spectroscopy, *Dr. V. Strehmel* for her help with TGA and DSC measurements as well as with administrative issues, *Dr. M. Page* (MPI) for stimulating discussions on worm-like micelles, *Dr. R. Sigel* and *Dr. S. Kubowicz* (MPI) for discussions about static and dynamic light scattering. Special thanks go to *S. Rai* (Ecole Nationale Supérieure de Chimie de Lille, France) for her practical help with counterion-modified gemini surfactants: her 2-month placement was a good experience to test my abilities as a supervisor. I also wish to thank *Prof. J.-M. Aubry* (ENSCL, France) who kindly introduced me to *Prof. Laschewsky* in 2003, and *Dr. V. Rataj* for her interest in dimeric surfactants for new developments in catalytic reactions. *Prof. M. Gradzielski* and *Dr. S. Prévost* (Technische Universität Berlin) are acknowledged for their interest in catanionic mixtures with gemini surfactants.

Also, I am grateful to *Dr. U. Buller* and *Dr. H.-P. Fink* who permitted me to work in the laboratories of the Fraunhofer institute (IAP). Particularly, I wish to express my appreciation to the scientists and technicians of the “FB 4” (division of water-based polymer systems) for the friendly environment and practical help. *Dr. E. Goernitz* is gratefully acknowledged for his useful comments on rheology and expertise with the rheometer. In addition, I would like to thank *Dr. B. Paulke* for access to the tensiometer, as well as *Dr. J. Storsberg*, *Dr. S. Bruzzano*, *Dr. J.-F. Lutz* for motivating scientific discussions. Special thanks to the lab and office mates for the nice work atmosphere: *Dr. J.-F. Baussard*, *Dr. M. Mertoglu*, *Dr. S. Garnier*, *K. Skrabania*, *J. Kristen*, *F. Salles*, *N. Zuber*, *A. Bivigou-Koumba*, *P. Ott*, *O. Mauger*, *E. Möller*, *Dr. M. Päch*.

I send my heartfelt thanks to my brother *Alexis*, sister *Mélanie* and friends in France and Berlin-Brandenburg for their important support all over these years and for giving me precious thesis-unrelated moments. I do not forget to thank my football mates of the *S.G. Saarmund* for their warm welcome in the club and for providing great times of entertainment.

I am forever indebted to my parents *Dany* and *Régine* for their understanding, help and encouragement whatever I have carried out in my life. Finally, I wish to express my love to *Carine* and thank her for her endless patience and support in every-day life, and for always being at my side whenever I need it.

All contributed to make my PhD work abroad a great experience and an enjoyable time.

*Merci à vous tous,
Laurent.*

ABSTRACT

The properties of a series of well-defined new surfactant oligomers (dimers to tetramers) were examined. From a molecular point of view, these oligomeric surfactants consist of simple monomeric cationic surfactant fragments coupled via the hydrophilic ammonium chloride head groups by spacer groups (different in nature and length).

Properties of these cationic surfactant oligomers in aqueous solution such as solubility, micellization and surface activity, micellar size and aggregation number were discussed with respect to the two new molecular variables introduced, i.e. degree of oligomerization and spacer group, in order to establish structure – property relationships. Thus, increasing the degree of oligomerization results in a pronounced decrease of the critical micellization concentration (CMC). Both reduced spacer length and increased spacer hydrophobicity lead to a decrease of the CMC, but to a lesser extent. For these particular compounds, the formed micelles are relatively small and their aggregation number decreases with increasing the degree of oligomerization, increasing spacer length and sterical hindrance. In addition, pseudo-phase diagrams were established for the dimeric surfactants in more complex systems, namely inverse microemulsions, demonstrating again the important influence of the spacer group on the surfactant behaviour.

Furthermore, the influence of additives on the property profile of the dimeric compounds was examined, in order to see if the solution properties can be improved while using less material. Strong synergistic effects were observed by adding special organic salts (e.g. sodium salicylate, sodium vinyl benzoate, etc.) to the surfactant dimers in stoichiometric amounts. For such mixtures, the critical aggregation concentration is strongly shifted to lower concentration, the effect being more pronounced for dimers than for analogous monomers. A sharp decrease of the surface tension can also be attained. Many of the organic anions produce viscoelastic solutions when added to the relatively short-chain dimers in aqueous solution, as evidenced by rheological measurements. This behaviour reflects the formation of entangled wormlike micelles due to strong interactions of the anions with the cationic surfactants, decreasing the curvature of the micellar aggregates. It is found that the associative behaviour is enhanced by dimerization. For a given counterion, the spacer group may also induce a stronger viscosifying effect depending on its length and hydrophobicity.

Oppositely charged surfactants were combined with the cationic dimers, too. First, some mixtures with the conventional anionic surfactant SDS revealed vesicular aggregates in solution. Also, in view of these catanionic mixtures, a novel anionic dimeric surfactant based on EDTA was synthesized and studied. The synthesis route is relatively simple and the compound exhibits particularly appealing properties such as low CMC and σ_{CMC} values, good solubilization capacity of hydrophobic probes and high tolerance to hard water. Noteworthy, mixtures with particular cationic dimers gave rise to viscous solutions, reflecting the micelle growth.

TABLE OF CONTENTS

LIST OF ACRONYMS	p.xi
1. GENERAL INTRODUCTION	p.1
1.1. Overview of surfactant science	p.3
1.1.1. Structure and classification of standard surfactants	p.3
1.1.2. Properties of low molar-mass surfactants in aqueous solution	p.6
<i>1.1.2.a. Surface-activity</i>	<i>p.6</i>
<i>1.1.2.b. Micelle formation</i>	<i>p.8</i>
<i>1.1.2.c. Micellar association models</i>	<i>p.11</i>
<i>1.1.2.d. Krafft point and cloud point</i>	<i>p.14</i>
1.1.3. Aggregation behavior of surfactants	p.15
<i>1.1.3.a. Type of aggregates</i>	<i>p.15</i>
<i>1.1.3.b. Packing parameter concept</i>	<i>p.16</i>
<i>1.1.3.c. Lyotropic liquid crystals</i>	<i>p.19</i>
1.2. Polymeric and oligomeric surfactants	p.20
1.2.1. Polymeric surfactants	p.20
1.2.2. Oligomeric surfactants	p.21
<i>1.2.2.a. Architecture of oligomeric surfactants</i>	<i>p.22</i>
<i>1.2.2.b. Linear surfactant oligomers</i>	<i>p.24</i>
<i>1.2.2.c. Overview on the properties of gemini surfactants</i>	<i>p.27</i>
<i>1.2.2.d. Applications of gemini surfactants</i>	<i>p.28</i>
1.3. Objectives and motivation of this work	p.30
1.4. References	p.32

2.	NEW SERIES OF SURFACTANT OLIGOMERS	p.37
2.1.	Choice of model cationic surfactants	p.37
2.1.1.	Presentation of the structures	p.37
2.1.2.	Synthesis routes	p.38
2.1.3.	Basic properties previously determined	p.40
2.2.	Novel anionic gemini surfactant	p.41
2.2.1.	Background and motivation	p.41
2.2.2.	Synthesis of “dimer EDTA”	p.44
2.2.3.	Characterization of “dimer EDTA”	p.45
2.2.3.a.	<i>NMR, IR, Mass Spectroscopy and Elemental Analysis</i>	<i>p.45</i>
2.2.3.b.	<i>Acid-base titration</i>	<i>p.47</i>
2.3.	References	p.50
3.	PROPERTIES OF THE SURFACTANT OLIGOMERS	p.52
3.1.	Properties of cationic surfactant oligomers	p.52
3.1.1.	Krafft Temperatures	p.52
3.1.2.	Surface activity and micellization	p.52
3.1.2.a.	<i>Spacer effect in dimeric surfactants</i>	<i>p.53</i>
3.1.2.b.	<i>Series of oligomeric surfactants</i>	<i>p.56</i>
3.1.2.c.	<i>Peculiar behaviour of tetramer p-X-4</i>	<i>p.61</i>
3.1.3.	Dynamic Light Scattering and NMR spectroscopy	p.63
3.1.4.	Micellar aggregation number	p.66
3.1.4.a.	<i>Background</i>	<i>p.66</i>
3.1.4.b.	<i>Comments on the method and fluorophore</i>	<i>p.67</i>
3.1.4.c.	<i>Discussion</i>	<i>p.70</i>
3.1.5.	Formation of microemulsions	p.75
3.1.5.a.	<i>Background</i>	<i>p.75</i>
3.1.5.b.	<i>Effect of cationic dimers on the formation of an inverse microemulsion</i>	<i>p.76</i>

3.2. Properties of the new anionic gemini surfactant	p.78
3.2.1. Krafft temperature	p.78
3.2.2. Surface activity and micellization	p.78
3.2.3. Dynamic light scattering and viscosity	p.82
3.2.4. Solubilization capacity in micellar environment	p.82
3.2.5. Tolerance to calcium ions	p.84
3.3. Summary	p.86
3.4. References	p.87
4. EFFECT OF ADDITIVES ON PROPERTIES OF SURFACTANT DIMERS IN SOLUTION	p.90
4.1. Addition of organic salts	p.90
4.1.1. Background and interests	p.91
4.1.2. Addition of sodium salicylate as model organic salt	p.93
<i>4.1.2.a. Micellization and surface activity</i>	<i>p.93</i>
<i>4.1.2.b. Viscosifying effect</i>	<i>p.97</i>
4.1.3. Addition of other hydrotropes	p.103
<i>4.1.3.a. Effects of various organic salts tested</i>	<i>p.103</i>
<i>4.1.3.b. Micellization and surface activity</i>	<i>p.106</i>
<i>4.1.3.c. Viscosifying effect</i>	<i>p.108</i>
<i>4.1.3.d. Polymerization in mixtures of gemini surfactants and polymerizable counterions</i>	<i>p.112</i>
4.1.4. Addition of cationic hydrotropes to dimer EDTA	p.117
4.2. Addition of oppositely charged surfactants	p.117
4.2.1. Background	p.117
4.2.2. Addition of SDS to cationic dimers	p.118
4.2.3. Addition of DTAC to dimer EDTA	p.121
4.2.4. Mixture of oppositely charged surfactant dimers	p.121
4.3. References	p.123

5. EXPERIMENTAL PART	p.127
5.1 Standard surfactants	p.127
5.2 Analytical methods	p.127
5.3 Synthesis and characterization of cationic dimers	p.130
5.4 Synthesis of the anionic gemini surfactant based on EDTA	p.130
5.5 Acidic titration of neutralized dimer EDTA	p.132
5.6 Determination of Krafft temperatures of oligomeric surfactants	p.132
5.7 Surface tension measurements	p.133
5.8 Determination of CMC of cationic oligomers by dye solubilization methods	p.135
5.9 Time resolved fluorescence quenching experiments (TRFQ)	p.137
5.10 Calculation of spacer lengths	p.140
5.11 Formulation of microemulsions	p.140
5.12 Determination of CMC of dimer EDTA via UV-Vis spectroscopy	p.141
5.13 Solubilization capacity of surfactants	p.143
5.14 Tolerance of surfactants to calcium ions	p.144
5.15 Synthesis of “EO-2 (MoO ₄)”	p.145
5.16 Preparation of mixtures surfactant/organic salts	p.147
5.17 Determination of CMC via conductimetry	p.148
5.18 Polymerization in mixtures of gemini surfactants and polymerizable counterions	p.149
5.19 Rheological studies of dimeric surfactants with additives	p.150
5.20 Mixtures of cationic surfactant dimers with anionic surfactants	p.156
5.21 References	p.157
6. GENERAL CONCLUSIONS	p.160

APPENDIX 1: Synthesis and characterization of cationic dimers	p.I
APPENDIX 2: Synthesis of N-methyldodecylamine	p.VIII
APPENDIX 3: Characterization of dimer EDTA	p.IX
APPENDIX 4: Determination of CMC via solubilization of 2-AN	p.XV
APPENDIX 5: Determination of CMC via solubilization of pinacyanol	p.XVI
APPENDIX 6: Supporting information for TRFQ experiments	p.XVII
APPENDIX 7: Thermal analyses	p.XIX
APPENDIX 8: List of Tables	p.XXI
APPENDIX 9: List of Figures	p.XXII
APPENDIX 10: Communications concerning this thesis	p.XXIX
APPENDIX 11: Surfactants studied in this work	p.XXX

LIST OF ACRONYMS

A	Average surface area per molecule [\AA^2]
ABS	Alkyl benzene sulfonate
acsal	Sodium acetylsalicylate
benz	Sodium benzoate
BDDAC	Benzylododecyldimethylammoniumchloride
C	Concentration of a solution [$\text{mol}\cdot\text{L}^{-1}$] or [$\text{g}\cdot\text{L}^{-1}$]
CAC	Critical aggregation concentration [$\text{mol}\cdot\text{L}^{-1}$] or [$\text{g}\cdot\text{L}^{-1}$]
cinn	Sodium cinnamate
CMC	Critical micellization concentration [$\text{mol}\cdot\text{L}^{-1}$] or [$\text{g}\cdot\text{L}^{-1}$]
CR	Count rate [kcps] (DLS)
CTAB	Cetyltrimethylammoniumbromide
CTAC	Cetyltrimethylammoniumchloride
D_H	Hydrodynamic diameter of aggregates [nm]
DHT	Sodium dihydroxyterephthalate
dimer EDTA	Anionic dimeric surfactant based on EDTA
DLS	Dynamic Light Scattering
DNA	Deoxyribose nucleic acid
DP	Sodium diphenate
DSC	Differential Scanning Calorimetry
DTAC	Dodecyltrimethylammoniumchloride
EDTA	Ethylene diamine tetraacetic acid
EO	Ethylene oxide
G'	Storage modulus [Pa]
G''	Loss modulus [Pa]
G₀	Plateau modulus [Pa]
HLB	Hydrophile lipophile balance
HNC	Sodium hydroxynaphthoate
IR	Infrared Spectroscopy
i-B	Iso-butenylene
k_B	Boltzmann constant ($= 1.38 \times 10^{-23} \text{ J}\cdot\text{K}^{-1}$)
m.p.	Melting point [$^{\circ}\text{C}$]
m-X	Meta-xylene
N_A	Avogadro's number ($= 6.02 \times 10^{23} \text{ mol}^{-1}$)
N_{agg}	Micellar aggregation number
NDC	Sodium naphthylidicarboxylate
NMR	Nuclear Magnetic Resonance Spectroscopy
o-X	Ortho-xylene
O/W	Oil in water
P	Packing parameter
pK_a	Decimal logarithm of the acid dissociation constant
p-X	Para-xylene
R	Gas constant ($= 8.31 \text{ J}\cdot\text{mol}^{-1}\cdot\text{K}^{-1}$)
R_g	Radius of gyration of a micelle [nm]
R_h	Hydrodynamic radius of a micelle [nm]
sal	Sodium salicylate
SANS	Small angle neutron scattering
SDS	Sodium dodecyl sulfate
SEM	Scanning electron microscopy
SL	Sodium laurate
SLS	Static Light Scattering
SSFQ	Steady State Fluorescence Quenching
SXS	Sodium xylene sulfonate

T	Temperature [°C] or [K]
tere	Sodium terephthalate
TGA	Thermogravimetric analysis
T_K	Krafft temperature [°C]
TLC	Thin Layer Chromatography
t-B	Trans-1,4-buten-2-ylene
tos	Sodium tosylate
TRFQ	Time Resolved Fluorescence Quenching
UV-vis	Ultraviolet/visible Light Spectroscopy
4-VB	Sodium 4-vinyl benzoate
W/O	Water in oil
Γ	Surface excess [mol·m ⁻²]
ε	Extinction coefficient [L·mol ⁻¹ ·cm ⁻¹]
σ	Surface tension [mN·m ⁻¹]
σ_{cmc}	Surface tension at the CMC [mN·m ⁻¹]
σ	Applied stress [Pa]
γ	Deformation or strain
γ̇	Shear rate [s ⁻¹]
τ	Relaxation time [s]
τ_{rep}	Relaxation time of reptation [s]
τ_{br}	Relaxation time of breaking [s]
η	Viscosity of a solution [Pa·s]
η₀	Zero-shear viscosity [Pa·s]
η*	Complex viscosity [Pa·s]
ν	Frequency [Hz]
ω	Angular Frequency [rad·s ⁻¹]
λ	Wave length [nm]
ν	Frequency of bending vibration of a chemical group (IR) [cm ⁻¹] (ν _s : symmetric, ν _{as} : asymmetric)

1. GENERAL INTRODUCTION

Surfactants, a common contraction of the term surface-active agents, are versatile chemical substances that modify the surfaces or interfaces of the systems in which they are contained. Surfactants find a wide range of applications in everyday life as well as in industrial processes, though often not realized. For instance, they are present in detergents, personal care products and cosmetics, agrochemicals, pharmaceuticals, food processing, dyestuffs, manufacturing of textiles and fibers, nanotechnologies, paints, paper coatings, inks and adhesives, etc. [1] In addition, they play a vital role in the oil industry, e.g. in enhanced oil recovery or oil slick dispersion for environmental remediation [2]. Surfactants may be readily available from the nature (e.g. saponins or else fatty acids, bile acids or glycerol based lipids which are vital to the cell membrane) or may be synthesized (from petroleum feedstocks).

The most familiar of all surfactants is undoubtedly soap, a simple substance which, in water, clearly demonstrates two effects: it produces foam due to its action at the air-water interface, and it transfers grease from grubby hands into the soapy water as a result of its activity at the water-oil (grease) interface. Soap can be traced back to Egyptian times, around 2500 BC. Already Sumerians used to combine animal and vegetable oils with alkaline salts in order to form a soap-like material which was used for treating skin diseases, as well as for washing [3]. The manufacture of soap has naturally been subject to many developments along the centuries, but it is still made by alkaline hydrolysis of animal fats or vegetable oils (a process known as saponification) and remains a widely used single surfactant, accounting for more than 30 % of the current surfactant market. Moving on from soaps – and into the 19th century – the next surfactants developed were the sulfates and sulfonates of vegetable oils. A classic example from the late 1800s is the reaction of castor oil with sulfuric acid, resulting in a mixture of sulfates and sulfonates which, after neutralization with sodium hydroxide, gives a product known as Turkey Red oil, useful in the dyeing of linen. Later, the development of sulfonation and sulfatation processes using other oils as reactants led to a move away from natural and renewable plant oils and animal fats to the use of petroleum products. For example, the introduction of alkyl benzene sulfonates (ABSs) was brought about by electrophilic substitution in the benzene ring using oleum ($\text{H}_2\text{S}_2\text{O}_7$) or sulfur trioxide. The ABSs represented a major contribution in changing the traditional soap powders to detergent powders for household laundry. Progress was not confined to the sulfonation of different oils, but was soon accompanied by ethoxylation, in which ethylene oxide (EO) molecules react with a fatty alcohol to form the surfactant molecule. Thus, alcohol ethoxylates, alcohol ether sulfates and alkyl phenol ethoxylates became available. Currently, pressure exists to move away from non-renewable petroleum feedstock and to move back towards plants as sources of raw materials. Therefore, efforts have recently concentrated on developing surfactants from oleochemical feedstock in an attempt to satisfy the modern consumers' desire for “more natural” products and for sustainable development [4]. Examples of such surfactants are

derivatives from the carbohydrates sorbitol, sucrose, glucose and from plant oils such as coconut or palm kernel. Sorbitan esters are used as emulsifiers in cosmetics and the sucrose esters in food manufacture. The alkyl polyglucosides find application as detergents rather than as emulsifiers and are making inroads into some everyday products. Also, it is notable that the recent emergence of efficient synthesis techniques such as e.g. controlled radical polymerizations has permitted the precise design of more complex surface-active structures like so-called polymeric surfactants (including “polysoaps” and amphiphilic block copolymer “macro-surfactants”) [5, 6]. These surfactants with tailor-made properties are promising agents for specific applications requiring high performance, e.g. for nanomaterial fabrication, drug delivery and encapsulation, etc. [7].

The surfactant industry represents a dynamic business field with large volumes and profits. The global surfactant market volume size is about 12 million tons (2003), with an overall rough value of 13 billion Euros [8]. This market is expected to grow further, especially within the emerging countries of the Asia-Pacific zone in the next years. Thus, the wide range of surfactant applications (*vide supra*), the large volumes of production as well as the expansion of the markets justify the intensive research in surfactant science. Progresses in the field are constant as exemplified by the continuous developments in the synthesis of detergents. Furthermore, novel surfactant structures carry the promise to expand the property profile and performance of nowadays surfactants. In this context, well-defined linear oligomeric surfactants, which represent intermediate structures between conventional and polymeric surfactants, are innovative and promising structures for the control of surfactant properties and behavior. Accordingly, this thesis will focus on the properties of such novel amphiphiles. The present general introduction is divided into three parts which shall situate the field.

Chapter 1.1 is an introduction to surfactant science, which gives an overview of the main features of common surfactant molecules, such as their chemical nature and fundamental properties. This part aims at bringing a theoretical background or reminder in this subtopic of colloid science and also aims at highlighting concepts of interest, relevant to comprehend the experimental work of this thesis.

Chapter 1.2 focuses on relatively recent developments in the field, in particular with the emergence of polymeric and oligomeric surfactants. The latter classes of surfactants will be presented with respect to their architecture and properties, with an emphasis on dimeric (so-called “gemini”) surfactants which are of particular interest for this work.

Chapter 1.3 presents the main goals and challenges of the present work concerning the development and properties of surfactant oligomers.

1.1 Overview of surfactant science

1.1.1. Structure and classification of standard surfactants

Surfactants have the ability to adsorb (or locate) at interfaces, thereby altering significantly the physical properties of those interfaces. The term “interface” is commonly employed here to describe the boundary in liquid/liquid (e.g. oil/water), solid/liquid and gas/liquid (e.g. air/water) systems, although in the latter case the term “surface” can also be used. This adsorption behaviour results from the amphiphilic nature of surfactants (from Greek, *amphi* = twofold; *philos* = friend). Indeed, classical surfactants combine both a polar and a non-polar part into a single molecule: the non-polar portion (usually a straight hydrocarbon chain containing 8-18 carbon atoms), also called hydrophobic “tail” is covalently attached to the polar functional portion or so-called hydrophilic “head-group” (which can be non-ionic, ionic or zwitterionic). Figure 1.1-1 shows a typical representation of a low molar mass surfactant compound.

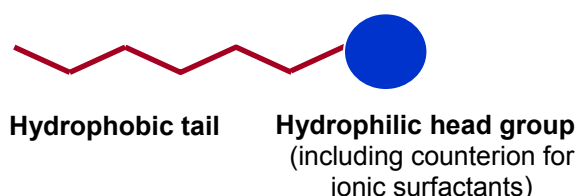


Figure 1.1-1: common schematic design of a low-molar mass surfactant molecule.

Surfactants are usually classified according to the nature of the hydrophilic head-group. Thus, one distinguishes between ionic (i.e. anionic, cationic or amphoteric) and non-ionic surfactants. Anionic surfactants are low cost and applied in most surfactant-based formulations and detergents. Commonly used anionic groups are carboxylates, sulfates, sulfonates and phosphates. Cationic surfactants, generally quaternary ammonium compounds, are more expensive to produce and therefore used in more specialized applications such as in disinfectant formulations, corrosion inhibitors, fabric softeners, etc. Amphoteric (zwitterionic) surfactants contain both cationic and anionic groups, and generally induce lower skin irritation and show good compatibility with other surfactants. Nonionic surfactants are ranked after the anionics in terms of industrial importance and often comprise repeating ethylene oxide units or carbohydrates as a hydrophilic group. On Figure 1.1-2 are depicted examples of surfactants presenting the standard amphiphilic design (see Fig. 1.1-1) with various hydrophilic head-groups and an arbitrarily fixed dodecyl chain as the hydrophobic part.

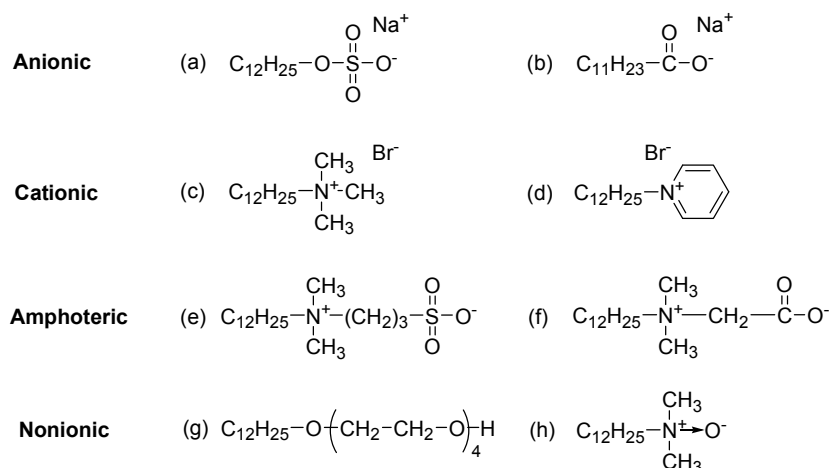


Figure 1.1-2: examples of surfactants having a dodecyl chain and various head groups. (a) sodium dodecyl sulfate (SDS); (b) sodium dodecanoate; (c) dimethyldodecylammonium bromide; (d) dodecylpyridinium bromide; (e) N,N'-dimethyl-N-(3-sulfopropyl)-dodecylammonium (dodecyl sulfobetaine); (f) N,N'-dimethyl-N-(carboxymethyl)-dodecylammonium; (g) hexaethylene glycol mono-*n*-dodecyl ether (C₁₂E₄ or trade name Brij 30); (h) dodecylamine oxide.

Not only the hydrophilic group can be modified, but also the hydrophobic portion can be of different nature and length. Typically, it consists in medium to long hydrocarbon chains (> C8), which can be linear or branched, and saturated or unsaturated (e.g. unsaturated fatty acids such as oleic acid cis C9:C8-COOH). Alkylbenzenes or alkylaromatics are also quite usual. Nevertheless, fluorocarbon [9] or partially fluorinated [10] chains, silicon chains [11] and polycyclic structures [12] can additionally be found, as illustrated in Figure 1.1-3.

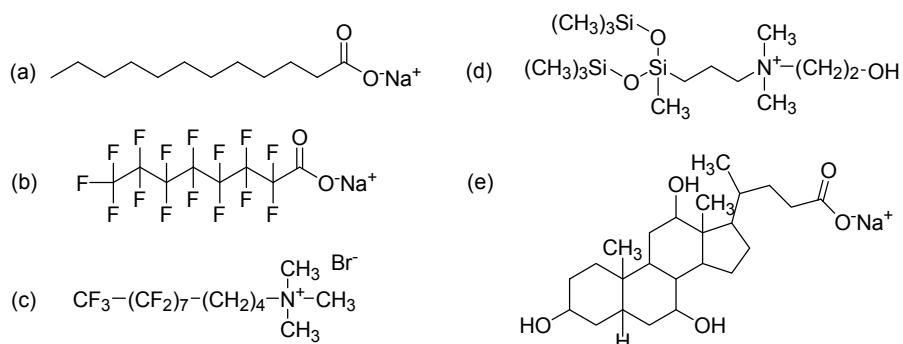


Figure 1.1-3: examples of surfactants with various hydrophobic moieties. (a) dodecyl hydrocarbon chain; (b) perfluorinated chain (sodium perfluorooctanoate); (c) partially fluorinated chain (perfluorooctylbutane trimethylammonium bromide from [10]); (d) silicon-based chain (cationic siloxane surfactant from [11]); (e) sodium cholate (From [13]).

The design of low molar-mass amphiphilic molecules is obviously not confined to the simple scheme “one hydrophobic tail connected covalently to one hydrophilic head-group” (Fig. 1.1-1), but can evolve to more complicated molecular structures, as will also be seen later in this chapter with

oligomeric surfactants and so-called “gemini” surfactants. Some possible designs of surfactants and corresponding examples are presented in Fig. 1.1-4.

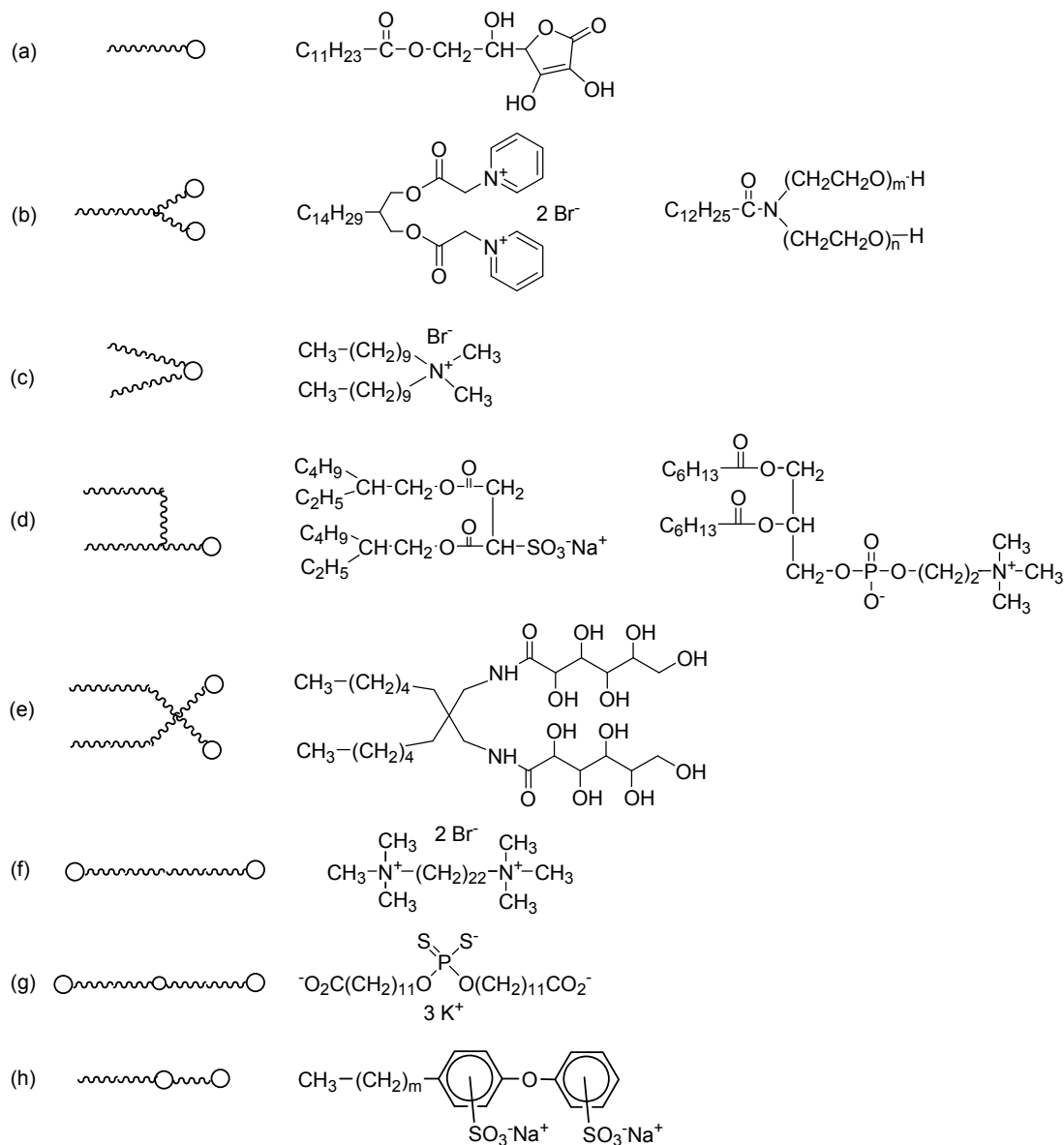


Figure 1.1-4: several designs of low molar-mass amphiphiles and corresponding examples. (a) Ascorbic acid based standard surfactant [14]; (b) double-headed pyridinium surfactant (left) [15] and ethylene glycol based surfactant (right); (c) double-chain surfactant: didecyldimethylammonium bromide; (d) other double chain surfactants: sodium bis(2-ethylhexyl) sulfosuccinate – trade name Aerosol OT – (left) [16] and lecithin (right) [17]; (e) gemini surfactant (see 1.2.2.b): non-ionic dihexyl glucamide [18]; (f) Bola-surfactant [19]; (g) Shamrock surfactant [20]; (h) two-headed surfactant, alkyldiphenyloxide disulfonate salts (trade name: Dowfax surfactants) [21].

1.1.2. Properties of low molar-mass surfactants in aqueous solution

1.1.2.a. Surface activity [22]

Surface tension is an effect at the surface of a liquid that makes the surface layer behave as an elastic sheet. As illustrated in Figure 1.1-5 (a), each molecule in the bulk liquid can interact in all directions with surrounding molecules due to various intermolecular attractive forces. In contrast, the molecules at the liquid surface only partially experience attractions with neighboring molecules from the liquid interior (Figure 1.1-5 (b)). Hence, they do not achieve the same level of interactions as bulk molecules (there may be a small outward interaction between surface and air molecules, but as air is much less dense than the liquid, it is negligible).

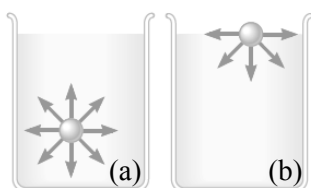


Figure 1.1-5: (a) A molecule within the bulk liquid interacts in all directions with other surrounding molecules. (b) A molecule at the surface only experiences attractive interactions with molecules from the liquid interior.

In other words, the molecules at the liquid surface exhibit an energy excess compared to the bulk ones, since they cannot minimize further their energy, interacting only with surrounding liquid molecule underneath the surface (cf. Figure 1.1-5 (b)). Therefore, the liquid squeezes itself together until it has the lowest surface area possible, in order to reduce the surface energy. The latter is defined as the surface tension of the liquid, which is expressed as a work done per unit area ($\text{J}\cdot\text{m}^{-2}$) and is commonly represented by the symbol σ . This means that if a surface with surface tension σ is expanded by a unit area, then the increase in the surface stored energy is also equal to σ . It is notable that the surface behaves in some respects as if it were a stretched film or membrane under tension. The force along a line of unit length parallel to the film also corresponds to the surface tension (in $\text{N}\cdot\text{m}^{-1}$). Noteworthy, if a liquid sample is not subject to external forces, it forms a sphere which is the geometrical shape with the minimum surface area for a given volume.

Water is a very cohesive liquid (see its high melting and boiling points) due to the formation of a 3-dimensional hydrogen bond network (see Figure 1.1-6) in addition to attractive van der Waals interactions. This induces that the amount of work required to expand the interface air-water, characterized by the surface tension, is relatively high ($72.6 \text{ mN}\cdot\text{m}^{-1}$, for pure water at 20°C).

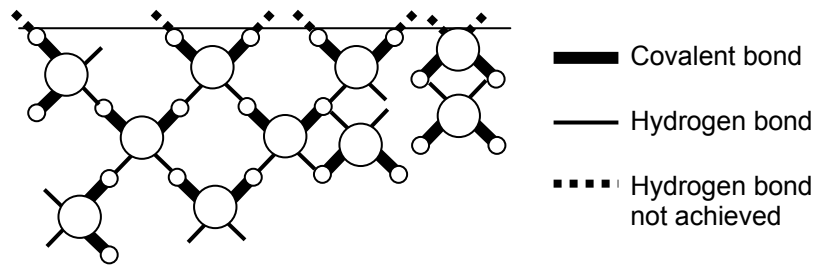


Figure 1.1-6: scheme representing water molecules at the interface liquid-air.

When surfactants are added to water, they adsorb at the water-air interface, which actually arises from their dualistic character. In aqueous solution the hydrophobic chain interacts weakly with the water molecules, whereas the hydrophilic head interacts strongly via dipole or ion-dipole interactions. It is this strong interaction that renders the surfactant soluble in water. However, the cooperative action of dispersion and hydrogen bonding between the water molecules tends to squeeze the surfactant chain out of the water (hence, these chains are referred to as hydrophobic). Therefore, surfactants tend to accumulate at the surface, which allows lowering the free energy of the phase boundary, i.e. the surface tension σ .

As shown on Figure 1.1-7, the soluble surfactants self-assemble into a condensed layer at the water-air interface, referred to as Gibbs monolayer (to be distinguished from Langmuir monolayers that form when insoluble surfactants are spread on the water-air interface), with the hydrocarbon chains pointing out of the water phase, and the hydrophilic head groups inside it [23].

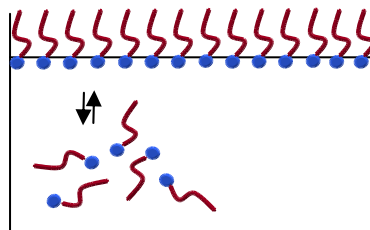


Figure 1.1-7: Equilibrium between surfactants in the monolayer and in the bulk, at low surfactant concentration in aqueous solution.

Typical surfactants have strong surface activity, i.e. the energy gained by a molecule when it migrates to the surface is much larger than the thermal energy $k_B T$. As a result, the concentration profile drops sharply to its bulk value within a molecular distance from the surface (hence the term monolayer). Such a monolayer can be regarded as a separate sub-system at thermodynamic equilibrium and in contact with a reservoir of surfactant molecules (see Fig. 1.1-7) that exchange with those of the monolayer. In general, hydrocarbon and fluorocarbon surfactants can reduce σ to value about $30 \text{ mN}\cdot\text{m}^{-1}$ and to $20 \text{ mN}\cdot\text{m}^{-1}$, respectively. Furthermore, the denser the surfactant layer, the larger the reduction in σ . Thus, the surface tension of an aqueous surfactant solution gradually

decreases with increasing its concentration, resulting from a gradual accumulation of surfactant in the monolayer. This behavior is described via the Gibbs adsorption isotherm, expressing the excess concentration of surfactant Γ in the surface layer as [24]:

$$\Gamma = -\frac{1}{nRT} \times \left(\frac{d\sigma}{d \ln C} \right)_T \quad \text{Equation 1.1-1}$$

with:

- Γ is the surface excess in mol/m²
- σ represents the surface tension in N/m
- C is the bulk surfactant concentration in mol/L
- $R = 8.31 \text{ J}\cdot\text{mol}^{-1}\cdot\text{K}^{-1}$ (gas constant)
- T = absolute temperature in K,
- n is a constant of proportionality which is 1 for nonionic surfactants and ionic ones at high salt concentration (thus treating the surfactants as one particle); it has a higher value for salt-free ionic surfactant solutions, where strong correlations between the different ions lead to non-ideal activity coefficients [23].

Because of the high surface activity of surfactant molecules, leading to a sharp concentration profile at the water–air interface, Γ^{-1} is commonly interpreted as the average surface area per molecule, A .

The reduction of the surface tension by surfactants is of interest in many common applications (e.g. the surface tension intervenes in various detergency mechanisms such as the wetting of surfaces or so-called “rolling-up”). The surface tension of liquids can be determined by different methods such as e.g. Du Noüy ring, Wilhelmy plate or spinning-drop tensiometer. The method involving a Du Noüy ring tensiometer is used many times in this work and is described in the experimental part.

1.1.2.b. Micelle formation

The physical properties of surfactant solutions differ from those of smaller or non amphiphilic molecules in a major aspect, namely the abrupt changes in their properties above a critical concentration, which is illustrated in Figure 1.1-8 with plots of several physical properties (osmotic pressure, solubilization, surface tension, conductivity, etc.) as a function of concentration of an ionic surfactant [25-27]. At low concentrations, most properties are similar to those of simple electrolytes. One notable exception is the surface tension which decreases rapidly with increasing surfactant concentration, as described before. However, from a fairly sharply defined region (see shaded area on Fig. 1.1-8), the properties exhibit sudden changes. This behavior results from the self-assembly of surfactant molecules in solution into so-called micelles (from the Latin “micella” meaning “small bit”). The concentration at which these aggregates form is known as the critical micellization

concentration (abbreviated CMC) [28]. Noteworthy, it is possible to determine the CMC via numerous different methods (allowing comparisons), as important changes occur in many physical properties at the CMC (see Fig. 1.1-8).

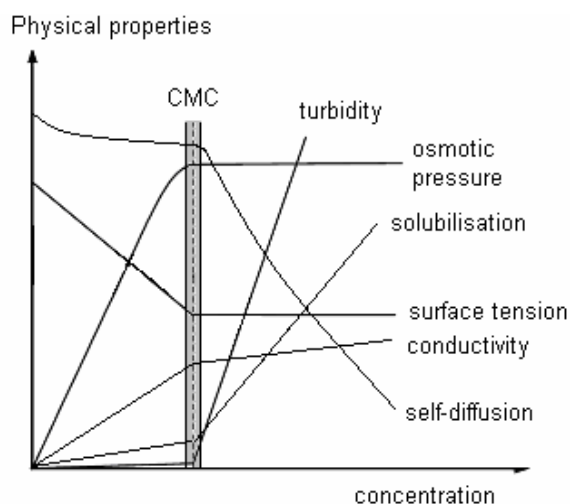


Figure 1.1-8: Schematic representation of the concentration dependence of some physical properties of surfactant solutions [29].

Micelles are spontaneously formed clusters of surfactant molecules (typically 40 to 200), whose size and shape are governed by geometric and energetic considerations (see also “packing parameter concept” below). They are loose, mostly spherical aggregates above their CMC in water or organic solvents [30]. Also, micellar aggregates are short-lived dynamic species, which rapidly disassemble and reassemble [31]. Hence, only average shape and aggregation numbers of micelles can be determined. Figure 1.1-9 represents a spherical micelle formed in aqueous solution, where the hydrophobic chains are directed towards the interior of the aggregate and the polar head-groups point towards water, hence allowing the solubility / stability of the aggregate (no phase separation). Micelles are also known to be disorganized assemblies which interiors consist of mobile, non-stretched hydrophobic chains [32]. Note in addition that water molecules can penetrate partially the micelle core to interact with surfactant hydrophobic tails [22].

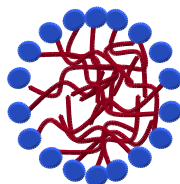


Figure 1.1-9: Scheme of a spherical micelle of surfactants in aqueous solution.

One of the most interesting properties of micellar aggregates is their ability to enhance the aqueous solubility of hydrophobic substances which otherwise precipitate in water (see “solubilisation” curve increasing above the CMC on Fig. 1.1-8). The solubility enhancement

originates from the fact that the micellar core can serve as compatible hydrophobic microenvironment for water-insoluble molecules. This phenomenon driven by hydrophobic interactions is referred to as solubilization [33]. It finds numerous applications such as e.g. for the environment friendly solubilization of organic solvents in water or for the design of drug delivery systems, or else in detergency applications.

Below the critical micellization concentration, surfactant adsorb at the surface of water, as shown in the previous section. At the CMC, the interface is at (near) maximum coverage and to minimize further free energy, molecules begin to aggregate in the bulk phase. Above the CMC, the system then consists of an adsorbed monolayer, free monomers and micellized surfactant in the bulk, with all these three states in equilibrium (see Figure 1.1-10). Additional surfactants increase the micelle concentration or allow micelle growth, while the concentration of the unassociated monomers remains almost constant.

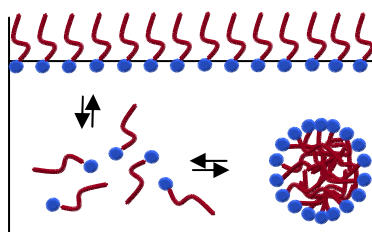


Figure 1.1-10: Schematic representation of the equilibrium in a surfactant solution above the CMC

The formation of micelles is a result of a complex interplay between hydrophobic forces and weak non directional repulsive forces. Hydrophobic forces which are opposed by electrostatic repulsion among the ionic head-groups at the micelle surface drive the micellization in water. This driving force is actually related to the formation of hydrophobic hydration shells around hydrophobic surfactant moieties. Traditionally, it was thought that water undergoes a structural enhancement in the hydrophobic hydration shell which is expressed in the formation of stronger and/or more hydrogen bonds per unit volume [34]. Upon aggregation these shells overlap and structured water is released. Thus, this process is accompanied by a gain in entropy. The current view is that water in hydrophobic hydration shells is not significantly more structured than that in the bulk [35-42]. It is widely accepted that water largely retains its original structure by accommodating the nonpolar solute in its hydrogen bonding network thereby maintaining as many hydrogen bonds as possible [35, 42-44]. It has been argued that in order not to sacrifice hydrogen bonds compared to bulk water, the hydrogen bonds of water in the hydrophobic hydration shells adjacent to the apolar moieties are predominantly oriented tangentially to the apolar surface [35-38, 43]. This leads to a loss of entropy due to a motion restriction of solvent molecules. At a certain surfactant concentration, the number of water molecules is not sufficient to form independent hydration shells, which results in interferences and mutual obstructions of hydration shells (i.e. water molecules have to be part of two hydration shells simultaneously, which is highly unfavorable). As a result, the tendency to form aggregates increases rapidly [35].

Subsequently, the entropy lost upon formation of the tangentially oriented hydrogen bonds is regained upon aggregation since part of the water molecules surrounding the individual solutes is released. Hence, the micellization of surfactants is considered to be an entropy-driven process.

Although water is the primary solvent in surfactant studies and applications, aggregation behavior is not restricted to water and there are examples of the formation of aggregates in a wide variety of polar organic solvents of high cohesive energy density such as hydrazine, formamide, alkane diols (e. g. ethylene glycol) and ethyl ammonium nitrate [35, 45], although the aggregate stability is generally lower than that in water [46]. In addition, the self-assembly is generally much less cooperative, the CMC much higher, and the micelles are smaller [2]. It is also notable that in apolar solvents the association is of low cooperativity and leads only to small and polydisperse aggregates. However, introduction of even small amounts of water can induce a cooperative self-assembly (via dipole-dipole interaction between the head-groups [47]), leading to reverse micelles.

Noteworthy, each surfactant has a characteristic CMC at a given temperature, depending among other parameters on its structural balance hydrophilicity/hydrophobicity. Thus, the length of the hydrophobic tail is a major factor to modify the CMC-value: for a homologous series of linear single-chain surfactants, the CMC decreases logarithmically with the carbon number. Furthermore, chain branching gives a higher CMC than a comparable straight chain surfactant [48]. For a given hydrophobic tail, the nature of the hydrophilic group is also of importance: varying the head-group from ionic to nonionic induces a strong decrease of the CMC-values (by one order of magnitude or more) since no electrostatic repulsion can oppose to micelle formation (driven by the hydrophobic effect). Varying the nature of conventional ionic groups, however, has only a less pronounced effect. Note that the intrinsic hydrophilicity of head-groups can be classified; for instance, among the common anionic hydrophilic groups the usual ranking (starting from the less hydrophilic group) is the following: sulfate ($-\text{OSO}_3^-$) < sulfonate ($-\text{SO}_3^-$) \ll carboxylate ($-\text{CO}_2^-$) [49]. The counterion nature of ionic surfactants also influences the CMC. An increase in the degree of ion binding will decrease the CMC as the electrostatic repulsion between ionic groups will decrease. The presence of an added electrolyte also usually causes a decrease in the CMC of most surfactants (greatest effect for ionic ones). It allows to screen partially the electrostatic repulsion between head-groups and hence to lower the CMC. Finally, the influence of the temperature on micellization is generally weak for ionic surfactants (slight increase of CMC with T) while more important for nonionic surfactants (especially for ethylene oxide based surfactants) with a decrease of the CMC-values (in addition see part *1.1.2.d* about Krafft temperature and cloud point).

1.1.2.c. Micellar association models [29, 50]

Surfactants form a liquid-like aggregate when associating into micelles. Since no obvious mechanism leads to a specific aggregation number, it is natural to describe the association in terms of

a stepwise addition of a monomer S to the aggregate S_{n-1} , which is described by the following equation:



When additional interactions between aggregates and between monomers are neglected, the previous equilibrium can be expressed as:

$$K_n = \frac{[S_n]}{[S] \times [S_{n-1}]} \quad \text{Equation 1.1-3}$$

The latter equation provides a general description of any stepwise association process in dilute solution. However, as it is almost impossible to specify all the K_n equilibrium steps, some simplified models must be considered.

A first model is the **phase separation model**. Micelle formation has indeed several features in common with the formation of a separate liquid phase. Hence, this model approximates aggregation as a phase separation process, in which the activity of the monomer remains constant above the CMC. Also, in terms of the association described in Equation 1.1-2, the phase separation model assumes that aggregates with large n dominate all others except the monomer. This assumption implies strong cooperativity because once aggregation has started, it becomes more and more favorable to add another monomer until a large aggregation number is reached. Above the CMC, monomers and aggregates coexist in equilibrium and the concentration of non micellar molecules remains constant. Thus, the surfactant possesses a certain chemical potential $\mu^0(\text{micelle})$ in the pseudo-separate phase which can be expressed as:

$$\mu^0(\text{micelle}) = \mu^0(\text{solvent}) + RT \ln [S] \quad \text{Equation 1.1-4}$$

$[S]$ can be considered as the CMC (neglecting dimers and oligomers). Hence, the standard free energy of micellization ΔG_{mic}^0 , which represents the difference between the standard chemical potential of a surfactant monomer in the micelle and in dilute aqueous solution, is:

$$\Delta G_{\text{mic}}^0 = \mu^0(\text{micelle}) - \mu^0(\text{solvent}) = RT \ln \text{CMC} \quad \text{Equation 1.1-5}$$

Note that the phase separation model captures several, but not all, essential features of micelle formation. Although it describes the start mechanism of the self assembly process, it does not describe the stop mechanism.

A second possible model, i.e. the **closed-association model**, describes both start and stop features. It assumes that one aggregation number N dominates. The micellization is considered as a one-step process where N surfactant monomers S associate to form aggregates containing N molecules. This is reflected in the following equilibrium:



The total surfactant concentration expressed in terms of moles of monomer is:

$$[S]_T = N[S_N] + [S] = NK_N[S]^N + [S] \quad \text{Equation 1.1-7}$$

The equilibrium constant K_N relates to the other equilibrium constants of Equation 1.1-3 by:

$$K_N = \prod_2^N K_n \quad \text{Equation 1.1-8}$$

The derivative $\frac{\partial \{N[S_N]\}}{\partial [S]_T}$ describes what fraction of surfactants enters into an aggregate. From the plots of this derivative against $[S]_T$ varying values of N , it is noticeable that the larger the N value, the more abruptly this function changes from a low concentration of zero to the high concentration value of unity [29]. When N becomes infinite, the phase separation model is regained with a discontinuity in the derivative (step function), defining the CMC. Small micellar aggregation numbers, however, lead to less well-defined CMC-values. Typical micellar aggregation numbers lie in the range $N = 30-100$ which ensures that N is large enough to make the CMC a reasonably well-defined quantity in the closed association model.

The CMC is the concentration at which added surfactants preferentially enter the micelles. The starting point of this phenomenon can be evaluated when added monomer is as likely to enter a micelle as to remain in solution; this can be expressed by:

$$\left. \frac{\partial \{N[S_N]\}}{\partial [S]_T} \right|_{CMC} = \left. \frac{\partial [S]}{\partial [S]_T} \right|_{CMC} = 0.5 \quad \text{Equation 1.1-9}$$

Solving this equation gives the following relationship:

$$[S]^{N-1}_{CMC} = (N^2 K_N)^{-1} \quad \text{Equation 1.1-10}$$

The CMC refers to the total surfactant concentration, and by combining Equations 1.1-7 and 1.1-10, one obtains:

$$CMC = [S]_{CMC} (1 + N^{-1}) = (N^2 K_N)^{-1/(N-1)} (1 + N^{-1}) \quad \text{Equation 1.1-11}$$

$$\text{Hence,} \quad \ln CMC \cong -\frac{1}{N} \ln K_N \quad (\text{when } N \gg 1) \quad \text{Equation 1.1-12}$$

$$= \frac{1}{RT} \Delta G_{mic}^\theta = \frac{1}{RT} \{ \mu^\theta(\text{micelle}) - \mu^\theta(\text{solvent}) \}$$

A third Model is the **isodesmic model**, which assumes that K_n is independent of n . In this case it can be shown that the product $[S] \times K$ is inferior to one, regardless of either the total concentration or of K . Hence, the aggregate distribution function decays exponentially with $[S_1] > [S_2] > [S_n]$. In this model, aggregation is a continuous process that does not exhibit the abrupt onset in a narrow concentration range that characterizes micelle formation. This model describes quite well the association of some dyes in aqueous solution. However, it does not reflect the cooperativity associated with amphiphilic aggregation as this model does not predict a CMC. Its basic shortcoming lies in making K_n independent of n and thus depriving the process of cooperativity.

1.1.2.d. Krafft point and cloud point

A prominent feature that distinguishes ionic and nonionic surfactants is the difference in response to temperature, which derives from the affinity of their head-groups with water. With ionic surfactants, the micelles are formed only above a temperature known as the Krafft temperature. This is related to the crystal energy of the compound (ion pairing effects). A typical phase diagram where surfactant concentration is plotted against temperature is shown in Figure 1.1-11. T_K represents the Krafft point, i.e. the temperature at which surfactant solubility equals the critical micellization concentration. Below T_K , surfactant monomers only exist in equilibrium with the hydrated crystalline phase, and above T_K , micelles are formed providing greater surfactant solubility. The Krafft temperature is crucial in many applications since below T_K the surfactant can not perform efficiently.

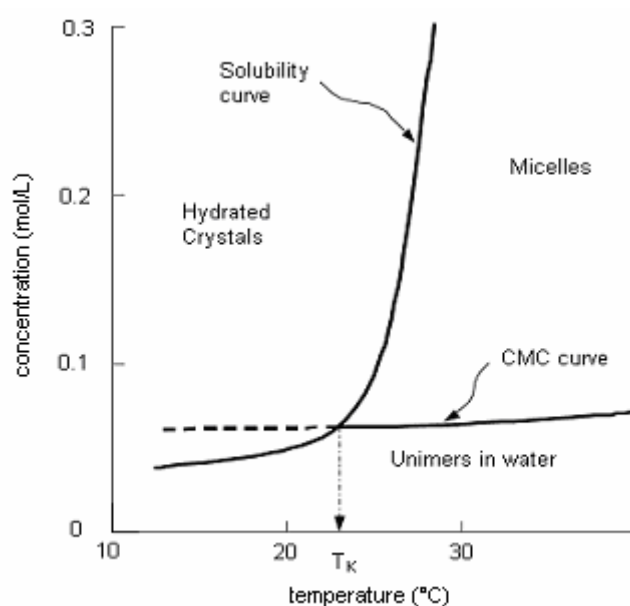


Figure 1.1-11: Schematic phase diagram for an ionic surfactant solution. T_K is the Krafft point.

For nonionic surfactants, the behavior is somehow inverse: when the temperature is increased, a common observation is that micellar solutions tend to become turbid at a well-defined temperature, referred to as “cloud point” (thermodynamic definition: lower critical solution temperature LCST). Above this temperature, the surfactant solution phase separates, which is accompanied by a sharp increase in aggregation number and a decrease in intermicellar repulsions [51-52], producing a difference in density of the micelle-rich and micelle-poor phases. This behavior is mainly attributed to the rupture of the hydrogen bonds formed between water and the head-groups (e.g. with polyoxyethylene (PEO) nonionics).

1.1.3. Aggregation behavior of surfactants

1.1.3.a. Types of aggregates

Early studies showed that spherical micelles are formed by ionic amphiphiles with single alkyl chain [53-54]. In 1936, Hartley described such micelles as spherical aggregates with alkyl groups forming a hydrocarbon liquid-like core and with polar groups providing a charged surface (see Fig. 1.1-9) [55]. Later, micelles of very different shapes were encountered. Aggregate morphology is mainly determined by a delicate balance between attractive hydrophobic interactions of surfactant alkyl tails and electrostatic repulsions of surfactant head groups [56]. In addition to repulsive interactions of electrostatic origin, repulsions due to hydration of the head groups must be taken into account. An opposing effect is exerted by the interfacial tension that tends to decrease the effective head group area. Thus, the different micellar geometries strongly depend on environmental conditions (e.g., concentration, temperature, pH, ionic strength, additives), which influence the balance mentioned just before. For instance, spherical micelles may grow to form cylinders or bilayers when the surfactant concentration or the salt content is increased, as illustrated in Figure 1.1-12.

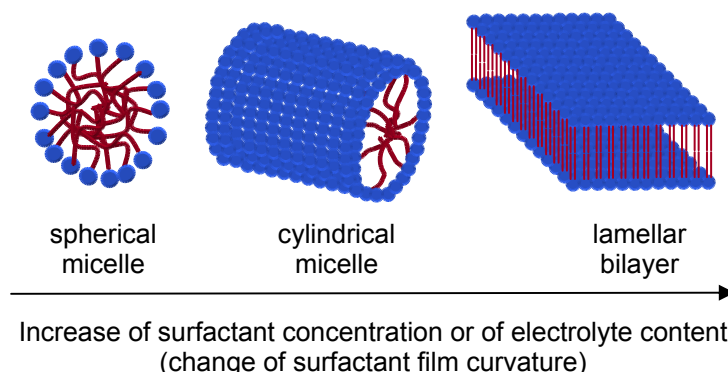


Figure 1.1-12: Idealized representation of various micellar morphologies [22].

The micellar geometry also depends on the molecular architecture of the surfactant; in other words, the type of aggregate into which a surfactant associates in aqueous solution is mainly related to its structure:

Spherical micelles

Typically, unbranched single-tailed surfactants possess a conical shape and aggregate to form spherical micelles in aqueous solution above their CMC [57]. On average almost all the chain volume is in a dry hydrophobic core. Still, all segments of the chain (methylene groups) spend some time in contact with the aqueous phase: the first two methylene groups of the surfactant (from the head group) have considerable contact with water in the aqueous solution. Even, the terminal group is to a certain extent exposed to the polar exterior, more often than groups nearer the chain centre [58]. Spherical micelles usually consist of 40-100 monomers [59] and are approximately 5 nm in diameter. Their size distribution is rather narrow (monodispersity). The lifetime of a typical spherical micelle is

of the order of milliseconds and the residence time of a monomer in a micelle is of the order of microseconds (see respectively slow and fast relaxation times τ_2 and τ_1 in Figure 1.1-13) [31, 60]. Monomer exchange is diffusion controlled.

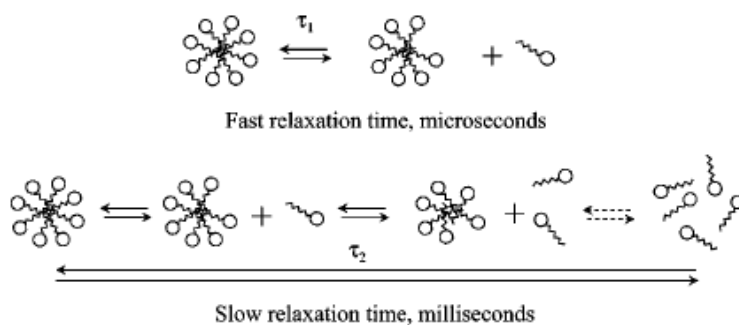


Figure 1.1-13: Mechanisms for the two relaxation times τ_1 and τ_2 for a surfactant solution above CMC. From reference [61].

Cylindrical micelles

Cylindrical micelles are formed by surfactants whose monomer shape resembles a truncated cone. Both theoretical and experimental reports show that these micelles are often long (so-called wormlike micelles can reach several tens of micrometers) and flexible and that they undergo transformations on relatively short timescales [62-65]. The presence of such micelles in aqueous solution is often reflected by an increase in relative viscosity [57]. Viscoelastic solutions are formed upon increasing the surfactant concentration which indicates the formation of an entangled network of wormlike micelles. Formation of wormlike micelles can often be induced by addition of strongly binding counter ions to ionic surfactants in aqueous solution, as will be seen later in this work.

Vesicles

In general, surfactant molecules possessing one head group and two alkyl tails form vesicles in aqueous solution. Actually, upon dissolving double-tailed surfactants in aqueous solution, bilayer fragments are formed that can be closed by the input of mechanical energy [66]. Vesicles range in diameter from 20 nm to several micrometers and can be either unilamellar or multilamellar. Vesicles formed from pure surfactants are metastable and eventually revert to the flat bilayer state and ultimately precipitate as crystalline materials.

1.1.3.b. Packing parameter concept

The concept of molecular packing parameter has been widely cited in the chemistry, physics, and biology literature because it allows a simple and intuitive insight into the self-assembly phenomenon [67]. The packing parameter approach permits indeed to relate the shape of the surfactant monomer to the aggregate morphology [68-70]. The molecular packing parameter P is defined as the

ratio v_0/al_0 , where v_0 and l_0 are the volume and the extended length of the surfactant tail, respectively and a is the *equilibrium* area per molecule at the aggregate interface (or mean cross-sectional {effective} head-group surface area), as illustrated in Figure 1.1-14.

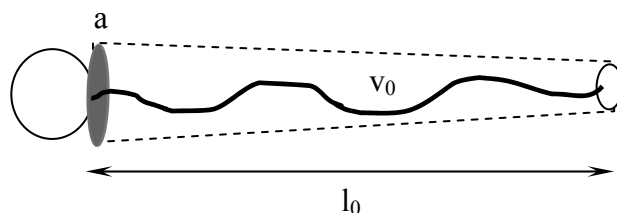


Figure 1.1-14: Illustration of the parameters v_0 , l_0 and a , involved in the calculation of the packing parameter P of a surfactant.

If we consider a spherical micelle with a core radius R , made up of N_{agg} molecules, then the volume of the core is $V = N_{agg} \times v_0 = 4\pi R^3/3$, the surface area of the core $A = N_{agg} \times a = 4\pi R^2$. Hence, it can be deduced that $R = 3v_0/a$, from simple geometrical relations. If the micelle core is packed with surfactant tails without any empty space, then the radius R cannot exceed the extended length l_0 of the tail. Introducing this constraint in the expression for R , one obtains $0 \leq v_0/al_0 \leq 1/3$, for spherical micelles. For spherical, cylindrical or bilayer aggregates made up of N_{agg} surfactant molecules, the geometrical relations for the volume V and the surface area A are given in Table 1.1-1. These geometrical relations, together with the constraint that at least one dimension of the aggregate (the radius of the sphere or the cylinder, or the half-bilayer thickness, all denoted by R) cannot exceed l_0 , lead to the following well-known [68] connection between the molecular packing parameter and the aggregate shape: $0 \leq v_0/al_0 \leq 1/3$ for sphere, $1/3 \leq v_0/al_0 \leq 1/2$ for cylinder, and $1/2 \leq v_0/al_0 \leq 1$ for bilayer. Inverted structures are formed when $P > 1$.

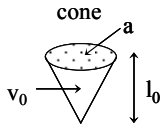






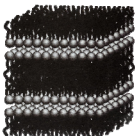


Table 1.1-1 Geometrical relations for spherical, cylindrical, and bilayer aggregates ^a

variable	sphere	cylinder	bilayer
volume of core $V = N_{agg} \times v_0$	$4\pi R^3/3$	πR^2	$2R$
surface area of core $A = N_{agg} \times a$	$4\pi R^2$	$2\pi R$	2
R	$3v_0/a$	$2v_0/a$	v_0/a
packing parameter	$v_0/al_0 \leq 1/3$	$v_0/al_0 \leq 1/2$	$v_0/al_0 \leq 1$

^a Variables V , A , N_{agg} refer to the entire spherical aggregate, unit length of a cylinder or unit area of a bilayer respectively, for the three shapes. R is the radius of spherical or cylindrical micelle or the half-bilayer thickness of the spherical vesicle. v_0 and l_0 are the volume and extended length of the surfactant tail ($R \leq l_0$) [67].

Table 1.1-2 summarizes the relationship between the architecture of surfactant monomer, packing parameter and aggregate morphology.

Table 1.1-2 Relationships between the shape of surfactant monomer and preferred aggregate morphology. [68]

possible surfactant type	$P (=V_0/a l_0)$	shape	structures formed*
single-chain surfactants with large headgroups	$< 1/3$	cone 	spherical micelles 
single-chain surfactants with small headgroups	$1/3 < P < 1/2$	truncated cone 	cylindrical micelles 
double-chain surfactants with large headgroups and flexible chains	$1/2 < P < 1$	truncated cone 	flexible bilayers, vesicles 
double-chain surfactants with small headgroups or rigid, immobile chains	$P \sim 1$	cylinder 	planar bilayers 
double-chain surfactants with small headgroups, very large and bulky hydrophobic groups	$P > 1$	inverted truncated cone or wedge 	inverted micelles 

* From reference [29].

Therefore, if the molecular packing parameter is known, the shape and size of the equilibrium aggregate can be readily identified as shown above. Noteworthy, a is often referred to as the “headgroup area” in the literature. This has led to the erroneous identification of a as a simple geometrical area based on the chemical structure of the headgroup in many papers, although a is actually an equilibrium parameter derived from thermodynamic considerations [67]. Needless to say, that for the same surfactant molecule, the area a can assume widely different values depending on the solution conditions such as temperature, salt concentration, additives present, etc.; hence, it is meaningless to associate one specific area with a given head group. For example, sodium dodecylbenzene sulfonate forms micelles in aqueous solution whereas bilayer structures are formed when alkali metal chlorides are added [71]. Moreover, the role of the surfactant tail has been virtually neglected. This is in part because the ratio v_0/l_0 appearing in the molecular packing parameter is independent of the chain length for common surfactants (0.21 nm^2 for single tail surfactants) and the area a depends only on the head group interaction parameter. Nagarajan showed that the tail length

influences the head group area (consideration of tail packing constraints) and thereby the micellar shape [67].

1.1.3.c. Lyotropic liquid crystals

Micellar solutions are one of several possible aggregation states. The existence of liquid crystalline phases constitutes an important aspect of surfactant science and a detailed description can be found in the literature (e.g. in [72] and [73]).

When the volume fraction of surfactant in a micellar solution is increased (typically above a threshold of about 40%) a series of regular geometries is commonly encountered. Interactions between micellar surfaces are repulsive (from electrostatic or hydration forces), so that as the number of aggregates increases and micelles get closer to each other, the only way to maximise separation is to change shape and size. This explains the sequence of surfactant phases observed in the concentrated regime. Such phases are known as mesophases or lyotropic (solvent-induced) liquid crystals. As the term suggests, liquid crystals are characterised by physical properties intermediate between crystalline and fluid structures. Certain of these phases have at least one direction that is highly ordered so that liquid crystals exhibit optical birefringence. The main structures associated with two-component surfactant–water systems are: cubic, hexagonal and lamellar. Some of these structures are depicted in Figure 1.1-15. Two main groups of cubic phases can be mentioned: the micellar cubic phases (I_1 and I_2) which are built up of regular packing of small micelles (or reversed micelles in the case of I_2). The micelles are short prolates arranged in a body-centred cubic close-packed array [74-75]. The bicontinuous cubic phases (normal V_1 and reversed V_2) are rather extended, porous, connected structures in three dimensions. They are considered to be formed by either connected rod-like micelles, similar to branched micelles, or bilayer structures. V_1 and V_2 are positioned between H_1 and L_α and between L_α and H_2 respectively (see Fig. 1.1-15). Cubic phases are optically isotropic systems and so cannot be characterized by polarizing light microscopy. The hexagonal phase is composed of a close-packed array of long cylindrical micelles, arranged in a hexagonal pattern. The micelles may be “normal” (in water, H_1) in that the hydrophilic head groups are located on the outer surface of the cylinder, or “inverted” (H_2), with the hydrophilic group located internally (less common). The lamellar phase (L_α) is built up of alternating water-surfactant bilayers. The hydrophobic chains possess a significant degree of randomness and mobility, and the surfactant bilayer can range from being stiff and planar to being very flexible and undulating. Noteworthy, it is possible for a surfactant to pass through several distinct lamellar phases.

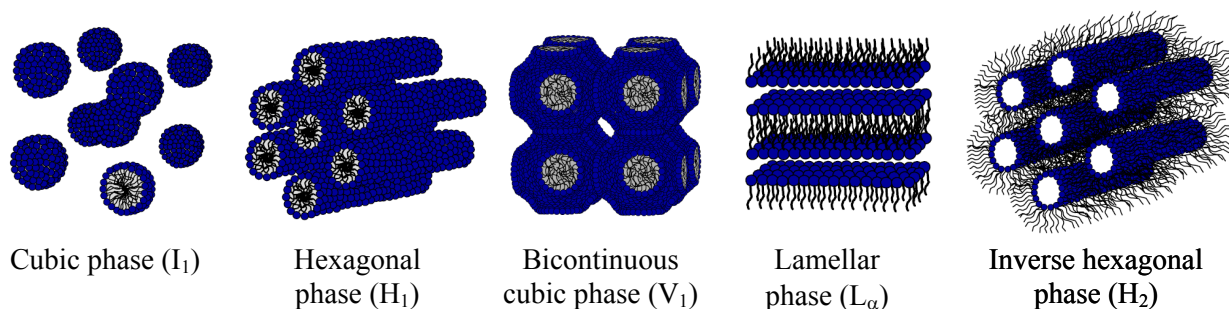


Figure 1.1-15: Common surfactant liquid crystalline phases.

As regards the viscosity of these phases, the following order can be found: cubic > hexagonal > lamellar. Cubic phases are generally the more viscous since they have no obvious shear plane. Hexagonal phases typically contain 30-60% water by weight but are very viscous since cylindrical aggregates can move freely only along their length. Lamellar phases are generally less viscous than the hexagonal phases due to the ease with which each parallel layer can slide over each other during shear.

1.2 Polymeric and Oligomeric surfactants

The search for new surfactants with new property profiles was for long concerned with the variation of the hydrophilic-lipophilic balance (HLB). Molecular variations focused on the nature of the hydrophilic head group, the general nature of the hydrophobic group (linear, branched, aliphatic, aromatic, perfluorocarbon, silicone, etc.) and its size (homologous series). More recently, the influence of the overall surfactant shape and size has been recognized as an important additional factor which controls the properties of surfactants. In this respect, new classes of amphiphiles, i.e. the polymeric and oligomeric surfactants respectively, have emerged. First, the former class will be briefly described before presenting the class of surfactant oligomers which is of interest for this work.

1.2.1 Polymeric surfactants

By their molecular structure, polymeric surfactants can be distinguished into two main general types: “polysoaps”, whose repeat unit is amphiphilic by itself, and amphiphilic block and graft copolymers, so-called “macro-surfactants”, whose overall macromolecule constitutes the amphiphile [7, 76]. Various designs of polymeric surfactants are illustrated in Figure 1.2-1.

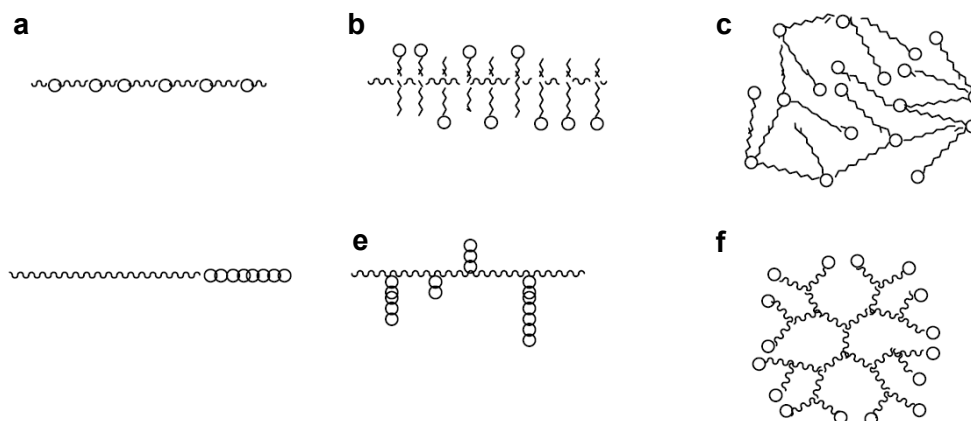


Figure 1.2-1: Scheme of different types of polymeric surfactants: a) ionene-type, b) polysoap, c) hyperbranched, d) block copolymer, e) graft copolymer, and f) dendrimer.

Compared to low molar mass surfactants, amphiphilic block copolymers usually exhibit low or very low CMC values ($10^{-9} - 10^{-4}$ M), can virtually reduce foaming to zero [7], show generally high solubilization capacity and good dispersing ability for solid particles (steric or electrosteric effects). The dissolution of these compounds is basically more time-consuming than that of standard surfactants and the molecular mobility is low. Moreover, the reduction of surface tension is in general low or moderate. For a deeper insight in the field, a report on recent progress [7] as well as a detailed review on synthetic strategies and self-aggregation aspects [33] can be consulted.

Polymeric surfactants made from individual surfactant monomer units (hydrophilic and hydrophobic groups scattered all over the macromolecule), so-called "polysoaps", are known since nearly 50 years [5]. Still, these molecules have attracted so far only limited interest. They have been generally considered as exotic macromolecules only, much more than as surfactants. Yet, they exhibit interesting features which has involved their use in many fields (as protective colloids, emulsifiers, lubricants, viscosity modifiers, etc.). Some properties such as e.g. the high solubilization capacity for hydrophobic molecules are found to be similar to those of standard surfactants, but other properties can differ considerably, as exemplified by their *intra*-molecular aggregation and the usually missing critical micellization concentration [77].

1.2.2 Oligomeric surfactants

Both academic and industrial interest has been focused on such novel surfactant structures since they exhibit an enhanced property profile and provide some unusual properties compared to conventional surfactants.

1.2.2.a. Architecture of oligomeric surfactants

Different architectures of well-defined surfactant oligomers are possible (see Figure 1.2-2). First, the degree of oligomerization ($n = 2, 3, 4 \dots$) can be precisely adjusted. In addition, the topology of the oligomers can be varied from linear to cyclic or star-like, and the position of the anchoring point can also be modified, e.g. the surfactant fragments can be coupled at the level of the hydrophilic head groups or at opposite ends of the hydrophobic chains giving intermediates namely of the "head type" and of the "tail-end type" (as defined for polymeric surfactants), respectively [76]. The combination of these molecular variables allows to enlarge the pool of amphiphilic molecules, creating original molecular designs [77]. Furthermore, these supplementary variables are expected to play an essential role for the control of the solution properties and aggregate morphologies of such new surfactants, giving possibly access to a wider range of applications.

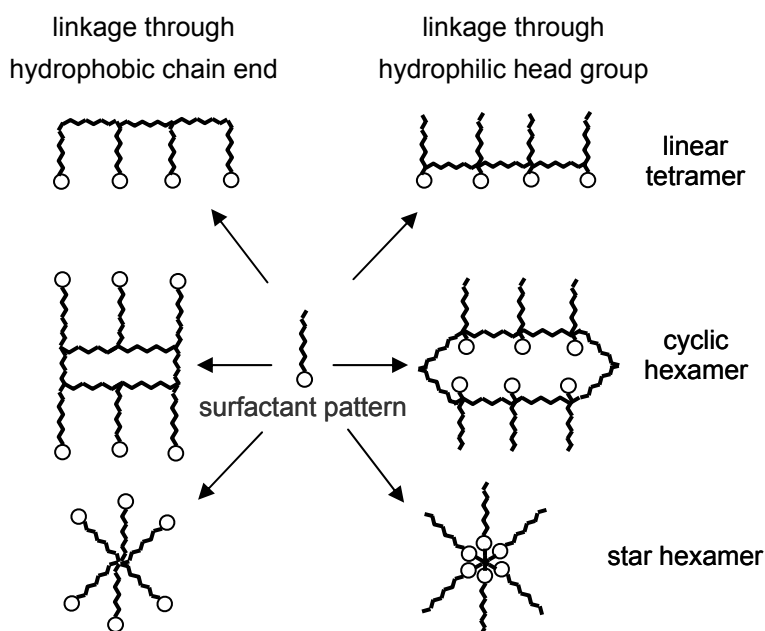


Figure 1.2-2: Different architectures of well-defined surfactant oligomers. Variables: hydrophilic head, hydrophobic tail; Additional factors: degree of oligomerization, topology of oligomers, position of anchoring point.

Cationic trimeric and tetrameric surfactant stars were reported in the context of Langmuir films, as well as a cationic cyclic hexameric surfactant (calix[6]arene-based porous amphiphile) [78]. Additionally, anionic trimeric surfactant stars [79-81] and trimeric or tetrameric cyclic surfactants [82-85] have been described occasionally. An example of a new trimeric-type anionic surfactant star with carboxylate head groups [81] is depicted on Figure 1.2-3.a. Such a structure provides for instance good emulsion stability. Regarding cyclic surfactants, novel oligoanionic amphiphiles based on dendro-calixarene (see Figure 1.2-3.d) were reported to self-assemble into completely uniform and structurally

persistent micelles (non deformable upon drying) [85]. The “T-shape” of the compound induces the formation of small and highly curved stable aggregates, each containing seven molecules. Such precisely defined and stable micelles resulting from the controlled self-assembly of specific amphiphiles can have potential nanotechnological applications as high performance drug-delivery capsules (vehicles for the delivery of apolar molecules) [86], for example.

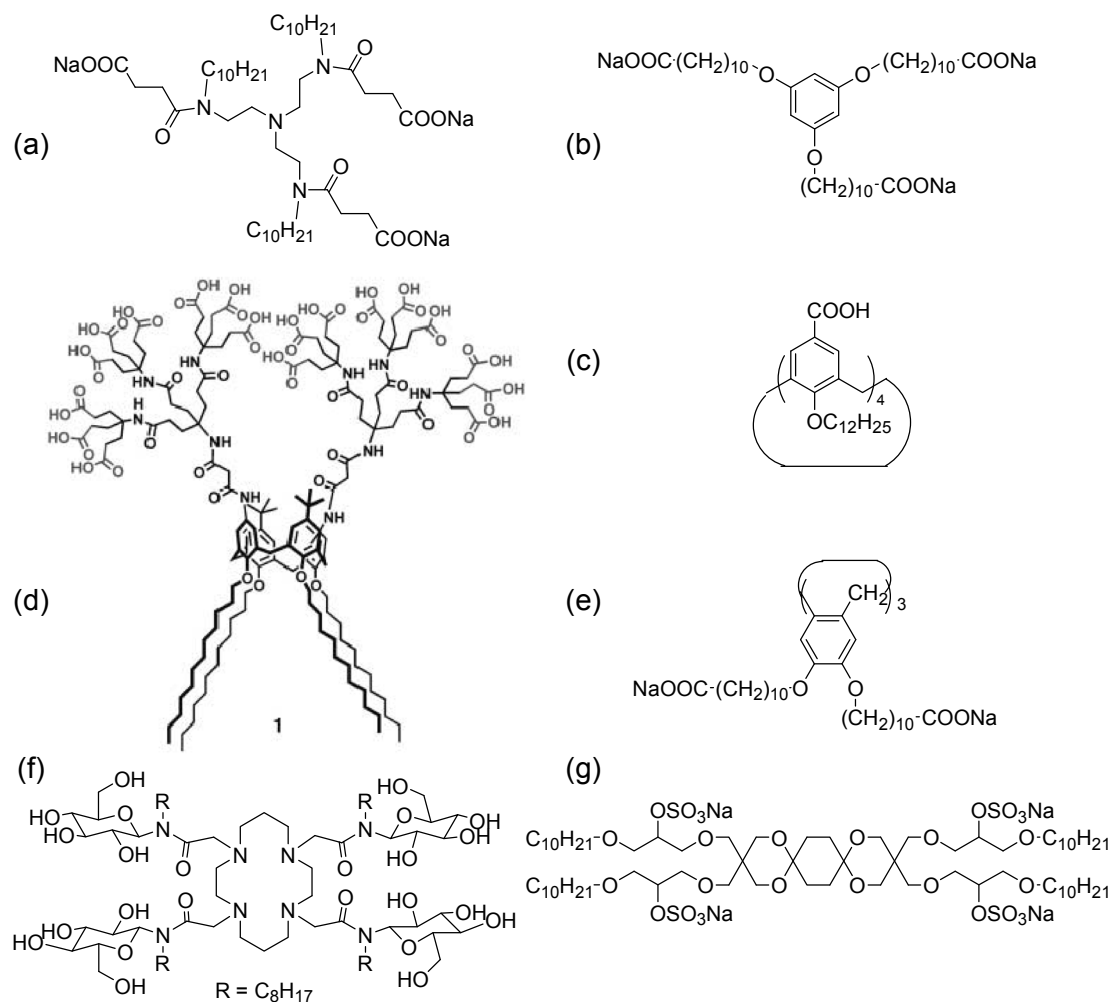


Figure 1.2-3: Examples of surfactant oligomers: (a) and (b) star-like trimeric surfactants from [81] and [87], respectively; (c), (d) and (e) calixarene-based cyclic surfactant oligomers from [88], [85] and [89], respectively; (f) macrocyclic sugar-based surfactant from [84]; (g) anionic tetrameric surfactant with multiple-ring spacer from [90].

More recently, the self assembly of amphiphilic calix[4]arenes with either a carboxylic acid (see Figure 1.2-3.c) or a trimethyl ammonium head group and different alkyl chains was investigated in aqueous solution [88]. The carboxylated calixarene forms vesicles in dilute solution and stable monolayer on water, while no aggregates are observed with the calixarene bearing ammonium head groups. Also, macrocyclic sugar-based surfactants (see e.g. Figure 1.2-3.f) were synthesized and characterized in recent years [84]. These macrocyclic surfactants self-aggregate in water into small

prolate micelles with a lipophilic core consisting of hydrocarbon chains and a hydrophilic shell containing the cages and the hydrated sugar moieties. They can potentially act as chelating surfactants and amphiphilic metal complexes, e.g. for use in enantioselective metal-catalyzed reactions in aqueous micellar media. Noteworthy, the complexation of copper (II) ions does not affect here the self aggregation. In addition to such novel amphiphilic structures, new anionic oligomeric (tetrameric) surfactants with multiple-ring spacers based on dioxane were also recently described (see Figure 1.2-3.g) [90].

It is notable that there is a rising interest in the rational design of such new surfactants that possess various chemical or biological functionalities and self-assemble into tunable and possibly predictable aggregate structures.

1.2.2.b. Linear surfactant oligomers

Linear surfactant oligomers represent another topological sub-class of surfactant oligomers (*vide supra*), in addition to cyclic and star oligomeric amphiphiles.

In simple cases, the “dimerization” of two independent surfactant fragments via the hydrophilic groups, results in so-called "gemini" surfactants, which were considered the starting point for surfactant oligomers [91]. This structure is opposed to "bola" surfactants which can be described as surfactants dimers that are coupled via the hydrophobic chain ends (see Figure 1.2-4). Both molecular structures have their biological counterparts: for example, cardiolipin (diphosphatidylglycerol) present in membranes of bacteria and of mitochondria is a gemini surfactant having four acyl groups and two phosphate groups. In the lipids of archaebacteria, biological counterparts of bola-amphiphiles can also be found (e.g. caldarchaeol).

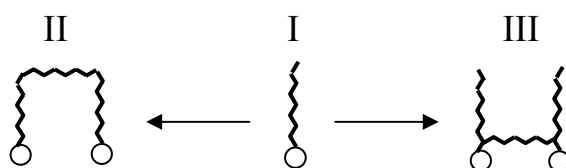


Figure 1.2-4: Scheme of the dimerization of “monomeric” surfactant (I) via the end of the hydrophobic chain (= "bola" amphiphile) (II), or via the hydrophilic group (= "Gemini" amphiphile) (III).

Bola amphiphiles exhibit properties different from those of gemini surfactants. The fundamental properties of gemini surfactants are generally more remarkable and hence, will be presented in more detail hereafter. Nevertheless, note that for bola amphiphiles [92] the critical micellization concentrations are usually larger [19, 93-94], and the sizes of the micelles are smaller [19, 94] than those of unipolar surfactants of the same carbon number. Bola-amphiphiles have also been shown to adopt a folded, reverse U-shape conformation at the air/water interface [94-95]. Moreover, special

bola-surfactants are of particular interest for the formation of monolayer membrane vesicles which are robust with respect to fusion and flip-flop of head-groups [96], and which provide great convenience for the membrane mimetic investigation [97]. Three examples of Bola-amphiphiles are presented in Figure 1.2-5: compound (a) was reported to be a very efficient gelling agent for water, by forming a dense network of nanofibers [98, 99]. Compound (b) was recently used with oppositely charged conventional surfactants for the formation of small spherical vesicles [97].

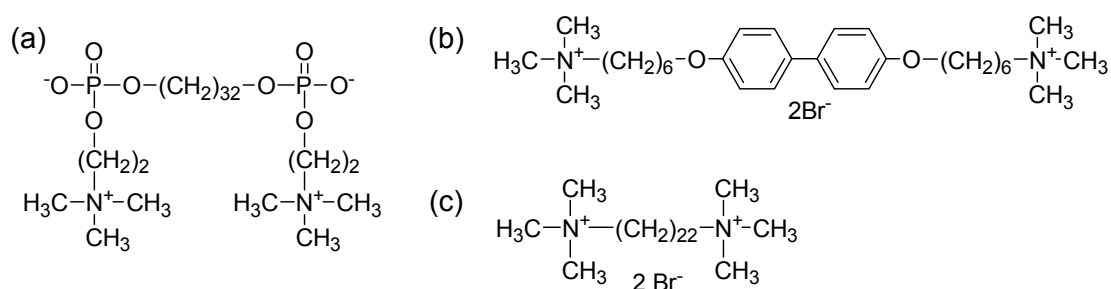


Figure 1.2-5: Examples of Bola-amphiphiles: (a) amphoteric one with phosphocholine headgroups, from [98]; (b) and (c) cationic ones, from [97] and [19], respectively.

As in the case of “head-type” polysoaps [77], a marked influence of the spacer group has been found for gemini surfactants. The spacer group between the two head groups can be either hydrophilic or hydrophobic, short or long, and rigid or flexible. Hence, the spacer represents a new structural parameter to tune the behavior and properties of amphiphiles, in addition to the classical variation of the nature of the hydrophilic head group and the hydrophobic tail (Fig. 1.2-6). The presence of the spacer group connecting the amphiphilic moieties permits the synthesis of dimeric surfactants with an enormous variety of structures and thus possibly opens the door to properties that cannot be achieved with pure (i.e. in the absence of additives) conventional surfactants.

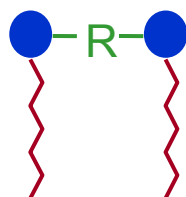


Figure 1.2-6: Design of “gemini” surfactants.

= hydrophilic head = hydrophobic tail and = spacer group

Noteworthy, when the two amphiphilic fragments are dissimilar (different chain length and/or head group), the resulting surfactant is referred to as heterodimer or “heterogemini” [100]. Typical structures of gemini surfactants with an aliphatic spacer group (classified by the nature of the head group) are depicted on Figure 1.2-7 [100-103].

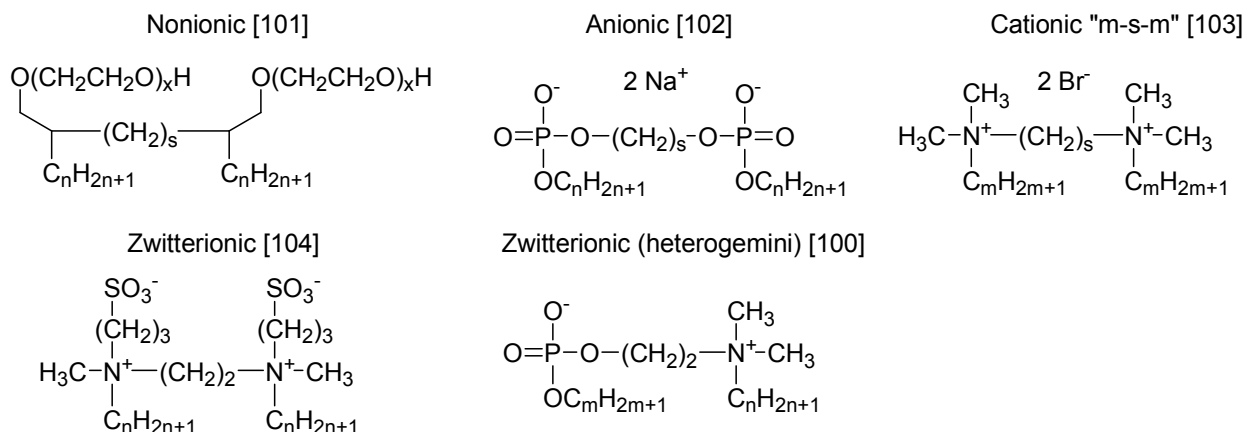


Figure 1.2-7: Examples of gemini surfactants [100-104].

The fact that the behavior of dimeric (gemini) surfactants can differ much from that of conventional surfactants can be qualitatively understood by the distribution of head group distances [105]. Indeed, unlike “monomeric” surfactants, dimeric amphiphiles exhibit a bimodal distribution of distances between the head groups, as shown in Figure 1.2-8.b. The head group distance distribution function shows a maximum at the thermodynamic equilibrium distance d_T (determined by the opposite forces at play in micelle formation) and another narrow maximum at a distance d_S corresponding to the length of the spacer (determined by the number of atoms in the spacer and its conformation). This bimodal distribution and the effect of the chemical link between head groups on the packing of surfactant alkyl chains in the micelle core are expected to strongly affect the curvature of surfactant layers, and thus, the micelle shape and the properties of the solution.

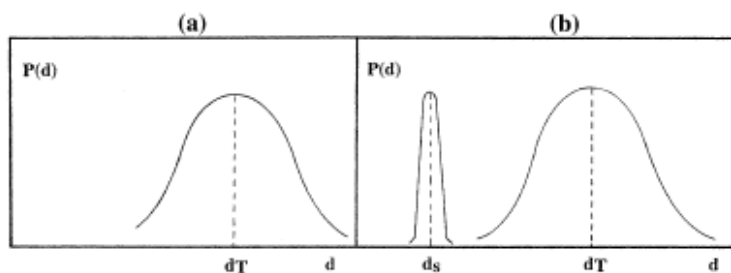


Figure 1.2-8: schematic representation of the distribution of distances between head groups in micelles of a conventional surfactant (a) and of a dimeric surfactant (b). Taken from [105].

In addition to gemini surfactants, higher oligomers, i.e. well-defined linear trimers or tetramers, can also be found. Nevertheless, trimers and tetramers are much rarer than dimers, since the syntheses and purifications of the former are very laborious. Most of such higher oligomeric surfactants are quaternized derivatives of diethylenetriamine [106-110] or dipropylenetriamine [111-116] and the naturally occurring tetramine spermine [116-117], bearing three or four linear alkyl chains, as exemplified in Figure 1.2-9.

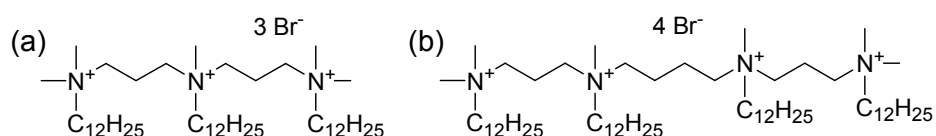


Figure 1.2-9: Examples of linear higher surfactant oligomers of the “head-type”: (a) trimeric surfactant “12-3-12-3-12” [111-116]; (b) tetrameric surfactant (from spermine) “12-3-12-4-12-3-12” [117].

Such oligomers are exotic structures so far, for the reasons evoked before. Therefore, the next part will focus on the properties of gemini surfactants which seem more promising for practical uses.

1.2.2.c. Overview on the properties of gemini surfactants

The 1990ies saw the up-rise of "gemini" surfactants due to their particularly appealing properties. These were recently reviewed by Zana, Menger and In [91, 105, 118-120]. Principally, dimeric surfactants exhibit remarkably lower critical micellar concentrations, compared to their monomeric analogues (generally one to two orders of magnitude). Table 1.2-1 briefly summarizes the main properties of dimeric surfactants versus monomeric surfactants in aqueous solution. It is evident from this table that the nature and the length of the spacer group linking individual surfactant units together are of major importance. For instance, it is notable that the CMC values for the cationic gemini surfactant series “m-s-m” (see Figure 1.2-7) with hydrophobic polymethylene spacer groups goes through a maximum upon increasing spacer carbon number at approximately $s = 6$, irrespective of the chain length [105]. Also it is notable that certain oligomeric surfactants were reported to form in aqueous solutions very large aggregates [121-122], so-called giant or worm-like micelles, and to exhibit strong viscosifying effects [116, 123-124]. Most such examples in the literature involve cationic dimeric surfactants with an ultra short C_2 -spacer. For instance, 1,2-bis(N,N,-dimethyl-N-dodecylammonio) ethane dibromide (bisquaternary ammonium with dodecyl chains and a C_2 -spacer, abbreviated "12-2-12") is an excellent thickener (as of ca. 2 % wt in pure water). However with increasing length of the spacer separating the two surfactant fragments, the marked thickening behavior disappears rapidly [119].

Noteworthy, when looking at the effect of the degree of oligomerization, In et al. showed for oligomeric surfactants with dodecyl chains and a C_3 spacers, that the micelle shape changes from spherical for the monomer to wormlike for the dimer to branched worm-like for the trimer [115] and to ring-like for the tetramer [114], parallel to an increase in the viscosity, as the micelle shape has a strong impact on the rheological behavior [116]. Nevertheless, almost no change of the micellar shape is observed for surfactants with longer spacers, and thus no marked thickening effect, in going from the monomeric (“12-3”) [125] to the dimeric (“12-6-12”) [121] and trimeric surfactant (“12-6-12-6-12”) analogs [116, 126].

Table 1.2-1: Comparison of typical properties of gemini surfactants vs. standard surfactants (all comparisons on equal amounts in weight).

- CMC is much smaller (ca. 1-2 orders of magnitude)
- $\sigma_{cmc} \cong$ equal or lower, depends on spacer group
- long relaxation times τ_1 and τ_2 (NMR)
- aggregation numbers depend on spacer length
 - medium to long spacer: N_{agg} is small; spherical micelles
 - short spacers: N_{agg} increases; worm-like micelles
- viscosifying effect depends on spacer length
 - medium to long spacer: small effect
 - short spacers: strong effect
 - appropriate counterions produce gelators [116, 121, 124, 127]
- foaming power varies strongly with spacer length
short spacers = strong foaming
- solubilization capacity \cong equal or higher

1.2.2.d. Applications of gemini surfactants

Rosen pointed out the enhanced performances of gemini surfactants which could make them the “new generation of surfactants” [128]. This has been somehow attested since then by the great number of patent filed on gemini surfactants [121] and by the topical academic interest in applications of these surfactant structures, as overviewed hereafter.

Most of the gemini surfactants have been cationic species, since they can be more easily synthesized for systematic studies. However, due to the lower compatibility with the human body compared to non-ionics or anionics, they have remained mostly an academic object. Still, they found applications as fabric softeners [91, 120], improved disinfectants (bactericidal and fungicidal agents because of their stronger biological activity) [129-130], as templating agents for mesoporous materials [131-133] or nanoparticles [134-137], as effective dispersants [138] and corrosion inhibitors [139-140]. Ultralow interfacial tension between crude oils and cationic gemini surfactant solutions was attained [141] and their use as enhanced oil recovery systems attracted interest [142]. Furthermore, removal of organic pollutant from soil surfaces by cationic geminis was found to be efficient [143]. Such surfactants were also effective in enhancing the rate of various reactions, as early noticed by Bunton et al. [144]. Micellar solutions of dimeric surfactants present a higher catalytic activity than corresponding monomeric surfactants in reactions such as e.g. decarboxylation and dephosphorylation [145], ester cleavage [146], cyclization [147], nucleophilic substitutions [105], etc. In the latter case,

triazole-based cationic gemini were shown to increase the rate of a nucleophilic aromatic substitution reaction [148]. Also, cationic gemini surfactants have found additional interest as non-viral transfecting agents (gene delivery systems) [149-158]. Certain geminis can indeed bind and compact DNA efficiently. Moreover, it is notable that phenol gemini derivatives can restrain the aggregation of organic molecules, e.g. cholesteryl esters which could cause atherosclerosis [159].

Special commercial nonionic gemini surfactants (with acetylene spacers) were also reported to be low foaming agents (for improved coating aesthetics) [160-161]. Glucosamide-based trisiloxane gemini surfactants were also synthesized and may be presumably used as wetting agents for cosmetic applications [162]. Sarcosine-based anionic dimeric surfactants were reported to be good flotative agents for collecting minerals [163]. Disulfonate or dicarboxylate dimeric surfactants with a spacer group that can be cleaved by ozonolysis were synthesized [164]. The cleavage results in a drop of the foam stability which can be useful for specific purpose. Some other anionic gemini surfactants were tested as new laundry surfactants [165]. Although formulations with these amphiphiles exhibited promising performances, this exploratory work was not pursued any further as the envisaged synthesis routes to these surfactants presumably involved high costs. Assumably, the potential of these molecules lays in specialized surfactant applications [165].

Thus, the given examples reflect the diversity of fields of applications for gemini surfactants. Only the very recent scientific literature regarding the uses of geminis was here mentioned, while the patent literature (which in fact concerns predominantly anionic and non-ionic geminis [91]) was not addressed. Hence, one can here figure out the great potential of these molecules as performance surfactants.

1.3 Objectives and motivation of this work

In the context described above, the synthesis and characterization of novel surfactants in the pursuit of interesting and unusual properties are worthwhile activities, given the importance of surfactants in applications.

The general aim of this work is to continue the search in the field of oligomeric surfactants with new linear surfactant oligomer structures in order to **establish structure – property relationships**. Such correlations are indeed useful for the choice of a given structure to obtain desired properties as well as for the prediction of the behavior of newly synthesized surfactants. Thus, this work includes the study and discussion of the fundamental properties of new series of surfactant oligomers with respect to the influence of the degree of oligomerization and the influence of the spacer group.

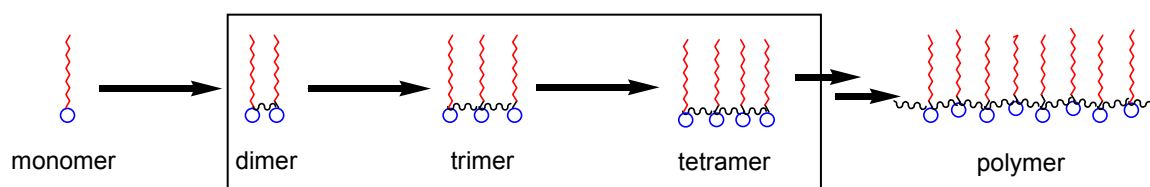


Figure 1.3-1: Oligomeric intermediates between monomeric and polymeric surfactants.

To reach this target, high-purity surfactants are needed for systematic studies: several cationic gemini surfactants with rational variation of the spacer group, as well as a novel anionic synthesized dimer will thus be examined (see chemical structures in the next chapter). It is also interesting to ask for the **behaviour of higher oligomeric analogues**, such as trimeric or tetrameric surfactants, which represent transitional structures between standard monomeric surfactants and polymeric ones (see Figure 1.3-1) [5]. Theoretical considerations predict that the critical micellization concentration decreases continuously with increasing degree of oligomerization, while preferentially small spherical micelles are formed at low concentration and wormlike micelles at high concentration [166]. Yet, there exist very few reports on such linear trimers and hardly any examples for tetramers (see especially 1.2.2.b). Hence, it is an objective of this work to point out the behavior of such higher oligomers, in comparison to the behavior of standard surfactants and polysoaps. Also, the role of the spacer group (length and chemical nature) will be examined.

In addition to the two new surfactant structural parameters that can be modified, namely the degree of oligomerization and the spacer group, it is also of interest to look at the **effect of the counterion**. In this respect, the addition of organic salts to gemini surfactant solutions will be studied since such additives are expected to strongly modify the morphology and properties of surfactant aggregates (possible anion exchange in-situ) [167]. The aim of such combinations is also to obtain a **synergistic effect** in the properties (while using lower amounts of material), in view of the relatively

high-cost of gemini surfactants. Moreover, dimeric surfactants are likely to interact with other additives such as oppositely charged surfactants (conventional or dimeric).

In the next chapter, the chemical structures used for this work as well as their interest will be described in more detail. Then, their fundamental properties such as Krafft temperature, micellization, surface activity, micellar aggregation number, and microemulsion formation will be presented and discussed in *Chapter 3*. *Chapter 4* will deal with the associative behaviour of geminis with organic salts: synergism in the micelle formation as well as morphology changes and viscosifying effects will be examined. Mixtures with oppositely charged surfactants will be also briefly addressed. *Chapter 5* is the experimental part describing the syntheses, techniques and methods (and related theories). Finally, *Chapter 6* is a general conclusion of the work, summarizing the evolution of the properties of surfactant oligomers with respect to the new structural parameters (degree of oligomerization, spacer, counterion effects), and addressing possible perspectives.

1.4 References

- [1] *Surfactants in Polymers, Coatings, Inks and Adhesives* (Applied Surfactant Series Vol. 1), Karsa, D. R. ed; Blackwell Publishing Ltd: Boca Raton, 2003.
- [2] Tadros, T. F. In *Applied Surfactants: Principles and Applications*; Wiley VCH Verlag: Weinheim, Germany, 2005.
- [3] Verbeek, H. In *Surfactants in Consumer Products: Theory, Technology and Applications*; Falbe, J., Ed.; Springer-Verlag: Berlin, Heidelberg, New York, London, Paris, Tokyo, 1987; Historical Review.
- [4] Pletnev, M. Y. *SÖFW-Journal* **2006**, *132*, 2-12.
- [5] Laschewsky, A. *Adv. Polym. Sci.* **1995**, *124*, 1-86.
- [6] Storsberg, J.; Laschewsky, A. *SÖFW-Journal* **2004**, *130*, 14-18.
- [7] Garnier, S.; Laschewsky, A.; Storsberg, J. *Tenside Surf. Det.* **2006**, *43*, 88-102.
- [8] Hauthal, H. G. *SÖFW-Journal* **2004**, *130*, 3-17.
- [9] Kotzev, A.; Laschewsky, A. *Polym. Prepr. Am. Chem. Soc. Div. Polym. Chem.* **1998**, *39*, 942-943.
- [10] Buhler, E.; Oelschlaeger, C.; Waton, G.; Rawiso, M.; Schmidt, J.; Talmon, Y.; Candau, S. J. *Langmuir* **2006**, *22*, 2534-2542.
- [11] Ralston, N. V. C.; Hunt, C. D. *Biochim. Biophys. Acta* **2001**, *1527*, 20.
- [12] He, M.; Lin, Z.; Scriven, L. E.; Davis, H. T.; Snow, S. A. *J. Phys. Chem.* **1994**, *98*, 6148-57.
- [13] Rawn, J. D. In *Traité de Biochimie*; Editions Universitaires: Paris, Montréal, Le Mont-sur-Lausanne, 1990.
- [14] Lo Nostro, P.; Ninham, B. W.; Ambrosi, M.; Fratoni, L.; Palma, S.; Allemanni, D.; Baglioni, P. *Langmuir* **2003**, *19*, 9583-9591.
- [15] Bhattacharya, S.; Haldar, J. *Langmuir* **2005**, *21*, 5747-5751.
- [16] Wennerström, H.; Lindman, B. *Phys. Rep.* **1979**, *52*, 1-86.
- [17] *Aggregation Processes in Solution: Studies in Physical and Theoretical Chemistry*; Wyn-Jones, E., Gormally, J. Eds.; Elsevier: Amsterdam, Oxford, New-York, 1983.
- [18] Eastoe, J.; Rogueda, P.; Harrison, B. J.; Howe, A. M.; Pitt, A. R. *Langmuir* **1994**, *10*, 4429.
- [19] Mackenzie, K.C.; Bunton, C.A.; Nicoli, D.F.; Saelli, G. *J. Phys. Chem.* **1987**, *91*, 5709.
- [20] Jaeger, D.; Mendoza, A.; Apkarian, R. P. *Langmuir* **2006**, *22*, 1555-1560.
- [21] Magdassi, S.; Moshe, M. B.; Talmon, Y.; Danino, D. *Coll. Surf. A* **2003**, *212*, 1-7.
- [22] Tsujii, K. In *Surface Activity: Principles, Phenomena, and Applications*; Academic Press Ed.: San Diego, London, New York, Tokyo, 1997.
- [23] Adamson, A. W.; Gast, A. P. In *Physical Chemistry of Surfaces*, 6th ed.; Wiley: New York, 1997.
- [24] *Surfactants in Consumer Products: Theory, Technology and Applications*; Falbe, J., Ed.; Springer-Verlag: Berlin, Heidelberg, New York, London, Paris, Tokyo, 1987.
- [25] Lindman, B. In *Surfactants*; Tadros, T. F. Ed.; Academic Press: London, 2003, pp 1984.
- [26] Holmberg, K.; Jönsson, B.; Kronberg, B.; Lindman, B. In *Surfactants and Polymers in Aqueous Solution* 2nd ed.; Wiley: Chichester, 2002.
- [27] Hoffmann, H. *Tenside Suf. Det.* **1995**, *32*, 6.
- [28] Shinoda, K.; Nakagawa, T.; Tamamushi, B.; Isemura, T. In *Colloidal Surfactants: Some Physicochemical Properties*. Academic Press: New York, London, 1963.
- [29] Evans, D.F.; Wennerström, H. In *The Colloidal Domain: where physics, chemistry, biology, and technology meet*; VCH Publishers, 1994.
- [30] Fuhrhop, J.-H.; Köning, J. In *Membranes and Molecular Assemblies: The Synergetic Approach. Monographs in Supramolecular Chemistry*; The Royal Society of Chemistry: Cambridge, 1994.

- [31] Patist, A.; Oh, S. G.; Leung, R.; Shah, D. O. *Coll. Surf. A* **2001**, *176*, 3-16.
- [32] Menger, F.M.; Zana, R.; Lindman, B. *J. Chem. Ed.* **1998**, *75*, 115.
- [33] Riess, G. *Prog. Polym. Sci.* **2003**, *28*, 1107.
- [34] Frank, H. S.; Evans, M. W. *J. Phys. Chem.* **1945**, *13*, 507.
- [35] Blokzijl, W.; Engberts, J. B. F. N. *Angew. Chem. Int. Ed.* **1993**, *32*, 1545.
- [36] Finney, J.L.; Soper, A.K. *Chem. Soc. Rev.* **1994**, *23*, 1.
- [37] Soper, A.K.; Luzar, A. *J. Phys. Chem.* **1996**, *100*, 1357.
- [38] Bowron, D.T.; Filipponi, A.; Lobban, C.; Finney, J.L. *Chem. Phys. Lett.* **1998**, *293*, 33.
- [39] Besseling, N.A.M.; Lyklema, J. *J. Phys. Chem. B* **1997**, *101*, 7604.
- [40] Jorgensen, W.L. *J. Phys. Chem.* **1982**, *77*, 5757.
- [41] Jorgensen, W.L.; Gao, J.; Ravimohan, C. *J. Phys. Chem.* **1985**, *83*, 3050.
- [42] Mancera, R.L. *J. Chem. Soc. Faraday Trans.* **1996**, *92*, 2547.
- [43] Bagno, A. *J. Chem. Soc., Faraday Trans.* **1998**, *94*, 2501.
- [44] Mancera, R.L.; Buckingham, A.D. *J. Phys. Chem.* **1995**, *99*, 14632.
- [45] Engberts, J. B. F. N.; Kevelam, J. *Curr. Opin. Colloid Interface Sci.* **1996**, *1*, 779-789.
- [46] Friberg, S. E.; Liang, Y. C. In *Microemulsions: Structure and Dynamics*. Boca Raton: CRC Press; 1987.
- [47] Friberg, S.; Ahmad, J. *Phys. Chem.* **1971**, *75*, 2001.
- [48] Rosen, M.J. In *Surfactants and Interfacial Phenomena*; John Wiley & Sons: USA, 1989.
- [49] Laughlin, R.G. *J. Soc. Cosmet. Chem.* **1981**, *32*, 371-392.
- [50] Hunter, R. J. In *Foundations of Colloid Science* (Volume I); Oxford Science Publications: Oxford, 1989.
- [51] Staples, E.J.; Tiddy, G.J.T. *J. Chem. Soc. Faraday Trans.* **1978**, *74*, 2530.
- [52] Tiddy, G.J.T. *Phys. Rep.* **1980**, *57*, 1.
- [53] McBain, J. W. *Trans. Faraday Soc.* **1913**, *9*, 99.
- [54] Reychler, *Kolloid-Z.*, **1913**, *12*, 283.
- [55] Hartley, G. S. In *Aqueous Solutions of Paraffin Chain Salts*; Hermann & Cie: Paris, 1936.
- [56] Tanford, C. In *The Hydrophobic Effect*, 2nd ed.; Wiley: New York, 1980.
- [57] Lindman, B.; Wennerström, H. *Top. Curr. Chem.* **1980**, *87*, 1.
- [58] Gruen, D. W. *R. Progr. Colloid Polym. Sci.* **1985**, *70*, 6-16.
- [59] Zana, R. In *Surfactant Solutions*; Zana, R., Ed.; Marcel Dekker Inc.: New York, 1987; Chapter 9.
- [60] Van Os, N.M.; Haak, J.R.; Rupert, L.A.M. In *Physico-Chemical Properties of Selected Anionic, Cationic, and Nonionic Surfactants*; Elsevier: Amsterdam, 1993.
- [61] Patist, A.; Kanicky, J. R.; Shukla, P. K.; Shah D. O. *J. Colloid Interface Sci.* **2002**, *245*, 1-15
- [62] Turner, M. S.; Marques, C.; Cates, M. E. *Langmuir* **1993**, *6*, 695.
- [63] Shikata, T.; Sakaigushi, Y.; Urakami, H.; Tamura, A.; Hirata, H. *J. Colloid Interface Sci.* **1987**, *119*, 291.
- [64] Lin, Z.; Scriven, L.E.; Davis, H. T. *Langmuir* **1992**, *8*, 2200.
- [65] Hoffmann, H.; Rehage, H. In *Surfactant Solutions*; Zana, R., Ed.; Marcel Dekker Inc.: New York, 1987; Chapter 4.
- [66] Engberts, J.B.F.N.; Hoekstra, D. *Biochim. Biophys. Acta-Rev. Biomemb.* **1996**, *1241*, 323.
- [67] Nagarajan, R. *Langmuir* **2002**, *18*, 31-38.
- [68] Israelachvili, J.N.; Mitchel, D.J.; Ninham, B.W. *J. Chem. Soc., Faraday Trans. 2* **1976**, *72*, 1525.
- [69] Israelachvili, J.N. In *Intermolecular and Surface Forces*; Academic Press: London, 1994.

- [70] Nagarajan, R.; Ruckenstein, E. In *Equations of State for Fluids and Fluid Mixtures*; Sengers, J.V., Kayser, R.F., Peters, C.J., White Jr., H.J., Eds.; Elsevier: Amsterdam, 2000, Chapter 15.
- [71] Sein, A.; Engberts, J. B. F. N. *Langmuir* **1995**, *11*, 455.
- [72] Laughlin, R.G. In *The Aqueous Phase Behaviour of Surfactants*; Academic Press: London, 1994.
- [73] Chandrasekhar, S. In *Liquid Crystals*; Cambridge University Press: New York, 1992.
- [74] Fontell, K.; Kox, K. K.; Hansson, E. *Mol. Cryst. Liquid Cryst. Letters* **1985**, *1*, 9.
- [75] Fontell, K. *Colloid Polym. Sci.* **1990**, *268*, 264.
- [76] Laschewsky, A. *Tenside Surf. Det.* **2003**, *40*, 246.
- [77] Laschewsky, A. *Adv. Polym. Sci.* **1995**, *124*, 53-59.
- [78] McCullough, D. H.; Janout, V.; Li, J.; Hsu, J. T.; Truong, Q.; Wilusz, E.; Regen, S. L. *J. Am. Chem. Soc.* **2004**, *126*, 9916.
- [79] Masuyama, A.; Yokota, M.; Zhu, Y. P.; Kida, T.; Nakatsuji, Y. *Chem. Commun.* **1994**, 1435.
- [80] Sumida, Y.; Oki, T.; Masuyama, A.; Maekawa, H.; Nishiura, M.; Kida, T.; Nakatsuji, Y.; Ikeda, I.; Nojima, M. *Langmuir* **1998**, *14*, 7450.
- [81] Yoshimura, T.; Kimura, N.; Onitsuka, E.; Shosenji, H.; Esumi, K. *J. Surfactants Deterg.* **2004**, *7*, 67.
- [82] Koide, Y.; Oka, T.; Imamura, A.; Shosenji, H.; Yamada, K. *Bull. Chem. Soc. Jpn.* **1993**, *66*, 2137.
- [83] Sugiyama, K.; Esumi, K.; Koide, Y. *Langmuir* **1996**, *12*, 6006.
- [84] Larpent, C.; Laplace, A.; Zemb, T. *Angew. Chem., Int. Ed.* **2004**, *43*, 3163.
- [85] Kellermann, M.; Bauer, W.; Hirsch, A.; Schade, B.; Ludwig, K.; Böttcher, C. *Angew. Chem. Int. Ed.* **2004**, *43*, 2959-2962.
- [86] Kerckhoffs, J.M.C.A.; van Leeuwen, F.W.B.; Spek, A. L.; Kooijman, H.; Crego-Calama, M.; Reinhoudt, D. N. *Angew. Chem. Int. Ed.* **2003**, *42*, 5717-5722.
- [87] Menger, F. M.; Angel, A. J.; Jaeger, D. A. *Chem. Commun.* **1984**, 546.
- [88] Strobel, M.; Kita-Tokarczyk, K.; Taubert, A.; Vebert, C.; Heiney, P. A.; Chami, M.; Meier, W. *Adv. Funct. Mater.* **2006**, *16*, 252-259.
- [89] Menger, F. M.; Takeshita, M.; Chow, J. F. *J. Am. Chem. Soc.* **1981**, *103*, 5938-5939.
- [90] Murguía, M.C.; Cabrera, M. I.; Guastavino, J. F.; Grau, R. J. *Coll. Surf. A* **2005**, *262*, 1-7.
- [91] In, M. *Surf. Sci. Ser.* **2001**, *100*, 59-110.
- [92] Yan, Y.; Huang, J.; Li, Z.; Zhao, X.; Zhu, B.; Ma, J. *Coll. Surf. A* **2003**, *215*, 263.
- [93] Meguro, K.; Ikeda, K.; Otsuji, A.; Yasuda, M.; Esumi, K. *J. Colloid Interface Sci.* **1987**, *118*, 372.
- [94] Yiv, S.; Kale, K.M.; Lang, R.; Zana, R. *J. Phys. Chem. B* **1976**, *80*, 2651.
- [95] Menger, F.M.; Wrenn, S. *J. Phys. Chem. B* **1974**, *78*, 1387
- [96] Fuhrhop, J.-H.; Wang, T. *Chem. Rev.* **2004**, *104*, 2901-2937.
- [97] Yan, Y.; Xiong, W.; Huang, J.; Li, Z.; Li, X.; Li, N.; Fu, H. *J. Phys. Chem.* **2005**, *109*, 357-364.
- [98] Köhler, K.; Förster, G.; Hauser, A.; Dobner, B.; Heiser, U. F.; Ziethe, F.; Richter, W.; Steiniger, F.; Drechsler, M.; Stettin, H.; Blume, A. *J. Am. Chem Soc.* **2004**, *126*, 16804-13.
- [99] Köhler, K.; Förster, G.; Hauser, A.; Dobner, B.; Heiser, U. F.; Ziethe, F.; Richter, W.; Steiniger, F.; Drechsler, M.; Stettin, H.; Blume, A. *Angew. Chem. Int. Ed.* **2004**, *43*, 245-247.
- [100] Menger, F. M.; Peresykin, A. V. *J. Am. Chem. Soc.* **2001**, *123*, 5614-5615
- [101] FitzGerald, P. A.; Davey, T. W.; Warr, G. G. *Langmuir* **2005**, *21*, 7121-7128.
- [102] Duivenvoorde, F. L.; Freiters, M. C.; van der Gaast, S. J.; Engberts, J. F. B. N. *Langmuir* **1997**, *13*, 3737.
- [103] Zana, R.; Benraou, M.; Rueff, R. *Langmuir* **1991**, *7*, 1072-1075.
- [104] Yoshimura, T.; Ichinokawa, T.; Kaji, M.; Esumi, K. *Coll. Surf. A* **2006**, *273*, 208-212.

- [105] Zana, R. *Adv. Colloid Interface Sci.* **2002**, *97*, 205.
- [106] Esumi, K.; Goino, M.; Koide, Y. *J. Colloid Interface Sci.* **1996**, *183*, 539.
- [107] Esumi, K.; Taguma, K.; Koide, Y. *Langmuir* **1996**, *12*, 4039.
- [108] Esumi, K.; Takeda, Y.; Goino, M.; Ishiduki, K.; Koide, Y. *Langmuir* **1997**, *13*, 2588.
- [109] Yoshimura T.; Yoshida, H.; Ohno, A.; Esumi, K. *J. Colloid Interface Sci.* **2003**, *267*, 167.
- [110] Yoshimura T.; Ohno, A.; Esumi, K. *J. Colloid Interface Sci.* **2004**, *272*, 191.
- [111] Zana, R.; Lévy, H.; Papoutsis, D.; Beinert, G. *Langmuir* **1995**, *11*, 3694.
- [112] Zana, R. *Coll. Surf. A* **1997**, *123-124*, 27-35
- [113] Kim, T. S.; Kida, T.; Nakatsuji, Y.; Ikeda, I. *Langmuir* **1996**, *12*, 6304.
- [114] In, M.; Aguerre-Chariol, O.; Zana, R. *J. Phys. Chem. B* **1999**, *103*, 7747.
- [115] In, M.; Warr, G. G.; Zana, R. *Phys. Rev. Lett.* **1999**, *83*, 2278.
- [116] In, M.; Bec, V.; Aguerre-Chariol, O.; Zana, R. *Langmuir* **2000**, *16*, 141.
- [117] Zana, R. In, M.; Lévy, H.; Duportail, G. *Langmuir* **1997**, *13*, 5552.
- [118] Menger, F.M. Keiper J.S. *Angew. Chem. Int. Ed.* **2000**, *39*, 1906-1920.
- [119] Zana, R. *J. Colloid Interface Sci.* **2002**, *248*, 203-220.
- [120] *Gemini Surfactants: Synthesis, Interfacial and Solution-Phase Behavior, and Applications*, Zana, R. Xia, J. Eds.; Dekker: New York, 2004.
- [121] Danino, D.; Talmon, Y.; Zana, R. *Langmuir* **1995**, *11*, 1448.
- [122] Buhler, E.; Mendes, E.; Boltenhagen, P.; Munch, J. P.; Zana, R.; Candau, S. J. *Langmuir* **1997**, *13*, 3096.
- [123] Weber, V.; Schosseler, F. *Langmuir* **2002**, *18*, 9705.
- [124] Oda, R.; Huc, I.; Candau, S.J. *Angew. Chem. Int. Ed.* **1998**, *37*, 2689-2691.
- [125] Lianos, P.; Lang, J.; Zana, R. *J. Colloid Interface Sci.* **1983**, *91*, 276.
- [126] Kästner, U.; Zana, R. *J. Colloid Interface Sci.* **1999**, *218*, 468.
- [127] Oda, R.; Huc, I.; Schmutz, M.; Candau, S.J.; MacKintosh, F.C. *Nature* **1999**, *399*, 566.
- [128] Rosen, M. J. *Chemtech* **1993**, *23*, 30-33.
- [129] Massi, L.; Guittard, F.; Gèribaldi, S. *Prog. Colloid Polym. Sci.* **2004**, *126*, 190.
- [130] Fisticaro, E.; Compari, C.; Róoycka-Roszak, B.; Viscardi, G.; Quagliotto, P. L. *Curr. Top. Colloid Interface Sci.* **1997**, *2*, 53.
- [131] Lyu, Y.-Y.; Yi, S. H.; Shon, J. K.; Chang, S.; Pu, L. S.; Lee, S.-Y.; Yie, J. E.; Char, K.; Stucky, G. D.; Kim, J. M. *J. Am. Chem. Soc.* **2004**, *126*, 2310-2311.
- [132] Kresge, C. T.; Leonowicz, M. E.; Roth, W. J.; Vartuli, J. C.; Beck, J. S. *Nature* **1992**, *359*, 710-712.
- [133] Van Der Voort, P.; Mathieu, M.; Mees, F.; Vansant, E. F. *J. Phys. Chem. B* **1998**, *102*, 8847.
- [134] Esumi, K.; Hara, J.; Aihara, N.; Usui, K. Torigoe, K. *J. Colloid Interface Sci.* **1998**, *208*, 578.
- [135] Sato, S.; Asai, N.; Yonese, M. *Colloid Polym. Sci.* **1996**, *274*, 889.
- [136] Sato, S.; Yoda, T.; Oniki, S. *J. Colloid Interface Sci.* **1999**, *218*, 504.
- [137] Tieke, B.; Dreja, M. *Langmuir* **1998**, *14*, 800-807.
- [138] Rabinovich, Y. I.; Kanicky, J. R.; Pandey, S.; Oskarsson, H.; Holmberg, K.; Moudgil, B. M.; Shah, D. O. *J. Colloid Interface Sci.* **2005**, *288*, 583-590.
- [139] Sharma, V.; Borse, M.; Jauhari, S.; Pai, K. B.; Devi, S. *Tenside Surf. Det.* **2005**, *42*, 163-167.
- [140] Qiu, L.-G.; Xie, A.-J.; Shen, Y.-H. *Corrosion Science* **2005**, *47*, 273-278.
- [141] Chen, H.; Han, L.; Luo, P.; Ye, Z. *J. Colloid Interface Sci.* **2005**, *285*, 872-874.
- [142] Bi, Z. C.; Qi, L. Y.; Liao, W. S. *J. Mat. Sci.* **2005**, *40*, 2783-2788.

- [143] Rosen, M. J.; Li, F. *J. Colloid Interface Sci.* **2001**, *234*, 418-424.
- [144] Bunton, C. A.; Robinson, L.; Schaak, J.; Stam, M. F. *J. Org. Chem.* **1971**, *36*, 2346.
- [145] Brinchi, L.; Germani, R.; Goracci, L.; Savelli, G.; Bunton, C. A. *Langmuir* **2002**, *18*, 7837.
- [146] Bhattacharya, S.; Kumar, V. P. *Langmuir* **2005**, *21*, 71-78.
- [147] Cerichelli, G.; Luchetti, L.; Mancini, G.; Savelli, G. *Langmuir* **1999**, *15*, 2631.
- [148] Qiu, L.-G.; Xie, A.-J.; Shen, Y.-H. *Colloid Polym. Sci.* **2005**, *283*, 1343-1348.
- [149] McGregor, C.; Perrin, C.; Monck, M.; Camilleri, P.; Kirby, A. J. *J. Am. Chem. Soc.* **2001**, *123*, 6215.
- [150] Dauty, E.; Remy, J.-S.; Blessing, T.; Behr, J.-P. *J. Am. Chem. Soc.* **2001**, *123*, 9227.
- [151] Ronsin, G.; Perrin, C.; Guédât, P.; Kremer, A.; Camilleri, P.; Kirby, A. J. *Chem. Commun.* **2001**, 2234.
- [152] Jennings, K. H.; Marshall, I. C. B.; Wilkinson, M. J.; Kremer, A.; Kirby, A. J.; Camilleri, P.; *Langmuir* **2002**, *18*, 2426.
- [153] Kirby, A. J.; Camilleri, P.; Engberts, J. B. F. N.; Feiters, M. C.; Nolte, R. J. M.; Södermann, O.; Bergsma, M.; Bell, P. C.; Fielden, M. L.; Rodriguez, C. L. G.; Guédât, P.; Kremer, A.; McGregor, C.; Perrin, C.; Ronsin, G.; van Eijk, M. C. P. *Angew. Chem. Int. Ed.* **2003**, *42*, 1448.
- [154] Bell, P. C.; Bergsma, M.; Dolbnya, I. P.; Bras, W.; Stuart, M. C. A.; Rowan, A. E.; Feiters, M. C.; Engberts, J. B. F. N. *J. Am. Chem. Soc.* **2003**, *125*, 1551-1558.
- [155] Dauty, E.; Behr, J.-P. *Polym. Int.* **2003**, *52*, 459-464.
- [156] Badea, I.; Verrall, R.; Baca-Estrada, M.; Tikoo, S.; Rosenberg, A.; Kumar, P.; Foldvari, M. *J. Gene Med.* **2005**, *7*, 1200-1214.
- [157] Bombelli, C.; Borocci, S.; Diociaiuti, M.; Faggioli, F.; Galantini, L.; Luciani, P.; Mancini, G.; Sacco, M. G. *Langmuir* **2005**, *21*, 10271-10274.
- [158] Säily, V. M. J.; Ryhänen, S. J.; Lankinen, H.; Luciani, P.; Mancini, G.; Parry, M. J.; Kinnunen, P. K. J. *Langmuir* **2006**, *22*, 956-962, and references therein.
- [159] Chen, J.; Yang, F.; Ji, G.-Z.; Yang, H.; Shen, Z.-W.; Zhou, X.-J. *Langmuir* **2005**, *21*, 10931.
- [160] Lehmann, K.; Hinrichs, P.; Maslek, S. *Eur. Coatings J.* **2004**, *5*, 32-36.
- [161] Galgocsi, E. C.; Chan, S. Y.; Yacoub, K. *J. Coatings Techn. Res.* **2006**, *3*, 77.
- [162] Han, F.; Zhang, G. *J. Surf. Det.* **2004**, *7*, 175.
- [163] Helbig, C.; Baldauf, H.; Lange, T.; Neumann, R.; Pollex, R.; Weber, E. *Tenside Surf. Det.* **1999**, *36*, 58.
- [164] Masuyama, A.; Endo, C.; Takeda, S.; Nojima, M.; Ono, D.; Takeda, T. *Langmuir* **2000**, *15*, 368.
- [165] van Zon, A.; Bouman, J. T.; Deuling, H. H.; Karaborni, D. S.; Karthaeuser, J.; Mensen, H. T. G. A.; van Os, N. M.; Raney, K. H. *Tenside Surf. Det.* **1999**, *36*, 84-86.
- [166] Maiti, P. K.; Lansac, Y.; Glaser, M. A.; Clark, N. A.; Rouault, Y. *Langmuir* **2002**, *18*, 1908.
- [167] Abdel-Rahem, R.; Gradzielski, M.; Hoffmann H. *J. Colloid Interface Sci.* **2005**, *288*, 570-582 and references therein.

2. NEW SERIES OF SURFACTANT OLIGOMERS

The surfactant structures used in this work, namely series of cationic surfactant oligomers and an anionic surfactant dimer, will be described in the following chapter.

2.1 Choice of model cationic surfactants

2.1.1 Presentation of the structures

Several series of model cationic surfactant oligomers, from dimers to tetramers, with various spacer groups were recently synthesized [1-3] (see synthesis below). On Figure 2.1-1, the architecture of these oligomers is represented, as well as the different spacer groups involved.

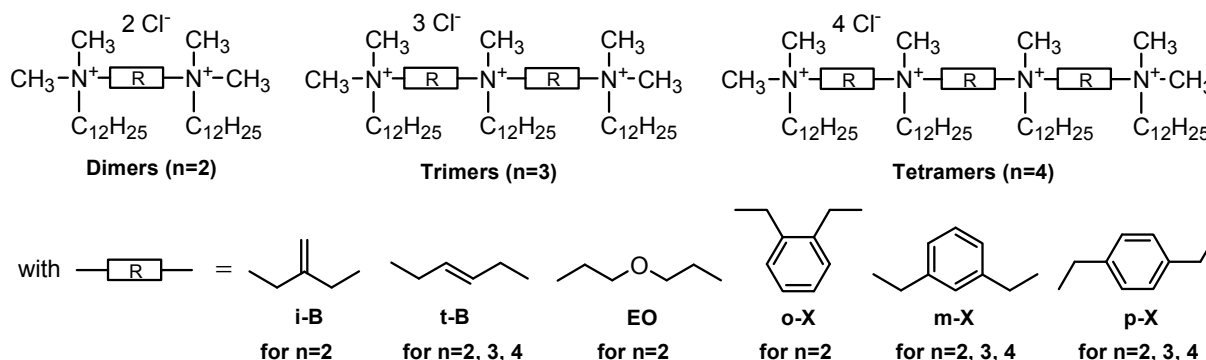


Figure 2.1-1: Structures of oligomeric surfactant with various spacer groups (n = degree of oligomerization).

These amphiphiles are derived from the parent compounds dodecyltrimethylammonium chloride **DTAC**, or benzyldodecyltrimethylammonium chloride **BDDAC**, respectively. The complete sets of chemical structures (and corresponding abbreviations) of the surfactants used throughout this work are depicted in Appendix 11.

Cationic surfactants were primarily chosen since well-defined series of such compounds are presumably more accessible for systematic studies [4]. Indeed, the reaction of alkylation (reaction of Menshutkin [5]) can be well controlled and hence allows a strict control of the degree of oligomerization of such ionenes. As regards the surfactant structural parameters, dodecyl chains were preferred as they are sufficiently hydrophobic to confer good surfactant properties to these compounds [6], while maintaining a good water solubility (short enough to expect water-soluble higher oligomers). The solubility of these cationic surfactants in water is further enhanced by employing chloride counter-ions (lower Krafft temperatures) [2], instead of the mostly used bromide [7] (ammonium bromide derivatives are easier to synthesize).

The series with different spacer groups between the surfactant fragments were selected, because the nature and the length of the spacer group linking the individual surfactant fragments together have been shown to be of major importance in the case of dimeric surfactants [2, 4, 7-9], in addition to the chemical nature of the hydrophilic group and of the hydrophobic chain of the surfactant fragment. Accordingly, it is expected that the spacer group exerts an important influence on the behavior of higher oligomeric surfactants, too.

Also, the spacer groups employed, namely iso-butenylene (**i-B**), trans-1,4-buten-2-ylene (**t-B**), o-xylylene (**o-X**), m-xylylene (**m-X**), and p-xylylene (**p-X**), can be considered as rigid, thus strictly fixing chemically the distance between the cationic groups within the same molecule. Noteworthy, most reports on the influence of the spacer group have been concentrated on the class of alkanediyl- α,ω -bis(dimethylalkylammonium bromide)s, i.e. geminis characterized by flexible alkyl segments as spacer groups [4, 8, 10-21]. Accordingly, the variation of the spacer length has gone mostly along with a change in its hydrophobic character, thus rendering it difficult to distinguish between architectural and compositional effects on the surfactant properties. In the present study, sets of isomeric compounds (see e.g. geminis with spacers **i-B** and **t-B**, and with spacers **o-X**, **m-X**, **p-X** on Figure 2.1-1) will be compared in order to keep the hydrophobicity of the spacer groups almost constant and only change the spacer length.

In addition, the spacer length was varied between C₃ and C₆, because the most pronounced changes in properties have been found in this range [4, 8]. The dimeric surfactant **EO-2** [22] with a very flexible diethyleneglycol spacer group was included in the study, for comparison.

2.1.2 Synthesis routes [1-3]

For systematic and reliable studies, high-purity surfactants are needed. The cationic oligomeric compounds were initially synthesized by R. Rakotoaly (PhD thesis [1]). The synthesis procedures developed for the dimers and the higher oligomers can be found in references [2] and [3], respectively. The dimeric compounds can be synthesized rather easily in large amounts. The higher oligomers, which are exotic structures so far, present more difficulties in their synthesis and purifications [1]. Hence, studies which consume much material were limited to the series of dimeric surfactants. The syntheses of larger amounts of the various dimeric surfactants were repeated whenever necessary in order to provide supplementary material for the determination of the property profile of these compounds and study their mixtures with numerous additives (see chapters 3 and 4).

Hereafter, a few remarks concerning the synthesis and purification of the series of cationic surfactant oligomers will be made.

The dimeric surfactants abbreviated **i-B-2**, **t-B-2**, **o-X-2**, **m-X-2**, **p-X-2** and **EO-2** are synthesized by alkylating an excess of N,N-dimethyldodecylamine by the appropriate dichloro

compound, as depicted on Figure 2.1-2. Though chlorides are often somewhat sluggish as alkylating agents, reactions proceeded smoothly even under mild conditions as the chlorines are activated in the reagents employed towards nucleophilic substitution by their allylic, or benzylic position, respectively, or by the ether moiety in β -position. Synthesis of the surfactants by this strategy was thus straightforward. The synthetic procedures and analyses of the dimeric surfactants that were resynthesized during this PhD work are described in more details in Appendix 1.

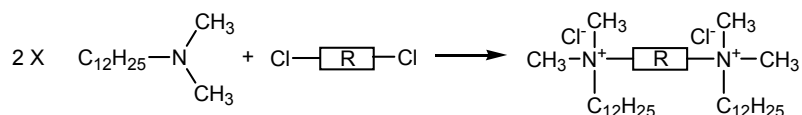


Figure 2.1-2: Scheme of reaction to synthesize the dimeric surfactants.

In agreement with the ease of alkylation, the thermal retro-alkylation is facilitated, too. The sterically somewhat congested dimers **i-B-2** and **o-X-2** decompose according the thermogravimetric analysis already above 160 °C, whereas decomposition starts for dimers **t-B-2** and **m-X-2** at 210 °C, and for dimers **EO-2** and **p-X-2** at about 220 °C only (cf. Ph.D. thesis of R. Rakotoaly [1]). Due to the thermal sensitivity, efficient and rigorous drying of the hygroscopic surfactants is difficult.

Advantageously, the dimers can be separated from the educts and monoalkylated by-products by recrystallization, e.g. from acetone (except for **o-X-2**). The surfactants were purified by repeated crystallization until no impurities could be detected by thin layer chromatography (TLC) or by NMR-spectroscopy [1]. When necessary, the stock surfactants were purified again before use. Still, the minimum in the surface tension vs. concentration curves of compound **o-X-2** (see chapter 3) indicates the presence of some strongly surface-active trace impurity that could not be removed. Putatively, this may be due to a slow hydrolytic decomposition of the compound, which is sensitive to nucleophilic attack as reflected in the low thermal stability.

The synthesis pathway towards the trimeric and tetrameric surfactants listed in Appendix 11 is schemed out in Figure 2.1-3 [1]. The complete procedures are detailed in the literature [3]. In the case of the trimers, N-methyldodecylamine is alkylated twice by a reactive quaternary ammonium surfactant that was prepared as intermediate. In the case of the tetramers, a symmetric tertiary diamine with two dodecyl chains is prepared first, which is subsequently alkylated twice by the reactive quaternary ammonium surfactant. This synthesis route to tri- and tetrameric surfactants enables molecular designs independent of the limited availability of tri- and tetramines as starting compounds. Also, this particular modular scheme was applied by R. Rakotoaly [1], as the intermediates show still sufficiently different property profiles to enable efficient purification by crystallization or precipitation. Certain properties of surfactants, such as their surface activity (cf chapter 3), are extremely sensitive to even small amounts of impurities. In fact, purification of the oligomeric surfactants by preparative column chromatography, which is most effective for simple model

surfactants, failed due to the multiple strong ionic and hydrophobic interactions of the compounds on normal phase as well as reversed phase stationary phases. Also, distillation and extraction with water/organic solvent are excluded because of the too high molar mass and the emulsifying ability of these surfactants, respectively. Hence, crystallization and dissolution/ precipitation cycles are the purification techniques of choice for such molecules. The surfactant trimers and tetramers obtained by the presented strategy were pure according to $^1\text{H-NMR}$, and devoid of the intermediate reagents according to TLC (see 5.3)

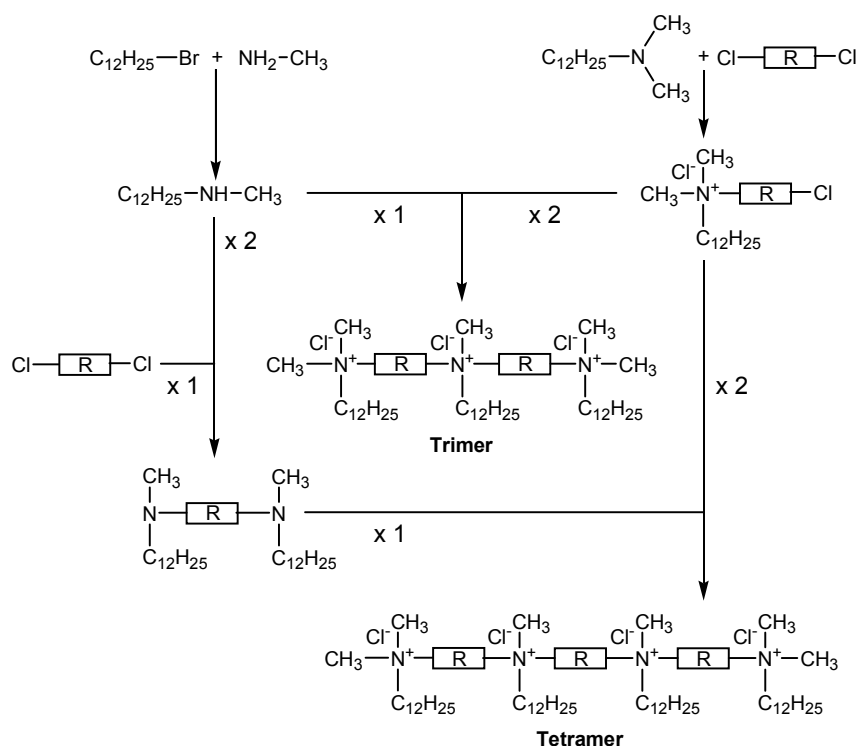


Figure 2.1-3: Synthetic routes to trimeric and tetrameric surfactants (with R = spacer group). Routes applied by R. Rakotoaly [1].

2.1.3 Basic properties previously determined [1-3]

The model surfactants presented above were formerly subject to some preliminary studies regarding some basic properties (see PhD thesis of R. Rakotoaly [1]). For all oligomers, the properties such as the foaming and solubilization of hydrophobic probes sensitively depend on the spacer group used [2] and degree of oligomerization [3]. Shorter spacer groups give rise to more stable foams and slightly higher solubilization capacities (in analogy to the reports of Dreja et al. and Dam et al. [23-24]), for a given degree of oligomerization [2-3]. Moreover, the evolution of the properties observed from standard to dimeric surfactants progresses with the trimers and tetramers, for a given spacer group [3]. In other words, for a fixed spacer group, the foam stability and the solubilization capacity (to a lesser extent) increase with the degree of oligomerization. Furthermore, for all the studied oligomeric surfactants the viscosifying effects are similarly small up to concentrations much above the

CMC. This observation suggests the absence of large aggregates. Hence, it differs from the general theoretical predictions made for oligomeric surfactants [25] and confirms that the thickening power of certain oligomeric surfactants is restricted to molecular structures with very short flexible spacer groups (namely C₂ or C₃) [26] (see chapter 1, part 1.2.2.c).

In the following section, a novel anionic surfactant dimer will be presented in detail (background, description and justification of the chosen system, synthesis and analysis).

2.2 Novel anionic gemini surfactant

2.2.1 Background and motivation

Most reports on gemini surfactants are related to cationic ones, namely to the family of alkanediyl- α,ω -bis(dimethylalkylammonium bromide)s. As already clarified before, the synthesis of bisquaternary ammonium surfactants often proceeds in a one pot reaction. In contrast, the synthesis of anionic surfactants is usually more complex. Therefore, systematic studies on such surfactants have been limited so far. Few anionic geminis such as sulfate [27-30] and phosphate [30-34] were synthesized and their properties such as CMC, surface tension, foaming and wetting abilities investigated. Pyrophosphate-based gemini surfactants were also described in the literature [35], as well as a peptide-based sulfonate dimeric surfactant (synthesized in five steps) [36]. A method for producing sulfonate geminis is to react a diepoxide with a long chain alcohol and subsequently convert the bis-diol to a propylsulfonic acid followed by alkali (see Figure 2.2-1.a) [27, 37]. Also, gemini surfactants can be efficiently prepared from 2-hydroxy-1-alkanesulfonates by coupling via a diester (transesterification) (see Figure 2.2-1.b) [38]. In another strategy, fatty acid methyl esters were reacted with sulphur trioxide resulting in α -sulfo fatty acid methyl esters, which can be transesterified with e.g. ethylene glycol to obtain a dimeric structure (see Figure 2.2-1.c) [39]. Other sulfonate geminis such as didodecyldiphenylether disulfonate, which are also commercial products, were studied in microemulsions [40]. Very recently, sulfonate gemini surfactants based on nonylphenol with varied alkyl spacer length were synthesized (see Figure 2.2-1.d), following a two-step procedure [41]. Also, a new family of dialkylaryl disulfonate geminis (see Figure 2.2-1.e) was synthesized in a single-step route using α -olefin sulfonic acid [42]. In this case, the sulfonyl group is attached to the alkyl chain (and not to the aromatic groups as usual) which confers additional interests (biodegradability, lower skin irritability, etc.) compared to true alkylbenzene sulfonate [43]. Besides, a series of homologous anionic gemini surface-active azo-initiators (see Figure 2.2-2.a) were prepared in one step by Ritter reaction. The latter sulfonate compounds are potentially useful in emulsion polymerizations as both initiators and emulsifiers (so-called "INISURFs") [44].

In addition, there are examples of gemini surfactants with carboxylate head groups [45-53]. *N*-acylated sarcosinate fragments covalently linked by a short ethyl spacer between the amide nitrogen (see Figure 2.2-1.f) gave gemini surfactants acting as effective flotative agents [45]. A simpler route to anionic geminis was also developed [47-49], involving the reaction of a diamine with 2-dodecen-1-ylsuccinic anhydride and subsequent neutralization. Nevertheless, this synthesis gives a mixture of regioisomers (see Figure 2.2-1.g). More recently, anionic dimers alkanediyl- α,ω -bis(sodium *N*-acyl- β -alaninates), $(\text{CH}_2)_m\text{-}\alpha,\omega\text{-[NCO(C}_n\text{H}_{2n+1}),\text{C}_2\text{H}_4\text{CO}_2\text{Na}]_2$ were described (see Figure 2.2-1.h) [51, 53]. For instance, sodium-1,2-bis(*N*-dodecanoyl-alaninate)-*N*-ethane was compared to corresponding monomeric surfactant in water, water-oil systems and microemulsions [54] and in water with added salts [51-53]. A new series of anionic gemini surfactant homologues (presenting some similarities with the amphiphiles described in [51]), namely 1,2-bis (*N*- β -carboxypropanoyl-*N*-alkylamino)ethane $(\text{CH}_2)_2[\text{N}(\text{C}_n\text{H}_{2n+1}),\text{COC}_2\text{H}_4\text{CO}_2\text{Na}]_2$ (see Figure 2.2-1.i), were synthesized by three-step reactions and their physicochemical properties investigated [50].

As for cationics, anionic surfactant dimers exhibit in general enhanced properties compared to their monomeric analogues.

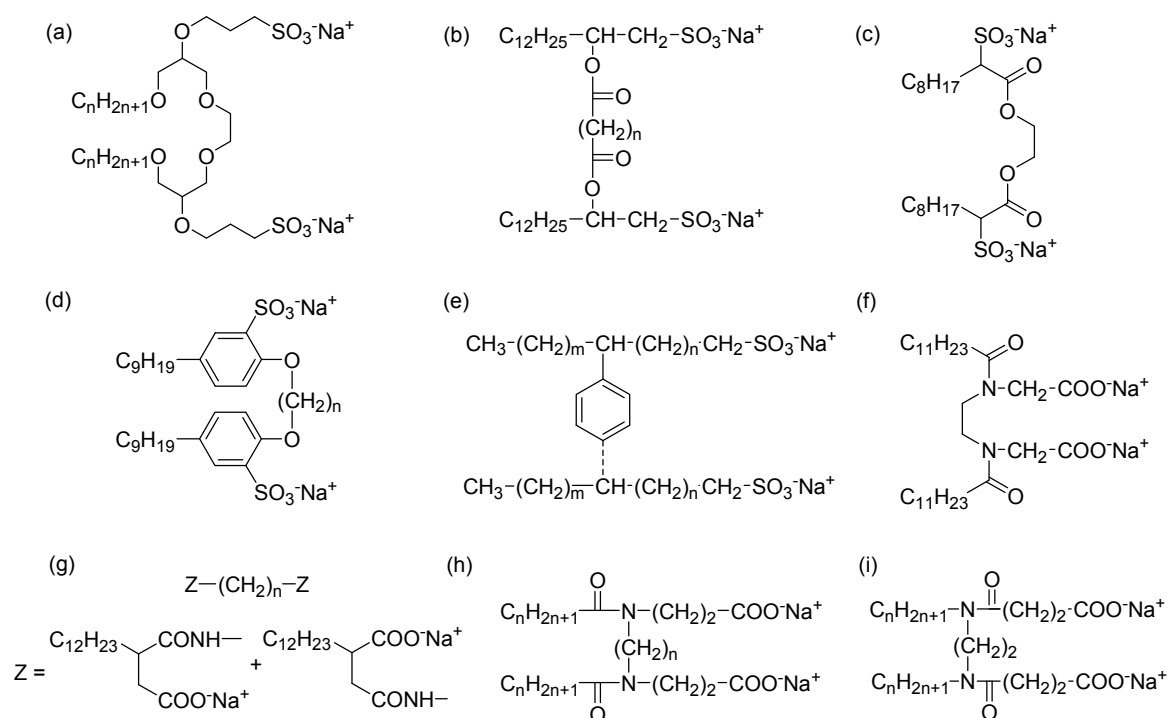


Figure 2.2-1: Examples of anionic dimeric surfactants from the literature: (a) [27]; (b) [38]; (c) [39]; (d) [41]; (e) [42]; (f) [45]; (g) [47]; (h) [51]; (i) [50].

Noteworthy, previous reports [55-56] described carboxylic dimeric structures cleavable at the level of the spacer group, in analogy to the sulfonate “Inisurfs” addressed above (see Figure 2.2-2.a) [44]. For example, amphiphilic 1,2-diazenes (see Figure 2.2-2.b) were tested as free radical initiators in lipid bilayers [55]. Another study presented a cystine-derivative with fluorocarbon chains

(see Figure 2.2-2.c) [56]. Such a compound can be mixed with polymerizable lipids to prepare liposomes with a phase-separated membrane (due to the perfluorinated chains). After UV-polymerization of the butadiene containing lipids, stable vesicles are obtained (polymerized and compartmented). Subsequent treatment of these liposomes with reductive agents leads to the cleavage of the disulfide structure (Figure 2.2-2.c) and the formation of water-soluble lysolipids that are pulled out of the membrane, leaving holes in the liposomes. This is obviously interesting for the release of entrapped materials from vesicles. Here, it is relevant to note that a similar strategy, i.e. the use of a chemically cleavable disulfide bridge as a spacer group, was recently applied for cationic lipids acting as nonviral transfecting agents. The reduction of the spacer (and subsequent cleavage of the cationic gemini into two parts) permits to overcome the poor release of DNA from lipoplexes [57]. Other bis(carboxylate) type gemini surfactants bearing cleavable carbon-carbon double bonds either in the spacer group (see Figure 2.2-2.d) or in the hydrophobic chain were more recently synthesized with unsaturated diglycidyl ether [58] by the same method as in reference [27] evoked above. These chemical structures can be cleaved by ozonolysis of the alkenes, giving candidates for environmentally friendly surfactants [37]. Note that this feature may also be interesting for the studied cationic surfactant dimers **i-B-2** and **t-B-2** having butenylen spacer groups.

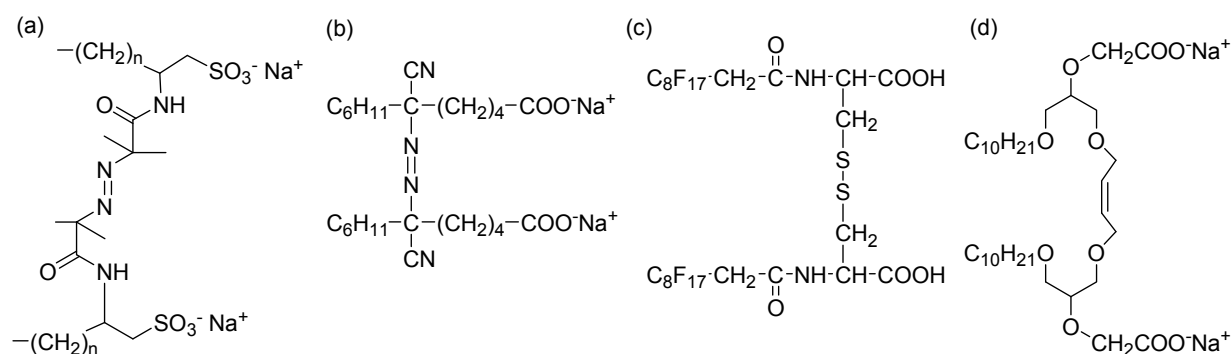


Figure 2.2-2: Examples of cleavable anionic dimeric surfactants. Thermally cleavable: (a) sulfonate “inisurf” [44]; (b) amphipathic 1,2 diazene [55]. Chemically cleavable: (c) cystine-derived gemini [56]; (d) double-bond containing dimer [58].

As addressed in the introduction, this work was intended to study the effect of additives on the behaviour of the cationic dimeric surfactants presented in part 2.1.1. Therefore, it was interesting to study not only a standard anionic surfactant but also an anionic dimeric surfactant in mixtures with these cationic dimers. Possibly, some remarkable effects can be induced on the solution properties by such combinations of oppositely-charged gemini surfactants (cf. chapter 4). As the synthesis of the known anionic dimeric surfactants is rather complicated (*vide supra*), an alternative, more accessible structure was aimed at. Accordingly, a straightforward synthetic route was designed to synthesize such a dimer, contrasting with most pathways towards the anionic structures exposed just before.

Hereafter, the synthesis of the novel anionic dimer is presented and the choice of the strategy and reagents justified. Also, as for the series of cationic dimers, the fundamental properties and behaviour of this compound will be examined and discussed with respect to the state-of-the-art on anionic geminis (cf. chapter 3).

2.2.2 Synthesis of “dimer EDTA”

A straightforward synthesis addressed above consists in opening an anhydride with a diamine to reach a mixture of carboxylate dimeric regioisomers [47]. In this work, an analogous strategy will be applied (i.e. reaction of an amine with a carboxylic anhydride), but here a symmetric dianhydride will be reacted with a simple secondary fatty amine to obtain a novel carboxylate gemini surfactant, without the drawbacks of regioselectivity involved in [47] for example. Moreover, tetracid dianhydrides may be more accessible than diamines, which presents an additional interest compared to the route followed in [47]. The synthesis route toward the target compound is illustrated in Figure 2.2-3.

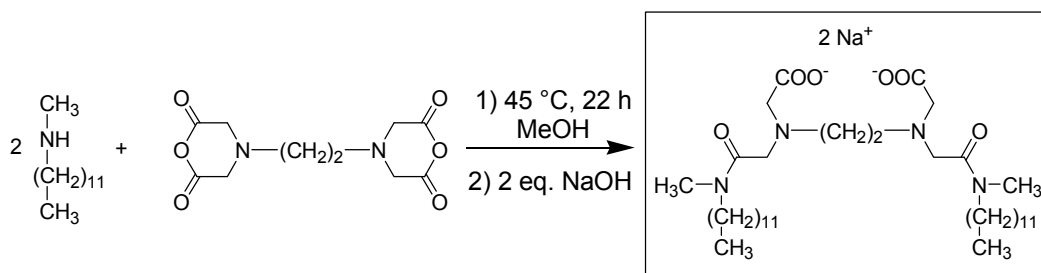


Figure 2.2-3: Scheme for the synthesis of the dimeric surfactant based on EDTA.

The synthesis involves N-methyldodecylamine and ethylene diamine tetraacetic acid dianhydride (EDTA-dianhydride) as reagents. The amine can be either synthesized in a first step, as described in Appendix 2 or can be purchased for a fair price. EDTA-dianhydride is also commercially available and relatively inexpensive, hence making the proposed synthesis attractive. The synthesis procedure is more precisely developed in the experimental part (see part 5.4). The reaction proceeds under mild conditions and is rather effective (note that the yield was not optimized).

Dodecylmethylamine was selected (instead of e.g. a primary dodecylamine) since the formed tertiary amides allow an increase of the hydrophilicity accompanied by a decrease of the Krafft temperature.

It is clear that the chosen system has model character. The synthetic concept can be easily extended to other types of amines (e.g. longer alkylmethylamine or dialkylamine) and dianhydrides, thus modifying widely the hydrophobic tail and spacer group of the formed dimeric surfactant, respectively.

2.2.3 Characterization of “dimer EDTA”

The values and graphs obtained from the analysis of the new anionic dimer are presented in more detail in the experimental part (see 5.4) as well as in Appendix 3.

2.2.3.a. NMR, IR, Mass Spectroscopy and Elemental Analysis

From all analyses performed on both acidic and neutralized form of the compound, it can be concluded that the aspired product was synthesized.

Various analyses were performed on the compound before neutralization (i.e. in its acidic form). First, the absence of free amine in the product was checked by thin layer chromatography (see 5.4). Elemental analysis shows that the content of C, N and H atoms in the product is consistent with the one for the proposed chemical structure, since the found weight percentage for each atom coincides with the calculated one within experimental errors. Mass spectrometry corroborates this result as the right molar mass peak was found (see 5.4). Also, the fragments generated from the product are consistent with the expected structure.

IR spectroscopy confirmed that the formation of the amide was successful (see Appendix 3 Figure A3-7). The band at 1656 cm^{-1} is characteristic for the tertiary amide $-\text{CO}-\text{N}(\text{CH}_3)-\text{CH}_2$ group. Moreover, comparing the spectra obtained for the product and for the dianhydride (see Appendix 3 Figure A3-8), one can see the absence of the bands at ca. 1808 cm^{-1} and 1758 cm^{-1} in the product. These two bands are characteristic for the six membered cyclic anhydride used. Hence, the product is free of the starting anhydride.

The ^1H -NMR spectra of the dimer EDTA (neutralized) are difficult to interpret since many peaks are overlapping (either in CDCl_3 or in D_2O , see Figures A3-1 and A3-2 in Appendix 3). Nevertheless, the main peaks as well as the integrals can be determined (cf. Experimental part 5.4). It should be emphasized that the ^1H NMR spectrum of the neutralized compound measured in CDCl_3 (see Figure A3-1) is sufficient to confirm the chemical structure of the new gemini surfactant and its purity. From the integrals, it is notable that the total number of protons in the sample is in agreement with that in the chemical formula of the expected product. As regards the spectrum of dimer EDTA (anionic form) in chloroform (see Figure A3-1 in Appendix 3), the triplet at 0.88 ppm is characteristic for the protons of the terminal methyl groups at the end of the hydrophobic chains. Also, multiplets at 1.17-1.37 ppm and 1.53 ppm correspond to the nine methylene groups comprised in each hydrophobic tail and to the methylene in beta-position of the amide group, respectively. Additionally, the CH_2 protons of the spacer group appear as a multiplet at 2.39 ppm. Moreover, another characteristic peak appears as a singlet at 2.92 ppm and can be assigned to the CH_3 -groups of the amides. From 2.95 ppm to 3.35 ppm, peaks overlap, resulting in a broad multiplet. Still, the overall integral of this multiplet

permits to confirm the presence of the 12 remaining protons, i.e. three couples of CH₂, respectively in alpha position of the amide, between the amide and the nitrogen of the spacer and in alpha position of the carboxylate. The spectrum does not present additional peaks, hence confirming the purity of the product.

When the measurement conditions are modified, the NMR spectra might become very complicated, for reasons that will be discussed hereafter. Comparing the ¹H NMR spectra in CDCl₃ and D₂O, it is notable that the peak at 0.88 ppm corresponding to the terminal CH₃ of the dodecyl chains is broadened in D₂O. This can be explained by the fact that the measurement is performed at a surfactant concentration above the critical micellization concentration (CMC) and that the exchange rate between molecularly dissolved surfactants and surfactants associated in micelles is slowed down for dimeric compounds [10, 59-62]. Also, it is notable that the peak corresponding to the protons of the spacer group (N-CH₂CH₂-N) at 2.4 ppm becomes broadened and presents somewhat a more complex shape. This observation can be accounted for by the conformations taken by the tertiary amides (cis or trans relative to the oxygen atom). Indeed, for tertiary alkylamides with two different N-substituents, two signals are often observed for the two conformers (see Figure 2.2-4), as the rotation around the CO-N bond is generally slow on the NMR time scale [63]. This effect seems more pronounced in water than in chloroform.

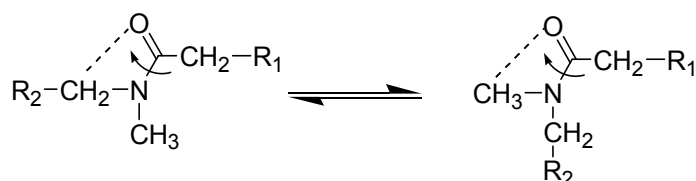


Figure 2.2-4: Trans-cis conformer equilibrium for one tertiary amide of dimer EDTA.

Furthermore, the various possible conformations of the tertiary amides (for the gemini, it means cis-cis, trans-trans and cis-trans) should also render the spectrum more complex for the other protons in the proximity of the amides. This is in fact the case as seen by the structures of the peaks above 2 ppm (see ¹H NMR spectrum of the neutralized surfactant in D₂O at pH 11 on Figure A3-2).

The same reason, namely the presence of different conformers in solution, can be addressed to try a clarification of the ¹³C NMR spectrum of the neutralized compound in CDCl₃, on which additional peaks are found (cf. Figure A3-3 in Appendix 3). With solvent CDCl₃, it seems that the effect of conformers is more visible on the ¹³C NMR spectrum than on the ¹H NMR spectrum.

The ¹H-NMR spectrum of the dimer in its acidic form in chloroform looks at first sight more defined than that of the anionic form, since the peaks above 2.8 ppm are better resolved (see Figure A3-4 in Appendix 3). Nevertheless, assigning exactly each proton or group of protons to each peak of this spectrum remains a complex issue, again due to conformer effects along with chiral effects

induced by protonation of the amines. The expected surfactant structure is a double zwitterion (see next part, acid-base titration), which is coherent with the deshielding observed for the protons in alpha position of the amines, compared to the previous spectra (Figures A3-1 and A3-2). For example, the multiplet found at 2.39 ppm for the neutralized dimer (corresponding to the protons comprised in the ethylene spacer) is strongly shifted to lower fields in the spectrum of the acidic form. Also, it appears in the form of two multiplets (2H + 2H) at 3.17 ppm and 3.34 ppm. In fact, the amines become chiral due to the protonation and therefore the two protons in alpha position of the amine are no longer equivalent, involving presumably two different signals of similar chemical shifts (with their couplings).

The peaks relative to the hydrophobic chain are found below 2 ppm as for the spectrum of the anionic form. Also, the peak for the CH₂ in alpha position of the amide (2H from each chain) is now discernable as a multiplet at 3.02 ppm. Noteworthy, the integrals give the expected number of protons.

In an attempt to assign more precisely the peaks, 2D NMR measurements of the acidic form in CDCl₃ were performed, showing the coupling C-H (see Figure A3-6 in Appendix 3). Still, the method is not sufficient to assign the protons unambiguously to corresponding peaks. Additional NMR methods are necessary (e.g. selective decoupling experiments) in order to definitely attribute the peaks, if needed.

2.2.3.b. Acid-base titration

Titration of the anionic dimer was performed in order to determine the different species present in solution as a function of the pH. These results will be useful for the discussion of the surface tension measurements, especially when performed with the anionic form of “**dimer EDTA**” at pH = 7-8 (see next chapter). The related titration curve can be seen in Figure 2.2-5 hereafter. The experiment is described in part 5.5 and added volumes of HCl and pH values for the equivalent points found are listed in Table 5.5-1 of the experimental part.

The derivative of the titration curve exhibit three maxima corresponding to three equivalent points (see Figure 2.2-5). The first equivalent point in this titration process (E₀) corresponds to the neutralization of the excess sodium hydroxide added before the titration to change the dimer from its acidic to its anionic form. The number of moles of HCl necessary to neutralize the NaOH excess reasonably coincides with the calculated one, assuming that the dimeric structure before neutralization (with MW = 654.94 g/mol) was actually obtained from the reaction presented above. As shown by the calculations in part 5.5, the second equivalent point E₁ at pH = 8.51 corresponds to the addition of one equivalent proton to the anionic dimer. In this case, it can be assumed that the protonation of one

tertiary amine takes place, as a tertiary amine is more basic than a carboxylate. The third equivalent point E_2 at $\text{pH} = 4.98$ refers logically to the protonation of the second amine of the spacer group. The different equilibria involved in the titration are represented in Figure 2.2-6.

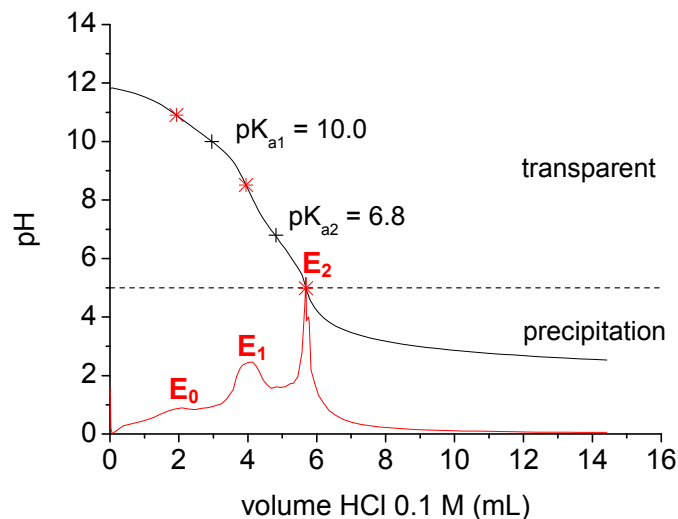


Figure 2.2-5: Titration curve by addition of HCl (0.1 M) to dimer EDTA previously neutralized with a known excess of NaOH (black curve) and its derivative (red curve) giving the equivalent points ($E_0 - E_2$). The dotted line indicates a visual change in the aspect of the solution (from transparent to turbid).

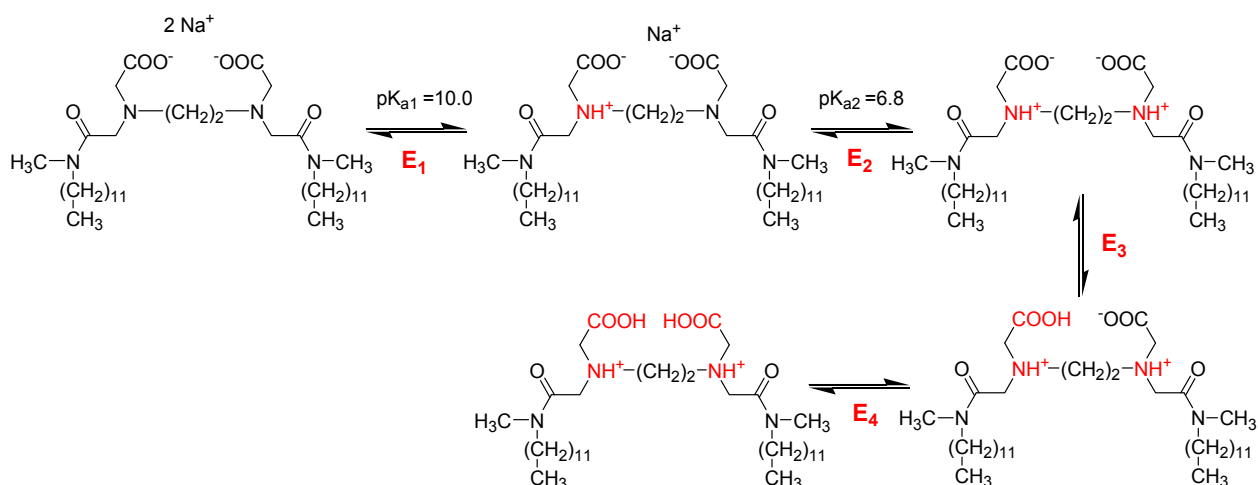


Figure 2.2-6: Hypothetical transitions occurring during the titration of anionic dimer with HCl.

From the titration data, the protonation constant pK_{a1} and pK_{a2} can be calculated using the following relation:

$$\text{pK}_a = \text{pH} + \log \left(\frac{[\text{base}]}{[\text{acid}]} \right) \quad \text{Equation 2.2-1}$$

with $\text{pK}_a = \text{pH}$ at the half equivalence. pK_{a1} and pK_{a2} were found to be **10.0** and **6.8**, respectively (see Figure 2.2-5), which is much higher than the pK_a values obtained for carboxylic acid based surfactants

(see e.g. ref. [64]). Hence, this indirectly corroborates that the protonation takes place on the amines of the compounds (and not on the carboxylates).

The product precipitates in the neutral form (below pH values of 5, see Figure 2.2-5), as may be expected for such a zwitterion. No redissolution of the compound was observed at lower pH.

Assumingly, further addition of HCl (i.e. further protonation) could result in a positively charged compound as depicted in the second range of Figure 2.2-6. Hence, the solubility of the product is likely to be recovered. Nevertheless, equivalent points E_3 and E_4 presumed on the scheme were not observed experimentally. The final pH of the titration is ca. 2.5, and it is supposed that these transitions might occur below this pH, in analogy to the compound $(\text{CH}_3)_3\text{N}^+-\text{CH}_2-\text{COOH}$ ($\text{pH}_e \cong 1.8$).

Other attempts to redissolve the precipitate (or dissolve the product in its zwitterionic form) by adding large amount of HCl (pH below 2.5) were not conclusive. This could possibly be accounted for a strong salt effect, resulting from the addition of hydrochloric acid (and additional presence of NaCl), hence reducing the overall solubility of the compound in solution. Another hypothesis would be that the protonated compound at low pH has a very high Krafft temperature, making it insoluble in water at ambient temperature.

2.3 References

- [1] Rakotoaly, R. H. Thèse de Doctorat, Louvain-la-Neuve, 2001.
- [2] Laschewsky, A.; Lunkenheimer, K.; Rakotoaly, R. H.; Wattebled, L. *Colloid Polym. Sci.* **2005**, *283*, 469.
- [3] Laschewsky, A.; Wattebled, L.; Arotçaréna, M.; Habib-Jiwan, J.-L.; Rakotoaly, R. H. *Langmuir* **2005**, *21*, 7170-7179.
- [4] Zana, R. *J. Colloid Interface Sci.* **2002**, *248*, 203.
- [5] March, J. In *Advanced Organic Chemistry 4th Edition*; Wiley & Sons: New York, Chichester, Brisbane, 1992.
- [6] Falbe, J. *Surfactants in Consumer Products: Theory, Technology and Applications*; Falbe, J. ed.; Springer: Berlin, Heidelberg, New York, 1987.
- [7] Wang, X. Y.; Wang, J. B.; Wang, Y. L.; Yan, H. K.; Li, P. X.; Thomas, R. K. *Langmuir* **2004**, *20*, 53.
- [8] *Gemini Surfactants: Synthesis, Interfacial and Solution-Phase Behavior, and Applications*, Zana, R.; Xia, J., eds., Dekker: New York, 2004.
- [9] Mathias, J. H.; Rosen, M. J.; Davenport, L. *Langmuir* **2001**, *17*, 6148.
- [10] Zana, R. *Adv. Colloid Interface Sci.* **2002**, *97*, 205.
- [11] Danino, D.; Talmon, Y.; Zana, R. *Langmuir* **1995**, *11*, 1448.
- [12] Devínski, F.; Lacko, I.; Imam, T. *J. Colloid Interface Sci.* **1991**, *143*, 336.
- [13] Zana, R.; Benraou, M.; Rueff, R. *Langmuir* **1991**, *7*, 1072.
- [14] Pisárčik, M.; Devínski, F.; Lacko, I. *Coll. Surf. A* **2000**, *172*, 139.
- [15] Bai, G. Y.; Wang, J. B.; Yan, H. K.; Li, Z. X.; Thomas, R. K. *J. Phys. Chem. B* **2001**, *105*, 3105.
- [16] Zana, R. *J. Colloid Interface Sci.* **2002**, *252*, 259.
- [17] Li, Z. X.; Dong, C. C.; Wang, J. B.; Thomas, R. K.; Penfold, J. *Langmuir* **2002**, *18*, 6614.
- [18] Sikirić, M.; Šmit, I.; Tušek-Božić, L.; Tomašić, V.; Pucić, I.; Primožić, I.; Filipović-Vinceković, N. *Langmuir* **2003**, *19*, 10044.
- [19] Alami, E.; Beinert, G.; Marie, P.; Zana, R. *Langmuir* **1993**, *9*, 1465.
- [20] Alami, E.; Levy, H.; Zana, R.; Skoulios, A. *Langmuir* **1993**, *9*, 940.
- [21] Zana, R. *J. Colloid Interface Sci.* **2002**, *246*, 182.
- [22] Kim, T. S.; Kida, T.; Nakatsuji, Y.; Hirao, T.; Ikeda, I. *J. Am. Oil Chem. Soc.* **1996**, *73*, 907.
- [23] Dreja, M.; Pyckhout-Hintzen, W.; Mays, H.; Tieke, B. *Langmuir* **1999**, *15*, 391.
- [24] Dam, Th.; Engberts, J. B. F. N.; Karthäuser, J.; Karaborni, S.; van Os, N. M. *Coll. Surf. A* **1996**, *118*, 41.
- [25] Maiti, P. K.; Lansac, Y.; Glaser, M. A.; Clark, N. A.; Rouault, Y. *Langmuir* **2002**, *18*, 1908.
- [26] In, M.; Bec, V.; Aguerre-Chariol, O.; Zana, R. *Langmuir* **2000**, *16*, 141.
- [27] Okahara, M.; Masuyama, A.; Sumida, Y.; Zhu, Y.-P. *J. Jpn. Oil Chem. Soc.* **1988**, *37*, 746-748.
- [28] Zhu, Y.-P.; Masuyama, A.; Okahara, M. *J. Am. Oil Chem. Soc.* **1990**, *67*, 459-463.
- [29] Zhu, Y.-P.; Masuyama, A.; Nagata, T.; Okahara, M. *J. Jpn. Oil Chem. Soc. (J. Oleo Sci.)* **1991**, *40*, 473.
- [30] Zana, R.; Lévy, H.; Danino, D.; Talmon, Y.; Kwetkat, K. *Langmuir* **1997**, *13*, 402-408.
- [31] Menger, F.M.; Littau, C. A. *J. Am. Chem. Soc.* **1993**, *115*, 10083.
- [32] Menger, F.M.; Littau, C. A. *J. Am. Chem. Soc.* **1991**, *113*, 1451.
- [33] Duivenvoorde, F. L.; Feiters, M. C.; van der Gaast, S. J.; Engberts, J. B. F. N. *Langmuir* **1997**, *13*, 3737.
- [34] Menger, F. M.; Eliseev, A. V. *Langmuir* **1995**, *11*, 1855.
- [35] Jaeger, D. A.; Wang, Y.; Pennington, R. L. *Langmuir* **2002**, *18*, 9259-9266.

- [36] Jennings, K.; Marshall, I.; Birrell, H.; Edwards, A.; Haskins, N.; Sodermann, O.; Kirby, A. J.; Camilleri, P. *Chem. Commun.* **1998**, 1951-1952.
- [37] Masuyama, A.; Endo, C.; Takeda, S.; Nojima, M. *J. Chem. Soc. Chem. Commun.* **1998**, 2023.
- [38] van Zon, A.; Bouman, J. T.; Deuling, H. H.; Karaborni, D. S.; Karthaeuser, J.; Mensen, H. T. G. A.; van Os, N. M.; Raney, K. H. *Tenside Surf. Det.* **1999**, *36*, 84-86.
- [39] Alargova, R. G.; Kochijashky, I. I.; Sierra, M. L.; Kwetkat, K.; Zana, R. *J. Colloid Interface Sci.* **2001**, *235*, 119-129.
- [40] Magdassi, S.; Ben Moshe, M.; Talmon, Y.; Danino, D. *Coll. Surf. A* **2003**, *212*, 1.
- [41] Zhu, S.; Cheng, F.; Wang, J.; Yu, J.-g. *Coll. Surf. A* **2006**, *281*, 35-39.
- [42] Li, Z.; Yuan, R.; Yin, F. *Tenside Surf. Det.* **2006**, *43*, 151-154.
- [43] Li, Z. S.; Liu, P. Q.; Xu, M. X. In *Synthesis and Technology of Surfactants (Chinese)*; The publishing Company of Light Industry: Beijing, 1995, p.98.
- [44] Sedláč, M.; Tauer, K. *Synlett.* **2004**, *2*, 299-300.
- [45] Helbig, C.; Baldauf, H.; Lange, T.; Neumann, R.; Pollex, R.; Weber, E. *Tenside Surf. Det.* **1999**, *36*, 58.
- [46] Zhu, Y.-P.; Masuyama, A.; Kobata, Y.; Nakatsuji, Y.; Okahara, M.; Rosen, M. J. *J. Colloid Interface Sci.* **1993**, *158*, 40.
- [47] Dix, L. R. *J. Colloid Interface Sci.* **2001**, *238*, 447-448.
- [48] Dix, L. R. *J. Colloid Interface Sci.* **2006**, *295*, 590 (Corrigendum).
- [49] Dix, L. R.; Gilblas, R. *J. Colloid Interface Sci.* **2006**, *296*, 762-765.
- [50] Yoshimura, T.; Esumi, K. *J. Colloid Interface Sci.* **2004**, *276*, 231-238
- [51] Tsubone, K.; Arakawa, Y.; Rosen, M. J. *J. Colloid Interface Sci.* **2003**, *262*, 516-524.
- [52] Tsubone, K.; Ghosh, S. *J. Surf. Det.* **2003**, *6*, 225-229.
- [53] Tsubone, K.; Ghosh, S. *J. Surf. Det.* **2004**, *7*, 47-52.
- [54] Kunieda, H.; Masuda, N.; Tsubone, K. *Langmuir* **2000**, *16*, 6438-6444.
- [55] Porter, N. A.; Petter, R. C.; Brittain, W. J. *J. Am. Chem. Soc.* **1984**, *106*, 813-814.
- [56] Büschl, R.; Folda, T.; Ringsdorf, H. *Makromol. Chem.* **1984**, *6*, 245-258.
- [57] Säily, V. M. J.; Ryhänen, S. J.; Lankinen, H.; Luciani, P.; Mancini, G.; Parry, M. J.; Kinnunen, P. K. J. *Langmuir* **2006**, *22*, 956-962, and references therein.
- [58] Masuyama, A.; Endo, C.; Takeda, S.; Nojima, M.; Ono, D.; Takeda, T. *Langmuir* **2000**, *16*, 368-373.
- [59] Oda, R.; Huc, I.; Danino, D.; Talmon, Y. *Langmuir* **2000**, *16*, 9759.
- [60] Huc, I.; Oda, R. *Chem. Commun.* **1999**, 2025.
- [61] Ulbricht, W.; Zana, R. *Colloid Polym. Sci.* **2001**, *487*, 183-185.
- [62] Groth, C.; Nydén, M.; Holmberg, K.; Kanicky, J. R.; Shah, D. O. *J. Surf. Det.* **2004**, *7*, 247-255.
- [63] Pretsch, E.; Bühlmann, P.; Affolter, C.; Badertscher, M. *Spektroskopische Daten zur Strukturaufklärung organischer Verbindungen*, 4th Edition; Springer: Berlin, Heidelberg, New York, 2001, p.224.
- [64] Huang, X.; Cao, M.; Wang, J.; Wang, Y. *J. Phys. Chem. B* **2006**, *110*, 19479-19486.

3. PROPERTIES OF THE SURFACTANT OLIGOMERS

In this chapter, the property profile of the surfactant structures previously described, namely the cationic oligomers and the anionic dimer, are examined with respect to the influence of the spacer group and of the degree of oligomerization.

3.1 Properties of cationic surfactant oligomers [1-3]

The following surfactant properties in aqueous solution for the series of oligomeric amphiphiles will be addressed here: Krafft point, micellization and surface activity, micellar structure (via dynamic light scattering, NMR spectroscopy and determination of aggregation numbers by time-resolved fluorescence quenching), formation of microemulsions.

3.1.1 Krafft Temperatures

The synthesized cationic dimeric, trimeric and tetrameric surfactants are readily soluble in water at ambient temperature, and have Krafft-temperatures below 0 °C (except dimeric compound **p-X-2**). This allows the use of oligomeric surfactants in cold water. The Krafft-temperature of **p-X-2** with a rather long rigid spacer p-xylylene is slightly higher than 20 °C. Putatively, this finding is attributed to a particularly favorable molecular packing in the solid state. Nevertheless, the exchange of the bromide counterion [4] with the chloride for **p-X-2** induced a substantial increase in solubility, as observed in another case [5]. Indeed, the analogous bromide salt of surfactants **p-X-2** was described before [6-8], exhibiting a high Krafft-temperature of about 44 °C [6]. Noteworthy, the Krafft-temperatures of the trimeric and tetrameric surfactants with the p-xylylene spacer (**p-X-3** and **p-X-4**) are below 0 °C, whereas the analogous dimer **p-X-2** surfactant has a Krafft temperature of 23 °C, i.e., the Krafft temperature is reduced by a higher degree of oligomerization. The method used to determine the Krafft temperatures is described in the experimental part 5.6. The T_K -values of all surfactant oligomers are summarized in Tables 3.1-1 and 3.1-2.

3.1.2 Surface activity and micellization

The determination of the critical micellization concentration (CMC) and of the surface activity is the basic step in the evaluation of the property profile of surfactants [9], typically by surface tension measurements. The procedure using a Du Noüy ring tensiometer is described in the experimental part 5.7.

3.1.2.a. Spacer effect in dimeric surfactants [1]

The surface-active behavior of the reference surfactant **BDDAC** and of the surfactant dimers is illustrated in Figure 3.1-1, and the characteristic parameters derived there from are listed in Table 3.1-1. The surface tension curves present virtually no minimum, thus indicating a rather good purity of the substances, though not necessarily guaranteeing sufficient surface-chemical purity in its strict requirement [10]. Except the substances **o-X-2** which reveals a clear minimum and **t-B-2** which shows a slight minimum in the σ_e vs. $\log(\text{concentration})$ isotherm, all other substances did not exhibit any noticeable minimum. Note that the isotherm for commercial reference surfactant **DTAC** is not shown since it exhibits a very strong minimum. For the surfactant exhibiting a minimum in their surface tension curve, the constant surface tension values which are observed at concentrations well above CMC are used to allow comparisons. The constant σ -values indicate that the surface-active impurity producing the minimum was solubilized in the micelles and does not longer influence the adsorbed layer.

All dimeric surfactants form micelles at room temperature, with similar values for the critical micelle concentration (CMC) between 1.2 and 2.2 mmol/L (respectively 0.7 g/L and 1.3 g/L). But the CMC values of dimers are considerably lower than those of the structurally related single tail surfactant "monomers" **DTAC** and **BDDAC**, which is true on molar and on weight basis (**BDDAC**: 7.0 mmol/L or 2.4 g/L; **DTAC**: 18.3 mmol/L or 4.8 g/L). This result is in agreement with the literature on dimeric surfactants [11], and makes gemini surfactants advantageous compared to conventional amphiphiles, e.g. for the solubilization of hydrophobic compounds in dilute surfactant solutions. Noteworthy, the CMC value of surfactant monomer **DTAC** determined experimentally (curve not shown) is consistent with that from reference [12] (with CMC value: 21.5 mmol/L or 5.6 g/L).

Table 3.1-1: Surface activity and micellization data of gemini surfactants and corresponding "monomers". Surface tension curves of dimeric surfactants made by K. Lunkenheimer.

Compound	T_{Krafft} [°C]	CMC [mmol/L]	CMC [g/L]	σ_{cmc} [mN/m]	C_{20} [mmol/L]	C_{20} [g/L]
DTAC ^b	<0	18.3	4.8	40.5	1.1	0.29
BDDAC	<0	7.0	2.4	39	1.5	0.51
i-B-2 ^a	<0	1.8	1.0	39.5	0.55	0.30
t-B-2 ^a	<0	2.0	1.1	41.4	0.8	0.44
EO-2 ^a	<0	2.2	1.25	44.9	0.9	0.51
o-X-2 ^{a,b}	<0	1.2	0.72	37	0.2	0.12
m-X-2 ^a	<0	1.5	0.90	42.8	0.6	0.36
p-X-2 ^a	22-23	2.1	1.3	45.0	0.8	0.48

^a = surface tension measurements performed by K. Lunkenheimer

^b = curves with a marked minimum

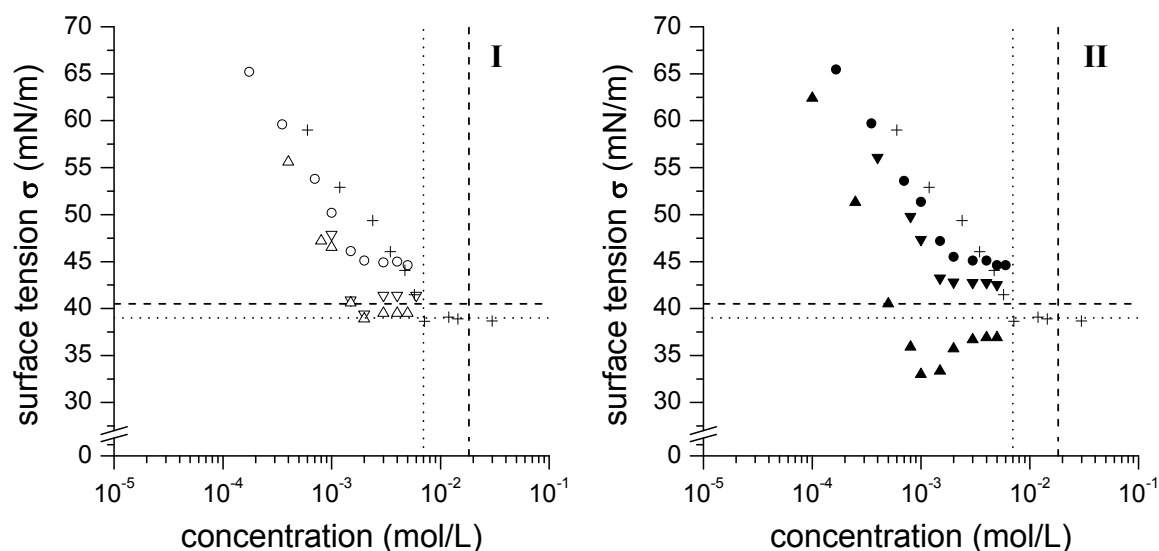


Figure 3.1-1: Surface tension vs. concentration curves of studied surfactants: (+) = **BDDAC**; I: (Δ) = **i-B-2**, (∇) = **t-B-2**, (o) = **EO-2**; II: (\blacktriangle) = **o-X-2**, (\blacktriangledown) = **m-X-2**, (\bullet) = **p-X-2**. Measurements of surfactant dimers performed by K. Lunkenheimer (MPI-KG, Golm) [1]. Vertical and horizontal lines are a guide for the eyes, respectively positioning CMC- and σ_{cmc} -values of reference surfactants: **DTAC** (dashes); **BDDAC** (dots).

The marked decrease of the CMC value when substituting one methyl group on the ammonium nitrogen in **DTAC** [12] by a benzyl group in **BDDAC**, underlines that spacer group effects in dimeric surfactants may at least partially result from a change in the hydrophilic-hydrophobic balance of the surfactants. Note that the CMC determined for dimer **EO-2** is about four times higher than the value reported previously in the literature [4], but only twice as high as the value reported for the CMC of its bromide analog [13] as would be expected [5]. Indeed, in the few reports comparing analogous cationic dimeric surfactants with chloride and bromide as counterions, the critical micellization concentration (CMC) values of the chlorides were reported to be about twice higher than the ones of the analogous bromides [5].

Analyzing the surface tension (σ) vs. concentration curves and the CMC values of the various dimeric surfactants, some differences are noticeable. The differences in the CMC value seem moderate, though clearly existing. Within the two series of isomeric dimeric surfactants, i.e. of such with a spacer group of identical hydrophobicity, namely butenylene and xylylene, the CMC values increase slightly with **i-B-2** < **t-B-2**, and with **o-X-2** < **m-X-2** < **p-X-2**. This means that the CMC values increase with increasing spacer length. This finding for the two rigid spacer groups coincides with a similar observation in the most studied series of dimeric surfactants with flexible spacers, the alkanediyl- α,ω -bis(dimethylalkyl ammonium bromide)s, for which a maximum for the CMC is observed for the C_6 -spacer [14]. Dimer **EO-2** whose flexible spacer is roughly equivalent to an

aliphatic C₅ unit, exhibits a CMC value that is slightly higher than the values for **i-B-2** and **t-B-2**. This behavior seems to fit into the general scheme, but may be fortuitous considering the different flexibility and polarity of the bisethyleneglycol spacer compared to the butenylene group. In any case, the different CMC values within the two series of isomeric compounds illustrate the importance of steric effects of the spacer for dimeric surfactants, despite a constant hydrophilic-hydrophobic balance. The effect of the spacer groups can be explained by steric constraints imposed on the self-organization of the surfactants. This could affect the packing density of the alkyl chains as well as the ability to minimize hydrophobic interactions intramolecularly by an appropriate conformation of the alkyl chains [12, 15-17].

Apart from the effect of the length of the spacer (steric effect), the chemical nature of the latter cannot be neglected, as exemplified by the comparison of the CMC values of xylylene and butenylene spacer series. The comparison of dimers **t-B-2** and **o-X-2** which both have a C₄-spacer unit between the surfactant fragments supports this finding, as reported for flexible C₄-spacers before [18]. Dimer **o-X-2** exhibits the lower CMC, which can be rationalized by the more hydrophobic xylylene spacer of **o-X-2** (see discussion for the standard surfactants **DTAC** and **BDDAC** above). In agreement, the CMC of **t-B-2** with the butenylene spacer matches well with the reported CMC of the similar dimeric ammonium chloride bearing a butinediyl spacer [5] with nearly identical hydrophobicity. Within this reasoning, the very close CMC values found for dimers **EO-2** and **p-X-2** should be seen as accidental, with the effects of differing spacer lengths and differing polarity just compensating. Note that this observation agrees well with the recent findings for the analogous pair of **EO-2** and **p-X-2** having the bromide counterion [15].

The similarity of the surface tension (σ) vs. concentration isotherms of the dimers (see Figure 3.1-1, I and II) indicates that their standard energy of adsorption is very similar and nearly independent of the type of the spacer. However some noticeable differences in their surface properties are found when comparing their σ_{cmc} -values (see Table 3.1-1). The σ_{cmc} -values increase with **o-X-2** < **i-B-2** < **t-B-2** < **m-X-2** < **p-X-2** \approx **EO-2** from 37 mN/m to 45 mN/m. The σ_{cmc} -values of the reference monomeric surfactants **DTAC** and **BDDAC** lie in between this range (respectively 40.5 mN/m and 39 mN/m). Looking separately at the two series of isomeric dimeric surfactants, the σ_{cmc} -values increase with **i-B-2** < **t-B-2** and with **o-X-2** < **m-X-2** < **p-X-2**. Hence, as for the CMC values, the σ_{cmc} -values increase with increasing spacer length for a given polarity of the spacer. In other words, the closer the two substituents are positioned, the higher will be their surface pressure at the CMC (π_{cmc}). This suggests that the isomers have different packing densities: the para isomer cannot be packed as tightly as the corresponding ortho isomer. If this explanation is true, this tendency will be reflected in the maximum surface excess determined from the equilibrium surface tension versus concentration isotherms of the amphiphiles. Still, the comparison of the two isomeric series of surfactants - with

butenylene and xylylene spacer - shows that not only the length but also the chemical nature of the spacer contributes to the extent of reduction of the surface tension. For a given spacer length, the xylylene spacer reduces the surface tension above the CMC more than the butenylene spacer (compare e.g. **t-B-2** and **o-X-2** approximately having the same spacer length). In analogy, comparing reference surfactants **DTAC** and **BDDAC**, it is noticeable that the benzyl group of **BDDAC** allows a slight reduction of surface tension at the CMC (see Table 3.1-1). For the pair **EO-2** and **p-X-2**, the different effects of their spacer groups seem to compensate, once more.

In addition, the C_{20} -value was determined for each surfactant (see Table 3.1-1). C_{20} represents the bulk surfactant concentration needed to reduce the surface tension of the solvent by an arbitrary $20 \text{ mN}\cdot\text{m}^{-1}$ (i.e. surfactant concentration in water for which σ equals $52 \text{ mN}\cdot\text{m}^{-1}$). This value commonly characterizes the efficiency of a surfactant to lower surface tension. It is found that the C_{20} -values of the studied dimers are slightly lower than that of the monomers (on a molar basis), reflecting that dimeric surfactants are a little more efficient than (or at least as efficient as) the analogous monomeric surfactants at decreasing the surface tension of water. This corroborates to some extent the finding that dimeric surfactants are more efficient than their monomeric counterparts, as pointed out by In [19] and Zana [11]. Nevertheless, the decrease in C_{20} is generally much more pronounced for common gemini surfactants (e.g. for bisquaternary ammonium bromides [11]). Noteworthy, the difference in the C_{20} -values between dimeric and analogous monomeric surfactants is here much smaller than the difference observed in the CMC-values (e.g. compare C_{20} -values of **i-B-2** and **DTAC**, as well as their CMC-values in Table 3.1-1).

As regards the spacer effect, comparing the C_{20} -values of surfactant dimers within the two isomeric series, it becomes clear that shorter spacers involve lower C_{20} (although the differences are small). For instance, C_{20} -value of **o-X-2** is smaller than that of **p-X-2**. This reflects a higher efficiency of surfactant dimers with short spacer to reduce the surface tension (slightly higher tendency to adsorb).

3.1.2.b. Series of oligomeric surfactants [2]

The surface active behavior of the nine surfactant oligomers (three series from dimer to tetramer) is illustrated in Figure 3.1-2 and compared with that of reference surfactant **BDDAC**. Also, for comparisons with higher oligomers, the curves of analogous dimeric structures are presented again. The characteristic parameters derived from the surface tension curves are listed in Table 3.1-2. All studied surfactants, with the exception of the tetrameric surfactant **p-X-4**, show a sharp break of the surface tension vs. $\log(\text{concentration})$ isotherm, which is indicative of a critical micellization concentration (CMC) and the formation of micelles. In the case of **p-X-4**, the isotherm exhibits a transition from a concentration regime with a marked decrease of the surface tension σ to a nearly flat

curve, too, but the transition is somewhat diffuse rather than to be a sharp discontinuity as for the other surfactants.

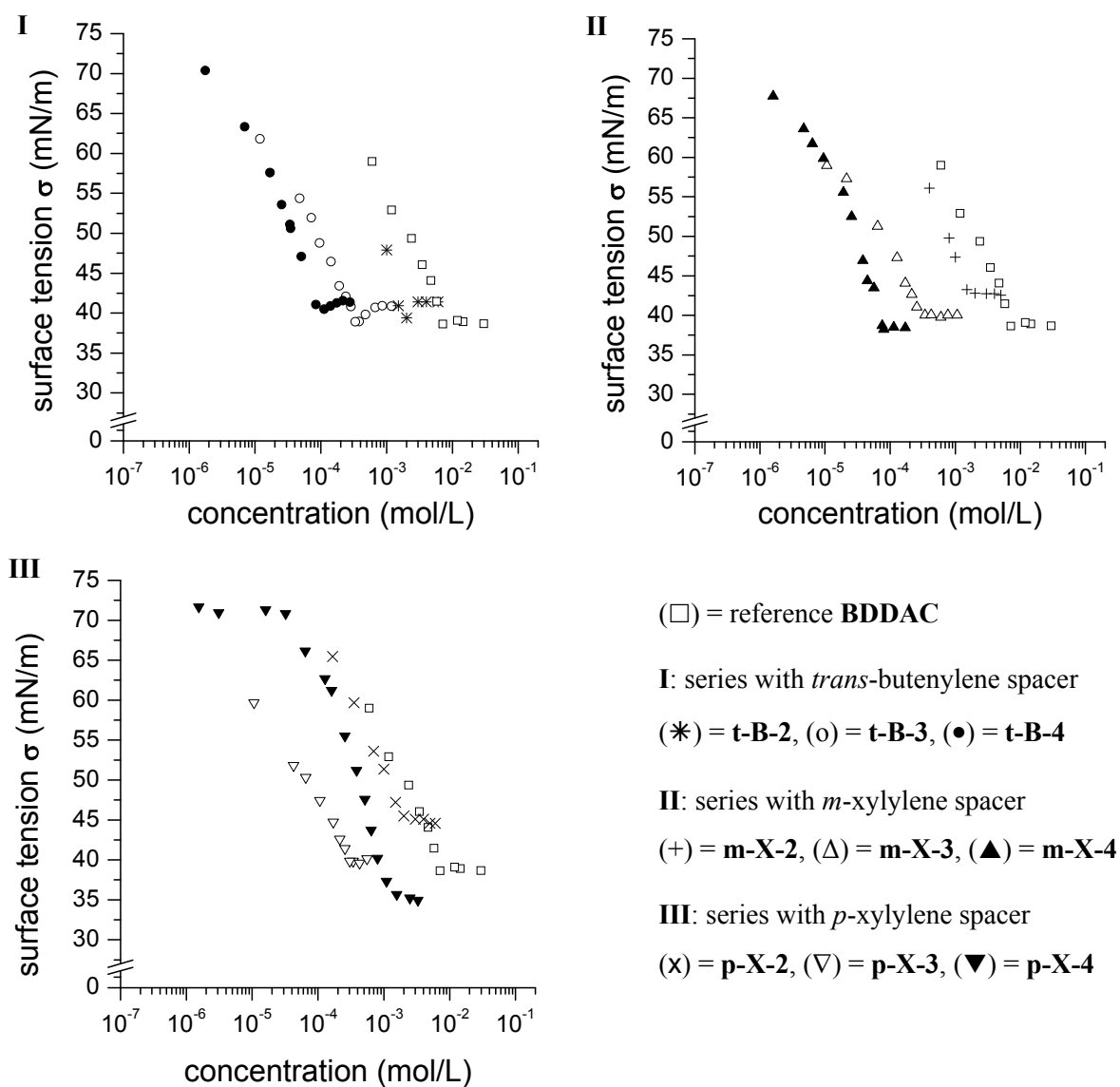


Figure 3.1-2: Surface tension vs. concentration isotherms of oligomeric surfactants.

Table 3.1-2: Surface activity and micellization data of studied oligomeric surfactants

Compound	T _{Krafft} [°C]	CMC ^a [g/L]	CMC ^a [mmol/L]	σ_{cmc} [mN/m]	CMC ^{b, e} [mmol/L]	CMC ^c [mmol/L]
DTAC	<0	4.8	18.3	40.5		
BDDAC	<0	2.4	7.0	39	7.7	5.5
t-B-2	<0	1.1	2.0 ^d	41.5		
m-X-2	<0	0.9	1.5 ^d	43		
p-X-2	22-23	1.3	2.1 ^d	45.0	1.7	1.5 ^e
t-B-3	<0	0.30	0.36	41	0.31	
m-X-3	<0	0.26	0.28	40	0.25	
p-X-3	<0	0.28	0.29	40	0.32	0.2
t-B-4	<0	0.13	0.12	41	0.12	
m-X-4	<0	0.11	0.09	38.5	0.08	
p-X-4	<0	1.7 *	1.3 *	35 *	0.7 *	3.5 *

^a = measured by tensiometry

^b = measured by fluorescence probe 2-AN

^c = measured by dye probe pinacyanol

^d = performed by K. Lunkenheimer (see previous section)

^e = performed by M. Arotçaréna (U.C. Louvain)

* apparent cmc

The surfactants with xylylene spacers did not exhibit a noticeable minimum in the surface tension vs. log(concentration) isotherms, while the substances with the t-butenylene spacer showed a small minimum only, indicating the high purity of the various substances. Comparing the surface activity within the surfactant oligomer series, it is found that the surface tension at the CMC (σ_{cmc}) decreases with the degree of oligomerization (for the somewhat contaminated surfactants, the true σ_{cmc} was estimated from the constant σ value at concentrations above the CMC). This effect is more pronounced for longer spacers (see Figure 3.1-2 and Table 3.1-2). Accordingly, for the series with p-xylylene spacer, **p-X-2**, **p-X-3**, and **p-X-4**, σ_{cmc} equals respectively to 45 mN/m, 40 mN/m and 35 mN/m for the dimer, trimer and the tetramer. For the series with shorter m-xylylene spacer, **m-X-2**, **m-X-3**, and **m-X-4**, σ_{cmc} equals to 43 mN/m, 40 mN/m and 38.5 mN/m, respectively, for the dimer, trimer and the tetramer. For the series with the even shorter t-butenylene spacer, **t-B-2**, **t-B-3**, and **t-B-4**, σ_{cmc} is close to 41 mN/m for all oligomers. For comparison, the σ_{cmc} -values of the monomeric reference surfactants **DTAC** and **BDDAC** are with 40.5 mN/m and 39 mN/m, respectively, in between the σ_{cmc} -values of the various oligomers. Accordingly, the maximum reduction of the aqueous surface tension that can be attained is comparable for monomeric and oligomeric surfactants.

The differences found between the surface activities of the various series of oligomeric surfactants may be attributed to differences in their packing densities at the air/water interface. A priori, this should be reflected in the surface areas A_{min} occupied by the various surfactants. By means

of the Gibbs equation (see chapter 1, part 1.1.2.a), the surface excess concentration Γ at the CMC can be worked out as:

$$\Gamma_{cmc} = \frac{10^{20}}{N_A \times A_{min}} = -\frac{1}{2.303 \times nRT} \left(\frac{\partial \sigma}{\partial \log C} \right)_T \quad \text{Equation 3.1-6}$$

with Γ_{cmc} in mol/m², $R = 8.31 \text{ J}\cdot\text{mol}^{-1}\cdot\text{K}^{-1}$ (gas constant) and $T =$ absolute temperature in K, whilst $\left(\frac{\partial \sigma}{\partial \log C} \right)$ is obtained from the tangency at the CMC. N_A is the Avogadro's number ($6.02 \times 10^{23} \text{ mol}^{-1}$).

¹). The surface area occupied by one surfactant molecule at the interface A_{min} is here expressed in Å². But a discussion of the state of adsorption at the air/water interface is a complex topic for the oligomeric surfactants [16-17, 20]. For instance, the calculation depends critically on the assumed degree of dissociation of the cationic surfactants, which is not known (represented by n in the equation). In the extreme cases, no dissociation is assumed, thus treating the surfactants as one particle in the Gibbs equation or complete dissociation is postulated. Then the surfactants must be treated as two, three, four or five particles respectively for monomers, dimers, trimers and tetramers. Neither of the extreme scenarios seems probable. Moreover, the degree of dissociation may vary between the various surfactants with the degree of oligomerization and the spacer length. Thus, even a relative comparison seems questionable without additional data. Therefore, a detailed analysis of the state of adsorption is beyond this study. Nevertheless, the different evolutions of the minimal surface tension obtained for the three series with different spacers with increasing degree of oligomerization (cf. Figure 3.1-2) suggest that the packing density of the dodecyl chains in the adsorbed monolayer stays approximately the same for the series with the *trans*-butenylene spacer, increases somewhat for the series with *m*-xylylene spacer, and improves much for the series with *p*-xylylene spacer.

Table 3.1-2 lists the CMC values derived from the break in the surface tension vs log(concentration) isotherms. The CMC values of oligomeric surfactants are much lower than those of the monomeric surfactants **DTAC** and **BDDAC**. If CMCs are expressed in moles of dodecyl chains per liter (which may be the more appropriate comparison), the values range respectively from 7.0 mM to 21.5 mM for monomers, from 3.0 mM to 4.2 mM for dimers, from 0.84 mM to 1.08 mM for trimers and from 0.28 mM to 0.44 mM for tetramers. Thus, also when normalized to the number of hydrophobic chains, the CMC decreases systematically with increasing degree of oligomerization. A closer look to the data reveals, that the decrease from monomers to dimers is more pronounced than the decrease from trimers to tetramers. The CMC decreases with the oligomerization degree in a somewhat hyperbolic manner (see Figure 3.1-3), as found for the only other reported series of quaternary ammonium oligomers [11, 21]. The general decrease of the CMC with increasing degree of oligomerization is mainly attributed to thermodynamical reasons [11], as basically, the entropic loss resulting from micellization of the surfactants becomes smaller.

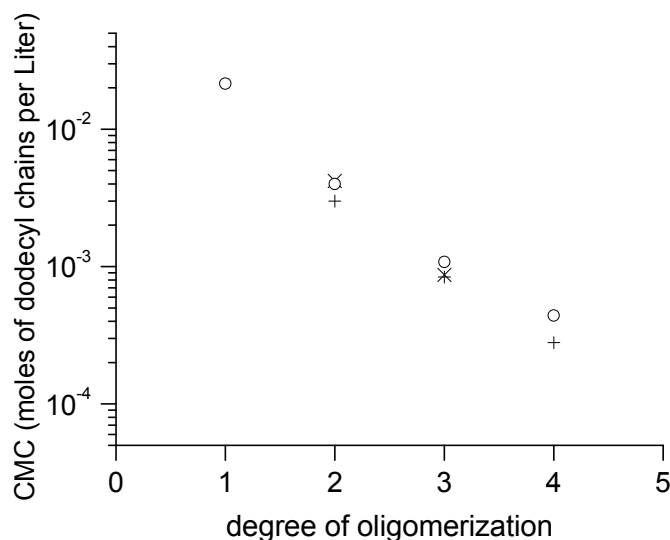


Figure 3.1-3: Evolution of the critical micellar concentration: CMC decreases with the degree of oligomerization. (o) = *trans*-butenylene spacer; (+) = *m*-xylylene spacer; (x) = *p*-xylylene spacer.

For a given degree of oligomerization, the differences in the CMC values between the three series with different spacer groups are small (Table 3.1-2). Comparing the effects of the isomeric *m*-xylylene and *p*-xylylene spacers, *i.e.* spacer groups of identical hydrophobicity, the CMC values increase slightly from *meta*- to *para*-xylylene for a given degree of oligomerization. This means that the CMC increase with increasing spacer length. This corroborates a similar observation in the most studied series of dimeric surfactants having flexible spacers, the alkanediyl- α,ω -bis(dimethylalkylammonium bromide)s [14]. The observations are also in line with the results presented in the previous part (3.1.2.b.) for the series of dimeric surfactants with rigid spacer groups [1]. In fact, it seems that the influence of the flexibility of the spacer of a given length on the CMC of analogous dimeric surfactants is very small, at least for rather short spacers [5]. To which extent differences in the spacer shapes may modify the CMCs is an interesting, but open question. The few existing studies on shape isomers of dimeric surfactants, induced by irradiation isomerization [22-24], have not been conclusive in this respect.

However, the chemical nature of the spacer has some influence on the CMC values, as the comparison for the series with the butenylene and *m*-xylylene spacer exemplifies. The oligomers with the *m*-xylylene spacer exhibit a lower CMC for a given degree of oligomerization, despite their increased spacer length. This can be easily rationalized by the more hydrophobic spacers of these compounds. Comparing the dimers and trimers with the butenylene spacer to the analogs with the even longer *p*-xylylene spacer, the CMC values are very close. Accordingly, the effects of the *p*-xylylene spacer being more hydrophobic (reducing the CMC), but being longer (increasing the CMC) seem to neutralize each other.

3.1.2.c. Peculiar behaviour of tetramer p-X-4

All the studied oligomeric surfactants stick to the above-discussed rules, with the remarkable exception of tetramer **p-X-4**. This compound shows not only a diffuse break point in the surface tension vs log(concentration) isotherm, but also, this point is observed at a higher concentration than the CMC of its trimer **p-X-3**. In order to clarify this unusual behavior, additional attempts were made to determine the CMC of the surfactants by the dye solubilization method. This method, presented in the experimental part **5.8**, is based on the sensitivity of the spectral properties of certain hydrophobic dyes to the polarity of the medium in which they are dissolved (solvatochromism). This makes them suitable to detect the presence of hydrophobic microdomains in aqueous solution, as the partition coefficient of the dye is favorable to the micelles. Upon increasing the surfactant concentration, the absorption spectrum of the dye shifts from that in aqueous solution to a spectrum similar to that in a less polar organic solvent when micelles are present. In the case of ionic surfactants, this method requires the use of non-ionic or of identically charged dyes, in order to avoid possible interferences by attractive electrostatic interactions [25].

Due to its sensitivity, the fluorescence probe 2-anilinonaphthalene (2-AN) was employed as hydrophobic, sparingly water-soluble dye. The fluorescence of 2-AN is very sensitive to its surrounding polarity, the emission wavelength decreasing with the polarity [26]. Indeed, all surfactants showed a clear solvatochromic effect at the CMC, shifting the emission wavelength of 2-AN from about 445 nm in dilute solution to values between 415 to 418 nm after association (see graphs in Appendix 4, corresponding to the measurements performed by M. Arotçaréna). Within a given series of oligomeric surfactants, the polarity effects for the probe deduced from the solvatochromic shift were negligible. Also, all three surfactant series with different spacer groups induced similar shifts of the emission wavelengths, in agreement with the only previous report on an oligomeric surfactant series [21]. This suggests similar solubilization sites for the probe in the various micellar aggregates, presumably in the palisade layer of the micelles.

The CMC values determined from the shift of the emission maximum are given in Table 3.1-2 above. They show excellent agreement with the surface tension derived data, except for tetramer **p-X-4**. Therefore, a second dye was used to determine the CMC of the oligomeric series with the p-xylylene spacer, namely the cationic dye pinacyanol, the absorbance maximum of which exhibits a pronounced solvatochromism [27-30]. The interaction of pinacyanol with the formed micelles produces a bathochromic shift ("red" shift) [31], as shown on the graphs in Appendix 5. The results of these measurements are listed in Table 3.1-2. Again, they show excellent agreement with the data obtained by the other techniques except for the tetramer **p-X-4**. On the one hand, the generally good agreement of the CMC values determined by different methods for the oligomeric surfactants is

reassuring. On the other hand, the systematic deviation found for **p-X-4** needs an explanation. Noteworthy, all methods seem to indicate that the CMC of the tetramer **p-X-4** is considerably higher than the CMC of the trimer **p-X-3**, despite the seeming inconsistency of the apparent CMC values for **p-X-4** determined by different methods.

The unusual behavior of **p-X-4** can be explained by the formation of premicellar aggregates in solution, reducing the concentration of free surfactant unimers at a given total concentration, and thus increasing the apparent CMC to higher values. Premicellar aggregation can occur in solutions of conventional surfactants that are sufficiently hydrophobic (at least 14 carbon atoms) [10, 32]. Premicellar aggregation was also evoked in certain cases for dimeric surfactants, for instance to explain the minimum of the apparent CMC as function of the alkyl chain length at the carbon number of 16 observed for the bromide analogs of **p-X-2** [7]. Similar observations for other series of dimeric surfactants with long alkyl chains ($\geq C_{14}$), especially at high ionic strengths, were explained by premicellar aggregates, too [8, 15, 33]. Analogously, the apparent CMC values determined from surface tension data for some trimeric anionic surfactants with long hydrophobic chains increase with the length of the alkyl chain. This was attributed to premicellar aggregates [34-35]. The assumed premicellar aggregates can easily explain not only the diffuse transition in the surface tension isotherm and the unexpectedly high apparent CMC value for **p-X-4**. They can also explain the markedly differing onset of solubilization by the two dye probes, which dispose of a strongly differing molecular structure. The smaller and more hydrophobic dye 2-AN should be more easily dissolved by small surfactant aggregates than pinacyanol (see chemical structures in experimental part), thus pretending a lower CMC.

The different results within the series **p-X-2** / **p-X-3** / **p-X-4**, as well as the occurrence of only moderately long dodecyl chains in **p-X-4** compared to the longer chains reported for the case of dimeric surfactants, demonstrate that the formation of premicellar aggregates is favored by an increasing degree of oligomerization. Also, the different results within the series **t-B-4** / **m-X-4** / **p-X-4**, exemplify that in addition to the length of the alkyl chains and the degree of oligomerization, the nature of the spacer group is important. It is an interesting question, why the p-xylylene spacer favors premicellar aggregation compared to the other ones. Possibly, the formation of small, dense aggregates by intermolecular interdigitation [8] of the dodecyl chains is easier in the case of **p-X-4**, as the longer p-xylylene spacer facilitates such a dense packing of the alkyl chains, whereas the m-xylylene and the butenylene spacers are too short for such an arrangement.

3.1.3 Dynamic Light Scattering and NMR spectroscopy

Dynamic light scattering of solutions of dimeric, trimeric and tetrameric surfactants (see experimental part) indicated only the presence of very small aggregates at the lower detection limit of the apparatus, i.e. of 2 nm diameter or smaller, up to 7 wt% of surfactant for dimers and up to 1 wt % of surfactant for higher oligomers, which is in agreement with the viscometric studies addressed in chapter 2. This confirms again the absence of large, rod-like aggregates, hence contradicting the general theoretical predictions made for oligomeric surfactants [36]. The thickening power of certain oligomeric surfactants is not a common feature for this class of compound but is rather restricted to special molecular structures with very short flexible spacer groups (namely C₂ or C₃) [21].

Some qualitative information on the structure of the surfactant micelles can be obtained by comparing their ¹H-NMR spectra in water below and above the CMC [37] (see Table 3.1-3, Figures 3.1-4 and 3.1-5). For dimeric surfactants (except dimer **p-X-2** which is not soluble with 1 wt% in water at ambient temperature), only very small changes of the chemical shift are observed for the protons of the hydrophobic chains, whereas the protons in the vicinity of the hydrophilic ammonium group as well as in the spacer undergo more notable changes. For the monomeric reference **BDDAC**, these protons (included the protons of the benzyl moiety) feel a shielding upon micellization. In contrast in the case of all dimeric surfactants, these protons feel a deshielding upon micellization. The effect is the least pronounced for **EO-2**, i.e. the dimer with the flexible spacer group. This observation suggests a basically different conformational change occurring in the hydrophilic portion of dimeric surfactants compared to their monomeric analogs. Interestingly, the changes in the ¹H-spectrum of **m-X-2** (see Figure 3.1-5a) correspond closely to the ones reported for its octyl bromide analog upon micellization, whereas the changes in the ¹H-spectrum of **o-X-2** are much weaker [37]. This implies that the length of the hydrophobic alkyl chain can influence the conformation adopted by the spacer group in the micelle.

Table 3.1-3: $^1\text{H-NMR}$ data of dimeric surfactants (except **p-X-2**) at 0.03 wt% (below the CMC, value in upper row) and 1 wt% (above the CMC, value in lower row) in D_2O .

sur- factant	chemical shift of groups [in ppm]							
	CH_3-	$-(\text{CH}_2)_9-$	$-\text{CH}_2-\text{C}-\text{N}^+$	CH_3-N^+	$-\text{CH}_2-\text{N}^+$ (chain)	N^+-CH_2- (spacer)	$\text{O}-\text{CH}_2-$	$=\text{CH}-$
BDDAC	0.78	1.21	1.70	2.94	3.25	4.41		7.46-7.48
	0.82	1.19	1.69	2.95	2.99	4.39		7.34-7.42
i-B-2	0.79	1.20	1.72	2.99	3.25	4.02		6.27
	0.80	1.23	1.77	3.08	3.32	4.10		6.34
t-B-2	0.78	1.20	1.71	3.00	3.19	3.98		6.26
	0.80	1.22	1.71	3.09	3.22	4.07		6.34
EO-2	0.78	1.20	1.71	3.03	3.27	3.51	3.88	
	0.82	1.23	1.71	3.08	3.32	3.56	3.95	
o-X-2	0.76	1.18	1.74	2.88	3.25	*		7.65
								7.64-7.73
m-X-2	0.79	1.19	1.75	3.02	3.38	4.75		
	0.76	1.18	1.76	2.96	3.18	4.45		7.52-7.67
	0.76	1.16	1.76	3.06	3.17	4.54		7.53-7.76

* signal hidden by solvent signal at 4.689 ppm

These experiments were not performed with higher oligomers because they exhibit very low CMC-values, hence involving little amount of materials and longer accumulation in NMR. Nevertheless, one can expect similar effects as for dimers, i.e. conformational changes occurring in the hydrophilic group due to the presence of spacer groups, compared to standard monomeric surfactants.

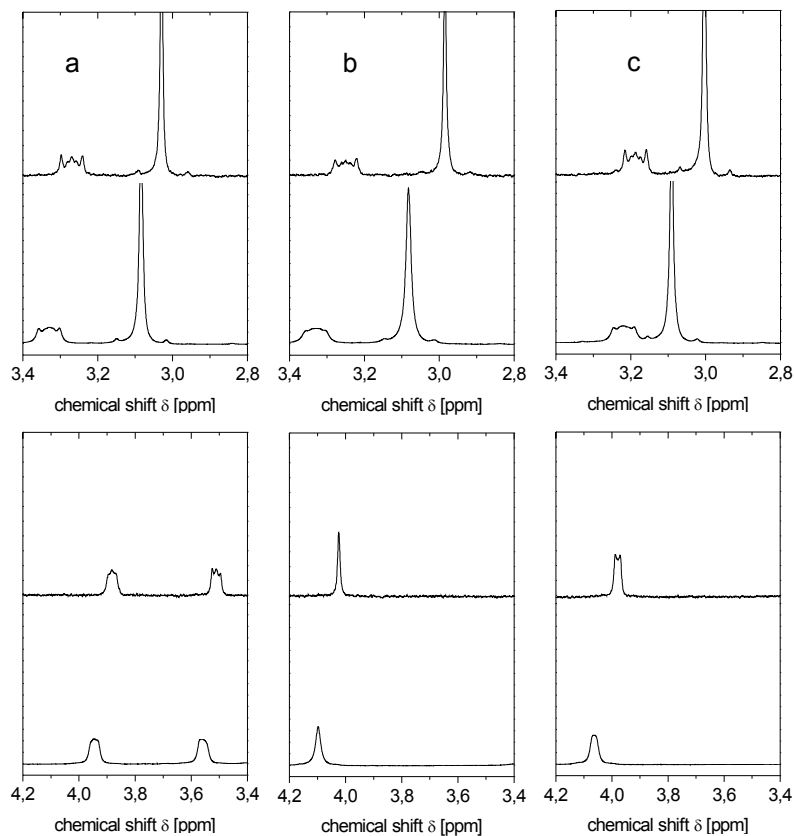


Figure 3.1-4: Selected parts of the ^1H -NMR spectra of dimeric surfactants in D_2O , at 0.03 wt% (below the CMC, upper graphs), and at 1 wt% (above the CMC, lower graphs). (a) = **EO-2**, (b) = **i-B-2**, (c) = **t-B-2**.

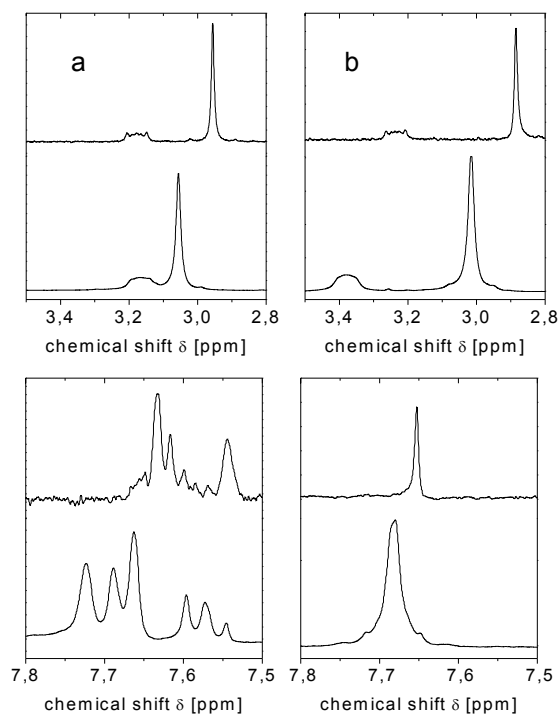


Figure 3.1-5: Selected parts of the ^1H -NMR spectra of dimeric surfactants in D_2O , at 0.03 wt% (below the CMC, upper graphs), and 1 wt% (above the CMC, lower graphs). (a) = **m-X-2**, (b) = **o-X-2**.

3.1.4 Micellar aggregation number [3]

3.1.4.a. Background

Here, the micelle aggregation numbers (N_{agg}) of the oligomeric surfactants are investigated. The aggregation number, i.e. the number of surfactants making up a micelle, is a structurally relevant parameter which contains indirect information on the micelle size and shape. The aggregation number is known to be affected by the chemical nature of the surfactant, its concentration [15], the temperature [38-41] and the addition of electrolytes [39, 42-44] or organic compounds [45-48]. Many methods can be used to determine the aggregation numbers [49], for instance, static light scattering (SLS), small angle neutron scattering (SANS) or fluorescence probing techniques. Light scattering requires extrapolation to low concentrations, close to the CMC (owing to intermicellar interactions) [50-51]. But by decreasing the concentration, the micelle size is possibly modified, as it is concentration dependent in most surfactant systems. Moreover, exploratory static light scattering measurements performed on micellar solutions of the surfactant dimer **EO-2** (in analogy to experiments reported in reference [51]) were unsuccessful as the intensities were too low for reliable analysis. Likewise, small angle neutron scattering (at high scattering vectors) allows the determination of micelle aggregation numbers and also yields information on the micelle shape in the actual experimental conditions [52]. Nevertheless, neutron scattering is very costly and the facilities are not generally available. Most problems evoked before can be avoided by using fluorescence probing methods [12, 33, 53-59]. This determination is affected neither by intermicellar interactions nor by the micellar shape. However, the fluorescence probes (and other necessary additives, such as quenchers) must be chosen carefully, and their concentration must be kept very low, in order to avoid possible changes of the micelle structure induced by the probe.

Steady-state fluorescence quenching (SSFQ) or time-resolved fluorescence quenching (TRFQ) can be applied. Both methods use a fluorescent probe, generally pyrene in the case of aqueous solutions, and an appropriate quencher of the probe. SSFQ involves measurements of the fluorescence emission intensity at increasing quencher concentration, using a spectrofluorometer. Since this apparatus is easily found in most laboratories, this method has been quite popular for determining N_{agg} -values in all types of surfactant-containing systems. Alternatively, TRFQ involves fluorescence decay experiments using single photon counting set-up. The decay curves are recorded in the presence of probe alone and in the presence of probe and quencher and are analyzed using an appropriate software with a nonlinear weighted least-squares procedure [42]. Performing and analyzing TRFQ measurements is more difficult compared to SSFQ experiments. Nevertheless, less restrictive assumptions are involved in TRFQ than in SSFQ from a theoretical point of view [12, 54-57, 60-62]. Alargova et al. pointed out and explained the discrepancies found between the results obtained from

SSFQ and TRFQ for various surfactant-containing systems [12]. They concluded that the range of aggregation numbers that can be explored with SSFQ is much more restricted than that with TRFQ.

Concerning the aggregation numbers of dimeric surfactants, much work has already been carried out [14, 33]. Quite complete sets of aggregation numbers were obtained for the so-called surfactant series m - s - m , which are bisquaternary ammonium bromide, with m representing the number of carbons comprised in the linear hydrophobic chain and s representing the number of methylene group making the flexible spacer. Aggregation numbers for the series 10- s -10 were determined by SANS [63-64]. It was found that the micelles are nearly spherical at concentrations close to the CMC and that the increase of N_{agg} with concentration is less pronounced as s increases. For the longer homologues 12- s -12, N_{agg} -values were obtained by TRFQ [65]. N_{agg} increases upon decreasing s , as reported for the 10- s -10 series and also for other series of gemini surfactants, namely 16- s -16 and the bis-anionic $\text{C}_{16}\text{H}_{33}\text{PO}_4^--(\text{CH}_2)_m-\text{PO}_4^-\text{C}_{16}\text{H}_{33}$, 2Na^+ (both studied by SANS) [66-68]. Aggregation numbers of two triquaternary ammonium surfactants (12-3-12-3-12, 3 Br^- and 12-3-12-3-12, 3 Cl^-) were also studied by TRFQ [69]. Interestingly, it was observed that an increase of the degree of oligomerization has the same effect as a decrease of the spacer carbon number s , i.e. a steeper micelle growth. Still, most studies on N_{agg} have dealt so far with surfactants (mostly dimers) bearing flexible spacer groups, but little has been done regarding oligomers with rigid spacer groups that may give rise to a completely different behavior. Moreover, the aggregation behavior of higher oligomers than dimers is virtually unknown.

The present study of aggregation numbers by TRFQ covers a larger set of molecules going from monomers to tetramers, which additionally have rigid spacer groups (except **EO-2**). It permits to focus both on the effect of the spacer and on the influence of the degree of oligomerization. Furthermore, 9,10 dimethylantracene is successfully used to replace pyrene as a fluorophore in the TRFQ experiments for the determination of micelle aggregation numbers. The different advantages of this probe will be presented.

3.1.4.b. Comments on the method and fluorophore

Most existing time-resolved fluorescence quenching experiments use pyrene as fluorescent probe (excitation wavelength: 335 nm; emission wavelength: 381 nm) [12, 49]. TRFQ procedures involving pyrene are well established and therefore continue to be intensively used nowadays. Nevertheless, the Laser techniques, to which the spectral features of pyrene were originally accommodated, have evolved over the years and consequently, other fluorescence probes may be more appropriate for TRFQ measurements with modern Lasers. In the experiments (see part 5.9), pyrene was substituted for another poorly water-soluble compound, namely 9,10 dimethylantracene, because

this probe seemed more suited to the set-up. Indeed, excitation of 9,10 dimethylantracene at 400 nm induces an intense fluorescence at 430 nm, as shown by the excitation spectrum in Figure 3.1-6, performed on a micellar solution of the standard surfactant **BDDAC**.

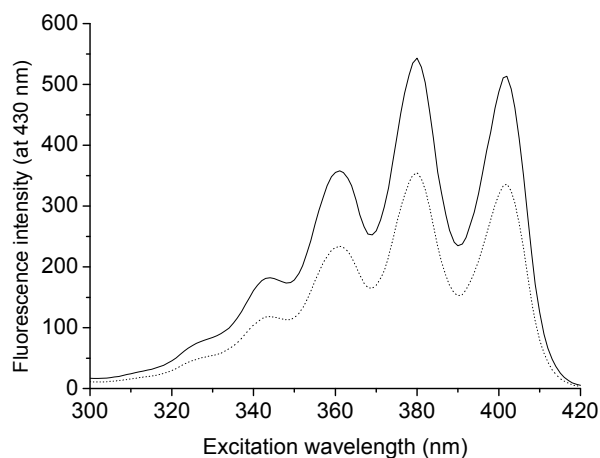


Figure 3.1-6: Excitation spectrum of 9,10 dimethylantracene (0.02 mmol/L) solubilized in a micellar solution of BDDAC (30 mmol/L) without quencher [solid line] and with quencher (1.2 mmol/L) [dotted line], taken at 430 nm.

More generally, spectral characteristics of 9,10 dimethylantracene are more appropriate than pyrene ones when modern solid lasers, such as frequency doubled Titanium / Sapphire (like in this work) or diode lasers are used. The fluorescence quantum yields of 9,10 dimethylantracene and pyrene, in polar solvents in the absence of oxygen, are close (respectively, 0.89 and 0.72), with a slightly higher efficiency for the first probe mentioned [70]. But when oxygen is present in the medium, the fluorescence of 9,10 dimethylantracene is much less sensitive to quenching than that of pyrene, giving rise to higher fluorescence intensities for 9,10 dimethylantracene. Furthermore, the latter fluorophore is less prone to aggregation due to its molecular structure (presence of methyl groups) and hence reduces the possibilities of excimer formation (self-quenching).

The toxicity of the fluorescence probe may be another relevant issue: in analogy to the differences of toxicity observed between toluene and benzene, 9,10 dimethylantracene is likely to be less toxic than pyrene, as the presence of the two CH_3 groups should facilitate its oxidation and subsequent elimination from the human body. In addition, it must be pointed out that fluorescence studies with this probe do not require obligatorily expensive equipment made of quartz (but allow for the use of glass), as they can be carried out in the visible range (excitation at 400 nm and emission at 430 nm, see Figure 3.1-6). The various practical advantages led to the use of 9,10 dimethylantracene as the fluorophore in TRFQ experiments, though hardly used in this context so far.

The luminescence of fluorophores can be partially or totally inhibited by quenchers. The tests made with the couple 9,10 dimethylantracene / 1-*n*-dodecyl pyridinium as fluorescent probe /

quencher were conclusive. For instance, the experimental and operating conditions were tested by measuring correct values of the aggregation number of two standard surfactants, namely sodium dodecyl sulfate **SDS** and dodecyl trimethyl ammonium chloride **DTAC** (reference “monomeric” surfactant in the study). As shown in Table 3.1-4, the average aggregation number of **SDS** was found to be 64 at a concentration of 0.095 M (literature value: 69 at 0.097 M [12]) and the N_{agg} of **DTAC** equaled 34 at a concentration of 0.104 M (literature value: 39 at 0.109 M [71]). The sample preparation and TRFQ experiment (equipment, equations used, etc.) are presented in more detail in the experimental part 5.9.

It was shown that the determination of aggregation numbers by TRFQ is not affected by the presence of dissolved oxygen [71]. Still, this was checked by comparing the N_{agg} -values obtained for solutions of the surfactant **BDDAC** in the presence of air or saturated with argon overnight which do not differ significantly ($N_{agg} = 14.2$ and $N_{agg} = 14.1$ respectively, at a concentration of 0.03 mol/L). Consequently, the experiments were performed without saturating the solution in argon or without removing air by freeze-pump-thaw cycles, prior to the decay measurements.

Table 3.1-4: Aggregation numbers of the studied series of oligomeric surfactants, expressed in number of dodecyl chains forming the micelles. The reproducibility of the experiment on the N_{agg} is ± 0.5 . CMC values were taken from Tables 3.1-1 and 3.1-2 [1-2], except for **SDS** which was taken from reference [12].

Surfactant	Concentration (moles of dodecyl chains / L)	Critical micellization concentration (mol/L)	Aggregation number (surfactants per micelle)	N_{agg} (dodecyl chains per micelle core)
SDS	0.095	0.008	64.1	64
DTAC	0.104	0.0215	34.3	34
BDDAC	0.110	0.0070	27.3	27
i-B-2	0.106	0.0018	16.1	32
t-B-2	0.104	0.0020	15.5	31
EO-2	0.108	0.0022	15.7	31
o-X-2	0.109	0.0012	12.7	25
m-X-2	0.109	0.0015	11.3	23
p-X-2	0.109	0.0021	10.5	21
t-B-3	0.038	0.00036	5.0	15
m-X-3	0.105	0.00028	5.4	16
p-X-3	0.105	0.00029	3.5	10.5
t-B-4	0.048	0.00012	3.8	15
p-X-4	0.034	0.0013	3.5	14

An example of decay curves without and with quencher is shown in Figure 3.1-7 for a micellar solution of **DTAC**. As can be seen, the photon accumulation is quite lengthy (max. intensity of 10^4) and the decay curve is recorded over a sufficiently long time (90 ns) to approximately reach the linear tail of the decay (intensity decreases over 3 decades to almost attain the level of the original

noise). These operating conditions are sufficient to perform a correct fitting of the curves and hence to get meaningful values. In Appendix 6, the fitted parameters (see equations in part 5.9) derived from the fluorescence decay curves of 9,10 dimethylantracene in micellar solutions are listed in Table A6-1, and other examples of fluorescence decay curves are shown in Figures A6-1 – A6-4.

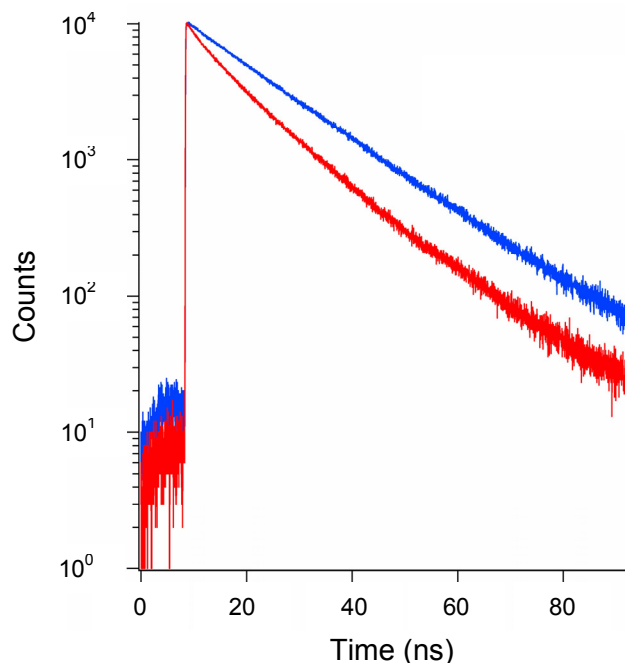


Figure 3.1-7: Example of decay curves for a micellar solution of **DTAC** (70 mmol/L) without quencher (upper curve) and with quencher (lower curve).

3.1.4.c. Discussion

Aggregation numbers

The aggregation numbers of the studied oligomeric surfactants are listed in Table 3.1-4, as well as the number of dodecyl chains making up a micelle core to facilitate comparisons. A first look at the results shows that the N_{agg} values are quite small (< 40 for solutions of ca. 3 wt %). This is mainly due to the use of chloride as counterion. Indeed, chloride counterions are less bound to the cationic head-groups (higher ionization degree) than their bromide counterparts [72], resulting in a stronger electrostatic repulsion of the hydrophilic heads as well as a steric hindrance due to higher hydration of the latter. Both effects can explain the lower N_{agg} values. Thus, for example, the substitution of the bromide counterions by chloride counterions in the so-called bisquaternary ammonium “12-*s*-12” series resulted in a significant decrease of N_{agg} [65, 69]. Also, the low values of aggregation number obtained at such concentrations (ca. 3 wt %) suggest that aqueous solutions of these surfactants essentially contain spherical micelles. This is in agreement with dynamic light scattering and viscometric measurements performed before on these systems [1-2]. One can also

notice that the surfactant **BDDAC** has an aggregation number smaller than that of the other reference surfactant **DTAC** (respectively, 27 and 34 at a C_{12} concentration of 0.1 M). This result is not surprising if the second smaller hydrophobic chain of **BDDAC**, namely the benzyl group which also makes up the micelle, is considered. On the one hand, the supplementary benzyl group makes the surfactant more hydrophobic, explaining the lower CMC value of **BDDAC** compared to **DTAC** [1]. On the other hand, the more polar benzyl groups is expected to lay in the outer layer of the micelle, seemingly involving an additional hindrance between the head-groups and a higher curvature of the interface, which can account for the lower N_{agg} compared to **DTAC**.

Effect of the concentration

Although this study is mainly focused on concentrated surfactant solutions (3 wt %), it was interesting to have an idea of the concentration effect on the aggregation numbers of oligomeric surfactants. Thus, TRFQ experiments were carried out by varying the concentration C for some surfactants, namely **DTAC**, **BDDAC**, **t-B-2**, **EO-2** and **p-X-2**. As shown in Figure 3.1-8, aggregation numbers increase with concentration for the studied surfactants, as typical for conventional ionic surfactants (chemical potential changes with C) [15, 73-74]. Nevertheless, the observed micelle growth is limited since the values of N_{agg} are low even at high concentration (3 wt %). Note that in previous studies [15, 69] the increase of N_{agg} with the concentration was found to be much more marked for gemini surfactants having shorter spacer groups. Though the examples studied here seem to exhibit the same tendency (e.g. compare **t-B-2** and **p-X-2** traces in Figure 3.1-8), the effects are much smaller and the few data are not sufficient to allow a general statement.

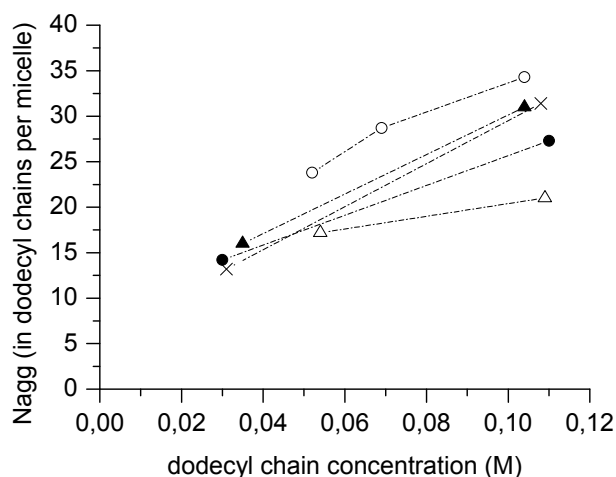


Figure 3.1-8: Micelle aggregation number N_{agg} as function of dodecyl chain concentration. (O) = **DTAC**, (▲) = **t-B-2**, (X) = **EO-2**, (●) = **BDDAC**, (△) = **p-X-2**; Dotted lines are a guide for the eyes.

Effect of the spacer

As regards the influence of the spacer, it is known that the length of the spacer plays a major role on the aggregation number of oligomeric surfactants. Generally, the shorter the spacer, the larger N_{agg} -values are [15, 63-65, 75]. For the dimeric surfactants, the spacer groups employed, namely isobutenylene, trans-1,4-buten-2-ylene, o-xylylene, m-xylylene, and p-xylylene, are hydrophobic and also rigid, thus fixing chemically the distance between the cationic groups within the same molecule. In contrast, the spacer group diethylether is less hydrophobic and very flexible. As shown in Table 3.1-4, for dimers at a concentration of 0.1 M of dodecyl chains, N_{agg} decreases with **i-B-2** > **EO-2** \geq **t-B-2** > **o-X-2** > **m-X-2** > **p-X-2** from 32 to 21 dodecyl chains. This is roughly consistent with the increase of the spacer length as can be seen on Figure 3.1-9, where the maximal length of each spacer was calculated (see experimental part 5.10).

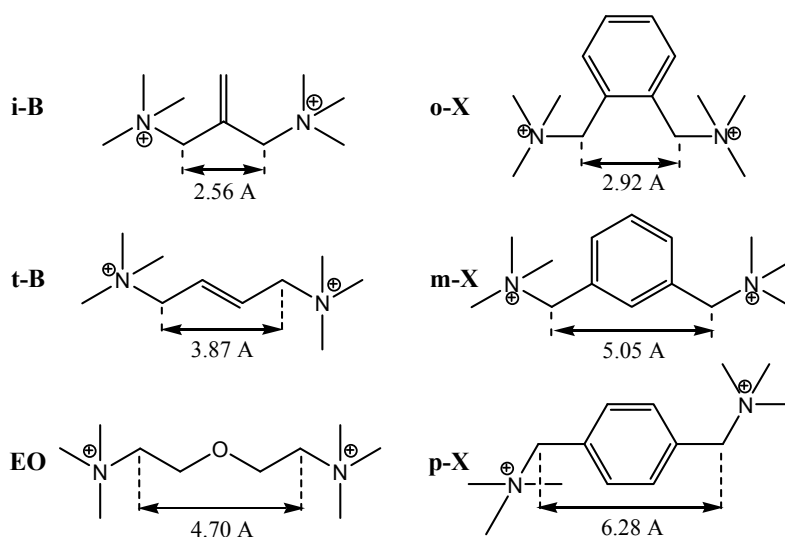


Figure 3.1-9: Calculated maximum length of the spacers involved in the oligomeric surfactant series.

The position of **EO-2** in the series can be explained by the fact that the diethylether spacer is a flexible spacer and therefore the calculated length (see Figure 3.1-9) may overestimate the true average distance. The higher flexibility and the reduction of the Coulombic repulsion between head-groups due to the better hydration around the spacer allow the long hydrophobic chains to pack more tightly, and hence to form larger aggregates [15]. The chemical nature of the spacer has also an impact on the N_{agg} as shown by the position of **o-X-2** in the series. Indeed, if the spacer length was the only parameter to influence the aggregation number, then **o-X-2** would be placed just after **i-B-2** (see Figure 3.1-9). Thus, it seems that other parameters are involved, too. Xylylene spacer could cause an additional steric hindrance hence reducing N_{agg} [15], in analogy to the differences observed for **DTAC** and **BDDAC**.

In Figure 3.1-10, aggregation numbers are plotted against the calculated maximum spacer length, for each set of isomeric dimers (namely isomers of butenylene and of xylylene). Interestingly,

the decrease of N_{agg} vs spacer length is virtually linear for the dimeric surfactants bearing xylylene spacer groups (**o-X-2**, **m-X-2**, **p-X-2**). For the butenylene series, the decrease of N_{agg} by going from iso-butenylene to the longer trans-butenylene spacer group is also evident. As already implied in the discussion above, the N_{agg} found for **EO-2** with the diethylether spacer (whose length is equivalent to a chain of five carbons) is higher than the value obtained by extrapolating the behavior of the butenylene spacer to a length of five carbons. This finding may seem surprising at a first look. As the diethylether spacer is more polar and less hydrophobic than a hypothetical pentenylene spacer, the micelles would be expected to have a higher curvature and thus be smaller, if there is a difference. The higher value of N_{agg} found is attributed to the different flexibility of the spacers, as already discussed above, namely to the discrepancy between calculated length of the EO spacer in the maximum stretched conformation and the true distance in the micelle due to its flexibility.

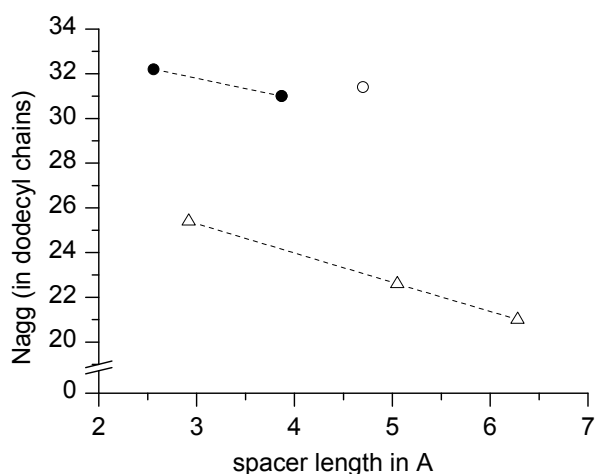


Figure 3.1-10: Micelle aggregation number N_{agg} as function of the spacer length for the sets of isomeric gemini surfactants, at a dodecyl chain concentration of ca. 0.1 M. (●) = butenylene spacer groups, (O) = diethylether spacer, (Δ) = xylylene spacer groups. Dotted lines are a guide for the eyes.

The increase of N_{agg} -values while decreasing the spacer length in each set of isomeric dimers suggests a denser packing of the surfactants with short spacer groups. This correlates with the surface tension values measured at the CMC for these series (i.e. $\sigma_{cmc} [\mathbf{o-X-2}] < \sigma_{cmc} [\mathbf{m-X-2}] < \sigma_{cmc} [\mathbf{p-X-2}]$ and $\sigma_{cmc} [\mathbf{i-B-2}] < \sigma_{cmc} [\mathbf{t-B-2}]$), which increase from 37 mN/M to 45 mN/m, and from 39 mN/M to 42 mN/M, respectively (*vide supra*) [1].

In the past, the aggregation of dimeric surfactants with octyl chains and isomers of xylylene spacer (i.e. homologues of **o-**, **m-** and **p-X-2** with bromide counterions) had been investigated [76]. At a concentration of 2.5 wt %, the surfactant with the ortho-xylylene spacer formed micelles whereas the meta-xylylene and para-xylylene surfactants gave rise to only very small aggregates with values for N_{agg} of 3-4. Here, the studied surfactants all form micelles due to the longer hydrophobic chains, but it is also found that **o-X-2** has a higher N_{agg} compared to **m-X-2** and **p-X-2** (with $N_{agg} (\mathbf{m-X-2})$ slightly higher than $N_{agg} (\mathbf{p-X-2})$).

For the higher oligomers (especially trimers), the following sequence is also observed: $N_{\text{agg}}(\mathbf{t-B}) > N_{\text{agg}}(\mathbf{m-X}) > N_{\text{agg}}(\mathbf{p-X})$. Obviously as for the dimers, the shorter the spacer, the better the packing and consequently the larger N_{agg} -values are.

Effect of the degree of oligomerization

It is seen in Table 3.1-4 that an increase in the degree of oligomerization involves a decrease in the aggregation numbers. For instance at a fixed concentration of ca. 0.1 M, N_{agg} decreases respectively with **BDDAC** (27.3), **m-X-2** (22.6) and **m-X-3** (16.2) for the m-xylylene spacer series. In the same way, N_{agg} decreases with **BDDAC** (27.3), **p-X-2** (21.0) and **p-X-3** (10.5) for the p-xylylene spacer series. For the t-butenylene spacer series, the following values are obtained: respectively, 23.8 for 0.05 M **DTAC**, 16.0 for 0.035 M **t-B-2**, 15.0 for 0.04 M **t-B-3**, and 15.2 for 0.05 M **t-B-4**. This means that N_{agg} also decreases with the degree of oligomerization but apparently in a less pronounced way (at this lower concentration). Presumably shorter spacers limit the decrease of N_{agg} .

This finding is contrary to that obtained with the most studied oligomeric surfactants of the "m-s-m" type, i.e. quaternary ammonium with alkylene spacers, which give rise to higher N_{agg} while increasing the oligomerization degree. But, those surfactants are structurally quite different insofar as they possess shorter flexible spacers (generally C₂ to C₄) and give rise to another kind of micelles at lower concentration range, namely cylinders (rod-like micelles). For example, the aggregation behavior of the surfactant trimer "12-3-12-3-12" was investigated by TRFQ [69]. The results showed a very strong tendency to micelle growth, much stronger than for "12-3-12", but similar to that of "12-2-12". Thus for this type of surfactants, an increase of the degree of oligomerization has the same effect as a decrease of the spacer carbon number (spacer length), that is, aggregation numbers become larger. In the present case, the different result, i.e. a decrease of N_{agg} with increasing degree of oligomerization, could be due to the fact that further addition of long rigid spacers between the head-groups reduces the overall flexibility of the structures and hence, makes it difficult for the higher oligomers to pack tightly. Consequently, the formed aggregates contain fewer dodecyl chains.

Noteworthy, the tetramer **p-X-4** seems to behave differently. Indeed, at a concentration of 0.03 M of dodecyl chains, $N_{\text{agg}}(\mathbf{p-X-4})$ equals 14.0, whereas the trimer **p-X-3** already has a lower aggregation number of 10.5 at a concentration of 0.10 M. In the previous part, the anomalous behavior of **p-X-4** was pointed out [2]. In fact, unlike the other studied surfactant, this tetramer does not have an obvious CMC but seems rather to form pre-micellar aggregates at low concentrations. Thus, it is not surprising to find a discrepancy in the N_{agg} with this compound.

3.1.5 Formation of microemulsions

3.1.5.a. Background

Microemulsions are transparent, isotropic, thermodynamically stable dispersions of two immiscible fluids, commonly water and oil, stabilized by amphiphilic molecules [77-79]. In many cases, short-chain alcohols, which are referred to as co-surfactants, are added to the mixture to enhance the solubilization properties of the surfactant molecules [80]. Microemulsions differ from (macro)emulsions insofar as they are thermodynamically stable systems (i.e. at equilibrium), while (macro)emulsions are metastable (or kinetically stable). In addition, microemulsion systems usually involve smaller structures, with droplet sizes from 10 to 100 nm.

From a structural point of view, microemulsions are formed by very small dispersed droplets of one phase in an external phase, with a monomolecular layer of amphiphilic molecules at the interface. Different types of microemulsions can be formed with surfactant-water-oil mixtures depending on the dispersed phase. An oil-rich microemulsion where water is the dispersed medium is commonly called water-in-oil (W/O) microemulsion or inverse-microemulsion (or else L_2 phase). Alternatively, a water-rich mixture where the oil is the dispersed medium is referred to as oil-in-water (O/W) microemulsion or direct microemulsion (or else L_1 phase). Noteworthy, a microemulsion in which the oil and water are intimately mixed (i.e. where both solvents form extended domains over macroscopic distances) is called bicontinuous microemulsion and is often represented by a sponge-like structure (the overall spontaneous curvature of the interface is zero).

Reports on the use of surfactant oligomers in microemulsions are relatively scarce and limited to dimeric surfactants. For example, polymerization of styrene was carried out in direct microemulsions formed by cationic gemini surfactants with oligo(oxyethylene) spacer groups, allowing to tune the size of the spherical particles with varying spacer length [81-82]. Also, phase diagrams were established for an anionic gemini surfactant, namely didodecyldiphenylether disulfonate, within the system surfactant/water/toluene/1-propanol and were compared to those obtained with the structurally related monomeric surfactants monododecyldiphenylether disulfonate and monododecyldiphenylether monosulfonate [83-84]. The dimeric surfactant showed a reduced isotropic microemulsion phase compared to the latter monomeric surfactant. Furthermore, Kunieda et al. reported on microemulsions and the phase behavior of the anionic gemini surfactant sodium 1,2-bis(*N*-dodecanoyl-alanate)-*N*-ethane (see Figure 2.2-1.h) [85].

Nevertheless, the effect of the spacer group and of the degree of oligomerization on the microemulsion formation has not been explicitly addressed yet. Here, these effects will be examined concerning the formation of inverse (W/O) microemulsions with the system surfactant/water/toluene/pentanol, already reported in the literature [86-89]. This four-component

system is reduced to a pseudo-ternary one by taking a mixture of the oil (toluene) and co-surfactant (pentanol) with a fixed ratio 1:1 (v/v).

3.1.5.b. Effect of cationic dimers on the formation of an inverse microemulsion

Partial pseudo-ternary phase diagrams were determined for the various cationic dimeric surfactants and their analogous monomeric counterpart **DTAC**, as described in the experimental part **5.11**. The oil-rich corner of the phase diagram, i.e. where the W/O microemulsions form, was explored. Note that these experiments consume large amounts of surfactant material and therefore, only the phase diagrams for the surfactant dimers were done, which still permits to see the influence of the dimerization as well as the influence of the spacer group on the formation of the inverse microemulsion (area and position). The different partial ternary phase diagrams thus obtained are represented in Figure 3.1-11.

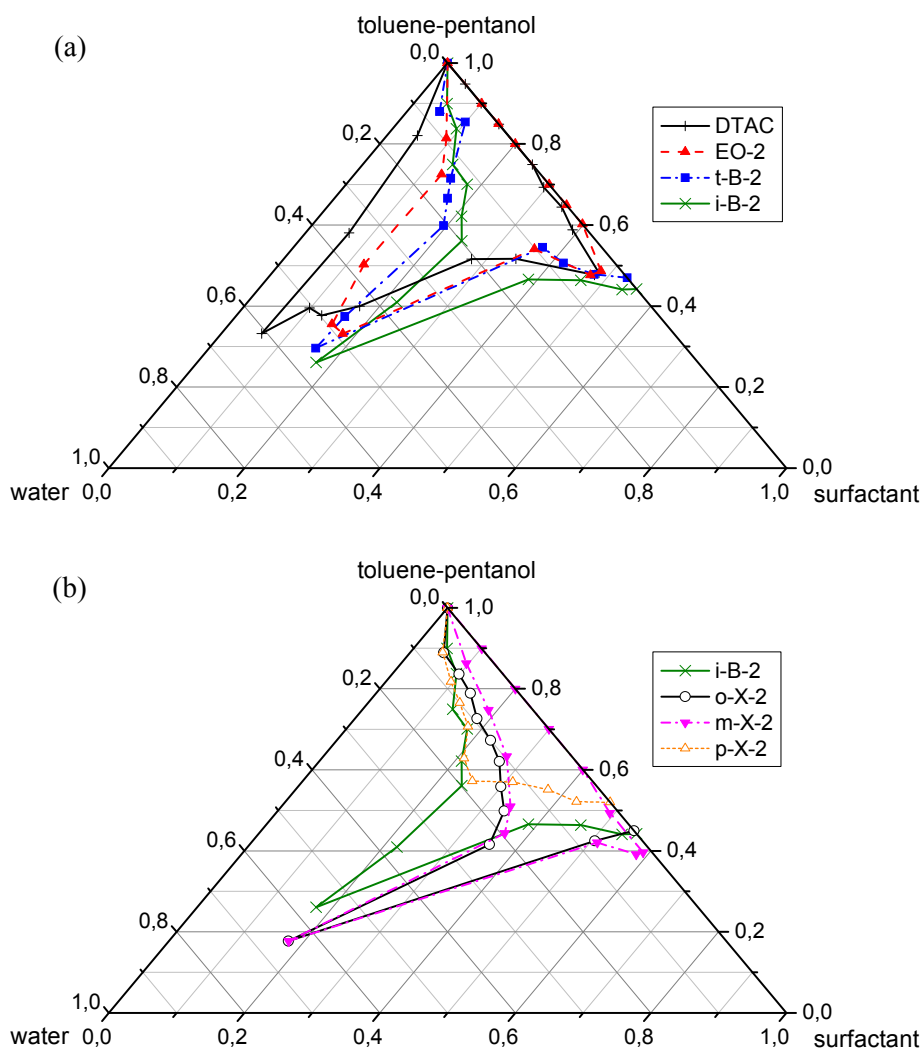


Figure 3.1-11: Partial ternary phase diagrams (in weight) for the system surfactant/water/toluene-pentanol (1:1 v/v); (a): **DTAC**, **EO-2**, **i-B-2**, **t-B-2**; (b): **i-B-2**, **o-X-2**, **m-X-2**, **p-X-2**. The delimited areas correspond to the L₂ phases (or W/O microemulsions).

Compared to the surfactant monomer **DTAC**, the studied surfactant dimers involve a reduction of the area of the optically-clear W/O microemulsion (except dimer **EO-2**), as well as a shift of the delimited zone towards the surfactant corner. Also, the effects of the spacer group are notable. Within the series of dimeric surfactants with the butenylene isomeric spacer groups, it is seen that the shorter iso-butenylene spacer displaces the region towards the surfactant corner (see Figure 3.1-11.a). For the series with the xylylene spacers, the spacer length is important, too (see Figure 3.1-11.b). At first sight, it does not seem to influence so much the extent of the shift as for the other series (see regions of **o-X-2** and **m-X-2** which superimpose). Nevertheless, the area is already strongly shifted for these surfactants with hydrophobic xylylene spacers. Noteworthy, for the **p-X-2** with the longest spacer group, the area of the inverse microemulsion is sharply reduced. In this case, the surfactant **p-X-2** does not behave at all like the other dimeric surfactants, as already noticed e.g. for the Krafft temperature.

Comparing the nature of the spacer group, i.e. comparing the two dimeric series with each other (aliphatic spacers and aromatic spacers), it is noted that more hydrophobic spacer groups (and sterically more hindered) involve a further shift of the microemulsion phase towards the surfactant rich part of the diagram (see position of the microemulsion area for **i-B-2** and **o-X-2** in Figure 3.11-1.b, respectively). Moreover, this is consistent with the shift observed when the polar diethylether spacer is replaced by the more hydrophobic trans-butenylene spacer within the aliphatic spacer series (see Figure 3.11-1.a).

The flexibility or rigidity of the spacer group seems also to be an important parameter. With the surfactant **EO-2** (bearing the more flexible diethylether spacer), almost no reduction (or slight reduction) of the microemulsion region is observed, whereas with all other surfactant dimers (having rigid spacer groups) the diminution of the region is significant, in comparison to the behaviour seen for the monomeric surfactant **DTAC**. The interfacial film formed by the surfactant monomer **DTAC** (and co-surfactant pentanol) is a priori the less rigid one, which is generally favourable for the formation of microemulsions (with high droplet curvatures) [90]. In contrast, by dimerizing the surfactant fragments via rigid spacers, the overall interface flexibility is decreased, diminishing the solubilization capacity of the microemulsion and hence its area on the phase diagram. A recent study supports these conclusions [85]. The studied dimeric surfactant sodium 1,2-bis(*N*-dodecanoylalanate)-*N*-ethane (see Figure 2.2-1.h) shows a very narrow single microemulsion phase compared to that of the monomeric surfactant analog sodium *N*-dodecanoyl-*N*-methyl β -alanate, for the investigated pseudo-ternary system (surfactant / hexanol / dodecane : 3 % NaCl aq 1:1 w/w), and presents a lamellar liquid crystal region instead. This behaviour was accounted for by the increased rigidity of the gemini surfactant layer [85].

A shift of the W/O microemulsion region towards the surfactant-rich corner reflects the need of more surfactant molecules to incorporate a defined amount of water. Presumably, this behaviour can be rationalized by the reduction of the hydration shell of the surfactant head-groups, since the shift coincides either with a decrease of the spacer length or with an increase of the spacer hydrophobicity. Hence, more surfactant is needed to incorporate water in the inverse micelles when “less hydrophilic” head-groups are implied (slightly modified hydrophilicity due to the spacer group used).

3.2 Properties of the new anionic gemini surfactant

In this section, the main properties of the novel anionic dimeric surfactant in aqueous solution are examined. For comparison, sodium laurate (**SL**, $C_{11}H_{23}COONa$) which is a common carboxylate surfactant will be studied. The use of sodium laurate as a reference “monomeric” surfactant is an approximation since the surfactant unit in the dimer comprises an amide group and an additional amine in its chemical structure. Nevertheless, it allows to derive reasonable comparisons between carboxylate amphiphiles having dodecyl hydrophobic tails. Noteworthy, sodium myristate ($C_{13}H_{27}COONa$) with a longer alkyl chain exhibits a high Krafft point (39 °C [91]), hence making it difficult to use it for comparative experiments. On the other hand, amino-acid based surfactants such as e.g. sodium lauroyl sarcosinate ($C_{11}H_{23}CON(CH_3)CH_2COONa$) could alternatively be considered as reference surfactants for the study. Yet, the chemical structure of the latter does not correspond to a true monomer of the anionic gemini based on EDTA.

3.2.1 Krafft temperature

The synthesized anionic dimeric surfactant based on EDTA (neutralized by an equivalent amount of sodium hydroxide) is soluble in water at room temperature (pH = 7-8) and, as found previously for the studied cationic dimeric surfactants, has a Krafft-temperature below 0 °C. This low Krafft point permits the use of this amphiphile in cold water. In comparison, sodium laurate exhibits a higher Krafft-temperature of about 21.5 °C [91].

3.2.2 Surface activity and micellization

The surface-active behaviour of **dimer EDTA** is illustrated in Figure 3.2-1, and the characteristic parameters derived there from are listed in Table 3.1-1. The surface tension curves present virtually no minimum, indicating the high purity of the substances [10]. **Dimer EDTA** form micelles at room temperature, at pH 7-8 and pH 12, with values for the critical micellization concentration (CMC) of 0.02 and 0.03 mmol/L (corresponding to 0.015 g/L and 0.020 g/L), respectively. These CMC values are considerably lower than that of the carboxylic type reference surfactant “monomer” sodium laurate (**SL**: 20.0 mmol/L or 4.4 g/L at pH = 10 [92]), as well as that

sodium *N*-dodecanoyl-*N*-methyl- β -alanate $C_{11}H_{23}CON(CH_3)CH_2CH_2COO^-Na^+$ (7.6 mmol/L or 2.3 g/L at pH 10.5) [93]. This result is in agreement with the various reports comparing monomeric and dimeric surfactants [11], as well as with the previous observations made with the studied cationic dimers (*vide supra*).

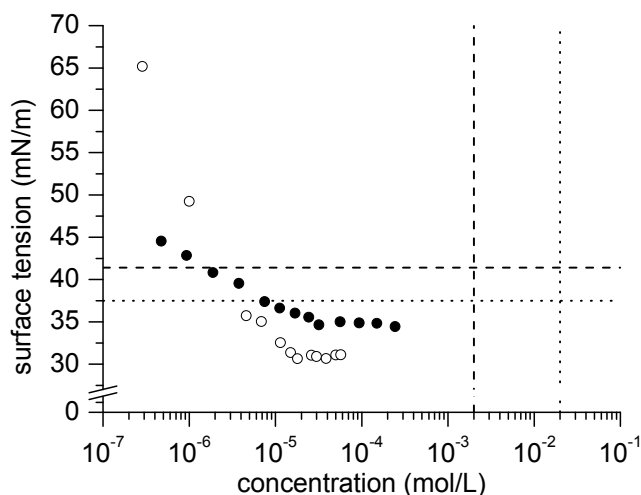


Figure 3.2-1: Surface tension vs. concentration curves of surfactant **dimer EDTA** at neutral pH (o) and pH = 12 (•). Vertical and horizontal lines are a guide for the eyes, positioning CMC- and σ_{cmc} -values respectively of reference surfactants: **SL** at pH = 10 (.....) and **t-B-2** (----).

Table 3.2-1: Surface activity and micellization data of surfactant dimer based on EDTA and reference carboxylic type surfactant “monomer” (sodium laurate). Data for cationic dimer **t-B-2** are also listed for comparison (see 3.1.2.a).

Surfactant	T_{Krafft} [°C]	CMC ^a [g/L]	CMC ^a [mmol/L]	σ_{cmc} ^a [mN/m]	CMC ^b [mmol/L]
SL	21.5 ^e	4.4 ^f	20 ^f	37.5 ^f	
dimer EDTA ^c	< 0	0.015	0.02	31	0.06
dimer EDTA ^d	< 0	0.020	0.03	35	
t-B-2	< 0	1.1	2.0	41.4	

^a = measured by tensiometry (Du Noüy ring method)

^b = measured by probe solubilization method (benzoylacetone)

^c = measured at pH = 7-8 (neutralized compound redissolved in water)

^d = measured at pH = 12 (phosphate buffer: $[Na_3PO_4] = 0.01$ M)

^e = value taken from ref. [91]

^f = measured at pH = 10, value taken from ref. [92]

Noteworthy, the CMCs found for the new compound are extremely low, but still lie in the same range as those found for other carboxylate gemini surfactants with dodecyl chains. For instance, 1,2-bis (*N*- β -carboxypropanoyl-*N*-dodecylamino)ethane (see Figure 2.2-1.i) exhibits a CMC value of 0.01 mM at pH = 11-12 [94]; the CMC value of *N,N'*-ethylenebis(sodium *N*-dodecanoyl- β -alanate)

(see Figure 2.2-1.h) is 0.04 mM at pH 10.5 [93]. The sodium salt of bis(1-dodecenylsuccinamic acid) (see Figure 2.2-1.g, with $n = 2$) has a CMC-value of 0.1 mmol/L at pH 10 [95], while the sodium salt of N,N'-didodecanylethylenediamine-N,N'-diacetic acid (see Figure 2.2-1.f) has a CMC-value of 0.25 mmol/L [96].

Compared to the studied cationic dimers, **dimer EDTA** shows a much lower CMC-value (as seen in Figure 3.2-1 and Table 3.2-1), which may be interesting e.g. for the solubilization of hydrophobic substances at low surfactant content.

In the strong basic environment created by the phosphate buffer (pH = 12), most of dimer EDTA molecules are fully deprotonated as divalent anions. In contrast, when the neutralized compound is dissolved as such in milliQ water, the pH value obtained lies between 7 and 8, which means that many surfactant molecules are monoprotinated in solution (as determined by acido-basic titration in chapter 2). Hence, a majority of the surfactant molecules possesses a zwitterionic unit and an anionic one. Nevertheless, the CMC values determined at different pH are similar (the CMC at pH 7 being slightly lower than that at pH 12). Recently, the CMC-values of a carboxylic acid type gemini surfactant (see anionic dimer “i” in Figure 2.2-1, with $n = 8$ and a propan-2-ol spacer group) found at pH 7 and pH 12 were also nearly alike [97].

Additionally, the CMC value of **dimer EDTA** at about neutral pH was determined by the probe solubilization method, as the surface tension isotherm was not fully conclusive (probably reflecting incomplete neutralization). The method is based on the keto-enol tautomerism of benzoylacetone (see 5.12) [98]. Typically when a surfactant is added, a sharp increase in the absorbance of the enol form (at 315 nm) is observed above the CMC, whereas the absorbance of the keto form (at 250 nm) decreases. This allows a very accurate CMC determination for common ionic surfactants. Thus, the absorbance of aqueous solutions of benzoylacetone at 315 nm was determined as a function of the concentration in **dimer EDTA**. The corresponding plot is shown in Figure 3.2-2.

The CMC is taken as the onset of the increase in the absorbance trace and is estimated to be equal to 0.06 mmol/L, which corroborates well the surface tension experiments within experimental errors. At such low concentrations, a slight difference in the CMC values determined by different techniques is not surprising.

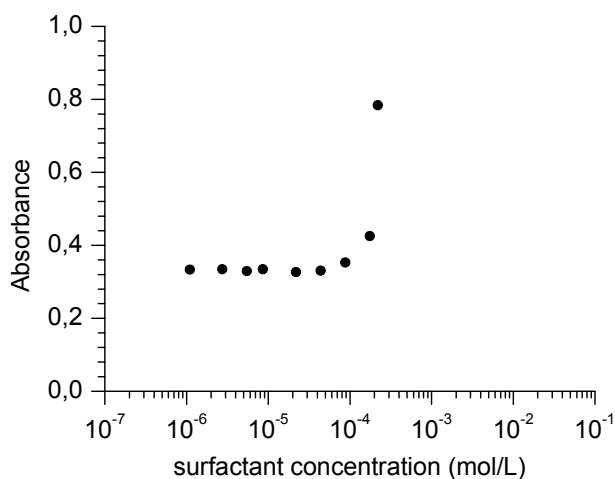


Figure 3.2-2: Evolution of the absorbance of the enol form of benzoylactone at 315 nm in aqueous solution (0.001 wt %) with increasing concentration of surfactant dimer EDTA.

For further comparison, other methods to determine the CMC value of **dimer EDTA** at pH 7-8 were tried. First, conductivity measurements were performed on aqueous solutions of this surfactant, but were unsuccessful as the conductivity values detected were very low (<10 μS), rendering the experiment unreliable. Also, DLS measurements were carried out over a wide range of concentrations but the scattering signal became already too low from concentrations supposed to be above the CMC determined by other techniques, making the method invalid for CMC determination.

Comparing the surface activity, it is found that the surface tension at the CMC (σ_{cmc}) of **dimer EDTA** is lower than that of surfactant monomer sodium laurate (in particular at pH values where most of both surfactant molecules are completely neutralized). Hence, the dimeric compound is quite effective at reducing the surface tension of water (which is even more noticeable for the dimer at neutral pH), which may be of interest e.g. for wetting processes. Also, the σ_{cmc} -value increases with pH (compare values in Table 3.2-1 at pH 7-8 and pH 12), as generally emphasized for carboxylic acid based surfactants [97, 99]. Assumingly, this reflects a tighter packing of the hydrophobic chains at the surface which may be explained by a change in the electrostatic repulsion between the molecules. Partial protonation of the molecules occurs in fact at pH 7-8, producing amphoteric surfactant fragments which may imply less repulsion between the surfactant head groups.

This is correlated by the comparisons of the slopes of the isotherms below the CMC. Indeed, according to the Gibbs equation, the minimum surface area occupied by a surfactant is inversely proportional to $\frac{\partial \sigma}{\partial \ln C}$ (see chapter 1). Here, the slope for **dimer EDTA** at pH 7 is steeper than that for **dimer EDTA** at pH 12, hence reflecting the smaller area occupied by the surfactant at the surface. Note that such difference in the slopes with pH was reported previously [97].

3.2.3 Dynamic light scattering and viscosity

Dynamic light scattering of solutions of dimer EDTA, either at pH 7-8 (neutralized product redissolved in MilliQ water) or at pH 12 (neutralized product redissolved in a phosphate buffer) showed only the presence of very small aggregates i.e. of 3 nm diameter or smaller, up to 5 wt % of surfactant without the addition of salts. In agreement with this result, the solutions did not reveal any strong thickening behavior due to the formation of entangled cylindrical micelles, as typically observed with a special gemini structure, namely quaternary ammonium bromides with ultra short alkyl spacer groups (see 3.1.3 above, as well as “properties of geminis” in 1.2.2.c).

Note that the presence of vesicular aggregates was recently reported for a carboxylic acid type gemini surfactant in aqueous solution (see anionic dimer “i” in Figure 2.2-1, with $n = 8$ and a propan-2-ol spacer group) when the pH drops from 12.0 to 7.0 [97]. It is well known that surfactants based on carboxylic acid (e.g. alkali-metal alkanoates such as decanoate or oleate) usually form micelles above the CMC at alkaline pH but start forming vesicles as the pH decreases (towards the pK_a) [100-101]. Such behaviour was not observed in this work, as the hydrodynamic diameters found in DLS with decreasing pH remain in the same range. This is presumably due to different protonation mechanisms. The supplementary amine groups (more basic than carboxylate groups) in the structure of the dimer based on EDTA get protonated with decreasing pH (see discussion of the acid-base titration in chapter 2). At pH values 7-8, most of the compound is mono-protonated, hence one surfactant fragment possesses a zwitterionic head-group and the other fragment has an anionic one. This system can be compared with mixtures of zwitterionic and anionic surfactant monomers which are often compatible and form mixed micelles [102]. In contrast, the carboxylic acid based gemini surfactant is singly protonated as monovalent anions at pH 7.0 [97], with hydrogen bonds between the carboxylic head-groups which generate a polymeric type of complex stabilizing the bilayer structure.

It is notable that when the pH of an aqueous solution of **dimer EDTA** is further decreased to pH 5, the solution appears bluish and a particle diameter of 38 nm can be measured via DLS. This is probably due to some insoluble particles which start forming in solution (the doubly protonated surfactant is dominant at this pH), as the compound precipitates at pH values below ca. 5 (see part 2.2.3.b).

3.2.4 Solubilization capacity in micellar environment

The low critical micellization concentration of the anionic EDTA based gemini (in aqueous solution around neutral pH) is likely to allow the solubilization of hydrophobic probes in the micelles at low surfactant content. This makes the latter amphiphile quite advantageous compared to conventional low molar-mass surfactants displaying higher CMC values. Still, it is of interest to

examine the ability of the new gemini to solubilize poorly water-soluble compounds at a given concentration above the CMC and compare this capacity with that of standard and other gemini surfactants in order to see if an enhancement is observed indeed.

The solubilization capacity is a key feature of surfactants. Usually, a marked solubilization effect is observed in aqueous solutions at concentrations only above the CMC [103]. Improved solubilization capacities were discussed for dimeric surfactants [53, 104-106], but the reports on the solubilization capacity of surfactant oligomers are scarce so far. The spacer group seems to influence the capacity, but no uniform picture has emerged yet. Whereas in some cases, an optimum length of the spacer was found for dimeric surfactants at intermediate spacer lengths (C₈-C₁₀) [81, 107], three other reports revealed decreasing capacity with increasing spacer length [1, 82, 106]. In contrast, increasing capacity was found with increasing spacer length, in another study [105]. Recently, the solubilization ability of series of cationic oligomeric surfactants (from monomers to tetramers) was examined [2]. In particular, the solubilization capacity of hydrophobic probes was found to be slightly improved with increasing the degree of oligomerization for a given spacer group. Also, the chemical nature of the spacer was preponderant, i.e. the results depend mainly on the couple surfactant – solubilizate used, as generally emphasized [103].

Using ¹H-NMR spectroscopy, preliminary quantitative solubilization studies with the hydrophobic probes *para*-xylene were performed for concentrated surfactant solutions (10 g/L), as described in the experimental part 5.13. The solubilization capacity of the surfactant **dimer EDTA**, as well as surfactant monomers (**sodium laurate**, **sodium dodecyl sulfate SDS**, **DTAC**) and surfactant dimers (**o-X-2**, **EO-2**) are listed in Table 3.2-2. The capacities are expressed in number of *p*-xylene molecules solubilized per surfactant molecule and per alkyl chains for significant comparisons.

Table 3.2-2: Solubilization capacity of solutions of monomeric and dimeric surfactants in D₂O for *para*-xylene, as determined by ¹H NMR (surfactant concentration: 1 wt %). Values calculated per alkyl chains are rounding ones (one decimal).

surfactant	<i>para</i> -xylene solubilized	
	per surfactant	per alkyl chain
sodium laurate	0.18	0.2
SDS	0.55	0.5
DTAC	0.28	0.3
dimer EDTA	1.46	0.7
o-X-2	1.62	0.8
EO-2	0.95	0.5

From Table 3.2-2, the solubilization capacity of the dimeric surfactants is found to be equal or higher than that of monomeric surfactants, as generally emphasized [53, 106], and lie in the same range. Comparing **dimer EDTA** with its (pseudo) structurally related monomeric analogue, namely

sodium laurate, it is seen that the dimer enhances the solubilization capacity of probe *p*-xylene. The dimer based on EDTA has also a slightly higher solubilization capacity than the commonly used surfactant **SDS**. In analogy, the cationic dimeric surfactants exhibit larger capacities than the analogous monomeric surfactant **DTAC**. Regarding the spacer effect, it seems that shorter spacer groups involve a higher solubilization capacity (compare **o-X-2** having a short spacer and **EO-2** having a long spacer), as previously determined for those compounds [1, 108].

Concerning the ¹H NMR spectra obtained (see the example given in chapter 5, Figure 5.13-1), it is noted that the characteristic peaks of the surfactant experience a shielding after addition of the probe, with the most pronounced effect for the protons at the level of the head groups. This reflects the *locus* of solubilization of the probe (relatively polar due to the benzene ring), namely in the palisade layer of the micelles (interface water-micelle core).

3.2.5 Tolerance to calcium ions

The stability of the new dimeric surfactant in hard water is a particularly interesting issue, since the compound is based on ethylene diamine tetraacetic acid (EDTA), a well-known chelating agent. The properties of common anionic surfactants in water are generally altered by the presence of calcium and magnesium ions (e.g. decreased solubility and solubilization capacity, etc.). Hence, sodium tripolyphosphate is often added to soften hard water, but it presents several drawbacks (e.g. environmental problems). Accordingly, the synthesis of surfactants that are stable in hard water is a promising way to reduce the use of softening agents while maintaining the surfactant efficiency [109-112].

The tolerance to calcium ions of dimer EDTA in aqueous solution (neutralized compound dissolved in MilliQ water) was tested and compared to that of the reference monomeric surfactant sodium laurate. The experiment consists in recording the turbidity under addition of a solution of calcium chloride to the surfactant solution (see experimental part **5.14** for more details). The corresponding turbidimetric curves are presented in Figure 3.2-3.

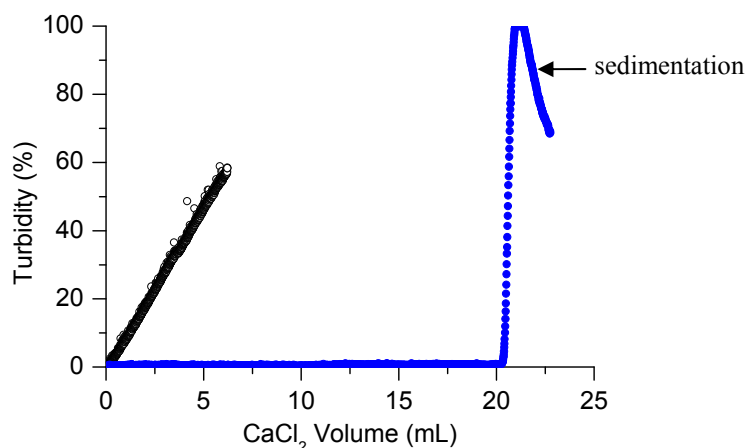


Figure 3.2-3: Turbidimetric titration of aqueous surfactant solutions (25 mL; 2 g/L) with calcium chloride ($[\text{CaCl}_2] = 0.5 \text{ g/L}$) at 30 °C, pH = 7. (O) = sodium laurate, (●) = dimer EDTA.

From Figure 3.2-3, it can be inferred that the stability of **dimer EDTA** against the addition of calcium ions in aqueous solution is much higher than that of the reference carboxylic type surfactant monomer. The solution containing the anionic dimer remains completely clear upon addition of a large amount of calcium chloride, until catastrophic precipitation is observed. In contrast, the sodium laurate containing solution becomes turbid after addition of a small amount of calcium chloride, and its turbidity increases progressively upon further addition. When 3 mL of calcium chloride solution added, the solution of sodium laurate is white, reflecting a high number of insoluble particles.

Carboxylate surfactants are usually found to be poorly soluble in hard water, as seen here with sodium laurate. In the case of **dimer EDTA**, the presence of the amine groups in the structure permits the chelation of calcium ions and hence, allows an enhanced tolerance of the surfactant to hard water. From the titration, one can try to calculate a calcium binding capacity for both surfactant, which would correspond to the maximum amount of calcium ions that the surfactant could tolerate. For dimer EDTA, a capacity of **75 mg Ca²⁺ / g surfactant** was found (i.e. 0.65 mol Ca²⁺ / mol head-group). For sodium laurate, a slight turbidity is observed from very low added amount of calcium (< 1 mL on the titration curve), but the solution remains stable. For the calculation of the tolerance to calcium ions, a higher volume of calcium chloride was arbitrarily used, namely the volume at which the solution is visually white. A capacity of **13 mg Ca²⁺ / g surfactant** (i.e. 0.07 mol Ca²⁺ / mol head-group) was calculated, which is much lower than the capacity found for the dimeric surfactant based on EDTA.

The dimeric surfactant synthesized can presumably chelate other kinds of ions, such as metal ions for instance, which could be a promising prospect for applications not only in detergents but also in other fields including metal anticorrosion, solid surface treatment, and catalysis (as amphiphilic metal complex).

3.3 Summary

The main properties of several series of cationic oligomeric surfactant and of a novel anionic dimeric surfactant, such as Krafft temperature, surface activity and micellization, micelle size and micellar aggregation number, solubilization capacity, were described.

Following the evolution of the properties of the cationic surfactants from the monomers via the dimers and the trimers to the tetramers, the critical micellization concentration CMC decreases strongly. Though the effects of the degree of oligomerization are dominant, the nature of the spacer groups cannot be neglected. For the systems studied, the CMC increases moderately with increasing spacer length and decreases with increasing hydrophobicity of the spacer. The increasing degree of oligomerization can also enhance the maximum attainable reduction of the surface tension, but this depends sensitively on the spacer group. All studied systems form small aggregates up to solutions containing several weight percent of the surfactants, as studied by DLS and TRFQ. The aggregation numbers N_{agg} of all oligomeric surfactants studied are relatively low (< 40 dodecyl chains per micelle), also at high concentrations (3 wt %). Both the nature of the spacer groups as well as the degree of oligomerization influence notably the aggregation numbers. Shorter spacers give rise to higher aggregation numbers, apparently resulting in a denser packing of the surfactant chains. In addition to the length of the spacer group, its detailed chemical structure plays an important role, too. For the three studied oligomeric series, aggregation numbers decrease with increasing degree of oligomerization, which differs from a singular study on two dimer/trimer ammonium surfactant pairs characterized by flexible C_3 -spacer groups. In addition, the effect of the spacer group of the surfactant dimers on the formation of inverse microemulsion was also examined.

The novel anionic dimeric surfactant based on EDTA exhibits a Krafft temperature below 0 °C and a very low CMC-value compared to the carboxylic type monomeric surfactant sodium laurate. The aggregates formed in solution are small (between pH 7 and 12) as studied by DLS. The surfactant dimer has also a high solubilization capacity as well as an enhanced tolerance to hard water.

In the next chapter, the properties of the dimeric surfactants combined with various additives (i.e. organic salts and oppositely charged surfactants) will be examined. Reports on such mixtures have been rare so far. Also, possible synergistic effects in the properties may arise from such combinations, which would make the synthesized surfactants even more attractive for further uses.

3.4 References

- [1] Laschewsky, A.; Lunkenheimer, K.; Rakotoaly, R. H.; Wattebled, L. *Colloid Polym. Sci.* **2005**, *283*, 469.
- [2] Laschewsky, A.; Wattebled, L.; Arotçaréna, M.; Habib-Jiwan, J.-L.; Rakotoaly, R. H. *Langmuir* **2005**, *21*, 7170-7179.
- [3] Wattebled, L.; Laschewsky, A.; Moussa, A.; Habib-Jiwan, J.-L. *Langmuir* **2006**, *22*, 2551-2557.
- [4] Kim, T.-S.; Kida, T.; Nakatsuji, Y.; Hirao, T.; Ikeda, I. *J. Am. Oil Chem. Soc.* **1996**, *73*, 907.
- [5] Menger, F. M.; Keiper, J.S.; Azov, V. *Langmuir* **2000**, *16*, 2062.
- [6] Zana, R. *J. Colloid Interface Sci.* **2002**, *246*, 182.
- [7] Menger, F.M.; Littau, C.A. *J. Am. Chem. Soc.* **1993**, *115*, 10083.
- [8] Song, L.D.; Rosen, M.J. *Langmuir* **1996**, *12*, 1149.
- [9] Wattebled, L.; Note, C.; Laschewsky, A. *Proceedings 53. SEPAWA Kongress (Würzburg)* **2006**, 73-87.
- [10] Lunkenheimer, K. In *Encyclopedia of Surface and Colloid Science*; Dekker: New York, 2002; p. 3739.
- [11] Zana, R. *Adv. Colloid Interface Sci.* **2002**, *97*, 205.
- [12] Alargova, R. G.; Kochijashky, I. I.; Sierra, M. L.; Zana, R. *Langmuir* **1998**, *14*, 5412.
- [13] Devinski, F.; Lacko, I.; Bittererova, F.; Tameckova, L. *J. Colloid Interface Sci.* **1986**, *114*, 314.
- [14] Zana, R. *J. Colloid Interface Sci.* **2002**, *248*, 203.
- [15] Wang, X.Y.; Wang, J.B.; Wang, Y. L.; Yan, H. K.; Li, P. X.; Thomas, R. K. *Langmuir* **2004**, *20*, 53.
- [16] Diamant, H.; Andelman, D. *Langmuir* **1994**, *10*, 2910.
- [17] Diamant, H.; Andelman, D. *Langmuir* **1995**, *11*, 3605.
- [18] Li, F.; Rosen, M. J.; Sulthana, S. B. *Langmuir* **2001**, *17*, 1037.
- [19] In, M. *Surf. Sci. Ser.* **2001**, *100*, 59-110.
- [20] Camesano, T. A.; Nagarajan, R. *Colloids Surf. A* **2000**, *167*, 165.
- [21] In, M.; Bec, V.; Aguerre-Chariol, O.; Zana, R. *Langmuir* **2000**, *16*, 141.
- [22] Karthaus, O.; Shimomura, M.; Hioki, M.; Tahara, R.; Nakamura, H. *J. Am. Chem. Soc.* **1996**, *118*, 9174.
- [23] Eastoe, J.; Dominguez, M. S.; Wyatt, P.; Beeby, A.; Heenan, R. K. *Langmuir* **2002**, *18*, 7837.
- [24] Faure, D.; Gravier, J.; Labrot, T.; Desbat, B.; Oda, R.; Bassani, D. M. *Chem. Commun* **2005**, 1167.
- [25] Hiskey, C. F.; Downey, T. A. *J. Phys. Chem.* **1954**, *58*, 835.
- [26] Brand, L.; Seliskar, J.; Turner, D. C., The effects of chemical environment on fluorescent probes, in: *Probes of Structure and Function of Macromolecules and Membranes*, Chance, B., Lee, C. P., Blaisie, J.-K., eds., Academic Press: New York 1971, p.17-39.
- [27] Sheppard S. E.; Geddes, A. L. *J. Chem. Phys.* **1945**, *13*, 63.
- [28] Mukerjee, P.; Mysels, K. J. *J. Am. Chem. Soc.* **1955**, *59*, 2937.
- [29] Weil, J. K.; Stirton, A. J. *J. Phys. Chem.* **1956**, *60*, 899.
- [30] Sabaté, R.; Freire, L.; Estelrich, J. *J. Chem. Educ.* **2001**, *78*, 343.
- [31] Sabaté, R.; Estelrich, J. *J. Phys. Chem.* **2003**, *107*, 4137.
- [32] Zana, R., State of gemini surfactants in solution at concentrations below CMC, *Surf. Sci. Ser.* **2004**, *117*, 93.
- [33] Rosen, M. J.; Mathias, J. H.; Davenport, L. *Langmuir* **1999**, *15*, 7340.
- [34] Masuyama, A.; Yokota, M.; Zhu, Y. P.; Kida, T.; Nakatsuji, Y. *Chem. Commun.* **1994**, 1435.
- [35] Sumida, Y.; Oki, T.; Masuyama, A.; Maekawa, H.; Nishiura, M.; Kida, T.; Nakatsuji, Y.; Ikeda, I.; Nojima, M. *Langmuir* **1998**, *14*, 7450.

- [36] Maiti, P. K.; Lansac, Y.; Glaser, M. A.; Clark, N. A.; Rouault, Y. *Langmuir* **2002**, *18*, 1908.
- [37] Hattori, N.; Yoshino, A.; Okabayashi, H.; O'Connor, C. J. *J. Phys. Chem. B* **1998**, *45*, 8965.
- [38] Israelachvili, J. N. *Intermolecular and Surface Forces*; Academic Press: London, 1991; Chapter 17.
- [39] Tanford, C. *The Hydrophobic Effect: Formation of Micelles and Biological Membranes*; Wiley: New York, 1980; Chapter 7.
- [40] Zana, R.; Weill, C. *J. Phys. Lett.* **1985**, *46*, 953.
- [41] Binana-Limbele, W.; Zana, R. *J. Colloid Interface Sci.* **1988**, *121*, 81.
- [42] Mazer, N. A. *Dynamic Light Scattering*; Pecora, R., Ed.; Plenum Press: London, 1991; Chapter 17.
- [43] Missel, P. J.; Mazer, N. A.; Carey, M. C.; Benedek, G. B. *J. Phys. Chem.* **1989**, *93*, 8354.
- [44] Alargova, R.; Petkov, J.; Petsev, D.; Ivanov, I. B.; Broze, G.; Mehreteab, A., *Langmuir* **1995**, *11*, 1530.
- [45] Rosen, M. J. *Surfactants and Interfacial Phenomena*; Wiley: New York, 1989.
- [46] Lianos, P.; Lang, J.; Strazielle, C.; Zana, R. *J. Phys. Chem.* **1982**, *86*, 1019.
- [47] Lianos, P.; Lang, J.; Zana, R. *J. Phys. Chem.* **1982**, *86*, 4809.
- [48] Grieser, F., *J. Phys. Chem.* **1981**, *85*, 928.
- [49] *Surfactant Solutions. New Methods of Investigation*; Zana, R., Ed.; M. Dekker Inc.: New York, 1987.
- [50] Underwood, A.L.; Anacker, E.W. *J. Colloid Interface Sci.* **1984**, *100*, 128.
- [51] Pisárčik, M.; Devinsky, F.; Lacko, I. *Colloids Surf. A* **2000**, *172*, 139.
- [52] Cabane, B. *Surfactant Solutions. New Methods of Investigation*; Zana, R., Ed.; M. Dekker Inc.: New York, 1987; Chapter 2, p 57.
- [53] Menger, F. M.; Keiper, J. S. *Angew. Chem. Int. Ed.* **2000**, *39*, 1907.
- [54] Zana, R. *Surfactant Solutions. New Methods of Investigation*; Zana, R., Ed.; M. Dekker Inc.: New York, 1987; Chapter 5 and references therein.
- [55] Infelta, P. *Chem. Phys. Lett.* **1979**, *61*, 88.
- [56] Yekta, A.; Aikawa, M.; Turro, N. *Chem. Phys. Lett.* **1979**, *63*, 543.
- [57] Barzykin, A. V.; Tachiya, M. *Heterog. Chem. Rev.* **1996**, *3*, 105.
- [58] Almgren, M. *Adv. Colloid Interface Sci.* **1992**, *41*, 9.
- [59] Gehlen, M.; De Schryver, F. C. *Chem. Rev.* **1993**, *93*, 199.
- [60] Lianos, P.; Zana, R. *J. Phys. Chem.* **1980**, *84*, 3339.
- [61] Tummino, P. J.; Gafni, A. *Biophys. J.* **1993**, *64*, 1580.
- [62] van Stam, J.; Depaemelaere, S.; De Schryver, F. C. *J. Chem. Educ.* **1998**, *75*, 93.
- [63] Hirata, H.; Hattori, N.; Ishida, M.; Okabayashi, H.; Furusaka, M.; Zana, R. *J. Phys. Chem.* **1995**, *99*, 17778.
- [64] Hattori, N.; Hirata, H.; Okabayashi, H.; Furusaka, M.; O'Connor, C. J.; Zana, R. *Colloid Polym. Sci.* **1999**, *277*, 95.
- [65] Danino, D.; Talmon, Y.; Zana, R. *Langmuir* **1995**, *11*, 1448.
- [66] Aswal, V.K.; De, S.; Goyal, P.S.; Bhattacharya, S.; Heenan, R.K. *Phys. Rev. E* **1998**, *57*, 776.
- [67] Aswal, V.K.; De, S.; Goyal, P.S.; Bhattacharya, S.; Heenan, R.K. *Phys. Rev. E* **1999**, *59*, 3116.
- [68] De, S.; Aswal, V.K.; Goyal, P.S.; Bhattacharya, S. *J. Phys. Chem.* **1996**, *100*, 11664.
- [69] Zana, R.; Lévy, H.; Papoutsis, D.; Beinert, G. *Langmuir* **1995**, *11*, 3694.
- [70] *Handbook of Photochemistry, Second Edition*; Murov, S. L.; Carmichael, I.; Hug, G. L., Eds.; Dekker: New York, 1993.
- [71] Alargova, R. G.; Kochijashky, I. I.; Zana, R. *Langmuir* **1998**, *14*, 1575.
- [72] Jiang, N.; Li, P.; Wang, Y.; Wang, J.; Yan, H.; Thomas, R. K. *J. Phys. Chem. B* **2004**, *108*, 15385.

- [73] Missel, P.J.; Mazer, N.A.; Benedek, G.B.; Young, C.Y.; Carey, M.C. *J. Phys. Chem.* **1980**, *84*, 1044.
- [74] Lin, T.L.; Chen, S.H.; Gabriel, N.E.; Roberts, M.F. *J. Phys. Chem.* **1987**, *91*, 406.
- [75] Wang, X.; Wang, J.; Wang, Y.; Ye, J.; Yan, H.; Thomas, R. K. *J. Colloid Interface Sci.* **2005**, *286*, 739.
- [76] Van Der Voort, P.; Mathieu, M.; Mees, F.; Vansant E.F. *J. Phys. Chem. B* **1998**, *102*, 8847
- [77] Langevin, D. *Acc. Chem. Res.* **1988**, *21*, 255.
- [78] Prince, L.M. *Microemulsions*; Ed. Academic: New York, 1977.
- [79] Shah, O. *Micelles, Microemulsions and Monolayers*, Science and Technology; M. Dekker Inc.: NY, 1998.
- [80] Stilbs, P.; Rapacki, K.; Lindman, B. *J. Colloid Interface Sci.* **1983**, *95*, 585.
- [81] Dreja, M.; Tieke, B. *Langmuir* **1998**, *14*, 800.
- [82] Dreja, M.; Pyckhout, W.; Mays, H.; Tieke, B. *Langmuir* **1999**, *15*, 391-399.
- [83] Magdassi, S.; Ben Moshe, M.; Talmon, Y.; Danino, D. *Coll. Surf. A* **2003**, *212*, 1-7.
- [84] Ben Moshe, M.; Magdassi, S.; Cohen, Y.; Avram, L. *J. Colloid Interface Sci.* **2004**, *276*, 221.
- [85] Kunieda, H.; Masuda, N.; Tsubone, K. *Langmuir* **2000**, *16*, 6438-6444.
- [86] Note, C.; Koetz, J.; Kosmella, S. *Coll. Surf. A* **2006**, *288*, 158-164.
- [87] Koetz, J.; Gunther, C.; Kosmella, S.; Kleinpeter, E.; Wolf, G. *Prog. Colloid Polym. Sci.* **2003**, *122*, 27-36.
- [88] Zhang, W.; Honeychuck, V.; Hussam, A. *Langmuir* **1996**, *12*, 1402-1403.
- [89] Note, C. PhD thesis, Universität Potsdam, 2006.
- [90] Binks, B.P.; Meunier, J.; Langevin, D. *Prog. Colloid Polym. Sci.* **1989**, *79*, 208.
- [91] Glukhareva, N. A.; Pletnev M. Y. *Colloid J. Russ. Acad. Sci.* **1993**, *55*, 530-534.
- [92] Zhu, Y.-P.; Masuyama, A.; Kirito, Y.; Okahara, M.; Rosen, M. J. *J. Am. Oil Chem. Soc.* **1992**, *69*, 626.
- [93] Tsubone, K.; Arakawa, Y.; Rosen, M. J. *J. Colloid Interface Sci.* **2003**, *262*, 516-524.
- [94] Yoshimura, T.; Esumi, K. *J. Colloid Interface Sci.* **2004**, *276*, 231-238
- [95] Dix, L. R. *J. Colloid Interface Sci.* **2001**, *238*, 447-448.
- [96] Helbig, C.; Baldauf, H.; Lange, T.; Neumann, R.; Pollex, R.; Weber, E. *Tenside Surf. Det.* **1999**, *36*, 58.
- [97] Huang, X.; Cao, M.; Wang, J.; Wang, Y. *J. Phys. Chem. B* **2006**, *110*, 19479-19486.
- [98] Shoji, N.; Ueno, M.; Meguro, K. *J. Am. Oil Chem. Soc.* **1976**, *53*, 165-167.
- [99] Kanicky, J. R.; Poniatowski, A. F.; Metha, N. R.; Shah, D. O. *Langmuir* **2000**, *16*, 172-177.
- [100] Hargreaves, W. R.; Deamer, D. W. *Biochemistry* **1978**, *17*, 3759-3768.
- [101] Roy, S.; Dey, J. *Langmuir* **2005**, *21*, 10362-10369.
- [102] Tadros, T. F. *Applied Surfactants: Principles and Applications*; Wiley: Weinheim, Germany, 2005.
- [103] Elworthy, P.H.; Florence, A.T.; MacFarlane, C.B. *Solubilization by surface-active agents*; Chapman and Hall: London, 1968.
- [104] Rosen, M. J. *Chemtech* **1993**, *23*, 30.
- [105] Zheng, O.; Zhao, J.-X. *J. Colloid Interface Sci.* **2006**, *300*, 749-754.
- [106] Dam, Th.; Engberts, J. B. F. N.; Karthäuser, J.; Karaborni, S.; van Os, N. M. *Coll. Surf. A* **1996**, *118*, 41.
- [107] Devínski, F.; Lacko, I.; Imam, T. *J. Colloid Interface Sci.* **1991**, *143*, 336.
- [108] Rakotoaly, R. H. Thèse de Doctorat, Louvain-la-Neuve, 2001.
- [109] Balzer, D. *Surf. Sci. Ser.* **2000**, *91*, 385.
- [110] Aratanic, K.; Oida, T.; Shimizu, T. *Commun. J. Com. Esp. Deterg.* **1998**, *28*, 45.
- [111] Holmberg, K. *Curr. Opin. Colloid Interface Sci.* **2001**, *6*, 148.
- [112] Wang, X.; Zhao, J.; Yao, X.; Chen, W. *J. Colloid Interface Sci.* **2004**, *279*, 548-551.

4. EFFECT OF ADDITIVES ON PROPERTIES OF SURFACTANT DIMERS IN SOLUTION

In this chapter, the effects of additives, such as organic salts and oppositely charged surfactants, on the main properties of dimeric surfactants will be described. Such combinations may be interesting in view of a possible enhancement of the properties while using lower amounts of surfactant material.

4.1 Addition of organic salts

4.1.1 Background and interests

Amphiphilic molecules self-assemble in aqueous solution into a variety of structures such as e.g. spherical or cylindrical micelles, vesicles, etc., depending on the molecular design and on the conditions under which aggregates are formed (cf. chapter 1) [1]. Single-tail surfactants usually form spherical micelles in aqueous solution above their critical micellar concentration (CMC) [2], which eventually grow to other shapes with an increase in surfactant concentration [3-4]. The growth of spherical micelles to cylinders can also be achieved by the addition of co-surfactants [5-7], of inorganic salts [4, 8-11], or of strongly binding organic salts [12-15]. Other ways towards micellar growth consist in using special surfactant structures, e.g. dimeric surfactants with a very short spacer group (namely an ethylene group linking covalently the head groups, as evoked in chapter 1) [16-17], hetero-gemini surfactants (see also *1.2.2.b*) [18], or mixtures of cationic and anionic surfactants [19-25]. The growth of micelles can be explained in terms of change in the surfactant packing parameter (see chapter 1) [26] due to decreased electrostatic repulsions and/or increased hydrophobic interactions, which results in a reduction of the spontaneous curvature of the surfactant assemblies.

It is now well-established from studies on single-chain surfactants that counterions have a strong influence on the CMC, aggregation number, size and shape of aggregates of ionic surfactant systems [27-34]. Alkyltrimethylammonium and alkylpyridinium surfactants are the most studied surfactant systems in this respect [12, 35-36]. Usually, spherical micelles are formed in combination with halide counterions, whereas aromatic counterions often induce the formation of rod-like micelles at relatively low surfactant and counterion concentrations [3-4, 37]. The formation of such rod-like micelles is attributed to the strong binding of organic counterions on surfactant micelles (at the level of the head groups of surfactants) to minimize the contact of their bulky hydrophobic part with water (see Figure 4.1-1). This results in a screening of charges. Hence, electrostatic repulsion between the ionic hydrophilic groups decreases, while hydrophobic interactions simultaneously increase in the palisade layer of the micelle, leading to a tighter packing of the surfactant-counterion mixed system (reduction

of the spontaneous curvature of the surfactant assemblies). This will therefore drive the micelle to change its microstructure.

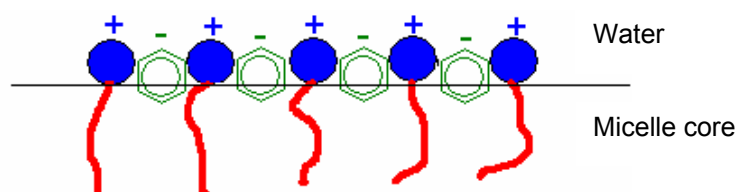


Figure 4.1-1: Schematic representation of the binding of organic anions at the micellar interface of cationic surfactants.

A possible consequence of the change of micellar morphology may be the appearance of a viscoelastic behaviour of the solution which arises from an entangled network of rod-like micelles. The latter micelles are often referred to as “living (secondary valence) polymers” because the association of surfactants results in long polymer-like chains which break and recombine (dynamic assembly process) [38-41]. In 1976 Gravsholt accounted for the marked viscoelasticity observed when adding some organic counterions such as salicylate to cationic surfactant solutions [3]. Anions such as salicylate are known to promote very efficiently the growth of cationic micelles. Solutions of worm-like micelles so formed have interesting rheological properties [42-44] and the theories of the structure and dynamics of these complex systems have been well developed [36, 45] (see also theory in **5.19**). Worm-like micelle containing systems [46] are discussed intensely as drag reducing agents (DRA) in recirculation systems [47-51] and in fracturing fluids in oil production [46, 52]. These viscoelastic surfactant based systems exhibit several advantages compared to high molar-mass true polymers for such applications [46]. Also, they were recently applied as high-efficiency viscosity agents in cement slurries, i.e. under high ionic strength and strongly alkaline conditions which are often too severe for polymers [53]. Additionally, entangled worm-like micelle systems were mentioned in many consumer products [46, 49].

Many investigations on cetyltrimethylammonium bromide (**CTAB**) mixed with various hydrophobic salts such as e.g. sodium salicylate [54-60], sodium tosylate [56], or anionic azo dyes (methyl orange and *p*-methyl red) [61] were reported. The influence of sodium salicylate on the aggregation of polymerizable cationic surfactants was also studied [62], as well as the effects of sodium salicylate and sodium tosylate on the phase behavior of a cationic surfactant with an erucyl tail (C_{22} , monounsaturated) [63]. Systems containing cetyltrimethylammonium (CTA) as a surfactant and salicylate [64-66], dichlorobenzoate [67], or isomers of sodium hydroxy-naphthoate [68-69] as a counterion were investigated, too. In analogy to the CTA / organic counterion surfactant systems, cetylpyridinium salicylate was studied [70]. Moreover, wormlike micellar and vesicular phases in aqueous solutions were evidenced for a series of *n*-alkyltrimethylammonium 5-ethylsalicylate surfactants (C_{12} , C_{14} and C_{16}) [13]. Thus, surfactant-counterion mixed systems have attracted

4. Effect of additives on properties of surfactant dimers in solution

considerable interest from both academic and industrial research. Nevertheless, there have been surprisingly few studies on organic salts combined with non-classical surfactants such as oligomeric surfactants, for example [71-76]. Reports on mixtures of gemini surfactants and different organic counterions have been limited so far, especially as regards the influence of dimerization and of the spacer group on the solution properties. Oda et al. described low molecular weight gelators of water and chlorinated solvents, based on gemini surfactant – counterion systems such as e.g. so-called “16-2-16” modified by L-tartrate counterions (bisquaternary ammonium with “16” and “2” representing the number of carbons in the linear hydrophobic chain and the number of methylene group making the spacer, respectively). Cryo-TEM examination of the gels revealed long and strongly entangled helical fibers [71-72]. Interactions of the dye “Methyl Orange” with a series of gemini amphiphiles, namely bisquaternary ammonium “12-n-12” (C_{12} linear hydrocarbon chains with spacer carbon number $n = 4, 8$ or 12) and a pyridinium-based gemini surfactant, were also studied [73]. Vesicles were found in the aqueous phase in addition to crystals as shown by transmission electron microscopy. More recently, new structures called “nucleo-gemini”, consisting of cationic gemini surfactants having nucleotides as counterions, were reported. Their behaviour at the air – water surface as well as in bulk solutions were examined [76].

The following study is aimed at describing more precisely the effect of the degree of oligomerization and of the spacer group on the properties of aqueous solutions of mixtures of surfactants and organic salts. Thus, different organic salts, also often called hydrotropes, were added to the studied cationic gemini surfactants and their monomeric analogs. Hydrotropes are commonly short amphiphilic molecules (often with a bulky “hydrophobic” part) that, without forming micelles, at high concentrations enhance the solubility of a variety of hydrophobic compounds in water, and that are generally slightly surface active. A wide range of organic salts were tested including sodium benzoate, sodium salicylate, sodium 6,2-hydroxynaphthoate and sodium vinyl benzoate, for instance. In these cases, the counterion of the surfactants is varied, namely due to possible anion exchange in-situ [39, 77-78]. The molar ratio surfactant / organic salt (based on the number of ionic groups in both components) is fixed at 1 to enable comparisons between the tested mixtures. High viscosities are indeed observed for aqueous mixtures with surfactant / organic salt ratios approaching the charge equimolarity [35, 39, 53, 56, 69].

The following experiments which are material consuming concentrate on surfactant dimers because they can be synthesized in large and pure amounts with reasonable efforts and costs compared to higher oligomers (see chapter 2).

4.1.2 Addition of sodium salicylate as model organic salt

As evoked before, sodium salicylate is the most studied organic salt in combination with conventional long-chain cationic surfactants. Hence, it represents a good model system to be tested with the cationic dimers.

4.1.2.a. Micellization and surface activity

Reports on associations of ionic surfactants and organic counterions generally focus on the viscosifying behaviour of the formed solutions, but less on the surface activity and micellization process, except in some cases [68, 79].

As stated for standard ("monomeric") surfactants, the counterion may influence the surfactant properties of charged dimeric surfactants. For instance, the bromide analogue of **EO-2** (CMC = 2.2 mmol/L) exhibits a reduced CMC of 0.5 mmol/L [80]. Also, the analog of **EO-2** with molybdate counterions MoO_4^{2-} (see synthesis via ion-exchange in **5.15**) shows different surface active behaviour (see Figure 4.1-2) with an even lower CMC value of 0.3 mmol/L, reflecting the lower hydrophilic character of the head groups due to this anion. In this line of reasoning, the properties of gemini surfactant solutions are expected to be dramatically changed by the addition of strongly binding anions such as salicylate.

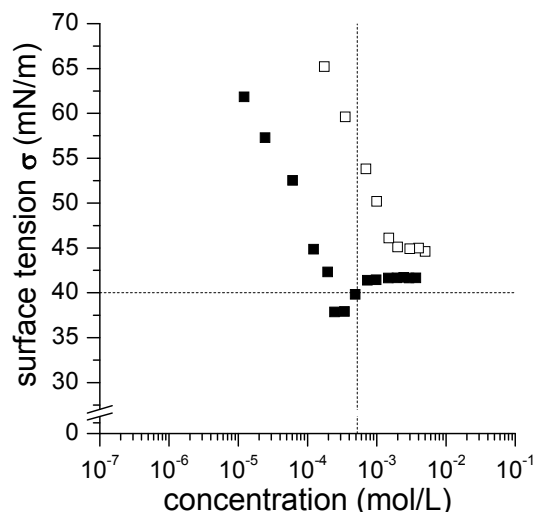


Figure 4.1-2: Surface tension curves of cationic dimer **EO-2** (**2Cl**) (∇) and of cationic dimer **EO-2** (**MoO₄²⁻**) (!). Vertical and horizontal dashed lines show CMC and σ_{cmc} -value of analog **EO-2** (**2Br⁻**) (From ref. [80]), respectively.

NOTE: the surface tension curve of **EO-2(MoO₄)** shows a minimum at the CMC, revealing the presence of some impurities in the sample, as discussed in the experimental part **5.15**. This is also a reason why organic anions were rather used as additives than as true counterions, since ion exchange processes (via the dihydroxide surfactants and subsequent addition of desired acid) may imply some

degradation of the product or incomplete exchange. Hence, the different purities of the samples would render the comparisons less accurate. It has for instance been shown that the cationic gemini surfactants in the dihydroxide form tend to degrade and hence cannot be stocked as intermediate compounds [81]. This is presumably due to the retro-nucleophilic substitution by hydroxide counterions, which is favored for spacer groups comprising an allylammonium or benzylammonium motif. In contrast, when organic salts are used as additives, the ratio surfactant/organic salt is well defined and the impurities introduced may be minimized. Numerous combinations can also be screened by this relatively fast method.

Effect of dimerization

A strong synergism in the properties of gemini surfactants combined with sodium salicylate is seen in surface tension measurements. For instance, Figure 4.1-3 illustrates the surface active behaviour of the dimeric surfactant **EO-2** and the corresponding behaviour of its mixture with the model organic salt sodium salicylate (1:2 molar ratio). For the latter mixture named here **EO-2(salicylate)₂**, an important shift of the surface tension curves towards lower concentration and lower surface tension values is noticed. The CMC and σ_{cmc} -values of dimer **EO-2** are respectively 1.25 g/L (2.2 mmol/L) and 45 mN/m, whereas for the mixture, they are 0.07 g/L (0.08 mmol/L) and 32 mN/m (in agreement with conductivity measurements: CMC = 0.1 mmol/L). Hence, the critical aggregation concentration (CAC: equivalent to CMC when additives are involved) as well as the surface tension at the CAC can be strongly reduced when particular hydrotropes are added to dimeric surfactants.

This synergistic effect is much stronger for dimeric surfactants than for standard monomeric ones. For reference monomeric surfactant **DTAC**, the CMC value is 4.8 g/L (18.3 mmol/L) while for the mixture **DTAC(salicylate)**, it is found to be 1.2 g/L (2.8 mmol/L), as determined by conductivity measurement (see Figure 4.1-4). Thus, the CMC value of **EO-2** is reduced by a factor 18 whereas that of **DTAC** is only reduced by a factor 4, when sodium salicylate is added in stoichiometric amount (on a hydrophobic chain basis) to the surfactant.

The marked decrease of the surface tension at the CMC by hydrotropes (compare σ_{cmc} for **EO-2** and **EO-2(salicylate)₂**), reveals a tighter packing of the surfactant chains at the interface. This is correlated by the comparison of the slopes of the isotherms below the CMC. Indeed, according to the Gibbs' equation, the minimum surface area occupied by a surfactant is inversely proportional to $\frac{\partial \sigma}{\partial \ln C}$. Here, the slope for **EO-2(salicylate)₂** is steeper than that for **EO-2** (see dashed line in Fig. 4.1-3), hence reflecting the smaller area occupied by the surfactant mixture at the surface. Note that the former finding, i.e. the low surface tension at the CMC, is particularly interesting for the use of such surfactant mixtures as wetting agents, e.g. in detergency applications.

4. Effect of additives on properties of surfactant dimers in solution

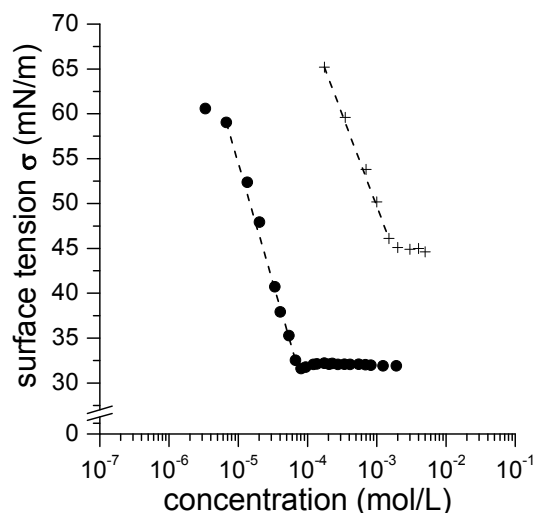


Figure 4.1-3: Surface tension curves of dimer **EO-2** and its mixture with sodium salicylate (1:2 molar ratio): (+) **EO-2**; (•) **EO-2(salicylate)₂**. Dashed lines are a guide for the eyes.

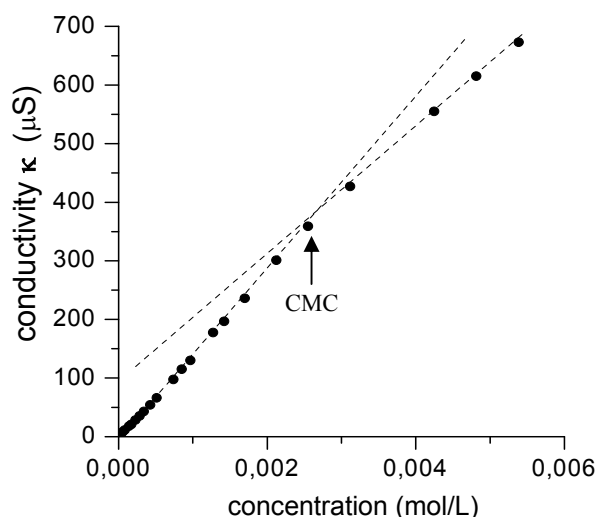


Figure 4.1-4: Conductivity measurement for a mixture of monomer **DTAC** with sodium salicylate (1:1 molar ratio): (•) **DTAC(salicylate)** (with $MW = 423.99 \text{ g/mol} = MW_{\text{DTAC}} + MW_{\text{NaSalicylate}}$). Dashed lines are a guide for the eyes. CMC corresponds to the break point in the curve.

It is also interesting to compare the CMC value obtained for the **EO-2** / sodium salicylate mixture with that of the **CTAC** / sodium salicylate mixture. **CTAC** (cetyltrimethylammonium chloride) is a higher homolog of **DTAC**, and therefore it is expected to exhibit a lower CMC value, (due to the longer hydrophobic chain). **CTAC** shows indeed a CMC 10 times lower than that of **DTAC** as seen in Table 4.1-1. The latter CMC value is also lower than that of dimeric surfactant **EO-2** (by a factor of ca. 3). When sodium salicylate is added to **CTAC**, the CAC is decreased by a factor of 4-5 (as observed between **DTAC** and **DTAC (salicylate)**). The CMC of **EO-2** is decreased by a factor of 18 via addition of salicylate, as seen before. Hence, the CMC of the mixture **EO-2(salicylate)₂** is even lower than that of the mixture **CTAC(salicylate)**, with the long chain surfactant **CTAC**. This

reflects again the stronger synergism induced when mixing dimeric surfactant with hydrotropes: the dimerization enables to enhance the associative behaviour.

Table 4.1-1: Surface activity and micellization data of cationic surfactant monomers and dimers and of their mixtures with sodium salicylate. The total molar mass for the mixtures corresponds to the sum of the molar masses of the chloride surfactant and of one or two equivalents of sodium salicylate.

surfactant / mixture	CMC (g/L)	CMC (mmol/L)	σ_{CMC} (mN/m)
DTAC	4.80	18.3	40.5
CTAC ^a	0.42	1.3	
EO-2	1.25	2.2	44.9
t-B-2	1.10	2.0	41.5
DTAC (sal) ^b	1.20	2.8	
CTAC (sal)	0.09	0.19	34.0
EO-2 (sal)₂	0.07	0.08	32.0
t-B-2 (sal)₂	0.05	0.06	32.0

^a = from ref. [82]

^b = measured by conductimetry

Effects of the spacer group

Mixtures of gemini surfactants **i-B-2**, **o-X-2**, **p-X-2** with sodium salicylate precipitate in aqueous solution. Only mixtures of gemini surfactant **EO-2**, **m-X-2**, and **t-B-2** with sodium salicylate remain clear (at least until 0.5 % wt). From this observation, it seems that shorter spacer groups involve a stronger association with salicylate, which results in a precipitate. The precipitate is made of stoichiometric amounts of the surfactant dication and salicylate, as checked by NMR in CDCl₃. Concerning **p-X-2**, this surfactant has already a Krafft temperature of 22-23 °C, hence by addition of strongly binding counterions precipitation also logically occurs.

Comparing the surface activity and micellization data obtained for mixtures **EO-2(salicylate)₂** and **t-B-2(salicylate)₂** (cf. Table 4.1-1), the effect of the spacer group is apparently negligible. The more hydrophobic and shorter spacer group of **t-B-2** induces only a slight decrease of the CMC value. No effect is observed on the surface tension at the CMC, which is already very low for these mixtures of surfactants having dodecyl chains and the very efficient hydrotrope sodium salicylate.

Nevertheless, it will be seen hereafter that the spacer group can cause larger differences in the viscosifying behaviour of the mixtures with salicylate, as well as in the surface activity for other organic salts.

4.1.2.b. Viscosifying effect

Effect of dimerization

In addition to the synergism observed in the surface active properties and micelle formation, viscous solutions can be obtained for mixtures gemini-organic salts at low concentrations, whereas no effect is observed for mixtures containing the analogous “monomeric” surfactant in the same concentration range.

Qualitative viscometric measurements demonstrating this behaviour were carried out. For mixtures with sodium salicylate, this is illustrated in Figure 4.1-5 where the relative viscosity measured by capillary viscometer is plotted against the concentration of the various complexes. Mixtures of **DTAC** and sodium salicylate (1:1) do not show significant change in the solution viscosity, up to 1 % wt (ca. 24 mmol/L). In contrast, mixtures of the dimers **EO-2**, **m-X-2**, **t-B-2** and sodium salicylate (1:2 in mole) produce highly viscous aqueous solutions even at concentrations as low as 0.3 % wt (ca. 2-3 mmol/L).

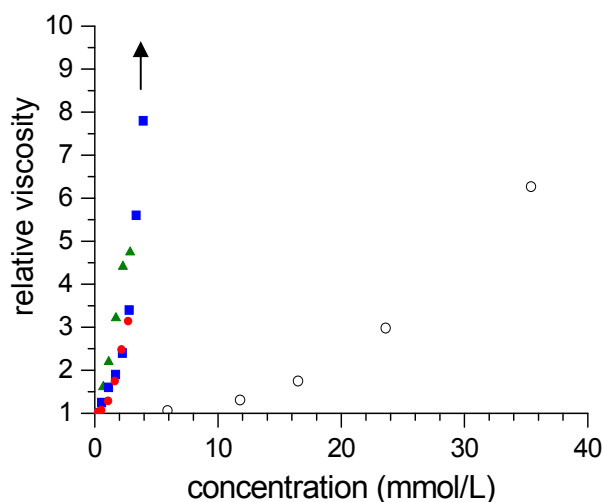


Figure 4.1-5: Relative viscosity of mixtures of monomer **DTAC**, dimers **EO-2**, **t-B-2**, **m-X-2** and sodium salicylate as a function of mixture concentration: (O) **DTAC(sal)**, (■) **EO-2(sal)₂**, (▲) **t-B-2(sal)₂**, (●) **m-X-2(sal)₂**. In the experimental conditions, shear rate $\dot{\gamma}$ is superior to 100 s^{-1} .

Thus, the dimerization of the surfactant fragments allows a strong and efficient viscosifying effect. This thickening behaviour reflects a strong growth of the micelles.

Viscoelastic behaviour for the mixtures dimer/sodium salicylate is also observed with the naked eye as a recoil of trapped air bubbles when the solution is rotated and suddenly stopped [3]. Therefore, to further characterize these viscoelastic systems, rheological measurements (rotation and oscillation) were performed. Figure 4.1-6 and Figure 4.1-7 illustrate the rheological behaviour of **EO-2(sal)₂** (0.8 % wt) (see also Figs. 5.19-3 and 5.19-4 for **EO-2(sal)₂** 0.6 % wt).

4. Effect of additives on properties of surfactant dimers in solution

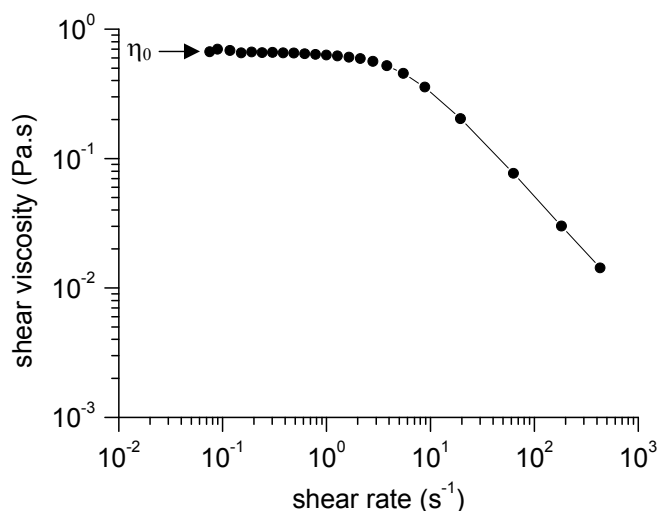


Figure 4.1-6: Shear viscosity η vs. shear rate $\dot{\gamma}$, for **EO-2(salicylate)₂** (0.8 % wt), at 25 °C.

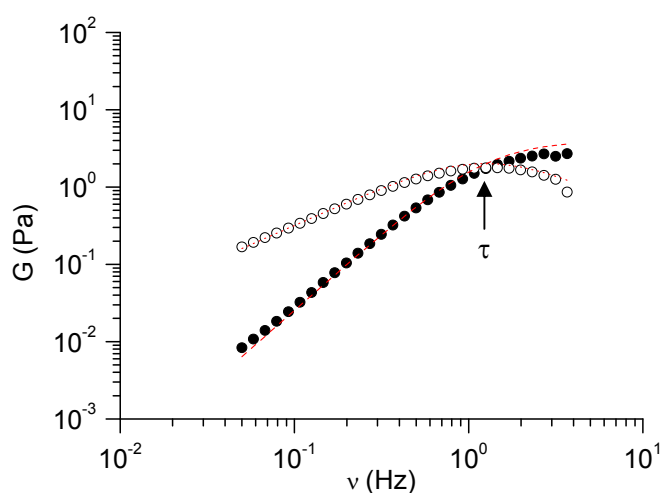


Figure 4.1-7: Frequency sweep experiment showing G' (●), G'' (○) for **EO-2(sal)₂** (0.8 wt %) at a shear stress of 1 Pa, at 25 °C. The dashed red lines correspond to the fitting of the curves with the Maxwell model presented in the experimental part.

The viscosity curve in Figure 4.1-6 is typical for viscoelastic solutions. It consists of two parts, namely the zero-shear viscosity range (Newtonian part) and the shear-thinning range (pseudoplastic part). In the former range, the viscosity is independent of the shear rate and is referred to as the zero-shear viscosity η_0 (value almost constant), as indicated on the graph. In contrast, the shear-thinning range corresponds to a linear decrease of the shear viscosity as a function of the shear rate (power law).

Frequency sweep experiments, as presented in Figure 4.1-7 (as well as in Fig. 5.19-3 for the mixture at 0.6 % wt), enable to determine the storage and loss moduli (G' and G'' respectively) vs. oscillation frequency (see 5.19). The curves obtained in the case of the studied mixtures can be well-fitted by the *Maxwell model* described in detail in the experimental part 5.19 (Equations 5.19-6 and 5.19-7). Also, the two curves cross over at a single point called relaxation time τ (time needed to

respond to a change of stress). The kinetic contribution to stress relaxation is the reversible chain scission process [45] (fast breaking limit).

Hence, the dynamic response evidenced for the dimeric surfactant/sodium salicylate systems corresponds to that of a Maxwell fluid with a single relaxation time and is characteristic for the presence of worm-like micelles in aqueous solution [43, 45, 63, 83].

Effect of concentration

The rheological measurements were carried out at various concentrations for the mixture **EO-2(sal)₂**, in order to examine the influence of the mixture concentration on the viscosifying and viscoelastic behaviour. Figure 4.1-8 represents the variation of the zero-shear viscosity as a function of the weight concentration of **EO-2(sal)₂**, determined from the viscosity curves (rotation experiments). The viscosity increases with concentration as expected, and reaches a maximum at ca. 0.6 % wt. Then, the viscosity decreases gradually. Note that near 2 % wt, the solution becomes turbid.

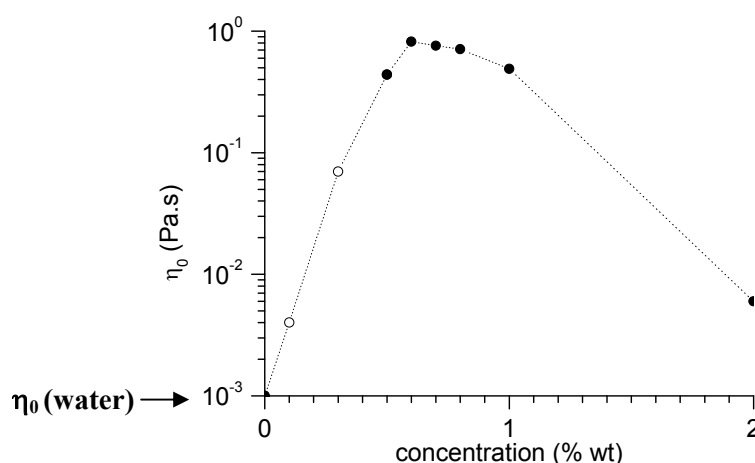


Figure 4.1-8: Zero-shear viscosity η_0 vs. concentration for the mixture **EO-2(sal)₂** at 25 °C. Points (o) are zero-viscosity values which are less accurate, since plateaus in the viscosity curves were hardly found for the system below 0.5 % wt in the measurement range. The dotted line is a guide for the eyes.

Viscosity maxima were also reported as a function of surfactant concentration at a constant ratio of salt to surfactant, for example for the CTAC / sodium salicylate system [84-85]. The reasons for these maxima are not yet clearly understood but the possibilities include a transition from linear to branched micelles [43, 86-87]. In fact, branched micelles are expected to show a lower viscosity than linear micelles because they have an additional pathway for stress relaxation (involving the sliding of branch points along the micelle) [88-80].

In Figure 4.1-9, the relaxation time and the plateau modulus (or elastic modulus) G_0 determined from the oscillation experiments are plotted against the mixture concentration.

4. Effect of additives on properties of surfactant dimers in solution

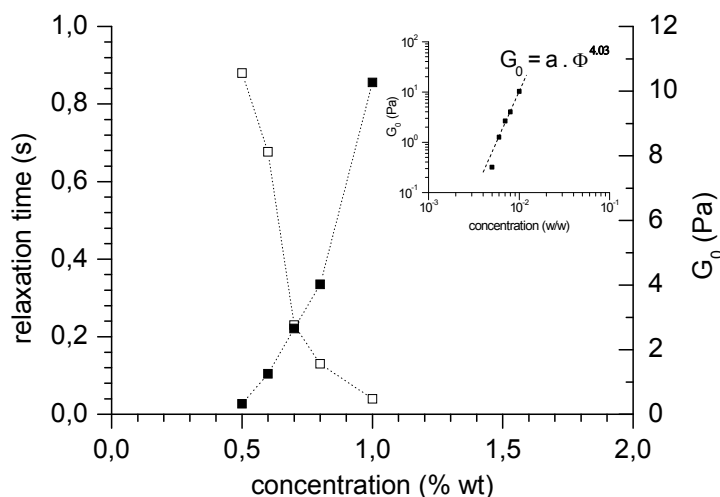


Figure 4.1-9: Relaxation time τ (□) and plateau modulus G_0 (■) vs. concentration, for the mixture **EO-2(sal)₂** at 25 °C. Dotted lines are a guide for the eyes. The inset shows the fitting of G_0 vs. concentration with a power law.

G_0 can be determined by direct measurement of the high frequency plateau in G' ($\omega^2\tau^2 \gg 1$, see Equation 5.19-6) or from η_0 and τ , according to equation 5.19-10, $\eta_0 = G_0\tau$. Note also that G_0 can be obtained from the fitting of the viscosity curves with the *Giesekus model* detailed in 5.19. In that case, the values of G_0 and τ are in good agreement with those obtained from the oscillation experiments.

In Figure 4.1-9, it is seen that the relaxation time decrease with the concentration. The strong decrease of the relaxation time may be related to the decrease of viscosity, presumably resulting from branching [90]. Also, it is often attributed to a salt effect which is known to shorten the relaxation times. Excess salts which strongly shield the charges of the micellar surface may favor intermicellar interactions / connections, and hence decrease the relaxation times (faster scission and recombination of micelles) [90].

Regarding the plateau modulus G_0 , an increase is noted with concentration of the mixture **EO-2 (salicylate)₂** (+ 2 NaCl excess salt). The plateau modulus depends upon the concentration of rod-like particles or, in the case of networks, upon the number density of the elastically effective chains [12]. Hence, the increase in concentration involves an increase of the number density of the rod-like micelle chains (or number density of entanglements in the system). The plot of the plateau modulus against the concentration can be fitted by a power law as shown in the inset in Figure 4.1-9. It is found that $G_0 \sim \Phi^4$. The value obtained for the scaling exponent is much higher than that expected for entangled wormlike micelles (2-2.25) [90]. Nevertheless, such a large exponent was reported for a mixture sodium dodecyl sulfate / p-toluidine hydrochloride, forming entangled rod-like micelles as well [89]. Moreover, deviation from the theoretical exponent, i.e. elasticity enhancement, was also found for a trimeric surfactant in aqueous solution in the entangled regime, which was rationalized by the formation of branching (corroborated by cryo-TEM pictures) [90]. Presumably, this supports the

hypothesis made for the changes observed in zero-shear viscosity, namely that branched wormlike micelles are present between 0.6 and 1 % wt, for the aqueous system **EO-2(salicylate)₂**.

Noteworthy, the turbidity (and subsequent phase separation) observed above 1.8-2 % wt for the system corroborates also the continual branching with increasing mixture concentration. The branching may indeed proceed until all the free ends are connected and a saturated network forms [63], as shown in Figure 4.1-10. In analogy, it was suggested in the literature that as branching progresses, the system might eventually phase separate into a saturated micellar network and a dilute surfactant solution [91-93]. The driving force for phase separation is the entropic attraction between network junctions [91]. The solution becomes clear again at a temperature of 28 °C, as followed by temperature-controlled turbidity measurements. With increasing temperature, the micelle size (and consequently the branching) should indeed decrease. Also, the solution is visually clear under shear, possibly reflecting the breakdown of the network.

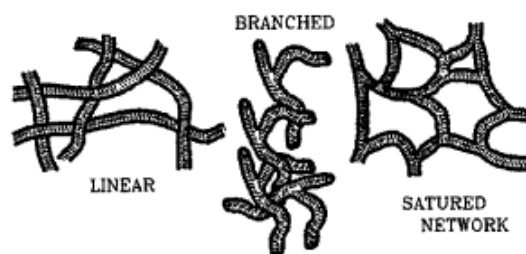


Figure 4.1-10: Linear, branched and saturated network of wormlike micelles. From ref. [94].

Effect of spacer: comparison **EO-2** / **t-B-2**

The data obtained from the rheological measurements of dimeric surfactants **EO-2** and **t-B-2** combined with sodium salicylate in aqueous solution are presented in Table 4.1-2.

Table 4.1-2: Rheological data for **EO-2(salicylate)₂** and **t-B-2(salicylate)₂** at a concentration of 0.5 % wt, measured by rotation (η_0) and oscillation experiments (G_0 , τ) at 35 °C. Values into brackets are the viscosities obtained from oscillation experiments (extrapolation of the complex viscosity at low frequency).

Mixture	η_0 (Pa.s)	τ (s)	G_0 (Pa)
EO-2(salicylate)₂	0.21 (0.19)	0.37	0.51
t-B-2(salicylate)₂	0.86 (0.57)	0.37	1.54

It is notable that the zero-shear viscosity η_0 of the aqueous mixtures gemini surfactant / sodium salicylate is increased by using a shorter hydrophobic spacer group, namely trans butenylylene, instead of the longer, polar diethylether spacer group. Hence, shorter hydrophobic spacer groups accentuate the viscosifying effect (within the wormlike micellar regime). This corroborates the studies

on pure bis-quaternary ammonium bromide gemini surfactants (abbreviated “m-s-m”, see chapter 1) for which a thickening behaviour arises for short alkyl spacers [95].

Still, without added hydrotrope, cylindrical micelles could not be found for the studied gemini surfactants up to 7 % wt in water (without additives), even for the shortest spacer groups of the series (namely, isobutenylene and *o*-xylylene), as proved by viscometric, light scattering and time-resolved fluorescence quenching measurements [96-98] (see chapter 3).

The relaxation times found are identical. This indicates a similar behaviour towards stress relaxation (dominated by scission-recombination of the micelles), independent of the spacer group, in that case. In contrast, the elastic modulus G_0 is much higher for the mixture of the gemini surfactant having a short hydrophobic spacer group (**t-B-2**). This high value for the elastic modulus reveals a densified network of rod-like micelles. Also, the increase in viscosity for the system with **t-B-2** may be attributed to the increase in the plateau modulus G_0 observed, which increased by approximately a factor 3 as the viscosity (approximately).

Finally, the results demonstrate that the spacer group in dimeric surfactants represents an additional variable to modify the viscosity of aqueous solutions, as regards mixtures between surfactants and organic salts (see also 4.1.3.c).

Comparison with longer chain surfactant CTAC

The findings exemplify that, in mixtures of surfactant / organic salts, introducing chemical bonds between two surfactant fragments with short alkyl chain lengths, can produce viscoelastic solutions (i.e. worm-like micelles) at relatively low concentration of only 0.3 % wt (*vide supra*). This behaviour is generally only observed for conventional cationic surfactants with longer alkyl chains (at least tetradecyl chains), as addressed in 4.1.1. Hence, it is interesting to compare the viscosity curves obtained for gemini surfactant / sodium salicylate mixtures to those obtained for similar mixtures with the long chain surfactant monomer **CTAC**. In Figure 4.1-11, the viscosity curves for such mixtures are presented.

The zero-shear viscosity values of the aqueous mixtures of **CTAC** / salicylate are higher than those for the dimeric surfactant mixture (here, **EO-2** as model dodecyl chain gemini). This can be rationalized by the longer hydrophobic chain of **CTAC**, which confers a higher cross sectional diameter to the formed rod-like micelles, and hence a higher volume fraction in solution. Still, the shear thinning behavior begins at higher shear rate for the dodecyl chain gemini surfactant than for higher homologue, apparently reflecting that the supramolecular structures containing the dimer complexes disentangle less easily at high flow rates. Thus, from a certain flow rate (ca. 10 s^{-1} for **EO-**

2(sal)₂ and **CTAC(sal)** 1 % wt), the shear viscosity of the mixtures with gemini surfactant become higher than for the higher homologue.

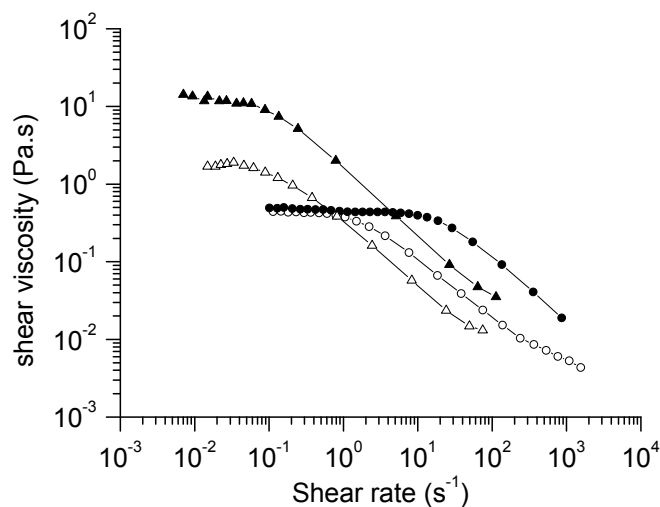


Figure 4.1-11: Shear viscosity η vs. shear rate $\dot{\gamma}$, at 25 °C, for mixtures: (○) **EO-2(sal)₂** 0.5 % wt; (●) **EO-2(sal)₂** 1.0 % wt; (△) **CTAC(sal)** 0.5 % wt; (▲) **CTAC(sal)** 1.0 % wt.

Hence, when using gemini, it is not necessary to use long chain surfactants to achieve high solution viscosity or viscoelasticity. Medium chain dimers can produce solutions with almost comparable viscoelastic properties and additional interesting features such as e.g. retarded shear thinning.

4.1.3 Addition of other hydrotropes

In addition to sodium salicylate, a wide range of other organic salts was added to the studied dimeric surfactants, which may potentially involve a synergism in the surfactant properties (i.e. surface active behaviour and/or viscosifying behaviour). The geometry and polarity of a given surfactant can be adjusted by electrostatic coupling with the appropriate organic counterion (such as the generation of a very bulky, hydrophobic head group). It is possible to adjust the hydrophilic-hydrophobic balance by choosing the counterion to be added [99]. Thus, the shape of the surfactant and the related spontaneous curvature of the surfactant assemblies can be broadly changed, resulting also in different solution properties, as will be seen in this section. Some tested systems will be presented hereafter in more details.

4.1.3.a. Effects of various organic salts tested

Selected organic salts are depicted in Figure 4.1-12. The complete set of tested organic salts is listed in the experimental part **5.16** (written either in acidic or sodium salt form). Many of the organic salts tested induced precipitation in aqueous solutions, as may be expected at the fixed

4. Effect of additives on properties of surfactant dimers in solution

stoichiometric ratio. It is noted that the organic salts comprising bulky sulfonate anions (e.g. sodium vinylbenzene sulfonate, sodium naphthalene sulfonate, disodium 4,5-dihydroxynaphthalene 2,7 disulfonate) give rise to turbid solutions more often than in the case of bulky carboxylate anions. This can be explained by the lower hydrophilicity of sulfonate group [100], which presumably involves stronger interactions with the cationic surfactant head groups. Also, “counterions” which are too hydrophobic induce precipitation when mixed with cationic gemini surfactants, as exemplified by mixtures of **EO-2** and sodium naphthalene carboxylate or sodium 3,2 hydroxynaphthalene carboxylate (**3,2 HNC**). Note that **3,2 HNC** is structurally comparable to sodium salicylate and hence should be strongly adsorbed on the micellar surface with the carboxylate and hydroxyl group protruding out of the micelle [69]. The naphthalene ring in **3,2 HNC** is expected to penetrate more in the micelle and therefore to confer more hydrophobicity on the molecule as compared to sodium salicylate. The precipitation observed may be explained by enhanced counterion binding via increased hydrophobic interactions in the palisade layer of the micelle.

Noteworthy, most of the precipitated systems did not redissolve upon heating, the interactions between the cationic dimeric surfactant and the organic salt being too strong.

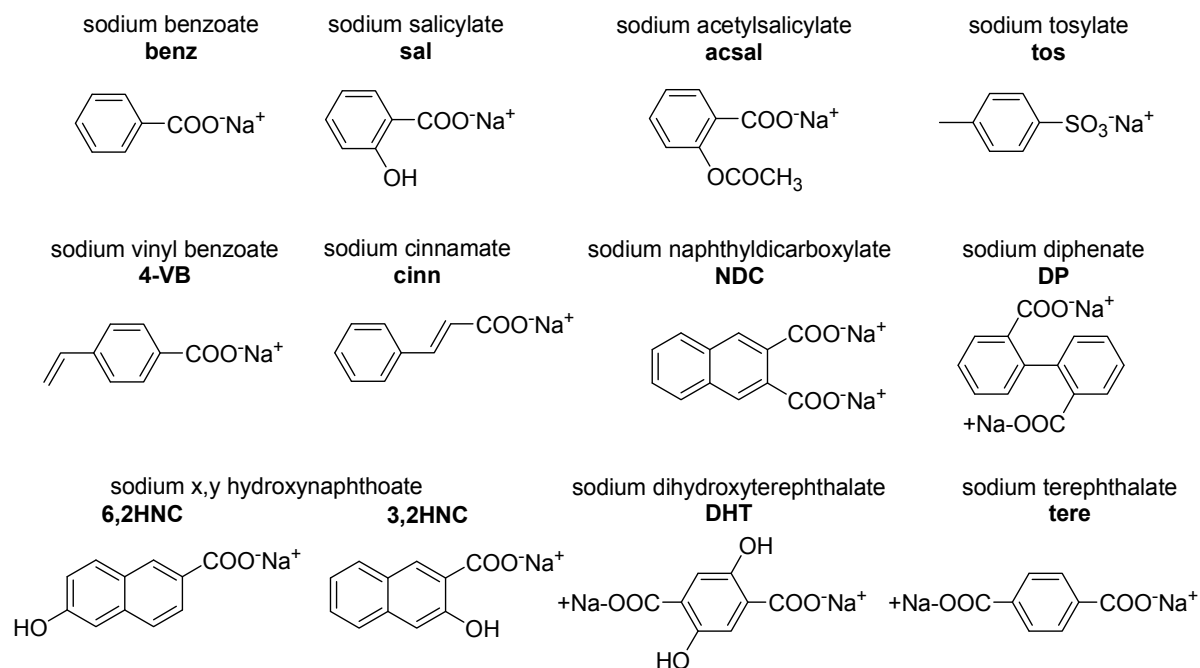


Figure 4.1-12: Examples of organic salts tested as additives to cationic dimeric surfactants. Abbreviations are in bold style.

However, not only the hydrophobicity of the counterion is a determining factor for the extent of interactions (and micellar growth or precipitation) of cationic surfactant/organic salt systems, but also the orientation of substituents on the aromatic ring is important [3-4]. It is noted that equimolar mixtures of cationic dimer **EO-2** with **3,2-HNC**, **2,1-HNC** and **1,2-HNC** precipitate in water while a mixture of **EO-2** and **6, 2 HNC** (see Fig. 4.1-12) gives a transparent and slightly viscous aqueous

4. Effect of additives on properties of surfactant dimers in solution

solution. Hence, the position of the hydroxyl group is essential for the resulting behaviour in aqueous solution for mixtures of cationic dimer and sodium hydroxynaphthalene carboxylate. Presumably, the increased distance between the carboxylate and hydroxyl groups for **6,2 HNC** prevents the naphthalene ring from penetrating the micelle like the other HNC [68], because the polar hydroxyl must keep a certain contact with water. The packing of the system **EO-2/6,2 HNC** should be less tight than for the other HNC, which results from lower hydrophobic interactions of the bulky part of the counterion with the surfactant hydrophobic tails (see Figure 4.1-13 and also discussion for surface tension of **EO-2/6,2 HNC** hereafter). Note that the addition of sodium 2-naphthoate (i.e. the parent anion of **6,2 HNC** but without OH group) leads to precipitation in mixtures with **EO-2**. This corroborates the strong influence of the hydroxyl group, which apparently changes the orientation of the naphthalene ring at the micellar surface (while naphthoate inserts markedly in the micelle).

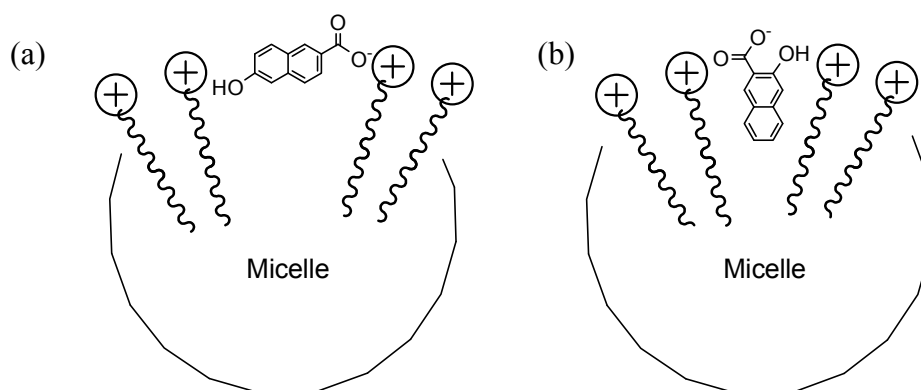


Figure 4.1-13: Scheme of the hypothesized orientation of naphthoate anions on the micellar surface of cationic surfactants: (a) **6,2 HNC**; (b) **3,2 HNC**. The latter anion induces precipitation.

It is noticeable that other dimeric surfactants with shorter and more hydrophobic spacers favour precipitation when organic salts are added. **EO-2** is the only surfactant dimer of the series which can be mixed with **6,2 HNC** or sodium tosylate, for instance, without observing precipitation. Hence, the spacer group has an important influence on the behaviour in water for such mixtures, as already evoked for sodium salicylate above. Notably, dimer **EO-2** implies much less precipitation in mixed systems with hydrophobic salts (probably due to the polarity of the spacer). **EO-2** is therefore the surfactant of choice for further studies and comparisons between the systems.

Noteworthy, other tested organic salts such as trimesic and pyromellitic acid sodium salts (sodium 1,3,5 benzene tricarboxylate and sodium 1,2,4,5 benzene tetracarboxylate respectively) also induce precipitation of surfactant **EO-2**. The recovered precipitates correspond to a stoichiometric complex of cationic surfactant/organic anion (relative amount checked by ^1H NMR in CDCl_3) and free of excess salt (checked by elemental analysis). In contrast, some added organic salts with multiple carboxylate groups on the bulky counterion (e.g. sodium phthalate, isophthalate, terephthalate) do not provoke precipitation of the mixtures, nor viscosifying effects (whatever the surfactant dimer). These

counterions are probably not sufficiently hydrophobic to induce a sharp transition to large aggregates or precipitates.

From all these observations, it can be concluded that there is a complex interplay between the surfactant and the organic salt, which may result in strongly different aqueous behaviour as a function of the selected counterion, due to modified electrostatic and hydrophobic interactions. For the systems which show no precipitation in solution, the solution properties were further examined.

4.1.3.b. Micellization and surface activity

Surface tension measurements were carried out on various mixtures of cationic dimers and organic salts in water. The data derived therefrom are listed in Table 4.1-3 (see also Table 4.1-1 for comparisons with monomeric analog). The effects observed strongly depend on the chosen counterion.

As in the case of sodium salicylate (see above), the CMC and σ_{CMC} values of the surfactant dimers are sharply reduced by adding the various counterions, reflecting the synergistic effects in mixtures cationic surfactants/anionic hydrotropes.

Table 4.1-3: Surface activity and micellization data of cationic surfactant dimer **EO-2** and its mixtures with various organic salts, determined by tensiometry. Values for **o-X-2** and one of its mixtures are also listed. (cf. corresponding abbreviations in Fig. 4.1-12).

surfactant mixture	CMC (g/L)	CMC (mmol/L)	σ_{CMC} (mN/m)
EO-2	1.250	2.2	44.9
o-X-2	0.720	1.2	37.0
EO-2 (sal)₂	0.071	0.08	32.0
EO-2 (tos)₂	0.067	0.07	32.0
EO-2 (6,2HNC)₂	0.020	0.02	38.5
EO-2 (NDC)	0.030	0.036	38.5
o-X-2 (NDC)	0.024	0.027	30.5
EO-2 (DP)	0.110	0.13	40.0
EO-2 (tere)	0.300	0.38	40.5
EO-2 (DHT)	0.240	0.30	38.0
EO-2 (acsal)₂	0.108	0.11	33.0

For surfactant dimer **EO-2**, the CMC value decreases with changing counterion (see chemical structure in Fig. 4.1-12) as follows:

EO-2 >> EO-2 (terephthalate) > EO-2 (dihydroxyterephthalate) > EO-2 (diphenate) \approx EO-2 (acetylsalicylate)₂ > EO-2 (salicylate)₂ \approx EO-2 (tosylate)₂ > EO-2 (naphthalene dicarboxylate) > EO-2 (6,2 hydroxynaphthalene carboxylate)₂. It is clear from this series that more hydrophobic anions involve considerably lower CMCs (compare e.g. naphthalene dicarboxylate and diphenate to terephthalate, all bearing two carboxylate groups, or else hydroxynaphthalene carboxylate and

salicylate). Also, the presence of a hydroxyl group in the structure of the counterion allows a slight decrease of the CMC (possibly due to additional interactions of the electron pairs of the oxygen with the ammonium head groups), as exemplified by the comparison between counterions dihydroxyterephthalate and terephthalate. Replacing the -OH group of salicylate by a -OCO-CH₃ group also corroborates the previous finding, since the CMC slightly increases with acetylsalicylate.

As regards the surface tension at the CMC, σ_{cmc} values decrease with varying the counterion in the following order for surfactant dimer **EO-2**:

EO-2 > EO-2 (terephthalate) > EO-2 (diphenate) > EO-2 (naphthalene dicarboxylate) \approx EO-2 (6,2 hydroxynaphthalene carboxylate)₂ > EO-2 (dihydroxyterephthalate) > EO-2 (acetylsalicylate)₂ > EO-2 (salicylate)₂ \approx EO-2 (tosylate)₂. Noteworthy, the ranking of the series for σ_{cmc} is different from that obtained for the CMC values. Hence, CMC and σ_{cmc} can be modified independently by selecting the appropriate organic salt as additive.

First, the surface tension at the CMC is reduced, independently of the organic salt, compared to that of the pure surfactant in water. Nevertheless, large variations are noted depending on the counterions' nature (hydrophobicity, number and nature of polar groups and position of the substituents). For instance, comparing σ_{cmc} for **EO-2(tere)** and **EO-2(NDC)**, it is found that the more hydrophobic naphthalene dicarboxylate implies a lower surface tension at the CMC (the naphthalene ring can penetrate further in the micellar core and hence, give a tighter packing). In contrast, **EO-2(6,2 HNC)**₂ exhibits a rather high σ_{cmc} compared to **EO-2(sal)**₂ for example, although the naphthalene ring is more hydrophobic than the benzene ring. This is mainly due to the position of the -OH group in **6,2 HNC** which changes the orientation of the counterion at the level of the surfactant head groups and therefore induces a less tight packing of the surfactants (as evoked in the previous section and depicted in Fig. 4.1-13).

The presence of hydroxyl substituents has also an influence on the surface tension at the CMC. Thus, the σ_{cmc} value of **EO-2(DHT)** is lower than the σ_{cmc} value of **EO-2(tere)**, showing that hydroxyl groups (in the appropriate position on the ring) may improve the surfactant chain packing at the surface. Finally, it is noted that sodium salicylate and sodium tosylate provoke sensitively the same effects on micelle formation and surface tension when mixed with dimer **EO-2**. As will be seen hereafter, this is not the case for the viscosifying behaviour.

In the present cationic gemini surfactants/hydrotropes mixtures, a marked effect on the surface activity and micellization is observed by varying the spacer group, while it is limited in the case of the very effective hydrotrope sodium salicylate (see previous part). For instance, adding disodium naphthalene dicarboxylate **NDC** to **EO-2** (having a long, flexible and polar spacer) or to **o-X-2** (with short, rigid and hydrophobic spacer) gives rise to two different surface tension isotherms, as presented in Figure 4.1-14. The CMC value is slightly lower for the mixture with surfactant dimer **o-**

X-2, while the σ_{cmc} value of **o-X-2(NDC)** is markedly inferior to that of **EO-2(NDC)**. In fact, by adding **NDC**, both pure dimeric surfactants experience a decrease of 6.5 mN/m of their σ_{cmc} value, as seen in Figure 4.1-14. The σ_{cmc} value of **o-X-2** was found to be much lower than the σ_{cmc} value of **EO-2** (difference of 8 mN/m; cf. horizontal lines in Fig. 4.1-14) due to the shorter xylylene spacer group (cf. chapter 3). Hence, the spacer effect on the σ_{cmc} value is preserved after addition of the organic salt **NDC**. Concerning the CMC, the micelle formation for the mixture with **o-X-2**, i.e. possessing a short hydrophobic spacer, is slightly favoured compared to the mixture with **EO-2** in analogy to the dimeric surfactants examined in pure state.

Note that the lower σ_{cmc} value found for the mixture **o-X-2(NDC)** compared to **EO-2(NDC)** reflects an even tighter packing of the surfactant chains at the surface, and is consistent with the steeper slope of the isotherm of **o-X-2(NDC)**, which reveals a lower area per headgroup.

As a result, the length and hydrophobicity of the spacer group is an additional parameter to modify the CMC and σ_{cmc} values in the studied mixtures.

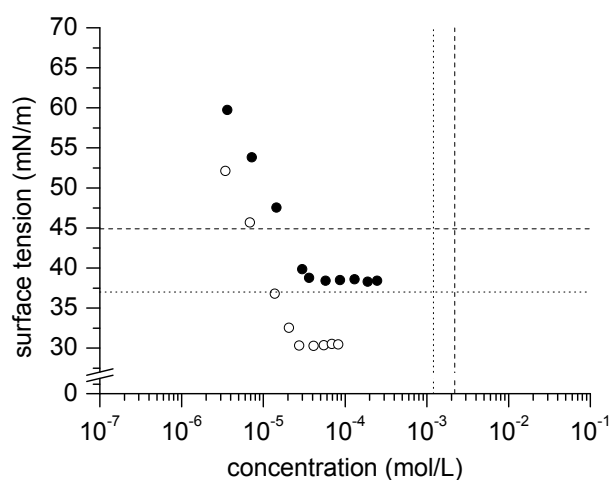


Figure 4.1-14: Surface tension curves of dimeric surfactants **EO-2** and **o-X-2** mixed with organic salt naphthalene dicarboxylate (**NDC**): (●) **EO-2 (NDC)**; (○) **o-X-2 (NDC)**. Vertical and horizontal lines are a guide for the eyes, respectively positioning CMC- and σ_{cmc} -values of pure dimeric surfactants: **EO-2** (dashes); **o-X-2** (dots).

4.1.3.c. Viscosifying effect

In addition to sodium salicylate which is the most common hydrotrope used for the formation of worm-like micelles with cationic surfactants, other organic salts may induce a viscosifying effect when mixed to cationic surfactants. The organic salts listed in experimental part **5.16** were tested in combination with dimer **EO-2**, and their thickening effect was evaluated.

Figure 4.1-15 shows the relative viscosity vs. concentration of mixtures of **EO-2** and three hydrotropes (sodium salicylate, tosylate and 6,2 hydroxynaphthalene carboxylate) inducing a

4. Effect of additives on properties of surfactant dimers in solution

thickening effect in water, compared to the pure dimeric surfactant. Sodium salicylate exhibits the strongest effect, followed by 6,2 HNC and then sodium tosylate.

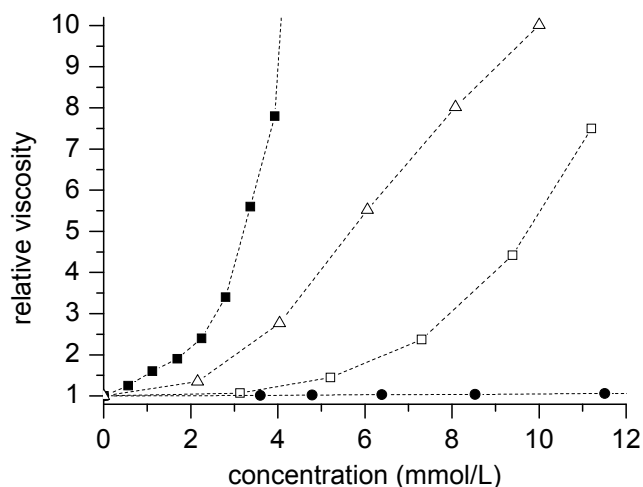


Figure 4.1-15: Relative viscosity vs. concentration: (■) $\text{EO-2(salicylate)}_2$, (Δ) EO-2(6,2 HNC)_2 , (\square) EO-2(tosylate)_2 , (\bullet) EO-2 . In the experimental conditions, shear rate $\dot{\gamma}$ is superior to 100 s^{-1} . Dashed lines are a guide to the eyes.

It is seen that **6,2 HNC** is less efficient than sodium salicylate (as for the surface tension reduction), although it is more hydrophobic. Again, this may originate from the orientation of the counterion at the micellar interface, which limits the reduction of head group area and thus the micelle growth. Note that although tosylate and salicylate presented the same characteristics for the decrease of the CMC and the reduction of the surface tension at the CMC in combination to dimer **EO-2**, these hydrotropes exhibit different viscosifying effects. Apparently, the presence of the hydroxyl group in the salicylate structure facilitates steeper micellar growth when increasing the concentration.

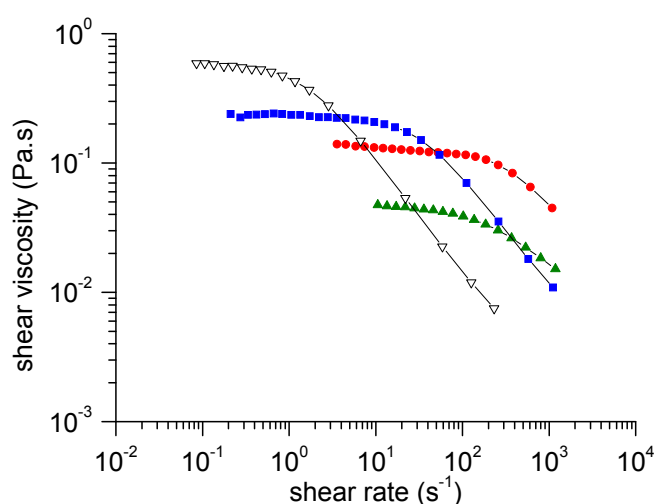


Figure 4.1-16: Shear viscosity η vs. shear rate $\dot{\gamma}$, for **o-X-2(benzoate)**₂ 2 % wt (\bullet), **t-B-2(benzoate)**₂ 2 % wt (\blacktriangle), **t-B-2(cinnamate)**₂ 1 % wt (\blacksquare) and **EO-2(vinylbenzoate)**₂ 0.5 % wt (∇), at 25 °C.

Organic salts which also thicken aqueous solutions of dimeric surfactants are among others sodium benzoate, sodium cinnamate and sodium vinylbenzoate, as shown by the rheological measurements in Figure 4.1-16. A mixture **EO-2**/sodium vinylbenzoate (0.5 % wt) implies a slightly stronger viscosifying effect ($\eta_0 = 0.60$ Pa·s) than the corresponding mixture with sodium salicylate ($\eta_0 = 0.44$ Pa·s). In contrast, sodium cinnamate, which is in fact an isomer of vinylbenzoate (cf. Fig. 4.1-12), does not induce a thickening effect with **EO-2**, though with **t-B-2**. Therefore, the nature and position of the substituents of the organic salts are decisive for the resulting viscosifying effects, as for the surface active properties and micellization.

Effect of dimerization

A strong viscosifying effect was found for mixtures of dimeric surfactants and sodium salicylate, while the effect was limited for the analogous monomeric surfactant (see 4.1.2.b). Thus, it seems that the dimerization allows a steeper micellar growth in mixtures surfactant/hydrotropes. This conclusion was confirmed by the examination of other organic salts. For instance, sodium benzoate (= salicylate without hydroxyl) was mixed to surfactant dimer **o-X-2**, analogous monomer **DTAC** and longer hydrophobic chain monomer **CTAC**. The combination with dimer **o-X-2** gives rise to viscous aqueous solutions at fairly low concentration (< 1 % wt), while no such behaviour is obtained for the monomers in the same range of concentrations, as seen in Figure 4.1-17.

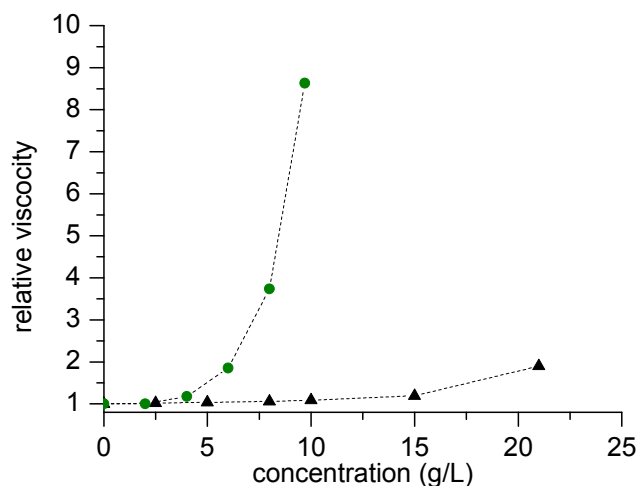


Figure 4.1-17: Relative viscosity of mixtures of monomer **CTAC**, dimer **o-X-2** with sodium benzoate as a function of mixture concentration: (▲) **CTAC(benz)**, (●) **o-X-2(benz)₂**. In the experimental conditions, shear rate $\dot{\gamma}$ is superior to 100 s⁻¹. Dashed lines are a guide to the eyes.

This behaviour is remarkable since generally, sodium benzoate is considered to be an inefficient organic salt for the formation of wormlike micelles with conventional cationic surfactants (including long chain ones). The finding proves that the dimerization and the use of the appropriate

spacer group (in the present case, a short hydrophobic xylylene group) allows a steep growth of the micelles when adding counterions that are usually inefficient.

Spacer Effect

In Figure 4.1-16, it is seen that a mixture **o-X-2**/sodium benzoate exhibits a higher zero shear viscosity than the same mixture with dimer **t-B-2**. In addition, no visual effect on the viscosity could be detected for the other dimers except **i-B-2** which also gives a high viscous solution. Hence, the spacer length seems to have an additional influence on the viscosifying effect, namely the shorter the spacer of the dimeric surfactant in the mixture, the higher the viscosity of the aqueous solution (as observed above with sodium salicylate).

This principle is corroborated by the viscometric experiments performed on mixtures of sodium acetylsalicylate (acsal) and the series of surfactant dimers, as visualized in Figure 4.1-18. The following ranking can be found as regards the viscosifying effect: **EO-2(acsal)₂** < **m-X-2(acsal)₂** < **t-B-2(acsal)₂** < **o-X-2(acsal)₂** ≤ **i-B-2(acsal)₂** (NB: **p-X-2(acsal)₂** is insoluble). This series coincides exactly with a decreasing spacer length of the dimers (see Fig. 3.1-9). Hence, a shorter spacer group in dimeric surfactants enables to reinforce the thickening behaviour observed in mixtures cationic surfactants/hydrotropes.

Noteworthy, sodium acetylsalicylate induces a general smaller thickening effect than sodium salicylate (the electron pair of the oxygen in the acetyl group which is involved in the resonance is less accessible than that in the hydroxyl group).

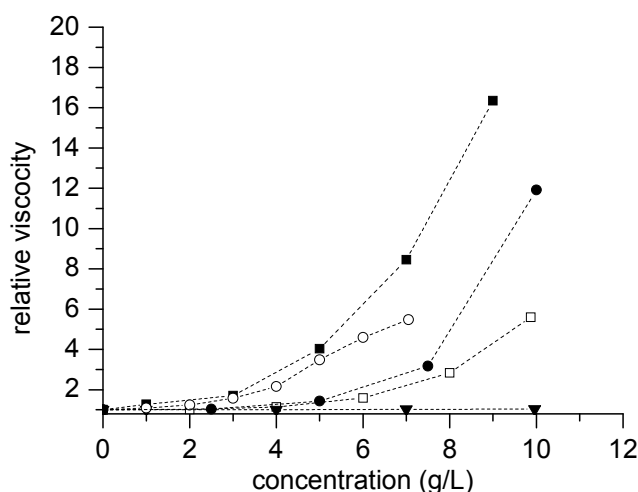


Figure 4.1-18: Relative viscosity of mixtures of surfactant dimers and sodium acetylsalicylate vs. mixture concentration: (■) **i-B-2(acsal)₂**, (□) **t-B-2(acsal)₂**, (▼) **EO-2(acsal)₂**, (○) **o-X-2(acsal)₂**, (●) **m-X-2(acsal)₂**. In the experimental conditions, shear rate $\dot{\gamma}$ is superior to 100 s^{-1} . Dashed lines are a guide to the eyes.

4. Effect of additives on properties of surfactant dimers in solution

To conclude, choosing an appropriate organic salt (more or less hydrophobic, presence of hydroxyl groups, etc.) as well as the proper spacer group of the gemini surfactant permits to access a wide range of viscosifying effect, at different concentrations.

4.1.3.d. Polymerization in mixtures of gemini surfactants and polymerizable counterions

The addition of functional organic anions such as sodium vinyl benzoate to cationic gemini surfactants is particularly interesting since the mixture can be subsequently polymerized via the organic anions, which are strongly bound to the cationic surfactant micelles, as described above.

Usually, polymerization in surfactant systems is performed via polymerizable groups inserted in the chemical structure of the surfactant (so-called “surfmers”) [101-102]. In this respect, polymerizable surfactants mixed with an oppositely charged hydrotropic salt were recently reported to form wormlike micelles whose structure can be fixed and stabilized after polymerization (at the level of the surfactant tail) [103-104]. In contrast, polymerization of surfactant aggregate structures via the surfactant counterions is less common. In recent years, this strategy was applied for wormlike micelles made of single chain cationic surfactants containing bulky polymerizable counterions [105-108]. Upon free-radical polymerization of the surfactants via the counterions, the wormlike micelles (which are dynamic self-assemblies) transformed into stable rodlike nanoparticles that remain well dispersed in water and that retain the cross-sectional structure of the initial micelles. After polymerization, the solutions became much less viscous, and are no longer viscoelastic.

When sodium vinyl benzoate (**4-VB**) is added to the model cationic gemini surfactants, viscoelastic solutions are obtained, resulting from the presence of entangled cylindrical micelles in solution (Maxwellian behaviour confirmed by oscillatory experiments). Free-radical polymerization in such aqueous mixtures was attempted. First, a mixture of **EO-2** / **4-VB** (molar ratio 1:2, 0.5 % wt in water) exhibiting a high viscoelasticity was polymerized for 90 min at 45 °C under nitrogen atmosphere, using 5 % (mol initiator / mol monomer **4-VB**) of water soluble initiator VA-44 (see also experimental part **5.18**). The final solution is turbid and yields in a white precipitate. This shows that the polymerization effectively occurred in these structured systems. In contrast, the polymerization of **4-VB** alone in water at such low concentration (11 mM) is inefficient since the vinyl protons of the monomer are still observed on the ¹H NMR spectrum after polymerization in D₂O, reflecting low conversion at such low monomer concentrations without surfactants added to the system. Moreover, it can be assumed that the precipitate results from the formation of strongly bound polymer-surfactant complexes [109]. The latter consist in anionic polymer chains synthesized in situ and bound cationic gemini surfactants (providing a stoichiometric amount of positive charges). The water-insolubility can be rationalized by the strong electrostatic and hydrophobic interactions between these species (as

generally observed for water-soluble polymers / gemini surfactants systems [110]), which do not permit the charge dissociation necessary to keep the structure dispersed.

Therefore, the molar ratio **EO-2** / **4-VB** was changed in order to create a charge excess which could increase the solubility of the complex after polymerization. Thus, a mixture of **EO-2** / **4-VB** (molar ratio 1:1, 1 % wt in water, not viscous) was polymerized for 3 h at 60 °C under nitrogen atmosphere, using 5 % (mol initiator / mol monomer **4-VB**) of VA-44. During the course of the polymerization, the solution passes through a white, turbid phase, and becomes clear again ca. after 1 week. To corroborate the changes visually observed in the aspect of the solution, the aggregate size was determined by dynamic light scattering before and after polymerization (see Figure 4.1-19). The surfactant **EO-2** forms micelles with small diameter at the detection limit of the apparatus (cf. aggregation numbers determined in chapter 3 [98]). The mixture with sodium vinyl benzoate before polymerization presents a slightly higher hydrodynamic diameter (3.5 nm), reflecting the micelle growth in the system. Still, this growth is not pronounced enough to involve the formation of entangled wormlike micelles. In agreement, no viscoelasticity is observed. One day after the polymerization, the solution is still turbid with particles having diameter of ca. 380 nm. One week after the polymerization, the system is clear and the structures show an average hydrodynamic diameter of 6 nm. Thus, the structure of the system reorganises with time after the polymerization.

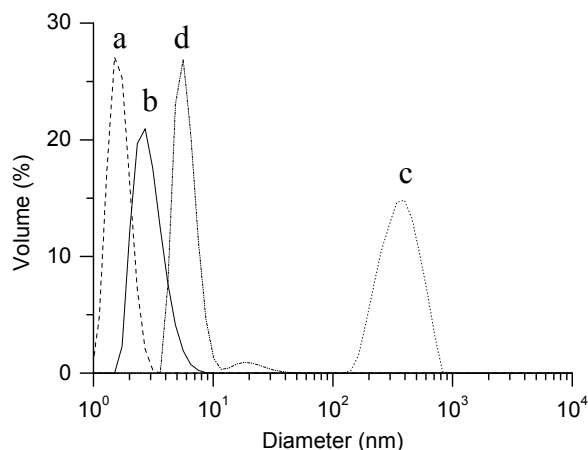


Figure 4.1-19: Effect of added equimolar amounts of sodium 4-vinylbenzoate "**4-VB**" on the association of dimeric surfactant **EO-2** in water; as studied by DLS showing the volume repartition vs. hydrodynamic diameter: a) (----) = pure **EO-2**; b) (—) = **EO-2(4-VB)** before polymerization (1 wt %); c) (····) = **EO-2 (4-VB)** at 1 day after polymerization (1 wt %); d) (-·-) = **EO-(4-VB)** at 1 week after polymerization (1 wt %).

In addition, ¹H NMR spectroscopy was used to study the chemical composition of the aggregates (before and after polymerization) as well as to provide a qualitative measure of component mobility in the aggregates or micelle dynamics [106]. Figure 4.1-20 shows the proton NMR spectra of **EO-2**, **4-VB**, **EO-2(4-VB)** (molar ratio 1:1, 1 % wt) before and after polymerization.

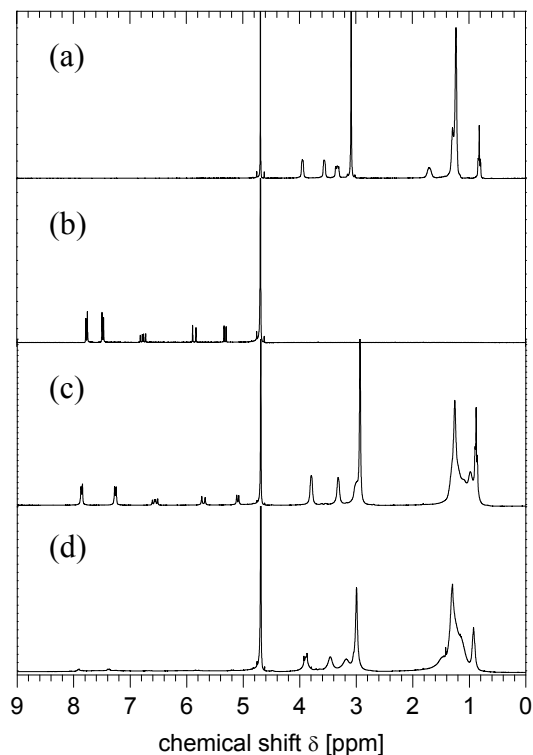


Figure 4.1-20: Effect of added equimolar amounts of sodium 4-vinylbenzoate "**4-VB**" on the association of dimeric surfactant **EO-2** in D_2O ; followed by 1H -NMR: (a) pure **EO-2**; (b) pure **4-VB**; (c) **EO-2(4-VB)** before polymerization (1 wt%); (d) **EO-2(4-VB)** after polymerization (1 wt%). Signal of solvent at 4.698 ppm.

Comparing the spectrum of the mixture before polymerization to the spectra of the components taken alone, characteristic differences are noted. The peaks in Fig. 4.1-20.c are slightly broader than those in Fig. 4.1-20.a and Fig. 4.1-20.b. This can be attributed to hindered mobility of the molecules within the self assembled structures [106]. Moreover, regarding the chemical shifts, the protons from the surfactant head-group (see Fig. 4.1-20.a: CH_3 at 3.08 ppm, CH_2 in α position of the ammonium at 3.32 ppm and CH_2 in β position at 1.71 ppm) and spacer group (see region from 3.5 to 4 ppm on Fig. 4.1-20.a) feel a shielding upon addition of **4-VB** (see same regions on Fig. 4.1-20.c). These upfield shifts of the head-group, and spacer group resonances suggest that all these protons experience the shielding cone portion of the aromatic ring current from nearby vinyl benzoate counterions [111]. It can be inferred therefrom that the added organic salts are preferentially located at the interface and intercalate among the dimethylammonium head-groups, the first few methylenes of the dodecyl chains (from the ammonium) and the diethylether spacer groups (also near the head-groups at the interface). This is corroborated by upfield shifts (shielding) felt by the vinyl and aromatic protons (except the protons adjacent to the carboxylic group) of the organic salt (compare Fig. 4.1-20.b and Fig. 4.1-20.c the spectrum regions between 5 and 7.5 ppm). Such shifts for organic salts also point to the intercalation of the respective protons into the micelle (a proton which is in a less polar environment than water such as the micellar interior, is more shielded [111]). In contrast, for the

4. Effect of additives on properties of surfactant dimers in solution

protons in ortho position of the carboxylic group (at 7.75 ppm in Fig. 4.1-20.b), downfield shifts are noticed. This suggests that these protons are more exposed to water at the micelle/water interface. Hence, an orientation of the added vinyl benzoate can be inferred.

Comparing the spectra of the mixture before and after polymerization (Fig. 4.1-20.c and Fig. 4.1-20.d respectively) in D₂O, it is noted that the signals in the region above 5 ppm disappear upon polymerization of the mixture (Fig. 4.1-20.d). While the disappearance of the vinyl signals (at 5.1, 5.7 and 6.5 ppm) seems to indicate high conversion, it is coupled to the complete loss of the aromatic peaks. This loss, which is surprising at first sight, is the result of a drastic change in molecular mobility of the counterions after polymerization relative to the NMR time scale. The polymerization effectively obstructs the dissociation of counterions out of the aggregates leaving the polymer constituents significantly immobilized in the aggregate and making them invisible to solution NMR [106]. The surfactant peaks are still broad, also showing their reduced mobility in the structure. They experience a very slight downfield shift, indicating a slightly more polar environment on average than before polymerization.

For comparisons, the polymerization was separately performed on monomer **4-VB** with the same experimental conditions as before. The amount of **4-VB** is equivalent to that present in the 1 % wt mixture (i.e. 13.5 mM in D₂O). Figure 4.1-21 shows the proton NMR spectra of **4-VB** in D₂O before and after polymerization (Fig. 4.1-21.a and Fig. 4.1-21.b respectively).

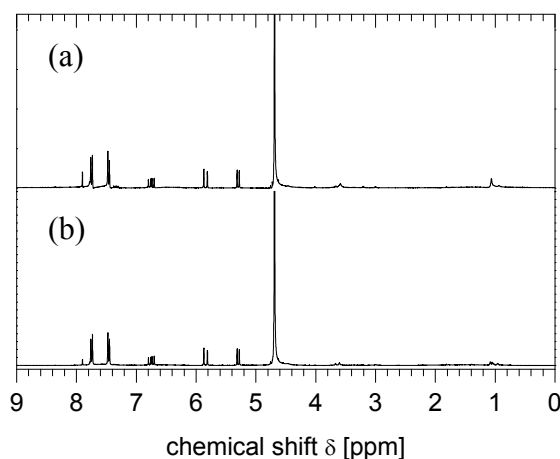


Figure 4.1-21: ¹H-NMR spectra of 4-vinylbenzoate "**4-VB**" (a) before polymerization, and (b) after attempted polymerization in D₂O (concentration 13.5 mM). Signal of solvent at 4.698 ppm.

The spectra are nearly identical. The spectrum after attempted polymerization (Fig. 4.1-21.b) does not present much change in the relative intensity of the peaks of the aromatic protons to that of the vinyl protons. Hence, monomer **4-VB** is not converted to a polymer under these conditions. This reflects the poor polymerization of the organic salt in D₂O at such low monomer content, and proves that the polymerization (in the defined conditions) only proceeds in an efficient way in micellar

solutions, as discussed above. High conversion is achieved because the majority of counterions is confined to the micelle core and in contact with a growing polymer chain. Assumingly, the reaction maintains a high efficiency because the monomer is held at high local concentrations in a structured environment where the monomer units are locally aligned along the surface of the micellar aggregate.

If the relative amount of anion is now increased, some variations are observed compared to the previous experiment. For example, a mixture **EO-2** / **4-VB** (molar ratio 1:1.5, 0.5 wt % in water) is slightly viscous before polymerization. During the polymerization under the same conditions as described before, the solution goes through a turbid phase. Nevertheless, 1 day after the polymerization, a very slightly turbid and non viscous solution is obtained. No precipitation is observed, even after several months. The ^1H NMR spectrum of the mixture before polymerization shows broader peaks than those seen in Fig.4.1-20.c, which indicates a reduced mobility of the molecules within the aggregates, as well as an increase of the sample's viscosity. Dynamic light scattering experiments performed before polymerization (see Fig.4.1-22.b) permitted to determine an average hydrodynamic radius of 11 nm for the aggregates present in solution (with a high polydispersity). This is bigger than the size determined for the pure surfactant in water (Fig.4.1-22.a) and than the size for the previous mixture (Fig.4.1-20.b).

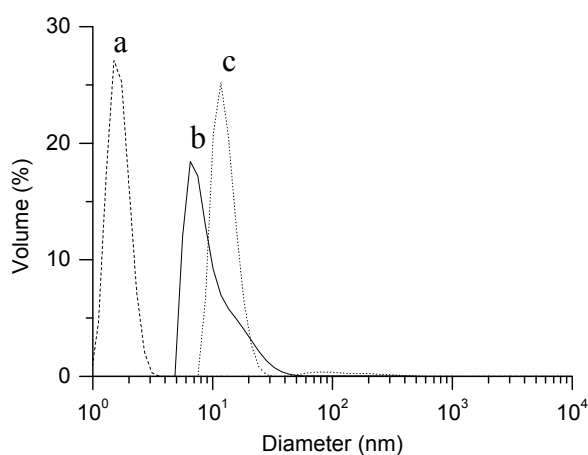


Figure 4.1-22: Effect of added amounts of sodium 4-vinylbenzoate "**4-VB**" on the association of dimeric surfactant **EO-2** in water; as studied by DLS showing the volume repartition vs. hydrodynamic diameter: a) (----) = pure **EO-2**; b) (—) = **EO-2(4-VB)** mixture with molar ratio 1:1.5 before polymerization (0.5 wt %); c) (····) = **EO-2 (4-VB)** mixture with molar ratio 1:1.5 after polymerization (0.5 wt %).

Hence, the micelles are further growing upon increase of **4-VB**, explaining the higher viscosity. After polymerization, it is seen that the main peak is slightly shifted to higher hydrodynamic radii (cf. Fig. 4.1-22.c). This shows that the system including polymer chains and surfactant molecules is structurally different. The slight turbidity of the solution visually observed can only be explained by

4. Effect of additives on properties of surfactant dimers in solution

the presence of big aggregates, which are responsible for a secondary shoulder on the distribution curve (Fig. 4.1-22.c) between ca. 100 and 300 nm.

4.1.4 Addition of cationic hydrotropes to dimer EDTA

Whereas hydrotrope effects for cationic surfactants have been extensively studied (*vide supra*), much less work has been done on analogous effects for anionic surfactants. Anionic wormlike micelles have been reported mainly in the presence of high concentrations of inorganic salts (e.g. 0.6 M NaCl) [112-115] or upon the addition of cationic surfactants [116]. Recently, hydrotrope-induced micellar growth in anionic surfactant solutions was reported [89, 117]. For instance, mixtures of sodium dodecyl sulfate **SDS** and organic salt *p*-toluidine hydrochloride (see Figure 4.1-23) produce worm like micelles in solution.

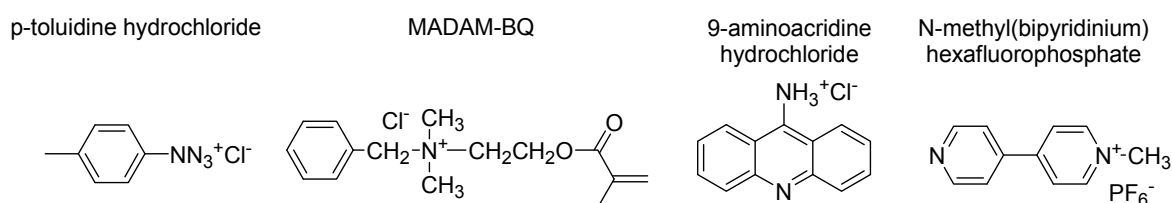


Figure 4.1-23: Examples of organic salts tested as additives to the anionic dimeric surfactant.

Thus, addition of some cationic hydrotropes to the anionic surfactant **dimer EDTA** was attempted (with equimolar ratio of charged groups), in view of producing viscoelastic solutions, as obtained in the case of the cationic dimers. The tested salts are depicted in Figure 4.1-23. The solutions obtained remain transparent and low viscous (except for *p*-toluidine hydrochloride, for which precipitation is observed after some hours). These preliminary tests seem to indicate that it is more difficult to make the micelles of **dimer EDTA** grow to stable entangled rodlike aggregates by addition of bulky counterions, compared to the studied cationic dimers. It also agrees with the general statement that the nature of the counterion has less dramatic influence on anionic surfactants than on cationic ones [118].

4.2 Addition of oppositely charged surfactants

4.2.1 Background

Studies of mixed micellization of dimeric surfactants with conventional surfactants were initially aimed at demonstrating a synergism of the surfactant properties, which would make the use of gemini surfactants more attractive, in view of their relatively high cost [95]. The reported results show that the presence or absence of synergism is very much dependent on the system [95]. In fact, no

general rule has emerged yet [119-125]. Nevertheless, mixtures of dimeric surfactants and conventional surfactants appear more prone to show synergism than binary mixtures of conventional surfactants [121].

No synergism in micelle formation was evidenced for mixtures of cationic dimers “m-s-m” with their analogous monomers **DTAB** or **CTAB** [119, 125] and with non-ionic ethoxylated surfactants $C_m(EO)_n$ [123]. In contrast, synergism in surface tension reduction and in mixed micelle formation was found in mixtures of amine oxide surfactants with anionic gemini surfactants such as the one depicted in Figure 2.2-1.a [120, 126]. Synergism in micelle formation was reported for mixtures of other anionic surfactant dimers with non-ionic ones $C_m(EO)_n$ [124-125]. Also, cationic gemini surfactants $C_{12}-C_s-C_{12}$, $2Br^-$ (with spacer C number $s = 3, 6, 12$) formed mixed micelles with nonionic surfactant Triton X-100 with lower aggregation numbers [127]. Shorter spacer involved a more pronounced decrease in aggregation number at fixed surfactant ratio, owing to larger steric repulsion between headgroups of *TX100*. Incorporation of the latter surfactant to gemini surfactants may lead to a more compact and hydrophobic micellar structure [127]. No synergism was observed in the micellization (CMC of mixtures is never inferior to that of *TX100*). On the contrary, mixtures of cationic gemini and zwitterionic surfactants show the presence of synergistic interactions in the mixed micelles, which increase with increasing length of the hydrophobic tail of the zwitterionic component, or with decreasing that of the gemini component [128]. Moreover, a marked synergism in surface tension reduction was found in mixtures of cationic dimeric surfactants and conventional anionic surfactants [122]. Also, the effect of additions of a disulfate dimeric surfactant with a hydrophilic poly(ethylene oxide) spacer group to a **CTAB** solution was investigated [129]. TRFQ and cryo-TEM showed that such additions resulted in a growth of the CTAB micelles and, at 10 % molar content of dimeric surfactant, in the formation of vesicles and very large aggregates (close to precipitation) [129]. The latter results do not support the existence of cross-linked micelles in mixtures of oppositely charged monomeric and dimeric surfactants [130], as hypothesized by Menger et al. in another report including a similar surfactant system [131].

4.2.2 Addition of SDS to cationic dimers

Mixtures of cationic dimeric surfactants with common oppositely-charged surfactants, such as e.g. sodium dodecyl sulfate (**SDS**) were explored here. The micellar morphology in aqueous solution is likely to change, in analogy to the micelle growth observed when surfactants are mixed with particular “counterions”. Such systems are also called catanionic mixtures (contraction of cationic and anionic) and have attracted much attention in the last two decades, especially oppositely-charged conventional surfactant systems [132]. Thus, mixing of oppositely charged surfactants can produce interesting microstructures such as vesicles [20], large lamellar sheets [133-134], or rod-like micelles [134-135], which are not formed by any of the pure compounds. Due to the strong electrostatic

4. Effect of additives on properties of surfactant dimers in solution

interaction between the head groups, cationic surfactant mixtures exhibit low critical aggregation concentrations and enhanced surface active properties [133, 136-139]. Furthermore, variation of the surfactant molecular structure and the stoichiometry of the mixture allows to tailor the microstructure. Recently, the use of aqueous cationic surfactant mixtures in the oil-in-water (o/w) microemulsion polymerisation of styrene was reported [140]. The studied systems included mixtures of dodecyltrimethylammonium bromide **DTAB** and sodium dodecylsulfate **SDS**, as well as decanediy-1,10-bis(dimethyldodecylammonium bromide) which is a cationic gemini surfactant of the form “12-10-12” and **SDS** [140].

The ratio gemini surfactant to **SDS** was varied as described in experimental part 5.20. Cationic surfactant **EO-2**, which is the most polar dimer in the studied series, was chosen as it may reduce the extent of precipitation when mixed with conventional anionic surfactant (having also a C_{12} chain). Interestingly, a mixture of dimeric surfactant **EO-2** and **SDS** (20/80 wt or 11/89 mol, total surfactant amount = 0.8 g/L) produces large polydisperse aggregates, which are observable by cryo-ultra high resolution scanning electron microscopy (see Micrograph in Figure 4.2-1). These presumably correspond to vesicular aggregates, in agreement with the persisting bluish tint of the solution, which is characteristic for vesicle containing solutions. Dynamic light scattering (DLS) also permits to evidence the aggregate size, revealing a broad distribution of aggregate sizes, with hydrodynamic diameters between 70 and 400 nm (mean peak at 160 nm, 100% volume), as seen in Figure 4.2-2 (peak e).

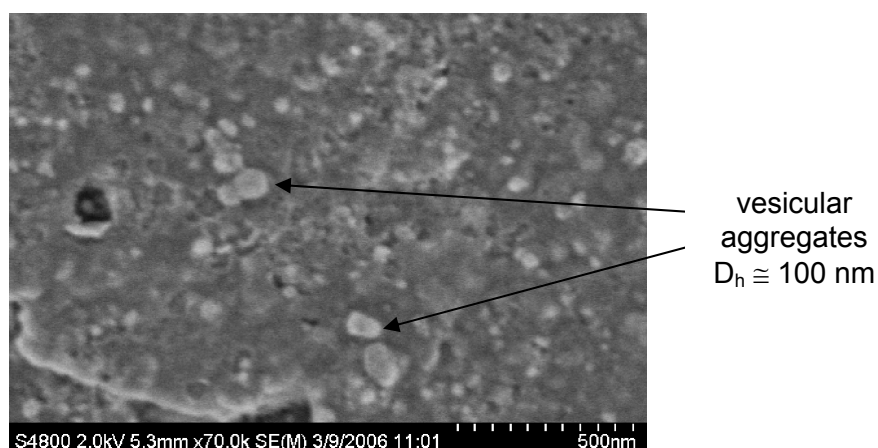


Figure 4.2-1: Cryo-SEM micrograph of a mixture of **SDS** / **EO-2** (80 / 20 in weight), 0.8 g/L in water, revealing the presence of small vesicular aggregates. (Pictures from *B. Tiersch*, Universität Potsdam).

For comparison, a 10 g/L mixture of **DTAC/SDS** (20/80 wt or 21/79 mol) is completely clear with the presence of small mixed micelles. The hydrodynamic diameter D_h measured by dynamic light scattering is 3.7 nm as shown in Figure 4.2-2 (peak c). Basically, it coincides with the diameter found for pure SDS in water (see peak b). Hence, the presence of big objects (i.e. strongly scattering) in this solution can be excluded. Moreover, when the latter solution is diluted ten times to 1 g/L,

precipitation is observed after some hours. Still, a freshly diluted solution (visually slightly white) can be measured in DLS and results in larger aggregates (peak d in Figure 4.2-2) which may be attributed to precipitate formation (crystals). This behaviour might be surprising at first sight but may be related to the behaviour observed for mixtures of charged polymers with oppositely charged surfactants, also precipitating upon dilution (due to large entropic gain via release of the counterions in dilute aqueous solution) [141]. This is also consistent with reports on catanionic systems composed of pure surfactants showing that transition from mixed micelles to vesicles occurs by dilution with water [23, 142].

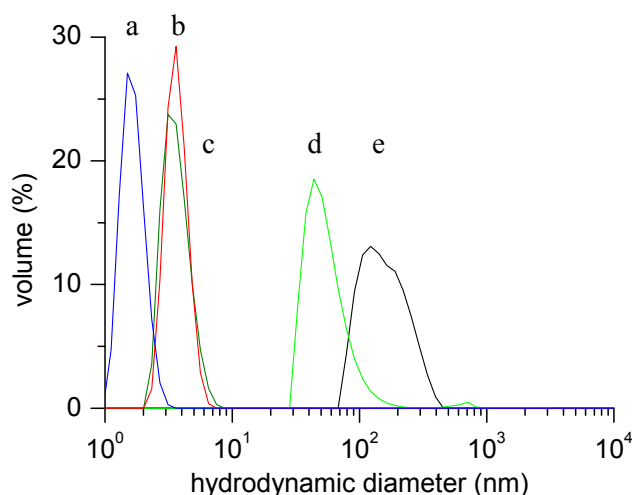


Figure 4.2-2: DLS measurements of pure surfactants and mixtures of oppositely charged surfactants in water, showing the volume repartition vs. hydrodynamic diameter: a) (—) = pure **EO-2** (4 g/L); b) (—) = pure **SDS** (4 g/L); c) (—) = **SDS** / **DTAC** (80/20 w/w, 10 g/L); d) (—) = **SDS** / **DTAC** (80/20 w/w, 1 g/L, measured just after dilution); e) (—) = **SDS** / **EO-2** (80/20 w/w, 0.8 g/L).

To conclude on this part, it is seen that the use of dimeric surfactant **EO-2** permits to accentuate the micelle growth and presumably to access bilayer formation as in vesicles, when added to commonly applied surfactant **SDS** at room temperature. Noteworthy, vesicles are of interest for numerous practical applications including drug delivery, cosmetics, imaging agents, herbicides (use as “vehicles” in these previous examples), micro-reactors for production of ultrafine particles, model system in biological studies, etc. The formed vesicles are stable over months (constant bluish tint of the solution, no precipitation). In contrast, the analogous monomeric surfactant **DTAC** (added to **SDS** in the same conditions) induces either small mixed micelles (concentrated solution) or crystalline precipitate (diluted solution).

Further experiments on such systems are under way in order to provide further insights into these complex systems [143]. In this respect, the role of the spacer group on the vesicle formation within these catanionic systems should be examined.

4.2.3 Addition of DTAC to dimer EDTA

A mixture **Dimer EDTA / DTAC** (molar ratio 1:1; 2 % wt) is transparent and not viscous. Even when **dimer EDTA** and **DTAC** (monomeric analog of **EO-2**) are mixed in stoichiometric amount (1:2; 1 % wt in water), the resulting solution is clear and low viscous. Hence, **dimer EDTA** notably exhibits a good compatibility with oppositely-charged surfactant monomer **DTAC**. This behaviour may be explained by the fact that at pH 7-8 in water the compound is in fact a mixture of monoprotonated (majoritary), diprotonated and dianionic species (minoritary), as shown by the acide-base titration in chapter 2. Hence, a charge excess may be preserved for the mixture. In addition, the presence of hydrophilic tertiary amides in the surfactant structure may help to keep a good solubility of the mixture. **Dimer EDTA** is apparently a surfactant which could be combined with many additives without inducing precipitation.

4.2.4 Mixture of oppositely charged surfactant dimers

Interestingly, the new gemini surfactant based on EDTA can be mixed with the studied cationic gemini surfactants. Such catanionic mixtures are original and have not been reported yet.

It is observed that a stoichiometric mixture of **dimer EDTA** and **EO-2** (1 % wt) precipitates in water, in contrast to the same mixture with **DTAC** seen just above. Hence, the interactions are stronger between the two oppositely charged dimeric surfactants than between **dimer EDTA** and the cationic monomer. This corroborates the general tendency for gemini surfactants to enhance associations.

To avoid precipitation, the ratio between cationic and anionic gemini surfactants must be changed. Thus, a mixture of **dimer EDTA / EO-2** (1:2 molar; 2 % wt), i.e. with the anionic dimer used as additive to the **EO-2**-rich solution, was prepared. The resulting solution is clear and low viscous. However, if **EO-2** is used as additive to a solution rich in **dimer EDTA**, the behaviour turns out to be different. This is exemplified by the mixture **dimer EDTA / EO-2** (2:1 molar; 2 % wt), which is clear and viscoelastic, reflecting the strong micelle growth. Hence, it seems that the micelle growth from small micelles to cylindrical micelles is more favoured for solutions rich in the anionic dimeric surfactant.

Rheological measurements were performed in order to corroborate the viscoelastic behaviour visually found for the catanionic mixture **dimer EDTA / EO-2** (2:1 molar; 2 % wt). Figure 4.2-3 illustrates the shear viscosity curve obtained for the latter mixture. The curve typically resembles that of a viscoelastic material (*vide supra*) and presents a zero-shear viscosity value for the mixture equal

to 0.4 Pa.s. Note that the mixture remains clear upon dilution and become less viscous, reflecting the progressive transition from entangled cylindrical micelles to small mixed micelles.

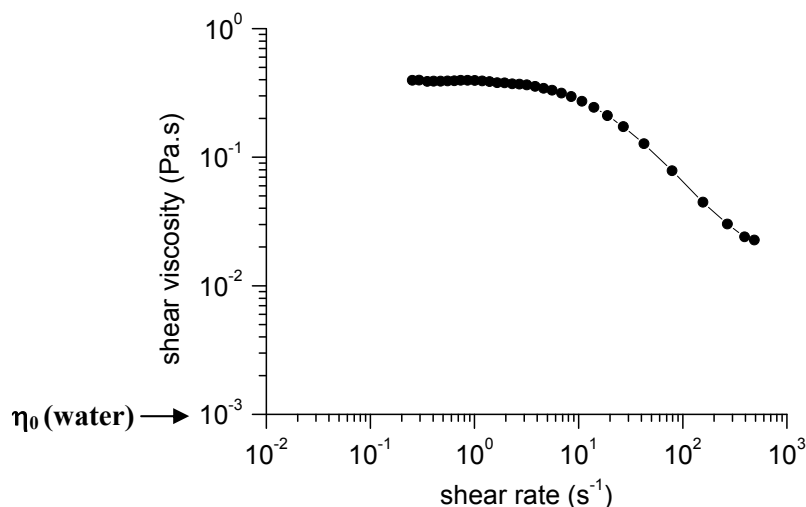


Figure 4.2-3: Shear viscosity η vs. shear rate $\dot{\gamma}$, for **dimer EDTA / EO-2** (molar ratio 2:1; 2 % wt), at 25 °C.

Apparently, the behaviour of the studied mixture “anionic” gemini / cationic gemini is quite different from that of the mixtures “anionic” gemini / cationic analogous monomer. It is noted that the catanionic mixture of oppositely charged gemini surfactants promotes the micelle growth towards stable entangled rod-like micelles while the corresponding mixture with DTAC gives rise to almost no micelle growth (see system **dimer EDTA/DTAC** 1:1, 2 % wt).

In this chapter, it has been demonstrated that the addition of organic salts and of oppositely charged surfactants to gemini amphiphiles may give rise to strongly enhanced solution properties, such as reduction of aggregation concentration and surface tension, as well as thickening effects (due to micellar growth). Combinations of gemini surfactants with additives are promising in view of the further use of these amphiphiles: improved properties can be easily attained with quite low amount of material in aqueous solution, which is appealing for potential applications while reducing the costs.

4.3 References

- [1] Laughlin, R. G. *The Aqueous Phase Behavior of Surfactants*; Acad. Press: London, 1994; Chapter 1.
- [2] Lindman, B.; Wennerström, H. *Top. Curr. Chem.* **1980**, *87*, 1.
- [3] Gravsholt, S. *J. Colloid Interface Sci.* **1976**, *57*, 575.
- [4] Imae, T.; Kamiya, R.; Ikeda, S. *J. Colloid Interface Sci.* **1985**, *108*, 215.
- [5] Porte, G.; Appell, J.; Poggi, Y. *J. Phys. Chem.* **1980**, *84*, 3105.
- [6] Imae, T.; Iwamoto, T.; Platz, G.; Thunig, C. *Colloid Polym. Sci.* **1994**, *272*, 604.
- [7] Oda, R.; Bourdieu, L.; Schmutz, M. *J. Phys. Chem. B* **1997**, *101*, 5913.
- [8] Lequeux, F.; Candau, S. J. *Structure and Flow in Surfactant Solutions* (ACS Symposium Series 578), Herb, C. A.; Prud'homme, R. K. eds.; Washington D.C., 1994.
- [9] Kern, F.; Lemarechal, P.; Candau, S. J.; Cates, M. E. *Langmuir* **1992**, *8*, 437.
- [10] Zhang, W.; Li, G.; Mu, J.; Shen, Q.; Zheng, L.; Liang, H.; Wu, C. *Chinese Science Bulletin* **2000**, *45*, 1854
- [11] Gamboa, C.; Sepúlveda, S. J. *J. Colloid Interface Sci.* **1986**, *113*, 566.
- [12] Rehage, H.; Hoffmann, H. *J. Phys. Chem.* **1988**, *92*, 4712.
- [13] Buwalda, R. X.; Stuart, M. C. A.; Engberts, J. B. F. N. *Langmuir* **2000**, *16*, 6780.
- [14] Cressely, R.; Hartmann, V. *Eur. Phys. J. B* **1998**, *6*, 57.
- [15] Imae, T.; Kakitani, M.; Kato, M.; Furusaka, M. *J. Phys. Chem.* **1996**, *100*, 20051.
- [16] In, M.; Bec, V.; Aguerre-Chario, O.; Zana, R. *Langmuir* **2000**, *16*, 141.
- [17] Bernheim-Groswasser, A.; Zana, R.; Talmon, Y. *J. Phys. Chem. B* **2000**, *104*, 12192.
- [18] Menger, F. M.; Peresykin, A. V. *J. Am. Chem. Soc.* **2001**, *123*, 5614.
- [19] Yan, Y.; Xiong, W.; Huang, J.; Li, Z.; Li, X.; Li, N.; Fu, H. *J. Phys. Chem. B* **2005**, *109*, 357.
- [20] Kaler, E. W.; Murthy, A. K.; Rodriguez, B. E.; Zasadzinski, J.A.N. *Science* **1989**, *245*, 1371.
- [21] Bhattacharya, S.; Haldar, J. *Coll. Surf. A* **2002**, *205*, 119.
- [22] Bhattacharya, S.; De, S. *Langmuir* **1999**, *15*, 3400.
- [23] Yacilla, M. T.; Herrington, K. L.; Brasher, L. L.; Kaler, E. W.; Chiruvolu, S.; Zasadzinski, J. A. *J. Phys. Chem.* **1996**, *100*, 5874.
- [24] Söderman, O.; Herrington, K. L.; Kaler, E. W.; Miller, D. D. *Langmuir* **1997**, *13*, 5531.
- [25] Malliaris, A.; Binana-Limbele, W.; Zana, R. *J. Colloid Interface Sci.* **1986**, *110*, 114.
- [26] Israelachvili, I. N.; Mitchell, D. J.; Ninham, B. N. *J. Chem. Soc., Faraday Trans. II* **1976**, *72*, 1525.
- [27] Gaillon, L.; Lelièvre, J.; Gaboriaud, R. *J. Colloid Interface Sci.* **1999**, *213*, 287.
- [28] Knock, M. M.; Bain, C. D. *Langmuir* **2000**, *16*, 2857.
- [29] Wang, Y.; Han, B.; Yan, H.; Cooke, D. J.; Lu, J.; Thomas, R. K. *Langmuir* **1998**, *14*, 6054.
- [30] Subramanian, V.; Ducker, W. A. *Langmuir* **2000**, *16*, 4447.
- [31] Wang, Y.; Lu, J.; Yan, H. *J. Phys. Chem. B* **1997**, *101*, 3953.
- [32] Hugerth, A.; Sundelöf, L.-O. *Langmuir* **2000**, *16*, 4940.
- [33] Lin, H.-P.; Kao, C.-P.; Mou, C.-Y.; Liu, S.-B. *J. Phys. Chem. B* **2000**, *104*, 7885.
- [34] Appell, J.; Porte, G.; Poggi, Y. *J. Colloid Interface Sci.* **1982**, *87*, 492.
- [35] Rehage, H.; Hoffmann, H. *Mol. Phys.* **1991**, *74*, 933.
- [36] Cates, M. E.; Candau, S. J. *J. Phys.: Condens. Matter* **1990**, *2*, 6869.
- [37] Rao, U. R. K.; Manohar, C.; Valaulikar, B. S.; Iyer, R. M. *J. Phys. Chem.* **1987**, *91*, 3286.

4. Effect of additives on properties of surfactant dimers in solution

- [38] Israelachvili, J. *Intermolecular and Surface Forces*, 2nd ed., Academic Press: London, 1992.
- [39] Shikata, T.; Hirata, H.; Kotaka, T. *Langmuir* **1987**, *3*, 1081.
- [40] Berret, J. F.; Appell, J.; Porte, G. *Langmuir* **1993**, *9*, 2851.
- [41] Wheeler, F. K.; Izu, P.; Fuller, G. G. *Rheol. Acta* **1996**, *35*, 139.
- [42] Hoffmann, H., et al. *Tenside Deterg.* **1985**, *22*, 290..
- [43] Raghavan, S. R.; Kaler, E. W. *Langmuir* **2001**, *17*, 300.
- [44] Candau, S. J., et al. *J. Phys. IV* **1993**, *3*, 197
- [45] Cates, M. E. *Macromolecules* **1987**, *20*, 2289.
- [46] Yang, J. *Curr. Opin. Colloid Interface Sci.* **2002**, *7*, 276.
- [47] Siriwatwechakul, W.; LaFleur, T.; Prud'homme, R. K.; Sullivan, P. *Langmuir* **2004**, *20*, 8970.
- [48] Zhang, Y.; Schmidt, J.; Talmon, Y.; Zakin, J. L. *J. Colloid Interface Sci.* **2005**, *286*, 696.
- [49] Rose, G. D.; Teot, A. S. *Structure and Flow in Surfactant Solutions*; American Chemical Society: Washington, DC, 1994; pp 352-369.
- [50] Rose, G. D.; Foster, K. L. *J. Non-Newtonian Fluid Mech.* **1989**, *31*, 59-85.
- [51] Sylvester, N. D.; Smith, P. S. *Ind. Eng. Chem. Prod. Res. Dev.* **1979**, *18*, 47-49.
- [52] Maitland, G. C. *Curr. Opin. Colloid Interface Sci.* **2000**, *5*, 301-311.
- [53] Yamamuro, H.; Koyanagi, K.; Takahashi, H. *Bull. Chem. Soc. Jpn.* **2005**, *78*, 1884-1886.
- [54] Sakaiguchi, Y.; Shikata, T.; Urakami, H.; Tamura, A.; Hirata, H. *Colloid Polym. Sci.* **1987**, *265*, 750.
- [55] Aswal, V.; Thiyagarajan, P.; Goyal, P. *J. Phys. Chem. B* **1998**, *102*, 2469.
- [56] Shikata, T.; Imai, S. *J. Colloid Interface Sci.* **2001**, *244*, 399.
- [57] Shikata, T.; Imai, S.; Morishima, Y. *Langmuir* **1998**, *14*, 2020.
- [58] Shikata, T.; Pearson, D. *Langmuir* **1994**, *10*, 4027.
- [59] Shikata, T.; Imai, S. *J. Phys. Chem. B* **1999**, *103*, 8694.
- [60] Shikata, T.; Hirata, H.; Kotaka, T. *J. Phys. Chem.* **1990**, *94*, 3702.
- [61] Buwalda, R.; Jonker, J. M.; Engberts, J. B. F. N. *Langmuir* **1999**, *15*, 1083.
- [62] Thuin, G.; Candau, F.; Zana, R. *Coll. Surf. A* **1998**, *131*, 303.
- [63] Raghavan, S. R.; Edlund, H.; Kaler, E. *Langmuir* **2002**, *18*, 1056.
- [64] Hashimoto, K.; Imae, T.; Nakazawa, K. *Colloid Polym. Sci.* **1992**, *270*, 249.
- [65] Munch, C.; Hoffmann, H.; Kalus, J.; Ibel, K.; Neubauer, G.; Schmelzer, U. *J. Appl. Crystallogr.* **1991**, *24*, 740.
- [66] Munch, C.; Hoffmann, H.; Ibel, K.; Kalus, J.; Neubauer, G.; Schmelzer, U.; Selbach, J. *J. Phys. Chem.* **1993**, *97*, 4514.
- [67] Geng, Y.; Romsted, L. S.; Froehner, S.; Zanette, D.; Magid, L. J.; Cuccovia, I. M.; Chaimovich, H. *Langmuir* **2005**, *21*, 562.
- [68] Abdel-Rahem, R. *Tenside Surf. Det.* **2005**, *42*, 95.
- [69] Abdel-Rahem, R.; Gradzielski, M.; Hoffmann, H. *J. Colloid Interface Sci.* **2005**, *288*, 570.
- [70] Hoffmann, H.; Platz, G.; Rehage, H.; Schorr, W.; Ulbricht, W. *Ber. Bunsenges. Phys. Chem.* **1981**, *85*, 255.
- [71] Oda, R.; Huc, I.; Candau, S.J. *Angew. Chem. Int. Ed.* **1998**, *37*, 2689.
- [72] Oda, R.; Huc, I.; Schmutz, M.; Candau, S.J.; MacKintosh, F. C. *Nature* **1999**, *399*, 566.
- [73] Buwalda, R. T.; Engberts, J. B. F. N. *Langmuir* **2001**, *17*, 1054.
- [74] Jiang, N.; Li, P.; Wang, Y.; Wang, J.; Yan, H.; Thomas, R. K. *J. Phys. Chem. B* **2004**, *108*, 15385.

4. Effect of additives on properties of surfactant dimers in solution

- [75] Thalody, B.; Warr, G. G. *Aust. J. Chem.* **2004**, *57*, 193.
- [76] Wang, Y.; Desbat, B.; Manet, S.; Aimé, C.; Labrot, T.; Oda, R. *J. Colloid Interface Sci.* **2005**, *283*, 555.
- [77] Shikata, T.; Hirata, H.; Kotaka, T. *Langmuir* **1987**, *4*, 354.
- [78] Cassidy, M. A.; Warr, G. G. *J. Phys. Chem.* **1996**, *100*, 3237.
- [79] Underwood, A. L.; Anacker, E. W. *J. Colloid Interface Sci.* **1987**, *117*, 296.
- [80] Rosen, M. J.; Mathias, J. H.; Davenport, L. *Langmuir* **1999**, *15*, 7340.
- [81] Rakotoaly, R. H. Thèse de Doctorat, Louvain-la-Neuve, 2001.
- [82] Mukerjee, P.; Mysels, K. J. *Critical Micelle Concentrations of Aqueous Surfactant Systems*; NSRDS-NBS 36, National Standard Reference Data Systems, NBS 36; NBS: Washington, DC, 1971.
- [83] Ferry, J. D. *Viscoelastic Properties of Polymers*, 3rd ed.; Wiley, New York, 1980.
- [84] Ait Ali, A.; Makhloufi, R. *Phys. Rev. E* **1997**, *56*, 4474.
- [85] Kern, F.; Zana, R.; Candau S. J. *Langmuir* **1991**, *7*, 1344.
- [86] Magid, L. J. *J. Phys. Chem.* **1998**, *102*, 4064.
- [87] Kern, F.; Lequeux, F.; Zana, R.; Candau S. J. *Langmuir* **1994**, *10*, 1714.
- [88] Lequeux, F. *Europhys. Lett.* **1992**, *19*, 675.
- [89] Hassan, P. A.; Raghavan, S. R.; Kaler, E. *Langmuir* **2002**, *18*, 2543-2548.
- [90] In, M.; Warr, G. G.; Zana, R. *Phys. Rev. Lett.* **1999**, *83*, 2278.
- [91] Drye, T. J.; Cates, M. E. *J. Chem. Phys.* **1992**, *96*, 1367.
- [92] Panizza, P.; Cristobal, G.; Curely, J. *J. Phys. Condens. Matter* **1998**, *10*, 11659.
- [93] Cristobal, G.; Rouch, J.; Curely, J.; Panizza, P. *Physica A* **1999**, *268*, 50.
- [94] Candau, S. J.; Oda, R. *Coll. Surf. A* **2001**, *183*, 5-14.
- [95] Zana, R. *Adv. Colloid Interface Sci.* **2002**, *97*, 205.
- [96] Laschewsky, A.; Lunkenheimer, K.; Rakotoaly, R. H.; Wattebled, L. *Colloid Polym. Sci.* **2005**, *283*, 469.
- [97] Laschewsky, A.; Wattebled, L.; Arotçaréna, M.; Habib-Jiwan, J.-L.; Rakotoaly, R. H. *Langmuir* **2005**, *21*, 7170.
- [98] Wattebled, L.; Laschewsky, A.; Moussa, A.; Habib-Jiwan, J.-L. *Langmuir* **2006**, *22*, 2551.
- [99] Antonietti, M.; Hentze, H.-P. *Adv. Mater.* **1996**, *8*, 840.
- [100] Laughlin, R. G. *J. Soc. Cosmet. Chem.* **1981**, *32*, 371-392.
- [101] Laschewsky, A. *Tenside Surf. Det.* **2003**, *40*, 246.
- [102] Laschewsky A. *Adv. Polym. Sci.* **1995**, *124*, 53-59.
- [103] Liu, S.; González, Y. I.; Danino, D.; Kaler, E. W. *Macromolecules* **2005**, *38*, 2482.
- [104] Zhu, Z.; González, Y. I.; Xu, H.; Kaler, E. W.; Liu, S. *Langmuir* **2006**, *22*, 949-955.
- [105] Kline, S. R. *Langmuir* **1999**, *15*, 2726.
- [106] Gerber, M. J.; Kline, S. R.; Walker, L. M. *Langmuir* **2004**, *20*, 8510.
- [107] Kim, T.-H.; Choi, S.-M.; Kline, S. R. *Langmuir* **2006**, *22*, 2844.
- [108] Gerber, M. J.; Walker, L. M. *Langmuir* **2006**, *22*, 941-948.
- [109] Thünemann, A. F. *Prog. Polym. Sci.* **2002**, *27*, 1473.
- [110] Zana, R. *J. Colloid Interface Sci.* **2002**, *248*, 203.
- [111] Kreke, P. J.; Magid, L. J.; Gee, J. C. *Langmuir* **1996**, *12*, 699.
- [112] Magid, L. J.; Li, Z.; Butler, P. D. *Langmuir* **2000**, *16*, 10028 and references therein.
- [113] Barker, C. A.; Saul, D.; Tiddy, G. J. T.; Wheeler, B. A.; Willis, E. *J. Chem. Soc., Faraday Trans. I* **1974**, *70*, 154.

4. Effect of additives on properties of surfactant dimers in solution

- [114] Kalur, G.; Raghavan, S. R. *J. Phys. Chem. B* **2005**, *109*, 8599.
- [115] Mu, J. H.; Li, G. Z.; Jia, X. L.; Wang, H. X.; Zhang, G. Y. *J. Phys. Chem. B* **2002**, *106*, 11685.
- [116] Raghavan, S. R.; Fritz, G.; Kaler, E. W. *Langmuir* **2002**, *18*, 3797.
- [117] Nakamura, K.; Shikata, T. *Langmuir* **2006**, *22*, 9853-9859.
- [118] Benrraou, M.; Bales, B. L.; Zana, R. *J. Phys. Chem. B* **2003**, *107*, 13432-13440.
- [119] Zhao, J.; Christian, S.D.; Fung, B.M. *J. Phys. Chem. B* **1998**, *102*, 761.
- [120] Rosen, M.J.; Gao, T.; Nakatsuji, Y.; Masuyama, A. *Coll. Surf. A* **1994**, *88*, 1.
- [121] Rosen, M.J.; Zhu, Z.; Gao, T. *J. Colloid Interface Sci.* **1993**, *157*, 2524.
- [122] Liu, L.; Rosen, M.J. *J. Colloid Interface Sci.* **1996**, *179*, 454.
- [123] Esumi, K.; Miyazaki, M.; Arai, T.; Koide, Y. *Coll. Surf. A* **1998**, *135*, 117.
- [124] Zana, R. Lévy, H. Kwetkat, K. *J. Colloid Interface Sci.* **1998**, *197*, 370.
- [125] Alargova, R.G.; Kochijashky, I. I.; Sierra, M. L.; Kwetkat, K.; Zana, R. *J. Colloid Interface Sci.* **2001**, *235*, 119-129.
- [126] Zhu, Y.-P.; Masuyama, A.; Nagata, T.; Okahara, M. *J. Jpn. Oil Chem. Soc.* **1991**, *40*, 473.
- [127] Wang, X.; Wang, J.; Wang, Y.; Ye, J.; Yan, H.; Thomas, R. K. *J. Colloid Interface Sci.* **2005**, *286*, 739-746.
- [128] Bakshi, M. S.; Singh, K. *J. Colloid Interface Sci.* **2005**, *287*, 288-297.
- [129] Zana, R.; Lévy, H.; Danino, D.; Talmon, Y.; Kwetkat, K. *Langmuir* **1997**, *13*, 402.
- [130] Stathatos, E.; Lianos, P.; Rakotoaly, R. H.; Laschewsky, A.; Zana, R. *J. Colloid Interface Sci.* **2000**, *227*, 476.
- [131] Menger, F.M.; Eliseev, A.V. *Langmuir* **1995**, *11*, 1855.
- [132] Li, X.; Kunieda, H. *Curr. Op. Colloid Interface Sci.* **2003**, *8*, 327.
- [133] Kondo, Y.; Uchiyama, H.; Yoshino, N.; Nishiyama, K.; Abe, M. *Langmuir* **1995**, *11*, 2380.
- [134] Kaler, E. W.; Herrington K. L.; Murthy, A. K.; Zasadzinski, J. A. N. *J. Phys. Chem.* **1992**, *96*, 6698.
- [135] Yaacob, I. I.; Bose, A. *J. Colloid Interface Sci.* **1996**, *178*, 638.
- [136] Lucassen-Reynders, E. H.; Lucassen, J.; Giles, D. *J. Colloid Interface Sci.* **1981**, *81*, 150.
- [137] Zhang, L. H.; Zhao, G. X. *J. Colloid Interface Sci.* **1989**, *127*, 353.
- [138] Li, X. G.; Liu, F. M. *Coll. Surf. A* **1995**, *96*, 113.
- [139] Yu, Z. J.; Zhao, G. X. *J. Colloid Interface Sci.* **1989**, *130*, 414.
- [140] Tieke, B. *Colloid Polym. Sci.* **2005**, *283*, 421-430.
- [141] Holmberg, K.; Jönsson, B.; Kronberg, B.; Lindman B. *Surfactants and Polymers in Aqueous Solution*, 2nd ed.; Wiley, Chichester, 2002.
- [142] Kamenka, N.; El Amrani, M.; Appell, J.; Lindheimer, M. *J. Colloid Interface Sci.* **1991**, *143*, 463.
- [143] Prévost, S.; Gradzielski, M.; Wattebled, L.; Laschewsky, A. to be published.

5. EXPERIMENTAL PART

Water used for all experiments was purified by a Millipore Qplus water purification system (resistance 18 M Ω cm).

5.1 Standard surfactants

Benzyltrimethyl-n-dodecylammonium chloride BDDAC (C₂₁H₃₈ClN, M_r = 339.99, puriss. \geq 99 %) and n-dodecyltrimethylammonium chloride DTAC (C₁₅H₃₄ClN, M_r = 263.89, purum. \geq 98 %) were purchased from Fluka. Sodium n-dodecyl sulfate SDS (C₁₂H₂₅SO₄Na, M_r = 288.38) and sodium laurate (C₁₁H₂₃COONa, M_r = 222.32) were obtained from Merck and Fluka, respectively.

5.2 Analytical methods

¹H (300 MHz) and ¹³C (75 MHz) NMR spectra were taken with a Bruker Avance 300 apparatus (128 scans for ¹H, 10000 scans for ¹³C).

IR-spectra were taken from KBr pellets using a Bruker IFS FT-IR spectrometer 66/s.

Mass spectra were recorded by a TSQ Quantum spectrometer (Thermo Finnigan) in Louvain-la-Neuve (by *Prof. J.-L. Habib-Jiwan*).

UV-Visible spectra were recorded with a Cary-1 UV-Vis spectrophotometer (Varian) equipped with temperature controller (Julabo F-10). Quartz cuvettes containing the sample were used, with a path length of 1 cm.

Elemental analysis was done with a model EA 1110 (CHNS-O) from CE Instruments.

Thermal properties of the dimeric surfactants **dimer EDTA** and **EO-2(MoO₄)** were measured with a TGA/SDTA 851 **thermal gravimetric analyzer (TGA)** (Mettler Toledo) and a DSC 822 **differential scanning calorimeter (DSC)** (Mettler Toledo) under nitrogen atmosphere. For TGA measurements, 2.0-5.0 mg of the synthesized products were scanned at a rate of 20 °C·min⁻¹ from 25 °C to 700 °C. The DSC instrument was calibrated by indium and zinc for temperature and enthalpy changes. For analysis by DSC, 2.0-5.0 mg of the samples were placed in an aluminium pan. They were scanned from 25 °C to 180 °C at a rate of 5 °C·min⁻¹. The melting point (T_m) was taken as the onset temperature of the endothermic peak which was observed in the heating trace.

Dynamic light scattering (DLS) for the characterization of the particle size distributions of micellar solutions was performed with a High Performance Particle Sizer (HPPS, from Malvern Instruments, UK) equipped with a He-Ne laser ($\lambda = 633$ nm, optical path 10 mm) and a thermo-electric Peltier temperature controller (temperature control range: 10-90 °C). The measurements were made at the scattering angle $\theta = 173^\circ$ (“backscattering detection”) at 25 °C (± 0.1 °C). The autocorrelation functions were analyzed with the CONTIN method. For all the samples, the results were calculated first using the “multi-modal distribution mode”. For monomodal size distributions, the measurement was repeated with the “mono-modal distribution mode”. 5 runs of 30 s were performed. The following refractive index n at 25 °C were taken: n of surfactant solutions = 1.5, n_0 water = 1.33. The following solvent viscosities η_0 were taken (in cP at 25 °C): η_0 water = 0.89. Prior to measurement, the surfactant solutions were filtered using a Sartorius Ministar-plus 0.45 μm disposable filter and were placed in a PS cuvette or glass cuvette (for high temperature measurements).

Principle and theory of DLS [1]

Light scattering is utilized in many areas of science, for instance to determine the particle size, the molar mass of polymers or aggregates, or the shape of aggregates, and was first systematically explored in 1871 by Tyndall [2].

If a small particle is illuminated by a source of light such as a laser, the particle will scatter the light in all directions.

Whereas the time average of the scattering intensity is measured in static light scattering (SLS), the fluctuations of the scattering intensity due to the Brownian motion of the particles are correlated by means of an intensity-time autocorrelator in DLS. The correlator monitors the scattering intensities in small time intervals τ over a total measurement time $t = n \cdot \tau$. The intensity-time autocorrelation function $g_2(h, t)$ is then calculated as:

$$g_2(h, t) = \frac{\langle I(t) \cdot I(t + \tau) \rangle}{\langle I(t) \rangle^2} \quad \text{Equation 5.2-1}$$

where h is the magnitude of the scattering vector:

$$h = \frac{4\pi n}{\lambda_0} \sin \frac{\Theta}{2} \quad \text{Equation 5.2-2}$$

with n the refractive index of the medium and Θ the scattering angle.

From $g_2(h, t)$ the correlation function of the electric field $g_1(h, t)$ is derived by:

$$g_1(h, t) = \sqrt{\frac{g_2(h, t) - \langle I(t) \rangle^2}{\langle I(t) \rangle^2}} \quad \text{Equation 5.2-3}$$

Moreover, for scattering centers undergoing Brownian motion, it can be shown that $g_1(h, t)$ is the Fourier transformation of a space – time correlation function. After mathematical transformations of $g_1(h, t)$, the following relation can be obtained:

$$g_1(h, t) = B \cdot e^{-Dh^2 t} \quad \text{Equation 5.2-4}$$

With the assumption of hard spherical particles, the hydrodynamic diameter D_H of the scattering objects is calculated from the diffusion coefficient D (see Equation 5.2-4), according to the Stokes-Einstein equation:

$$D_H = \frac{kT}{3\pi\eta D} \quad \text{Equation 5.2-5}$$

where k is the Boltzmann constant and η the viscosity of the solution.

Static fluorescence measurements were performed with a Cary Eclipse spectrometer from Varian.

Conductivity measurements were carried out on surfactant solutions at room temperature with a conductimeter MPC227 from Mettler Toledo (electrode NTC, 0 – 200.0 mS). The instrument is calibrated before measurements with both air and a standard solution (12.88 mS at 25 °C).

Turbidimetry involved the use of a temperature controlled turbidimeter model TP1 (E. Tepper, Germany) with heating and cooling rates of 1 °C·min⁻¹.

Viscometric measurements were performed with a semiautomatic Ubbelohde viscometer (Schott, Type 53110/I) at 30° C (thermostatic bath). The minimal start volume of the sample is 15 mL. The dilution is carried out in the tank of the capillary with MilliQ water, via a water dispenser (665 Dosimat). Particular attention is paid to avoid the formation of foam by controlling precisely the speed of ascension of the surfactant solutions in the capillary. Photoelectric cells connected to a chronometer (VB2 Lauda) allow the determination of the run time by detecting the meniscus of the solution in the capillary. The reference run time is measured for MilliQ water in the same capillary.

Rheological measurements were carried out with a dynamic stress rheometer DSR200 from Rheometrics (stress-controlled). The rheometer is connected to a thermostat (Polyscience) for temperature control. Both a cone plate (Titanium, diameter 40 mm, cone angle 0.0401 radians with gap 0.053 mm) measuring system and a coaxial cylinder system (Couette system with cup diameter 32 mm, bob diameter 29.5 mm and bob length 44 mm; cup in Aluminium and bob in Titanium) were used. The latter system is applicable for solutions of low viscosity, while the cone plate is more often

used for highly viscous solutions. Stress is applied by means of a torsional force to the cone or bob. Both rotation and oscillation experiments were performed on the surfactant mixtures as described in 5.19.

Cryo-high resolution scanning electron microscopy (Cryo-SEM) micrographs of the aqueous mixtures of surfactant dimer EO-2 with SDS were recorded with a S-4800 microscope from Hitachi. Each sample was cooled by plunging into nitrogen slush at atmospheric pressure. Afterward, the samples were freeze-fractured at -180°C , etched for 60 seconds at -98°C and sputtered with Platinum in the GATAN Alto 2500 Cryo-preparation chamber and then transferred into the Cryo-FE-SEM. The micrographs were taken by *Dr. B. Tiersch* (University of Potsdam, Inst. of Chemistry).

5.3 Synthesis and characterization of cationic dimers

A set of compounds was kindly provided by *Dr. R. H. Rakotoaly*. The dimeric compounds can be synthesized conveniently, whereas the higher oligomers present more difficulties in their synthesis and purifications as briefly addressed in chapter 2 [3]. Larger amounts of the surfactant dimers were synthesized according to [3-4] (synthesis procedures occasionally adapted, see Appendix 1), so as to have enough material for the product-consuming investigations. The purity of the compounds was checked by ^1H NMR spectroscopy (cf. Appendix 1). Concerning the higher oligomers, ^1H NMR spectra were taken on stock material in order to validate the purity of the compounds (no degradation) before use for the characterization of the properties.

5.4 Synthesis of the anionic gemini surfactant based on EDTA (“Dimer EDTA”)

Materials

N-methyldodecylamine (97%, MW=199.38 g/mol) and ethylene diamine tetraacetic acid dianhydride (98%, MW=256.22 g/mol) were purchased from Aldrich and used as received. Methanol was distilled prior to use or was analytical grade. Acetone was technical grade.

Procedure

N-methyldodecylamine (3.20 g, 16 mmol) and EDTA anhydride (2.05 g, 8 mmol) suspended in 50 mL of methanol are reacted for 22 h at $40-45^{\circ}\text{C}$. The EDTA anhydride particles progressively disappear as the reaction progresses. After cooling of the sample to room temperature, the remaining particles are filtered off. Subsequently, the reaction mixture is evaporated to give a yellowish oil. Acetone is then added until a white solid precipitates. The precipitate is filtered off over

a fritted glass (N° 4) and is further purified by dissolution in chloroform and precipitation in acetone, to yield a white powder (3.7 g, 71%). Finally, the product is neutralized with sodium hydroxide (1M aq) and the obtained solution is freeze-dried.

Analysis of compound before neutralization with NaOH

The absence of free amine in the product was checked by thin layer chromatography (TLC) with a mixture methanol / dichloromethane 1:1 (v/v) and developed by I₂ vapour.

Elemental analysis (C₃₆H₇₀N₄O₆, MW = 654.94 g/mol): Calculated: C 66.02; N 8.55; H 10.77; Found: C 65.97; N 8.93; H 11.22.

Mass Spectrometry (APCI, +) Signal at m/z = 655.52 [M+1].

¹H NMR (CDCl₃, 300 MHz, δ in ppm): 0.88 (t, 6H, CH₃-); 1.17-1.37 (m, 36H, -(CH₂)₉-); 1.45-1.60 (m, 4H, -CH₂-C-N-C=O); 2.92 (s, 6H, CH₃-N-C=O); 2.98-3.08 (m, 4H, C-CH₂-N-CO); 3.14-3.20, 3.31-3.37 (2m, 2H+2H, N-CH₂-CH₂-N); 3.50, 3.79 (2m, 4H+4H, CH₂-CO-N + CH₂-CO-O).

¹³C NMR (CDCl₃, 125 MHz, δ in ppm): 14.0 (CH₃-); 22.65 (CH₃-CH₂-); 26.74, 26.87, 27.11 (N-CH₂-CH₂-CH₂-); 28.16 (N-CH₂-CH₂-CH₂); 29.32, 29.56, 29.60, 31.88 (-(CH₂)₆-); 33.60, 34.34 (CH₃NCH₂); 48.39, 49.14 (N-CH₂-CH₂-N); 52.73, 52.90, 52.95 (CH₃NCH₂); 56.08, 56.14 and 57.70, 57.82 (CH₂-CO-N and CH₂-CO-O); 169.35, 169.01 (N-C=O); 172.73, 172.90 (O-C=O).

FT-IR spectroscopy (KBr, selected bands in cm⁻¹) 2958, 2921, 2852, 1712, 1656, 1639, 1373, 1196, 893.

TGA: neither solvent rests nor water is contained in the sample (cf. Appendix 7, Figure A7-1, no weight loss below 150 °C); the thermal decomposition starts above 180 °C.

Analysis of the compound after neutralization with NaOH

¹H NMR (CDCl₃, 300 MHz, δ in ppm): 0.88 (t, 6H, CH₃-); 1.15-1.35 (m, 36H, -(CH₂)₉-); 1.46 (m, 4H, -CH₂-C-N-CO); 2.39 (m, 4H, N-CH₂-CH₂-N); 2.86 (s, 6H, CO-N-CH₃); 2.95-3.35 (m, 4H+4H+4H, C-CH₂-N-CO, N-CO-CH₂-N, N-CH₂-COO).

¹³C NMR (CDCl₃, 75 MHz, δ in ppm): 14.06 (CH₃-); 22.65 (CH₃-CH₂-); 27.09 (N-CH₂-CH₂-CH₂-); 28.45 (N-CH₂-CH₂-CH₂); 29.5-29.7 (-(CH₂)₆-); 31.89 (CH₃-CH₂-CH₂-); 33.76, 34.52 (CH₃NCH₂); 48.11, 49.11 (N-CH₂-CH₂-N); 52.23 (CH₃NCH₂); 55.66, 59.36 (CH₂-CO-N + CH₂-CO-O); 170.91 (N-C=O); 177.75, 178.13 (O-C=O).

Elemental analysis (C₃₆H₆₈N₄O₆Na₂, 2H₂O MW = 734.96 g/mol): Calculated: C 58.83; N 7.62; H 9.87; Found: C 58.63; N 7.75; H 9.41.

TGA: ca. 5 wt % water are contained in the sample (cf. Appendix 7, Figure A7-2), which is consistent with the dihydrate form found via elemental analysis; the thermal decomposition starts above 180 °C. (see also all Figures in Appendix 3 concerning the characterization of the compound)

5.5 Acidic titration of neutralized dimer EDTA

Acid-base titration was performed automatically using a 670 Titroprocessor (Metrohm). Hydrochloric acid was added progressively to the anionic dimer solution via a Metrohm 665 Dosimat, and the pH was measured with a pH electrode Metrohm 6.0233.100.

Dimer EDTA under its acidic form (0.1217 g, $n_{\text{NH}^+ \text{-CH}_2 \text{-COO}^-} = 0.372 \text{ mmol} = 2 \times 0.186 \text{ mmol}$) was first neutralized with an excess sodium hydroxide (6 mL of NaOH 0.1N from Merck, i.e. 0.6 mmol). Hence, the calculated molar excess of NaOH is 0.228 mmol ($= 0.600 - 0.372 \text{ mmol}$). The initial pH value is 11.80. Subsequently, the solution was titrated with hydrochloric acid (HCl, 0.1M from Merck). The titration curve and its derivative are shown in chapter 2, Figure 2.2-5. From the derivated curve, three equivalent points are found: the first equivalent point is E_0 with $V_0 = 1.93 \text{ mL}$ and $\text{pH}_0 = 10.90$. Basically, it corresponds to the neutralization of the excess NaOH in solution within experimental errors (cf. Table 5.5-1). The second equivalent point is E_1 with $V_1 = 3.95 \text{ mL}$ and $\text{pH}_1 = 8.51$, and the third equivalent point is E_2 with $V_2 = 5.69 \text{ mL}$ and $\text{pH}_2 = 4.98$. These points correspond to two transitions from a basic form of the dimer to a more acidic one, which are discussed in more detail in part 2.2.3.b. The end volume of HCl added is 14.44 mL, and the solution consists in a white precipitate at a final pH below 2.5.

Table 5.5-1: Volumes of HCl (0.1M) and corresponding numbers of moles, added between each equivalent point.

Equivalent Points	volume HCl (mL)	n_{HCl} (mmol)	pH
E_0	1.93	0.193	10.90
$E_1 - E_0$	2.02	0.202	8.51
$E_2 - E_1$	1.74	0.174	4.98

5.6 Determination of Krafft temperatures of oligomeric surfactants

Krafft-temperatures were estimated by observing the dissolution of a small crystal of the surfactants in water by a microscope (Olympus BH-2) equipped with a hot stage (Linkam TP 92).

5.7 Surface tension measurements

Surface tension is probably the most common means of determining the critical micellization concentration (CMC). The method is convenient, relatively fast, and non-destructive. It is often advisable to make measurements on samples that have rested undisturbed for many hours [5], since surfactant molecules need time to accumulate at the surface and attain the equilibrium. In general, the higher is the molar mass of an amphiphile, the longer is the time necessary to obtain a well-equilibrated surface. In addition, equilibration times can be also even longer below the CMC. Below the CMC, surfactant molecules adsorb at the air/water interface and thus lower the surface tension. It decreases gradually as the concentration of surfactant increases. Above the CMC, any added surfactant joins a micelle rather than to increase the concentration of molecularly dissolved surfactants. Therefore, newly added surfactants do not increase the concentration in the interfacial film (see parts *1.1.2.a* and *1.1.2.b*). Hence, the surface tension becomes constant. As a result, a plot of surface tension versus surfactant concentration decreases below the CMC and levels off above it. The CMC is determined by the discontinuity in the plot of the surface tension as a function of the logarithm of concentration (as derived from the transformation of Gibbs' equation) [6-8].

Surface tensions were measured at room temperature (about 296 K) with a Du Noüy ring tensiometer K12 from Krüss (Hamburg, Germany) taking into account necessary modifications for the measurement of surfactant solutions [9-10].

Description of the method

The ring method [11-13] involves a Platinum-Iridium ring, suspended from a precision balance and immersed horizontally into the liquid. The surface tension is calculated from the force required to pull the ring through the surface.

A height-adjustable sample carrier is used to bring the liquid to be measured into contact with the ring. The liquid is raised until contact with the surface is registered (a force acts on the balance as soon as the ring touches the surface). The sample is then lowered again so that the liquid film produced beneath the ring is stretched. As the film is stretched, a maximum force is experienced (the film breakage is generally avoided during the measurement). If the circumference of ring is known, this maximal force measured can be used to calculate surface tension (or interfacial tension). A further requirement is that the ring must have a very high surface energy (contact angle θ must be 0° at the maximum force measured), hence explaining the use of a platinum-iridium alloy.

In a first approximation, the calculation is made according to the following equation (established from equilibrium between the forces applied on the ring):

$$F_{\max} = 2 \times 2\pi R \sigma \quad \text{Equation 5.7-1}$$

with σ is the surface tension, R is the mean radius of the ring and F_{\max} corresponds to the maximum force recorded when pulling the ring from the interfacial film. Note that the weight of the ring (which remains constant) is taken into account in F_{\max} via the tare made when running the measurement.

Nevertheless, this calculation requires a correction factor, mainly because the weight of the liquid column lifted by the ring cannot be neglected. This empirical correction factor was determined by *Harkins and Jordan* [12] and is incorporated as follows:

$$\sigma = f \cdot \sigma^* = f \cdot \frac{F_{\max}}{4\pi R} \quad \text{Equation 5.7-2}$$

where f is the dimensionless Harkins and Jordan factor and σ^* the measured surface tension value (uncorrected). Harkins & Jordan drew up tables of correction values by determining different surface tensions with rings of different diameters. The Harkins & Jordan correction offers great accuracy. The correction factor can also be determined from the following equation published by *Zuidema and Waters*, based on the extrapolation of the tables developed by *Harkins and Jordan* [14]:

$$f = 0.725 + \sqrt{\frac{0.01452 \cdot \sigma^*}{\frac{1}{4}U^2(\rho_1 - \rho_2)} + 0.04534 - \frac{1.679}{R/r}} \quad \text{Equation 5.7-3}$$

where r is the radius of the cross section of the wire (typically 0.2 mm), U is the wetting length (twice the circumference of the ring), ρ_1 and ρ_2 are the densities of the liquid phase and the gas phase (or liquid phase) above it, respectively.

This correction is carried out automatically by the tensiometer K12.

Preparation of the samples and measurements

A concentrated stock solution of surfactant is prepared by dissolving a defined amount of surfactant powder (after freeze drying) with MilliQ water in a 100 mL graduated flask. Subsequently, a range of surfactant solutions (ca. 14 concentrations) is prepared by dilution of precise volumes of the stock solution in 25 mL graduated flasks with MilliQ water. After homogenization, the solutions were placed in crystallizing dishes with rigorously the same geometry (40 mL, 50 mm diameter, 30 mm height from Roth, Germany) and were allowed to equilibrate minimum 12 h before measurement. Efforts were particularly made to avoid the evaporation of water in the equilibration periods.

In every preparation step, the glassware was extensively cleaned with MilliQ-water, and any contact between the surfactant solutions and materials which could cause the contamination by dirt or grease traces (e.g., from parafilm) was avoided. Indeed, the presence of only a small amount of grease could dramatically decrease the surface tension of the solutions and thus falsify the measurements.

The reference $\sigma_{\text{MilliQ-water}} = 71.5 \text{ mN}\cdot\text{m}^{-1}$ ($\pm 0.5 \text{ mN}\cdot\text{m}^{-1}$) for the geometry of the ring used was measured before each measurement series. After each measurement, the ring was carefully cleaned with MilliQ-water. The absence of residual surfactant or of dust traces on the ring and the conservation of the form of the ring were regularly verified by measuring the surface tension of MilliQ-water as a reference.

For surfactant dimer based on EDTA (anionic form), note that surface tension measurements were also performed at higher pH, namely at a pH value of 12. A buffer solution of sodium phosphate ($\text{Na}_3\text{PO}_4 \cdot 12 \text{ H}_2\text{O}$; $M_r = 380.12$; > 98 % from Aldrich) 0.01 mol/L in MilliQ water was used to prepare the stock surfactant solution of **dimer EDTA** (previously neutralized) and for the further dilutions. The surface tension of the buffer solution (pH = 12) was measured: $\sigma_{\text{buffer}} = 67.1 \text{ mN}\cdot\text{m}^{-1}$. This relatively low value compared to milliQ water can only be explained by the presence of surface active impurities in the sodium phosphate salt supplied.

5.8 Determination of CMC of cationic oligomers by dye solubilization methods.

An alternative method for the determination of the CMC of surfactants is the so-called dye solubilization method. Upon increasing the surfactant concentration, the absorption spectrum of a dye shifts from that in aqueous solution to a spectrum similar to that in apolar solvents when micelles are present (partition coefficient of the dye favourable to the micelles). Frequently used dyes for determining CMCs are for example pinacyanol chloride [15-18] or bromophenol blue [18]. Here, the dye selected for these experiments are pinacyanol chloride ($M_r = 388.94$; see Figure 5.8-1) and 2-anilinonaphthalene ($M_r = 219.29$; see Figure 5.8-2), both used as received from Aldrich.

Pinacyanol chloride (PIN) is a cationic dye belonging to the class of symmetric trimethinecyanine, a class of dyes which exhibits solvatochromic behaviour and which finds an important use as sensitizers in photography. The presence of nitrogen atoms in this molecule involves unbounded electrons (n-electrons) as well as π -electrons. Moreover, due to its amphipathic nature, PIN is soluble in a wide range of solvents, including water and chloroform. It is notable that PIN has already been used to determine the CMCs [19] and that, in combination with cationic surfactants, its solubilization site is at the aqueous micellar interface [20]. PIN was chosen as its ionic charge is the same as that of the surfactant oligomers studied [21], thus preventing the dye from influencing too much the micellization (favored aggregation process due to strong electrostatic interactions is avoided).

CMCs of the cationic surfactant oligomers with the *p*-xylylene spacer group (i.e. **BDDAC**, **p-X-2**, **p-X-3**, **p-X-4**) were determined by following the wavelength of absorbance maximum of pinacyanol (602 nm in dilute aqueous solution, see chemical structure of the dye in Figure 5.8-1) as function of the surfactant concentration, using a CARY UV-vis spectrophotometer (Varian).

The dye (100 μL of 5×10^{-5} M in water) was added to precise volumes of a starting surfactant solution and the whole mixture is adjusted to 5 ml with water. The solutions were then poured in cuvettes and allowed to equilibrate for at least 1 h before measuring the wavelength of the absorbance maximum. The concentration, at which a spectroscopic shift starts, was taken as CMC (see graphs in Appendix 5). The experiment with surfactant **p-X-2** was performed by *Dr. M. Arotçaréna* (U.C.Louvain-la-Neuve).

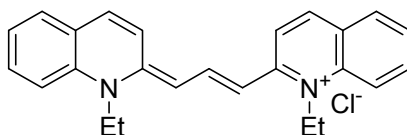


Figure 5.8-1: Chemical structure of dye pinacyanol chloride (quinaldine blue); 1,1'-diethyl-2,2'-carbocyanine chloride.

Also, CMCs were determined by following the wavelength of the fluorescence emission maximum of the sparingly water-soluble 2-anilinonaphthalene (2-AN, see chemical structure of the dye in Figure 5.8-2) as function of the surfactant concentration, using a thermostated spectrometer Salinco SLM 48000 (excitation at 294 nm). The experiments were performed for the three trimers and three tetramers in addition to **BDDAC** and **p-X-2**, by *M. Arotçaréna* and *A. Baudoult* (U.C.L.). CMC determination using spectral characteristics of dye 2-AN was already reported previously [22-24].

A saturated solution of 2-AN in water was used to prepare stock solutions of the surfactants which were diluted by pure water to the desired concentrations, to maintain a constant ratio of probe to surfactant. The emission maximum shifts gradually from ca. 445 nm to lower wavelengths with increasing surfactant concentration. The concentration, at which the emission wavelength starts becoming stable (between 420 nm and 415 nm) was taken as CMC (see some examples of graphs in Appendix 4).

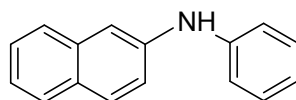


Figure 5.8-2: Chemical structure of dye 2-anilinonaphthalene (2-*N*-phenylnaphthylamine).

5.9 Time resolved fluorescence quenching experiments (TRFQ) [25]

Materials

9,10 dimethylantracene ($C_{16}H_{14}$, $M_r = 206.28$, 99 %) and 1-n-dodecylpyridinium chloride ($C_{17}H_{30}ClN$, $M_r = 283.9$, 98 %) were purchased from Aldrich and used as received. Water used for all experiments was purified by an Elgastat water purification system (resistance 18 M Ω cm).

Method

For the time-resolved fluorescence quenching (TRFQ) experiments, 9,10 dimethylantracene and 1-n-dodecylpyridinium chloride were used respectively as fluorescent probe (FP) and quencher (Q) (see chemical structures in Figure 5.9-1). The excitation wavelength was 400 nm. The fluorescence decay curves were recorded using a single photon counting apparatus with a PicoQuant Fluotime 200 set-up, at an emission wavelength of 430 nm. The excitation source is a Coherent Mira 900F pumped by a Verdi 10W delivering pulses of ca 130 fs. The repetition rate of the Mira is reduced to 3.8 MHz with a Coherent Pulse-Picker 9200 and the frequency is doubled by a Mira 9300 harmonic generator. The overall instrument response function is below 30 ps. The decay curve is recorded over a sufficiently long time (90 ns) to approximately reach the linear tail of the decay (intensity decreases over 3 decades to almost attain the level of the original noise). The decay traces were deconvoluted with the PicoQuant Fluofit software 3.0 [26-27]. The concentration of 9,10 dimethylantracene was kept at low level so that $[FP]/[micelle] < 0.03$ (to prevent the formation of excimers). The molar concentration ratio $R = [Q]/[micelle]$ was adjusted to be close to 1, as generally recommended (i.e. an average of one quencher per micelle) [28].

9,10 dimethylantracene is dissolved in n-pentane to make a stock solution of fluorophore (0.04 mmol/L). Required amounts of fluorophore (75 to 150 μ L) are then dropped in 5 ml graduated flasks and the n-pentane is evaporated by a stream of argon. Precise volumes of the surfactant stock solutions and when necessary, quencher stock solution (15 mmol/L) are added to the graduated flasks and filled with water. The surfactant concentrations were high enough to ensure that the probe 9,10 dimethylantracene and quencher were completely solubilized in the micelles. The solutions are sonicated until the full solubilization of 9,10 dimethylantracene is achieved (no trace of fluorophore observed on the glass under a UV lamp). Subsequently, they are poured in spectroscopy cuvettes (quartz) and allowed to equilibrate for at least 30 min before measuring the decay curves. All measurements were done at 21.0 ± 0.5 °C. The experiments were repeated twice in most cases and the results were consistent ($N_{agg} \pm 0.5$).

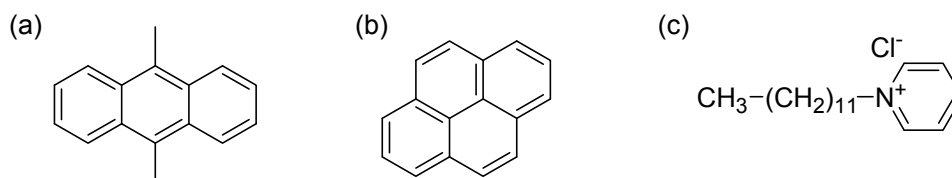


Figure 5.9-1: Chemical structure of (a) 9,10 dimethylantracene, (b) pyrene and (c) 1-n-dodecylpyridinium chloride.

Result Analysis

First, performing the experiments without quencher gives rise to single exponential decay curves ($I(t) = I(0) \exp \{-t/\tau_0\}$), which permits to obtain τ_0 , i.e. the probe fluorescence lifetime in the micellar environment. Then, the experiments are performed with quencher. The presence of quencher affects the decay traces, which are no longer mono-exponential but obey the following equation [28-33]:

$$I(t) = I(0) \exp \{-t/\tau_0 - R[1 - \exp(-k_q t)]\} \quad \text{Equation 5.9-1}$$

$I(t)$ and $I(0)$ are the fluorescence intensities at time t and zero, following the excitation. k_q is the rate constant for intramicellar quenching, and R is the molar ratio of quencher to micelle. Using a fitting program (software Igor), the fluorescence decay curves are fitted to this equation, the parameter τ_0 being fixed. The R -values are obtained there from and consequently, aggregation numbers N_{agg} can be calculated as:

$$N_{agg} = R \times \frac{(C - CMC)}{[Q]} \quad \text{Equation 5.9-2}$$

C is the total surfactant concentration, $[Q]$ the quencher concentration.

In Appendix 6, the fitted parameters k_q , R and τ_0 derived from the fluorescence decay curves of 9,10 dimethylantracene in micellar solutions are listed in Table A6-1, and the fluorescence decay curves in micellar solutions of SDS and **t-B-2**, **t-B-3**, **t-B-4** with and without quencher present are shown in Figures A6-1 – A6-4.

Additional comments on the method and results

The fluorescent probe 9,10 dimethylantracene could be also dissolved in the micellar solutions without sonication but dissolution was very slow, requiring extended times. The solutions were therefore sonicated to speed up their homogenization. This should minimize also possible contaminations of the measuring solutions, e.g. due to leaching of ions from the glassware, or due to growth of bacteria upon extended incubation times. There was no indication for the presence of microcrystals as result of this sample preparation method. In any case, the test measurements with the

reference surfactants **SDS** and **DTAC** gave very satisfactory results when comparing to literature data, and so, the same procedure was applied to the oligomeric surfactants.

Generally, a ratio [fluorophore]/[micelle] inferior to 0.05 is considered to be sufficient to prevent the formation of excimers etc. As described before, the ratio [fluorophore]/[micelle] was always inferior to 0.03 in the present study. So, there is one or zero fluorophore per micelle.

As explained above (and specified in Table A6-1 in Appendix 6), the concentration of the quencher was set as 0.3 to 1 molecules per micelle in average. As normally done, the quencher surfactant was selected to bear the same charge as the surfactants investigated, in order to have a uniform distribution of the quencher in the micelles.

Concerning the effect of the distribution of micelle size on the aggregation numbers determined by TRFQ, no analytical expression can be given (cf. double exponential Eq. 5.9-1), and thus no general discussion is possible a priori. Extensive numerical solutions would be needed to discuss this point. However characteristically, this is not done in the literature using TRFQ, even not in studies focused on the TRFQ method as such. Accordingly, it is not considered to be useful for the study where TRFQ is used only as a tool. Citing the review of Zana on gemini surfactants [34], studies of 12-s-12 surfactants showed that the polydispersity decreases with the micelle size, i.e., as the micelles are less and less elongated. Such a behavior is in agreement with the theoretical prediction that spherical micelles are nearly monodisperse [35]. When dimeric surfactant micelles grow, their shape changes and their polydispersity increases. But in the study, micelles are small so that it can be assumed that the distribution of micelles is narrow for the surfactants studied.

Excited states of the probe 9,10 dimethylantracene are short in comparison to pyrene (compare the curves for DMA in Appendix 6 and e.g. the decay curve given in Fig. 3 by Wang et al. [36]). This could a priori induce errors when the decay profiles are erroneously coupled with probe diffusion from one micelle to another. This possible difficulty was considered, but according to all indications, the problem does not apply. Indeed, the curves could be well fitted with the given equation; there is no indication of another short decay constant. Moreover, the measurements performed with standard surfactants dodecyltrimethylammonium chloride (**DTAC**) and sodium dodecyl sulfate (**SDS**) provided N_{agg} -values which match those found in the literature by using pyrene (see chemical structure in Fig. 5.9-1.b) as fluorescence probe (see ref. [28]). Also, it was pointed out before that “when quencher and /or probe are mobile on the fluorescence time scale (residence times in the micelles comparable or shorter than the probe lifetime), TRFQ can still be used for obtaining N ”, unlike SSFQ. (see Reference [28] and references 14-19 therein).

It is difficult to specify the accuracy of the aggregation numbers due to the complex character of the equations. Typically, detailed figures are missing in the literature. It is generally assumed, that the calculated aggregation numbers are good within 10 % (see e.g. ref. [37]). From this point of view, the third digit of the aggregation numbers in Table 3.1-4 is mostly not meaningful. However, the numbers for the systems studied here are small so that any rounding at an early stage of calculation may result in misleading numbers later on, or would provide apparently incorrect relations (e. g. between N_{agg} and alkyl chains per micelle). Presumably for similar reasons, many articles concerning aggregation numbers present also one decimal in order to facilitate comparisons (see e.g. refs. [28] and [38]). To compromise on these points, the numbers of alkyl chains per micelle are given as integers in Table 3.1-4, while the aggregation numbers are maintained with one decimal.

Concerning a physical interpretation of the parameters in Table A6-1, it is known that the value of k_q is proportional to the reciprocal of the (micro)viscosity felt by the probe and quencher in their motion in the micelle (see refs. [39] and [40]). k_q decreases with increasing micelle size as $1/N^a$ ($a \sim 1$ for spherical micelles, and $a > 1$ for elongated micelles) or when the microviscosity of the probe/quencher environment increases [28]. Comparing the values given in Table A6-1, the fitted k_q increases slightly with (i) increasing spacer length and (ii) increasing degree of oligomerization, implying a slightly decreasing microviscosity of the environment of the probe in the micelles. This behavior may be a consequence of increasing difficulties of the respective surfactants to pack tightly in the micelles, in agreement with the reduced aggregation numbers. However, the effects are small, and the putative explanation is only hypothetical.

5.10 Calculation of spacer lengths [25]

The spacer group lengths were calculated using the following bond lengths and angles:

i-B-2: (C-C) = 1.497 Å, (C-C-C) = 117.20°; **t-B-2:** (C-C) = 1.497 Å, (C=C) = 1.337 Å, (C-C=C) = 122.00°; **EO-2:** (C-C) = 1.514 Å, (C-O) = 1.402 Å, (O-C-C) = 107.40°, (C-O-C) = 106.80°; **o-X-2, m-X-2, p-X-2:** (C-C) = 1.497 Å, (C=C) = 1.42 Å, (N-C-C) = 109.47°, (C-C=C) = 120.0°.

5.11 Formulation of microemulsions

The microemulsions were prepared following the procedure used by *C. Note* [41]. Toluene was used as oil, milliQ-water as aqueous phase, **DTAC**, **BDDAC** and **cationic dimers** as surfactants, and pentanol as the cosurfactant. The phase diagrams were determined optically by titrating various oil-alcohol/surfactant mixtures with water in test tubes at room temperature (ca. 23 °C). First, 1 g of mixtures of the surfactant, oil and alcohol were prepared (oil / alcohol: 50/50 v/v). Then, milliQ water was added drop-wise to the systems under vigorous stirring. The aspect of the mixtures was

subsequently observed at rest. Known amounts of water were added until a change in the appearance of the solutions could be detected (e.g. clear-turbid transitions, phase separation). This allows the determination of the region of the isotropic phase in the phase diagram [42].

5.12 Determination of CMC of dimer EDTA via UV-vis spectroscopy

Principle

The CMC of the anionic dimeric surfactant based on EDTA was determined by the probe solubilization method (see also above in part 5.8), in addition to the determination by surface tension measurements. Compared to section 5.8 (where two different dyes are involved for the CMC determination of the cationic surfactant oligomers), another probe was here used, namely benzoylacetone ($M_r = 162.19$; 98 %; purchased from Fluka). Benzoylacetone seemed to be an appropriate probe for the CMC determination of the anionic gemini, since it is neutral, hence avoiding possible electrostatic interactions with the surfactant which could disturb the system. For instance, it is clear that the cationic probe pinacyanol (*vide supra*) should not be used in this case, because it would strongly interact with the anionic surfactant, and hence possibly favor the micelle formation (reduction of the true CMC value of the surfactant).

The method is based on the keto-enol tautomerism of benzoylacetone (see keto-enol equilibrium in Figure 5.12-1) [43-44]. Benzoylacetone is more enolized in both polar and nonpolar organic solvents than in water [45].

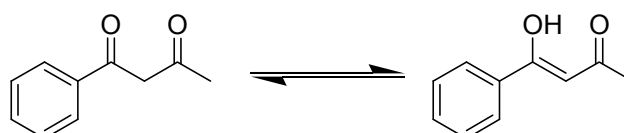


Figure 5.12-1: Keto-enol tautomerism of benzoylacetone: left = ketone form; right = enol form.

Benzoylacetone shows two absorption bands at about 250 nm and 315 nm in aqueous solution which correspond to the ketone and enol form, respectively. As the keto-enol equilibrium depends sensitively on the molecular environment, solubilization in micelles (the core of which is nonpolar) induces marked spectral changes. Typically when a surfactant is added, a sharp increase in the absorbance of the enol form is observed above the CMC, whereas the absorbance of the keto form decreases. This allows a very accurate CMC determination for common ionic surfactants [43].

Solution preparation and measurements

A stock solution of benzoylacetone is prepared by dissolution of 0.01 g in 200 mL of water (0.05 g/L) and stirred overnight to ensure complete homogenization. A range of concentration is prepared from a starting surfactant solution (exact amount of surfactant powder weighed in a graduated flask, after freeze drying) in the following way: various volumes of the stock surfactant solution are diluted in the graduated flask by adding precise volumes of the stock solution of benzoylacetone and completing with milliQ water, so that the final concentration of the probe benzoylacetone in each surfactant solution prepared is 10^{-2} g/L (or 0.001 wt %). Solutions are left to equilibrate some hours and then UV-vis spectra are measured in Quartz cuvettes (reference cuvette with milliQ water).

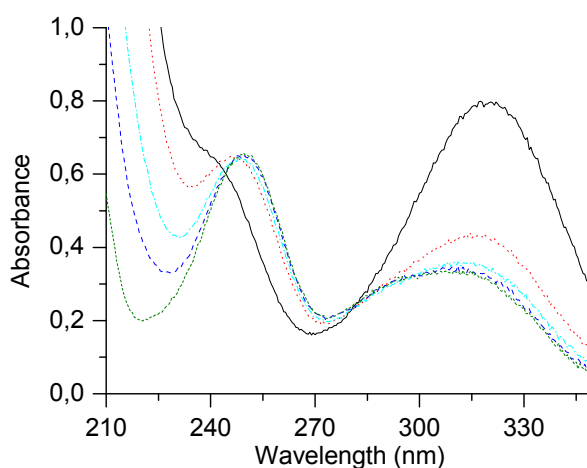


Figure 5.12-2: UV-vis spectra of 0.001 wt % aqueous solution of benzoylacetone after adding 0.002 g/L (□), 0.030 g/L (□), 0.06 g/L (□), 0.120 g/L (□), 0.15 g/L (□) dimer EDTA. Keto band at 250 nm decreases with increasing surfactant concentration whereas enol band at 315 nm increases. Presence of an isosbestic point at $\lambda = 280$ nm (single intersect between the curves), indicating an equilibrium between two species in solution.

Thus, Figure 5.12-2 shows some UV spectra which were taken for dilute aqueous solutions of benzoylacetone with increasing concentration of gemini surfactant “dimer EDTA” (compound neutralized, pH of solutions near 7). As expected, from a certain concentration on, an increase in the absorbance at 315 nm of the enol form of benzoylacetone is observed, as well as a decrease of the absorbance at 250 nm for the keto form, revealing the micellization of the surfactants in the medium. Hence, by plotting the absorbance at 315 nm (or the absorbance at 250 nm) versus the concentration of surfactant (see chapter 3), the onset of micelle formation, that is the CMC, can be determined. The experiment was repeated twice.

5.13 Solubilization capacity of surfactants

For solubilization studies, 10 mg of surfactant are dissolved in 1 ml of D₂O (10 g/L is well above the CMC of the studied surfactants). After adding about 0.4 ml (large excess) of organic liquid *para*-xylene (1,4 dimethylbenzene; M_r = 106.17; > 98 % from Aldrich), the mixture is vigorously shaken and allowed to phase separate for 24 h. The relative amounts of surfactant and solubilized material are quantified by ¹H-NMR, by comparing the integration of a characteristic signal of the surfactant to the integration of the singlet at about 2 ppm, characteristic for the methyl groups of *para*-xylene.

The following surfactants were tested: dodecyltrimethylammonium chloride (**DTAC**), sodium laurate and sodium dodecyl sulfate (**SDS**) for the reference surfactants (one cationic and two anionic); **EO-2**, **o-X-2** and **dimer EDTA** (neutralized and freeze dried) for the gemini surfactants (2 cationics and one anionic).

Peaks referring to protons near the surfactant head-groups, where the hydrophobic probe is solubilized (benzyl ring containing probe are commonly solubilized in the palisade layer of micelles), were chosen to determine the integrals, for valid comparisons:

- ❖ For **DTAC**, the singlet at 3.00 ppm corresponding to the (CH₃)₃-N⁺ - was compared to the singlet of the methyl protons of *p*-xylene at 2.13 ppm.
- ❖ For **sodium laurate**, the multiplet at 1.43 ppm corresponding to the CH₂ protons in β position of the carboxyl group was compared to the H_{benzyl} singlet of *p*-xylene at 6.81 ppm. The peak of the methyl protons of *p*-xylene could not be used as it overlapped with the CH₂ in α position of the carboxyl group of sodium laurate.
- ❖ For **SDS**, the triplet at 3.90 ppm corresponding to the CH₂ protons in α position of the sulfonate group was compared to the peak of the methyl protons of *p*-xylene at 2.03 ppm.
- ❖ For **EO-2**, the singlet at 3.03 ppm corresponding to the (CH₃)₂-N⁺ - was compared to the singlet of the methyl protons of *p*-xylene at 2.10 ppm.
- ❖ For **o-X-2**, the singlet at 2.99 ppm corresponding to the (CH₃)₂-N⁺ - was compared to the singlet of the methyl protons of *p*-xylene at 1.97 ppm.
- ❖ For **dimer EDTA**, the multiplet at 1.34 ppm corresponding to the CH₂ in β position of the amide was compared to the singlet of the methyl protons of *p*-xylene at 2.00 ppm.

Noteworthy, the results coincided when using the H_{benzyl} peak instead of the CH₃ peak of the probe *p*-xylene for the integrals. The experiments were repeated thrice (and at different moments) and show good agreement with each other. Thus, the numbers expressing the solubilization capacity of the various surfactants (given in Table 3.2-2 in chapter 3) are mean values. The error in the calculation is

estimated to be ± 0.05 , but the overall error (incertitude) on the experiment is probably larger. Still, the results remain significantly different to perform comparisons between the compounds.

An example of ^1H -NMR spectrum obtained is presented in Figure 5.13-1.

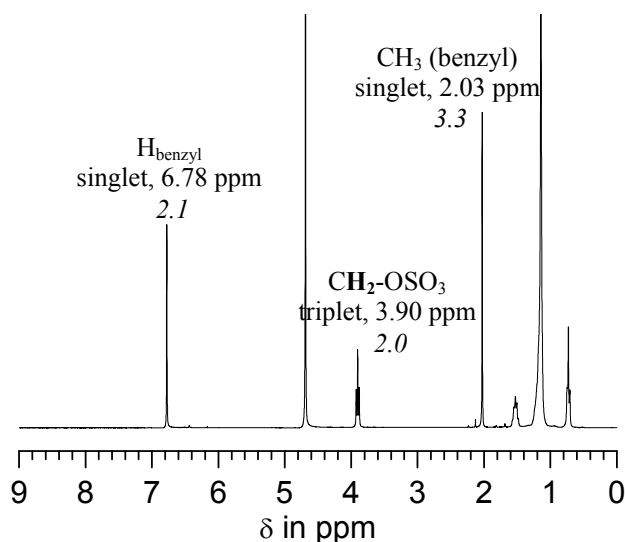


Figure 5.13-1: Example of ^1H -NMR spectrum (128 scans, 300 MHz) obtained for the solubilization study of p-xylene in micellar solution of SDS in D_2O (10 g/L). Values in *italic* corresponds to the integrals of the signal.

5.14 Tolerance of surfactants to calcium ions

The stability of surfactants in hard water was determined by recording the turbidity of surfactant solutions upon addition of aliquots of a stock solution of calcium chloride. Increasing turbidity and precipitation reflect the poor tolerance of the surfactant to calcium ions, while clear solutions denote a good stability in hard water. The computer-assisted titration was performed in a thermostated glassware ($T = 30\text{ }^\circ\text{C}$, above Krafft temperature of sodium laurate) under stirring. The turbidity was recorded as a function of the volume of calcium chloride added to 25 mL of surfactant solution via a self-made turbidity sensor described in [46-47]. The rate of addition of calcium chloride to the surfactant solution is 5 ml/h.

A stock solution of calcium chloride ($M_r = 110.98$; > 97 % from Aldrich) with a concentration of 0.5 g/L (4.5 mmol/L) and micellar solutions of sodium laurate and dimer EDTA (anionic form) with a concentration of 2 g/L (9 mM and 5.7 mM of alkyl chains, respectively) were prepared in graduated flasks with milliQ water. The measurements were repeated twice.

5.15 Synthesis of “EO-2 (MoO₄)”

The synthesis of dimeric surfactant **EO-2 (MoO₄)** consists in ion-exchanging the chloride counterions (Cl⁻) of **EO-2** with hydroxide counterions and making the latter species react with molybdenum trioxide to form the molybdate (MoO₄²⁻) containing surfactant, as illustrated in Figure 5.15-1.

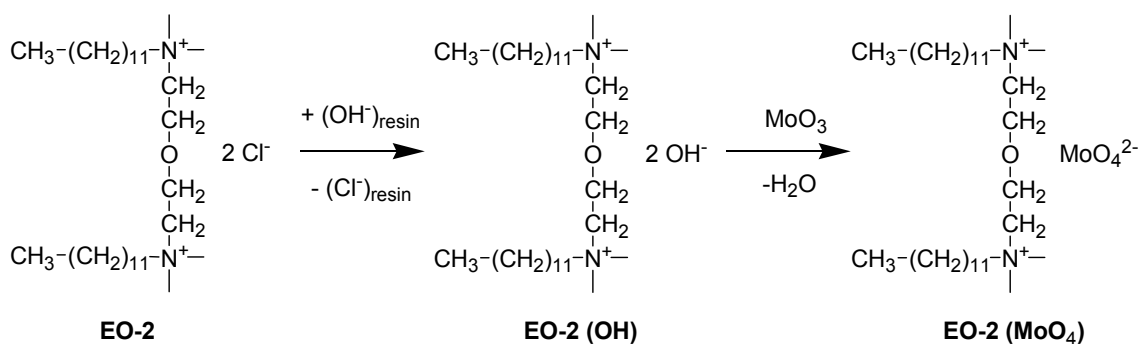


Figure 5.15-1: Scheme of the synthesis route towards EO-2 (MoO₄).

Procedure

140 mL of an Amberlite Ira-400(Cl) resin (Aldrich) are allowed to swell in 300 mL MilliQ water for 10 min. The resin is then introduced in a glass column (height = 40 cm, diameter = 2 cm) over a height of ca. 30 cm. Precautions are taken to keep the resin wet and to obtain a homogenous repartition of the resin beads within the column. The resin is rinsed in the column with 300 mL MilliQ water. Subsequently, it is activated (exchange Cl⁻/OH⁻) by passing slowly (ca. 2 mL/min) 400 mL of a 10 wt % solution of sodium hydroxide through the column. Then, it is washed with MilliQ water until pH value of 7 is obtained.

After that, a surfactant solution of **EO-2** (5 g - or 8.8 mmol - in 100 mL H₂O) is progressively passed through the resin (2 mL/min) and the resulting solution is collected in a double necked flask (500 mL) under a stream of Argon. Two fractions of MilliQ water (2 × 100 mL) are finally added to recover a maximum amount of ion-exchanged product.

Then, the collected solution is reacted at room temperature with a stoichiometric amount (1.26 g; 8.8 mmol) of molybdenum trioxide MoO₃ (M_r = 143.94; 99.5 %; from Aldrich) under stirring over 12 h in an atmosphere of Argon. After reaction, the possible excess of MoO₃ is filtered off on a Büchner funnel with small pore size. The filtrate is finally freeze dried to recover a white hygroscopic powder corresponding to the product **EO-2 (MoO₄)** (T_K < 0 °C).

NOTE: An acid-base titration can be carried out on a sample of the collected solution of **EO-2 (OH)** in order to know the concentration of hydroxide ions present and thus calculate the exact amount of

MoO₃ necessary for the final reaction (knowing that $2 \text{OH}^- + \text{MoO}_3 \rightarrow \text{MoO}_4^{2-} + \text{H}_2\text{O}$). For instance, the base can be titrated with a solution of HCl in presence of the bromothymol blue indicator [48].

Analyses

¹H NMR (300MHz, CDCl₃, 128 scans, δ in ppm): 0.88 (t, 6H, CH₃-); 1.20-1.40 (m, 36H, -(CH₂)₉-); 1.70 (m, 4H, -CH₂-C-N⁺); 3.37 (s, 12H, CH₃-N⁺); 3.49 (m, 4H, -CH₂-N⁺); 3.93 (m, 4H, -O-C-CH₂-N⁺); 4.25 (m, 4H, -CH₂-O-).

The spectrum does not present any additional peaks a priori showing a good purity of the sample.

Elemental analysis (C₃₂H₇₀MoN₂O₅, MW = 658.85 g/mol): Calculated: C 58.34; N 4.25; H 10.71; Mo 14.56. Calculated for dihydrate (C₃₂H₇₀MoN₂O₅, 2H₂O; MW = 694.88 g/mol: C 55.31; N 4.03; H 10.73; Mo 13.81. Found: C 55.24; N 4.08; H 10.49; Mo 13.00; Cl 0.70.

Element Mo was determined by Inductive Coupled Plasma (emission spectrometry) and element Cl by titration with AgNO₃.

TGA: ca. 5 wt % water are contained in the sample (cf. Appendix 7, Figure A7-3), which is consistent with the dihydrate form found via elemental analysis; the thermal decomposition starts above 160 °C, almost similar to the behaviour of the dimeric ammonium chlorides (yet, at slightly lower temperatures than the decomposition of **EO-2**).

UV Spectroscopy: molybdate anions in aqueous solution present an absorbance maximum in the UV spectrum at 208 nm [48]. The extinction coefficient ε at 208 nm of the MoO₄²⁻ anion is determined by measuring the absorbance of aqueous solutions of sodium molybdate (Na₂MoO₄, 2H₂O; M_r = 241.95; > 99.5 %; from Aldrich) with concentrations ranging from 0 to 0.1 mmol/L (absorbance at 208 nm is thus comprised between 0 and 1). The slope of the absorbance (A) vs. the concentration in molybdate [MoO₄²⁻] gives the extinction coefficient, as derived from Lambert-Beer's law ($A = \epsilon \cdot l \cdot C$): ε = 10430 L·mol⁻¹·cm⁻¹. The absorbance of a surfactant solution **EO-2(MoO₄)** with known concentration (ca. 0.05 mmol/L theoretically) was measured by UV spectroscopy and allowed to determine the true concentration of molybdate ions dissolved in solution, assuming the same extinction coefficient as the one measured for sodium molybdate at 208 nm in Lambert-Beer's law (with path length l = 1 cm).

Calculations of the amount of molybdate ions by elemental analysis and UV spectroscopy are consistent, revealing a sample modified beyond 97 % (molar) with molybdate counterions. The rest of the sample presumably consists in unmodified dimeric surfactant **EO-2** (the amount of chloride in the sample is about 0.7 wt %, as shown by elemental analysis) or unreacted **EO-2 (OH)**. All these sub-products can hardly be identified on the ¹H NMR spectrum of the sample (since only the counterion is

different). The surface tension curve of the compound exhibits a minimum at the CMC (see chapter 4), confirming the presence of some impurities. The minimum could possibly arise from a counterion effect. Another possibility for the presence of more surface active impurities may be the formation of tertiary amines in solution before measurements (solutions are indeed at rest 12 h minimum) resulting from the degradation of low amounts of unreacted product **EO-2 (OH)** (due to hydroxide ions which can attack at the level of the spacer group via retro-nucleophilic substitution). Very small amounts of tertiary amines would be sufficient to decrease strongly the surface tension and to involve a marked minimum at the CMC.

5.16 Preparation of mixtures surfactant/organic salts

Acetylsalicylic acid ($M_r = 180.16$; > 99 %), 9-aminoacridine hydrochloride ($M_r = 248.71$; > 96 %), benzenesulfonic acid sodium salt ($M_r = 180.16$; 98 %), 1,2,4-benzenetricarboxylic acid ($M_r = 210.14$; 98 %), citric acid ($M_r = 192.12$; 99 %), 2,5 dihydroxyterephthalic acid ($M_r = 198.13$; 98 %), isophthalic acid ($M_r = 166.13$; 99 %), mucic acid ($M_r = 210.14$; 97 %), 1,4,5,8-naphthalene-tetracarboxylic acid ($M_r = 304.21$; 97 %), sodium benzoate ($M_r = 144.1$; 99 %) and sodium xylene sulfonate ($M_r = 208.21$; 95 %; 40 % g/g in water) were purchased from Aldrich.

2-benzoylbenzoic acid ($M_r = 226.23$; 98 %), 1-hydroxy-2-naphtoic acid ($M_r = 188.18$; 99 %), 3-hydroxy-2-naphtoic acid ($M_r = 188.18$; > 98 %), 6-hydroxy-2-naphtoic acid ($M_r = 188.18$; 98 %), 5,5'-methylenedisalicylic acid ($M_r = 288.26$; 95 %), 2,3-naphthalenedicarboxylic acid ($M_r = 216.19$; 95 %), 2,7-naphthalenesulfonic acid disodium salt ($M_r = 332.26$; 95 %), 2-naphthalenesulfonic acid sodium salt ($M_r = 230.22$; 96 %), 2-naphtoic acid ($M_r = 172.18$; > 97 %), phthalic acid ($M_r = 166.13$; 99 %) and p-toluenesulfonic acid sodium salt ($M_r = 194.19$; 99 %) were purchased from Acros.

Diphenic acid ($M_r = 242.23$; > 95 %), 2-hydroxy-1-Naphtoic acid ($M_r = 188.18$; 97 %), natrium octyl sulfate ($M_r = 232.27$; > 97 %), o-coumaric acid (trans-2-hydroxycinnamic acid: $M_r = 164.16$; 97 %), p-toluidine hydrochloride ($M_r = 143.61$; > 99 %), pyromellitic acid ($M_r = 254.15$; > 97 %), sodium salicylate ($M_r = 160.10$; 99.5 %) trans cinnamic acid ($M_r = 148.16$; 99 %), terephthalic acid ($M_r = 166.13$; > 99 %), trimesic acid ($M_r = 210.14$; > 97 %) and 4-vinylbenzoic acid ($M_r = 148.16$; 97 %) were purchased from Fluka.

Sodium tartrate dihydrate ($M_r = 230.1$; 99.5 %) was purchased from Riedel-de-Haen.

Methacryloylethyldimethylamine-benzyl quaternized (MADAM-BQ) was a gift from *Dr. S. Bruzzano* (FhG-IAP, Golm).

All salts (sodium or ammonium salts) were used as received while the compounds under their acidic form were neutralized and freeze-dried prior to use. Precise amounts of acids were suspended in water and neutralized by adding equimolar volume of NaOH (titrated solution 0.1 N from Merck). The solutions are stirred overnight to ensure complete neutralization, before freeze-drying.

Mixtures of cationic surfactants and organic anions were prepared by dissolving the necessary amounts of each component separately in water and adding progressively one solution to the other one, under stirring.

5.17 Determination of CMC via conductimetry

Principle [49]

The conductivity method is a useful tool for the determination of the critical micellization concentration (CMC) of ionic surfactants [50-51]. The measurements are simple and accurate. The technique is based on the different equivalent conductivities of an ionic surfactant dissolved molecularly or in micellar form in water. In the ideal case, an ionic surfactant is completely dissociated below the CMC, and in this region the conductivity is a linear function of the concentration with a steep slope equal to the sum of individual ionic molar conductivities. Above the CMC, counterions dissociate only partially from the micelles. Moreover, charged micelles exhibit electrophoretic mobility as shown for sodium dodecylsulfate by the dynamic light scattering electrophoretic method [52]. Accordingly, the conductivity continues to increase with the concentration, but with a slope lower than that below the CMC (lower ionic mobility of micelles), which makes it possible to estimate the CMC from the kink in this plot [53].

A typical plot of conductivity as a function of the amphiphile concentration is illustrated in Figure 5.17-1. As the concentration of dodecyltrimethylammonium bromide (**DTAB**) exceeds 0.015 mol/L, the concentration dependence of the conductivity changes notably as a result of the transition from amphiphile unimers to micelles. The point at which the concentration dependence of the conductivity drastically changes corresponds to the CMC. The conductivity is referred to as κ in Siemens per meter (S/m).

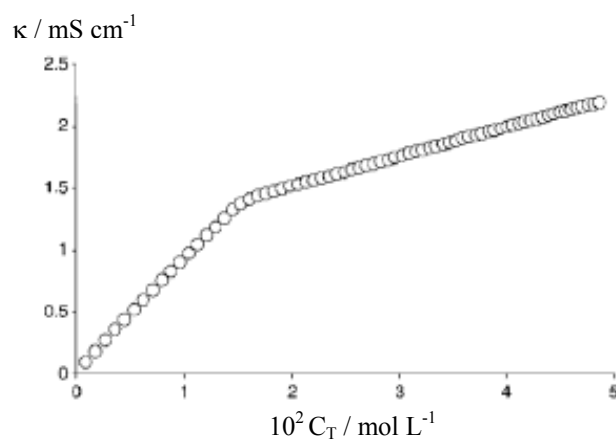


Figure 5.17-1: Concentration dependence of the conductivity for DTAB solutions in water at 25°C. Graph taken from ref. [54].

Procedure

A series of solutions with various concentration were prepared as for surface tension measurements. The measurements are performed under stirring in 25 ml beaker, taking the conductivity value κ when equilibrium is observed (generally, one minute is necessary for the signal to stabilize).

Conductivity measurements were carried out for the following compounds or mixtures: surfactant monomer **DTAC**, mixtures “**DTAC (salicylate)**” and “**EO-2 (salicylate)₂**”. This allowed to confirm the CMC values which were determined by other techniques such as surface tension measurements. Particularly, for the compound **DTAC** and its mixtures, it represents a method of choice as the commercial sample of surfactant **DTAC** exhibits a marked minimum in its surface tension curve near the CMC due to impurities, not acceptable as such.

It is noted that attempts to measure conductivity with anionic gemini surfactant **dimer EDTA** were unfruitful. Indeed, the measured values of conductivity were very low ($< 10 \mu\text{S}$) at the low concentration range of interest around the CMC. The incertitude on the measurement is important in this case and the sensitivity of the instrument (electrode) is clearly not sufficient to get reliable data.

5.18 Polymerization in mixtures of gemini surfactants and polymerizable counterions

Vinylbenzoic acid and D_2O (99.9% enriched) were purchased from Fluka and Aldrich respectively, and were used as received. The water soluble free radical initiator VA-44 (2,2'-azobis[2-(2-imidazolin-2-yl)-propane] dihydrochloride) was obtained from Wako Chemicals (Neuss, Germany). Vinylbenzoic acid was neutralized by adding an equimolar amount of NaOH (titrated solution 0.1 N from Merck) under stirring, and was subsequently freeze-dried.

Samples for polymerization are prepared with water (total volume 5 mL) as follows: the surfactant and sodium vinylbenzoate (4-VB) are mixed as described above, and the necessary amount of predissolved initiator is injected in the mixture. The oxygen is removed from the mixture by bubbling with nitrogen over 45 min. Then, the polymerizations are run:

- ❖ *EO-2 / 4-VB* (molar ratio 1:2, 0.5 wt % in water) is polymerized for 90 min at 45 °C under nitrogen atmosphere, using 5 % (mol initiator / mol monomer *4-VB*) of VA-44.
- ❖ *EO-2 / 4-VB* (molar ratio 1:1, 1 % wt in water) and *EO-2 / 4-VB* (molar ratio 1:1.5, 0.5 wt % in water) are polymerized for 3 h at 60 °C, also using 5 % of VA-44.

The same polymerization reactions were also carried out in D_2O in order to perform the NMR experiments.

5.19 Rheological studies of dimeric surfactants with additives

Rheology [55-56] is the study of the deformation and deformability of materials. This can range from the strength and durability of solids, to the flow properties of liquids.

Surfactant solutions containing small micellar aggregates exhibit low viscosity. The theoretical basis for the viscosity η of globular particles is Einstein's law, according to which the viscosity is linearly increasing with the volume fraction ϕ of the particles:

$$\eta = \eta_s(1 + 2.5\phi) \quad \text{Equation 5.19-1}$$

where η_s is the viscosity of the solvent. The equation of state for a Newtonian fluid is:

$$\sigma = \eta\dot{\gamma} \quad \text{Equation 5.19-2}$$

where σ is the shear stress (Pa) and $\dot{\gamma}$ is the shear rate (s^{-1}).

In many colloidal systems, a general phenomenon called viscoelasticity can be observed. Typical examples are gels, liquid crystalline phases or concentrated emulsions, foams or dispersions. The occurrence of such phenomena depends in a sensitive way on the molecular structure of the samples. Surfactants dissolved in aqueous solutions generally show both rheological contributions: a viscous resistance, resulting from liquid flow, and an elastic response that is caused by the deformation, orientation or change of supra-molecular micellar structures.

The solid- and liquid-like properties of a material depend intimately on the time scale of the measurement. If the network is deformed by a shear stress σ in a shorter time than it can reach equilibrium, it behaves like any solid material with a Hookean constant G , which is called the shear modulus and the following simple relation is obtained.

$$\sigma = G \cdot \gamma \quad \text{Equation 5.19-3}$$

where γ is the deformation.

If the network is deformed slowly it behaves like a viscous fluid with a zero-shear viscosity as it is described by equation 5.19-2.

Theory related to viscoelastic micellar solutions

Entangled solutions of threadlike micelles are often described as "living polymers", whose chains are subject to reversible scission and recombination processes [57-59]. In analogy to polymer solutions, these anisometric aggregates are denoted as "pseudo-polymers" or "worm-like micelles" [57-59]. The lengths of these particles depend in a complicated way on the surfactant concentration, the temperature and the ionic strength of the solution [60-62]. Viscoelastic properties usually occur at conditions, where the lengths of the rod-shaped particles are much longer than their mean distance of

separation [61-65]. The overlap threshold of anisometric micelles can be very low, and it is often observed in the millimolar range.

Relaxation time

Two different processes, namely diffusion and micellar kinetics, control usually the transient properties of entangled solutions of worm-like micelles. The treatment proposed by Cates et al. [58, 66-68] considers stress relaxation as a cooperative process of reptation, with characteristic relaxation time τ_{rep} , and chain scission-recombination characterised by a breaking time, τ_{br} . Reptation is a model for relaxation of semidilute and concentrated polymer solutions. It describes relaxation of individual chains that are confined by neighbouring entangled chains, by considering them confined in a theoretical "tube", from which they can escape only by one dimensional diffusion along their own axis. A description of reptation theory and its implications for relaxation times can be found for example in [69].

At experimental conditions where the average life-time of anisometric micelles is much smaller than the diffusion process of the whole aggregate (reptation), there are numerous breaking and reformation processes within the time scale of observation [59, 70]. The overall relaxation time is then determined by the combination of reptation and breaking of the aggregates. In the limit of fast breaking ($\tau_{br} \ll \tau_{rep}$) this is given by:

$$\tau = \sqrt{\tau_{br} \cdot \tau_{rep}} \quad \text{Equation 5.19-4}$$

In this limit, the rheological data have a single relaxation time and can be described by simple theories, namely they may be analysed using a Maxwell model. It is well established that these phenomena mostly occur in the regime of elevated surfactant concentrations or/and large amounts of excess salt. Under these experimental conditions, the average lifetime of the anisometric aggregates is relatively short in comparison to diffusion processes.

The Maxwell model

The Maxwell model for viscoelastic behaviour considers the material to be a series of elements, each consisting of a perfectly elastic (Hookean) spring, and a perfectly viscous (Newtonian) dashpot arranged in series (mechanical analogy shown in Figure 5.19-1).

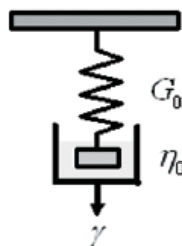


Figure 5.19-1: Schematic mechanical model of a Maxwell-Material, with a spring and a dashpot.

The elastic spring corresponds to a finite shear modulus G_0 and the dashpot represents the constant zero-shear viscosity η_0 . The spring and the dashpot represent the elastic portion and the viscous portion, respectively, for the response of a viscoelastic material. The dynamic properties of the Maxwell-element can be represented by a linear differential equation:

$$\dot{\gamma} = \frac{\dot{\sigma}}{G_0} + \frac{\sigma}{\eta_0} \quad \text{Equation 5.19-5}$$

The solutions of this equation (under harmonic oscillations) give the desired material functions [71]:

$$G'(\omega) = G_0 \frac{\omega^2 \tau^2}{1 + \omega^2 \tau^2} \quad \text{Equation 5.19-6}$$

$$G''(\omega) = G_0 \frac{\omega \tau}{1 + \omega^2 \tau^2} \quad \text{Equation 5.19-7}$$

where $G'(\omega)$ and $G''(\omega)$ are the storage modulus (elastic) and loss modulus (viscous), respectively. τ denotes the single stress relaxation time, G_0 is the zero-shear modulus (or plateau modulus), ω the angular frequency (ω is equal to $2\pi\nu$, where ν is the experimental oscillatory frequency in s^{-1}). The plateau modulus G_0 is obtained by direct measurement of the high frequency plateau in G' ($\omega^2 \tau^2 \gg 1$, see Equation 5.19-6). Noteworthy, the model is applied in the regime of linear viscoelasticity (i.e. for sufficiently small deformations).

Experimentally, these functions give the relaxation time as the reciprocal of the angular frequency at the crossover of G' and G'' , since when $G'(\omega) = G''(\omega)$:

$$\tau = \frac{1}{\omega} = \frac{1}{2\pi\nu} \quad \text{Equation 5.19-8}$$

The magnitude of the complex viscosity is given by:

$$|\eta^*(\omega)| = \frac{\sqrt{G'^2(\omega) + G''^2(\omega)}}{\omega} = \frac{\eta_0}{1 + \omega^2 \tau^2} \quad \text{Equation 5.19-9}$$

The zero-shear viscosity η_0 is observed in the low frequency limit as a plateau in η^* . Any of these three parameters (η_0 , G_0 and τ) can be determined from the other two, according to:

$$\eta_0 = G_0 \tau \quad \text{Equation 5.19-10}$$

Note that G_0 is directly proportional to the density of relaxing elements in the system.

*Oscillatory shear rheology: Theory and techniques*Oscillatory shear

Consider the application of a sinusoidally oscillating strain (of frequency ω rad·s⁻¹):

$$\gamma(t) = \gamma_0 \sin(\omega t) \quad \text{Equation 5.19-11}$$

where γ_0 is the strain amplitude. In the linear viscoelastic region, this oscillatory motion will give rise to a time-varying shear stress:

$$\sigma(t) = \sigma_0 \sin(\omega t + \delta) \quad \text{Equation 5.19-12}$$

Experimentally, on the controlled stress instrument, an oscillating stress of known amplitude is applied, and the resulting strain amplitude and its phase angle, δ , is measured with respect to the stress. It can then be shown that [71]:

$$G' = (\sigma_0 / \gamma_0) \cos \delta \quad \text{Equation 5.19-13}$$

and

$$G'' = (\sigma_0 / \gamma_0) \sin \delta \quad \text{Equation 5.19-14}$$

Stress sweep

Fundamental to the usefulness of oscillatory shear experiments is the assumption of infinitesimal strain. In order to check this assumption, stress sweeps over several frequencies were performed. Oscillatory measurements are taken at constant frequency, over a large range of shear stress amplitudes. A typical stress sweep experiment is shown in Figure 5.19-2. Note that below a critical stress (and strain) value, the various moduli are independent of the stress and strain. This corresponds to the approach to infinitesimal stress and strain, and below this point is considered to be the linear viscoelastic region. The experiment is repeated for a given sample at several representative frequencies, and a stress is chosen for subsequent oscillatory experiments (frequency sweep experiments) that is great enough to provide sufficient signal to noise, whilst remaining in the linear viscoelastic region. Note that with the apparatus used, only the stress can be chosen. However it is often better to fix a strain (a strain of 0.1 is commonly used in the linear region [72]).

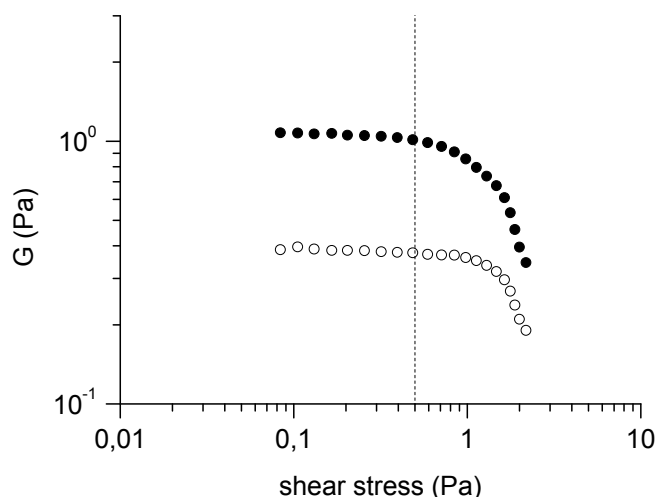


Figure 5.19-2: A typical stress sweep experiment showing G' (\bullet), G'' (\circ) as a function of the amplitude of oscillatory shear stress, for **EO-2(salicylate)₂** (0.6 wt %) at a frequency of 1 Hz, at 25 °C. The vertical dashed line represents the critical stress, marking the end of the linear viscoelastic region.

Frequency sweep

Frequency sweep measurements were taken by selecting a stress amplitude within the linear region (0.1 Pa in most cases, cf. Figures 5.19-2 and 5.19-3) to provide a measure of G' and G'' as a function of frequency. Typical frequency sweep measurements were performed over the approximate range 0.05 to 2 Hz (above 2 Hz, the measurements are no longer reliable). An example showing G' , G'' and $|\eta^*|$ is given in Figure 5.19-3.

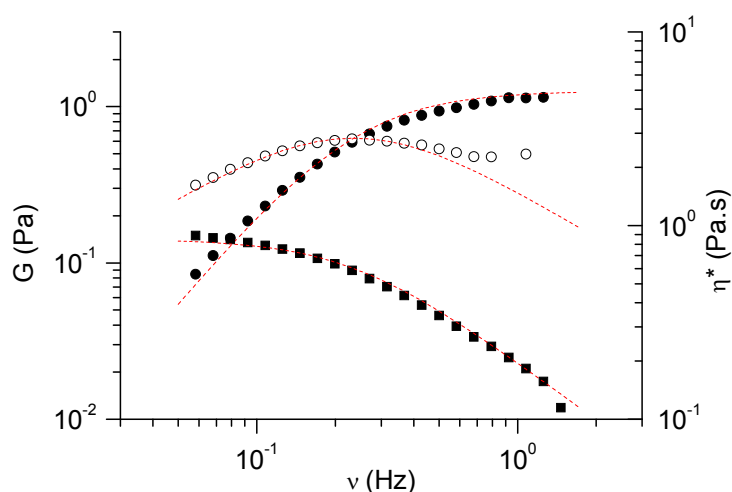


Figure 5.19-3: A typical frequency sweep experiment showing G' (\bullet), G'' (\circ) and η^* (\blacksquare), for **EO-2(salicylate)₂** (0.6 wt %) at a shear stress of 0.1 Pa, at 25 °C. The dashed red lines correspond to the fitting of the curves with the Maxwell model.

*Steady state measurements*Rotation

This type of measurement allows the determination of the flow curve of the viscoelastic fluids. Experimentally, in this work, the shear stress is varied and the shear rate produced in the sample is measured. A typical flow curve for viscoelastic fluids is represented in Figure 5.19-4.

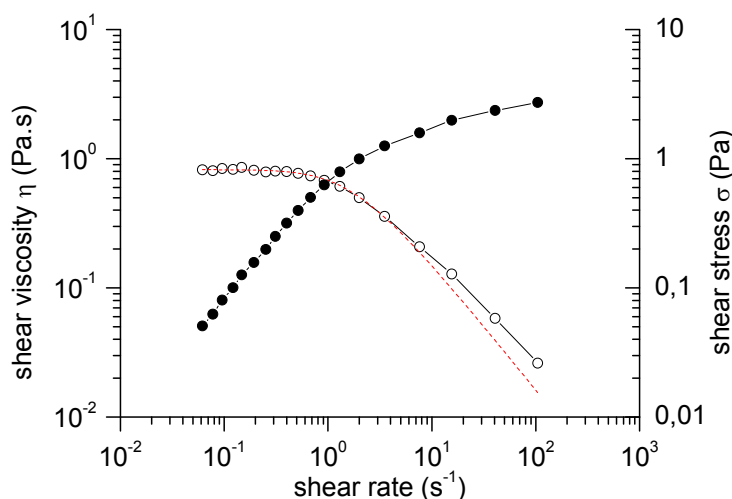


Figure 5.19-4: A typical flow curve showing the shear stress σ (●) and the shear viscosity η (○) vs. the shear rate $\dot{\gamma}$, for **EO-2(salicylate)₂** (0.6 wt %), at 25 °C. Lines are a guide for the eyes. The dashed red line corresponds to the fitting of the viscosity curve with the Giesekus model [73-81].

Nonlinear viscoelastic properties of entangled solutions of rod-shaped micelles [73]

The Maxwell model can successfully describe monoexponential stress relaxation properties. This holds for the regime of small deformations, shear rates or shear stresses. In the region of elevated mechanical forces, however, severe deviations occur. In viscoelastic surfactant solutions, it is often observed that the shear viscosity decreases markedly with increasing shear (see Figure 5.19-4). This typical behaviour is called shear thinning or pseudo-plastic. The non-Newtonian behaviour of such solutions is of great practical interest, and it is intimately connected with orientation processes or structural changes which occur during flow. Nonlinear rheological processes can be described by a theoretical model, first proposed by Giesekus [74-80]. In this theory, non-linear effects are introduced by taking into account an average anisotropy of the molecular conformation during flow. In the simplest case, there is only one configuration tensor controlling the anisotropic mobility [74, 76-78]. For steady state flow conditions, the Giesekus model can be represented as a set of equations [74, 76-78], holding for an anisotropy factor $\alpha=0.5$. The special value $\alpha=0.5$ was often observed in viscoelastic

surfactant solutions [60, 81]. Thus, it was shown that the shear viscosity of steady-state shear flow can be expressed by the following equation [74-78]:

$$\eta(\dot{\gamma}) = \frac{\sigma(\dot{\gamma})}{\dot{\gamma}} = \frac{G_0}{2\tau\dot{\gamma}^2} (\sqrt{1 + 4\tau^2\dot{\gamma}^2} - 1) \quad \text{Equation 5.19-15}$$

This law gives a decreasing viscous resistance with increasing shear rate and it describes, hence, shear thinning or pseudo plastic behaviour.

All rheological curves were fitted with the various models using the Nonlinear Least Squares Fitter (NLSF) – tool of the software Origin 7.0.

5.20 Mixtures of cationic surfactant dimers with anionic surfactants

Catanionic mixtures (0.05 g) of dimeric surfactant **EO-2** and standard monomeric surfactant **SDS** were prepared in test tubes. The molar percentage of **EO-2** was varied from 5 % to 95 %. The necessary amounts of each compound were dissolved separately in MilliQ-water and mixed together in the tubes (starting volume 5 ml; 1 % wt). The aspects of the solutions were noted upon dilution. Mixtures having a persisting bluish color were further studied by DLS.

5.21 References

- [1] Hunter R. J. In *Foundations of Colloid Science*, vol. I and II, Clarendon Press, Oxford, 1989.
- [2] Tyndall, J. *Phil. Mag.* **1869**, 37, 384.
- [3] Rakotoaly, R. H. Thèse de Doctorat, Louvain-la-Neuve, 2001.
- [4] Laschewsky, A.; Lunkenheimer, K.; Rakotoaly, R. H.; Wattebled, L. *Colloid Polym. Sci.* **2005**, 283, 469.
- [5] Menger, F. M.; Littau, C. A. *J. Am. Chem. Soc.* **1993**, 115, 10083.
- [6] Song, L. D.; Rosen, M. J. *Langmuir* **1996**, 12, 1149.
- [7] Laschewsky, A. *Adv. Polym. Sci.* **1995**, 124, 1-86.
- [8] Brown, W.; Schillén, K.; Almgren, M.; Hvidt, S.; Bahadur, P. *J. Phys. Chem.* **1991**, 95, 1850.
- [9] Lunkenheimer, K.; Wantke, K.-D. *Colloid Polym. Sci.* **1981**, 259, 354.
- [10] Lunkenheimer, K. *Tenside Deterg.* **1982**, 19, 272.
- [11] Adamson, A. W. In *Physical Chemistry of Surfaces (4th Edition)*; Wiley & Sons: New York, Chichester, Brisbane, Toronto, 1982.
- [12] Harkins, W. D.; Jordan, H. F. *J. Am. Chem. Soc.* **1930**, 52, 1751.
- [13] Miller, R.; Joos, P.; Fainerman, V. B. *Adv. Colloid Interface Sci.* **1994**, 49, 249.
- [14] Rusanov, A. I.; Prokhorov, V. A. In *Interfacial Tensiometry*; Möbius, D., Miller, R., Eds.; Elsevier: Amsterdam, 1996.
- [15] Weil, J. K.; Stirton, A. J. *J. Phys. Chem.* **1956**, 60, 899.
- [16] Mukerjee, P.; Mysels, K. J. *J. Am. Chem. Soc.* **1955**, 59, 2937.
- [17] Sheppard S. E.; Geddes, A. L. *J. Chem. Phys.* **1945**, 13, 63.
- [18] Sabaté, R.; Freire, L.; Estelrich, J. *J. Chem. Educ.* **2001**, 78, 343.
- [19] James, A. M.; Prichard, F. E. In *Practical Physical Chemistry (3rd Edition)*; Longman: Harlow, U.K., 1974; Chapter 10.
- [20] Sabaté, R.; Gallardo, M.; de la Maza, A.; Estelrich, J. *Langmuir* **2001**, 17, 6433.
- [21] Hiskey, C. F.; Downey, T. A. *J. Phys. Chem.* **1954**, 58, 835.
- [22] Shinkai, S.; Mori, S.; Koreishi, H.; Tsubaki, T.; Manabe, O. *J. Am. Chem. Soc.* **1986**, 108, 2409.
- [23] Kovatchev, S.; Vaz, V. L. C.; Eibl, H. *J. Biol. Chem.* **1981**, 20, 10369.
- [24] Basu, A.; Glew, R. H. *J. Biol. Chem.* **1985**, 24, 13067.
- [25] Wattebled, L.; Laschewsky, A.; Moussa, A.; Habib-Jiwan, J.-L. *Langmuir* **2006**, 22, 2551-2557.
- [26] Baussard, J.-F.; Habib-Jiwan, J.-L.; Laschewsky, A. *Langmuir* **2003**, 19, 7963.
- [27] Taziaux, D.; Soumillion, J.-Ph.; Habib Jiwan, J.-L. *J. Photochem. Photobiol. A: Chemistry* **2004**, 162, 599.
- [28] Alargova, R. G.; Kochijashky, I. I.; Sierra, M. L.; Zana, R. *Langmuir* **1998**, 14, 5412.
- [29] Infelta, P. *Chem. Phys. Lett.* **1979**, 61, 88.
- [30] Yekta, A.; Aikawa, M.; Turro, N. *Chem. Phys. Lett.* **1979**, 63, 543.
- [31] Barzykin, A. V.; Tachiya, M. *Heterog. Chem. Rev.* **1996**, 3, 105.
- [32] Almgren, M. *Adv. Colloid Interface Sci.* **1992**, 41, 9.
- [33] Gehlen, M.; De Schryver, F. C. *Chem. Rev.* **1993**, 93, 199.
- [34] Zana, R. *Adv. Colloid Interface Sci.* **2002**, 97, 205.
- [35] Oda, R.; Bourdieu, L.; Schmutz, M. *J. Phys. Chem. B* **1997**, 101, 5913.
- [36] Wang, X.; Wang, J.; Wang, Y.; Ye, J.; Yan, H.; Thomas, R. K. *J. Colloid Interface Sci.* **2005**, 286, 739.

- [37] Aoudia, M.; Zana, R. *J. Colloid Interface Sci.* **1998**, *206*, 158.
- [38] Wang, X. Y.; Wang, J. B.; Wang, Y. L.; Yan, H. K.; Li, P. X.; Thomas, R. K. *Langmuir* **2004**, *20*, 53.
- [39] Lianos, P.; Lang, J.; Strazielle, C.; Zana, R. *J. Phys. Chem.* **1982**, *89*, 1019.
- [40] Zana, R. In *Surfactant Solutions. New Methods of Investigation.*; Zana, R. Ed.; M. Dekker Inc.: New York, 1987; Chapter 5.
- [41] Note, C. PhD thesis, Universität Potsdam, 2006.
- [42] Note, C.; Koetz, J.; Kosmella, S. *Coll. Surf. A* **2006**, *288*, 158-164.
- [43] Shoji, N.; Ueno, M.; Meguro, K. *J. Am. Oil Chem. Soc.* **1976**, *53*, 165-167.
- [44] Favresse, P.; Laschewsky, A. *Colloid Polym. Sci.* **1999**, *277*, 792-797.
- [45] Morton, R. A.; Hassan, A.; Calloway, T. C. *J. Chem. Soc.* **1934**, 883.
- [46] Kosmella, S.; Koetz, J.; Shirahama, K.; Liu, J. *J. Phys. Chem. B* **1998**, *102*, 6459.
- [47] Koetz, J. Dissertation, Teltow-Seehof, 1986.
- [48] Caron, L. Thèse de Doctorat, Université des Sciences et Technologies de Lille, 2005.
- [49] Atkins, P.W.; de Paula, J. In *Physical Chemistry*, 7th Ed.; 2002, Chapter 24.
- [50] Mysels, K. J.; Mukerjee, P. *Pure Appl. Chem.* **1979**, *51*, 1083.
- [51] Kallay, N.; Tomašić, V.; Žalac, S.; Chittofrati, A. *Colloid Polym. Sci.* **1994**, *272*, 1576-1581.
- [52] Kemeyama, K.; Tagaki, T. *J. Colloid Interface Sci.* **1990**, *140*, 517.
- [53] White, P.; Benson, G. C. *Trans. Faraday Soc.* **1959**, *55*, 1025.
- [54] Jalšenjak, N.; Težak, D. *Chem. Eur. J.* **2004**, *10*, 5000.
- [55] Barnes, H. A.; Hutton, J. F.; Walters, K. In *An introduction to Rheology*; Elsevier science publishing company INC, 1989.
- [56] Goodwin, J. W.; Hughes, R. W. In *Rheology for chemists an introduction*; Royal Society of Chemistry, 2000.
- [57] Cates, M. E. *J. Phys. Condens. Matter* **1996**, *8*, 9167-9176.
- [58] Cates, M. E. *Macromolecules* **1987**, *20*, 2289-2296.
- [59] Marques, C. M. ; Turner, M. S. ; Cates, M. E. *J. Non-Cryst. Sol.* **1994**, *172*, 1168-1172.
- [60] Fischer, P.; Rehage, H. *Rheol. Acta* **1997**, *36*, 13-27.
- [61] Hoffmann, H.; Rehage, H. *Surf. Sci. Ser.* **1987**, *22*, 209-239.
- [62] Hoffmann, H.; Platz, G.; Rehage, H.; Schorr, W.; Ulbricht, W. *Ber. Bunsen-Ges. Phys. Chem.* **1981**, *85*, 255-266.
- [63] Hoffmann, H.; Rehage, H.; Reizlein, K.; Thurn, H. *ACS Symp. Ser.* **1985**, *272*, 41-66.
- [64] Hoffmann, H.; Platz, G.; Rehage, H.; Schorr, W. *Adv. Colloid Interface Sci.* **1982**, *17*, 275-298.
- [65] Hoffmann, H.; Platz, G.; Rehage, H.; Schorr, W. *Ber. Bunsen-Ges. Phys. Chem.* **1981**, *85*, 877.
- [66] Granek, R.; Cates, M. E. *J. Chem. Phys.* **1992**, *96*, 4758.
- [67] Turner, M. S.; Cates, M. E. *Langmuir* **1991**, *7*, 1590.
- [68] Spenley, N. A.; Cates, M. E.; Mcleish, T. C. B. *Phys. Rev. Lett.* **1993**, *71*, 939-942.
- [69] De Gennes, P-G. In *Scaling Concepts in Polymer Physics*; Cornell University Press: New York, 1979.
- [70] Grand, C.; Arrault, J.; Cates, M. E. *J. Phys. II* **1997**, *7*, 1071-1086.
- [71] Ferry, J. D. In *Viscoelastic properties of polymers*; Wiley: New York, 1980.
- [72] Page, M. PhD thesis, University of Sydney, 2003.
- [73] Rehage, H.; Pflaumbaum, M.; Fischer, P.; Fuchs, R. *Proceedings Sepawa Kongress (Würzburg)* **2005**, 207-222.

- [74] Giesekus, H. In *Phänomenologische Rheologie*; Springer Verlag: Berlin, 1994.
- [75] Giesekus, H. *J. Non-Newtonian Fluid Mech.* **1982**, *11*, 69-109.
- [76] Giesekus, H. *J. Non-Newtonian Fluid Mech.* **1984**, *14*, 47-65.
- [77] Giesekus, H. *J. Non-Newtonian Fluid Mech.* **1985**, *17*, 349-372.
- [78] Giesekus, H. *Rheol. Acta* **1995**, *34*, 2-11.
- [79] Giesekus, H. *Rheol. Acta* **2003**, *29*, 500-511.
- [80] Giesekus, H. *Rheol. Acta* **1966**, *5*, 29-35.
- [81] Holz, T., Fischer, P. Rehage, H. *J. Non-Newtonian Fluid Mech.* **1999**, *88*, 133-148.

6. GENERAL CONCLUSIONS

The property profile of several series of well-defined cationic surfactant oligomers based on the monomer dodecyltrimethyl ammonium chloride and of a novel anionic surfactant dimer based on EDTA was examined, with respect to the influence of the degree of oligomerization and to the influence of the spacer group (nature and length) linking chemically the surfactant units via the head-groups. For the studied class of compounds, structure – property relationships can be derived. The present study demonstrates the molecular potential behind the concept of oligomeric surfactants: in addition to common tunable parameters such as length and nature of the hydrophobic chain and size and nature of the hydrophilic head (including the counterion type), two other molecular variables can be exploited efficiently, namely the degree of oligomerization and the spacer group, in order to tailor the solution properties and aggregate morphology.

Concerning the cationic surfactant oligomers (from monomers to tetramers), the critical micellar concentration CMC decreases strongly with increasing the degree of oligomerization. Though the effects of the degree of oligomerization are dominant, the nature of the spacer groups cannot be neglected. Thus, the CMC increases moderately with increasing spacer length and decreases with increasing hydrophobicity of the spacer. The increasing degree of oligomerization can also enhance the maximum attainable reduction of the surface tension, but this depends sensitively on the spacer group. Generally speaking, many tendencies which are observed when going from a monomeric surfactant to its dimeric form, can be extrapolated further for the trimeric and tetrameric analogs. The behavior of the tetrameric surfactant having a *p*-xylylene spacer group differs from the one of the other compounds, as it seems to form premicellar aggregates at very low concentrations. This shifts the apparent CMC to higher values than expected. Accordingly, the formation of premicellar aggregates is favored on the one hand by an increasing degree of oligomerization, and on the other hand by an appropriate length of the spacer group.

All studied systems form small aggregates up to solutions containing several weight percent of the surfactants, as studied by dynamic light scattering (DLS). Time-resolved fluorescence quenching (TRFQ) is a powerful tool to investigate the micellar properties of surfactant solutions, including oligomeric surfactants, and to observe and analyze the effects of structural modifications of surfactants. The fluorescent probe 9,10 dimethylanthracene was employed favorably instead of the commonly used pyrene, as its spectral characteristics offer several practical advantages. The aggregation numbers N_{agg} of all oligomeric surfactants studied are relatively low (< 40 dodecyl chains per micelle), also at high concentrations (3 wt %). The values of N_{agg} increase only moderately with the concentration, as typically found for standard “monomeric” surfactants, thus indicating the presence of small micelles. Still, both the nature of the spacer groups as well as the degree of oligomerization influence notably the aggregation numbers. Shorter spacers give rise to higher

aggregation numbers, as previously described for other dimeric surfactants, apparently resulting in a denser packing of the surfactant chains. In addition to the length of the spacer group, its detailed chemical structure plays an important role, too. Oligomeric surfactants bearing e.g. aromatic spacers have smaller N_{agg} values compared to analogs bearing aliphatic spacers of the same length. This may be attributed to an increased sterical hindrance to efficient packing. For the three studied oligomeric series (i.e. from monomer to trimer or tetramer), aggregation numbers decrease with increasing degree of oligomerization. This finding differs from a singular study on two dimer/trimer ammonium surfactant pairs characterized by flexible C_3 -spacer groups. The N_{agg} values of the latter were notably higher for the trimers, as the transition from small spherical to large worm-like micelles is favored. The different behavior of the newly studied series of surfactant oligomers is rationalized by the higher rigidity of the spacer groups employed here, which inherently interferes with an efficient packing of the surfactant chains. In any case, the results exemplify that the effect of increasing the degree of oligomerization on the properties of oligomeric surfactants cannot be generalized as regards their aggregation behavior. All structural parameters (length, nature and rigidity of the spacer group; counterion nature; degree of oligomerization) must be taken into account for the overall property profile. In particular, the results demonstrate that it is possible to increase the degree of oligomerization of surfactants without inevitably increasing the viscosity of their solutions, since the N_{agg} -values remain low for appropriate surfactant structures.

The formation of inverse microemulsions was also addressed with respect to the effect of the spacer group on the resulting phase diagram. Dimerization via rigid spacers involves a reduction of the microemulsion area. In addition, shorter spacers as well as more hydrophobic ones shift the isotropic phase towards higher surfactant concentrations, reflecting the decrease of the hydration shell of the head groups, since more surfactant material is needed to incorporate water.

Furthermore, a simple synthetic route towards a novel anionic dimeric surfactant was described, contrasting with other reports in the field. The opening of a carboxylic dianhydride (here, based on EDTA) with a secondary amine allows to obtain a surfactant with interesting properties. The surfactant has a Krafft temperature below 0 °C and exhibits a very low CMC as well as a low surface tension at the CMC (both at pH 7 and pH 12). The compound shows also a high solubilization capacity and an improved tolerance to calcium ions compared to standard anionic surfactants. Such a surfactant can find potential uses as chelating agent, corrosion inhibitor, amphiphilic metal complex for catalyzed micellar reactions, or else as flotation agent in separation technology.

Dimeric surfactants, which are more conveniently synthesized than the higher oligomers, are promising amphiphiles. The addition of organic salts (also called hydrotropes), such as sodium salicylate, vinylbenzoate or tosylate, to the gemini surfactants markedly modifies the solution properties and aggregate morphology. In this case, another parameter of the surfactants, namely the

counterion is varied due to possible anion exchange in-situ. Surface tensions and critical aggregation concentrations can be markedly reduced compared to the surfactants in the pure state. This makes such mixtures advantageous, e.g. for wetting processes and for the solubilization of hydrophobic compounds at low surfactant contents. Remarkably, the observed synergism is much more pronounced for gemini surfactants than for analogous monomeric surfactants when combined with the same hydrotropes, meaning that dimerization strongly enhances the associative behaviour.

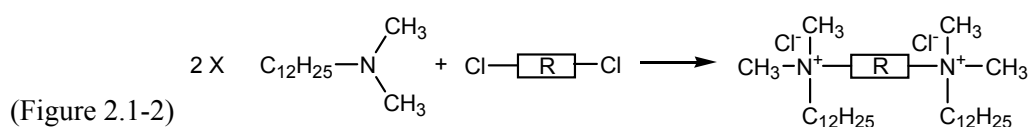
Moreover, dimeric surfactants with an appropriate spacer group produce viscoelastic solutions after addition of certain organic anions. This occurs for gemini surfactants bearing alkyl chains as short as dodecyl, whereas no effect is observed when involving the "monomeric" analogs. The viscosifying behaviour is present already at low concentrations, and reflects a marked growth of the micelles. Rheological measurements revealed a Maxwellian behaviour characteristic for entangled worm-like micelles. Noteworthy, dimeric surfactants with a short hydrophobic spacer allow the micelle growth with usually inefficient organic salts such as sodium benzoate. Perspectives for the further use of dimeric surfactants include mixtures with oppositely charged conventional surfactants. For example, some mixtures with the oppositely charged SDS gave rise to vesicular aggregates, not observed for mixture of the monomeric analog and SDS under the same conditions. Also, mixtures of two dimeric surfactants, namely a cationic surfactant with the diethylether spacer group and the anionic surfactant based on EDTA produce highly viscous aqueous solutions, revealing the marked micelle growth for these catanionic mixtures.

To conclude, surfactant oligomers represent an interesting class of amphiphilic compounds by virtue of their enhanced property profile compared to standard "monomeric" surfactants. The systematically studied parameters additionally introduced in the surfactant structure allow to change widely and conveniently the properties. The transfer of surfactant oligomers from research in the application domain will depend on the efforts of chemists to find simple and cost-effective routes to produce such amphiphiles, as well as on efforts to formulate them with particular additives in order to keep or improve their performance within reasonably low material content. It is expected that breakthroughs will arise in the next few years from such an extensive research.

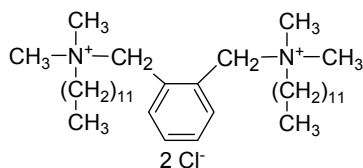
APPENDIX 1: Synthesis and characterization of cationic dimers

The synthesis procedures and analyses of the cationic dimers that were resynthesized in the course of this PhD work are presented in this section. Also, the purification steps were repeated in order to have surfactants as pure as possible for investigations of their properties.

The following reaction scheme was applied for the synthesis of the six cationic dimeric surfactants:

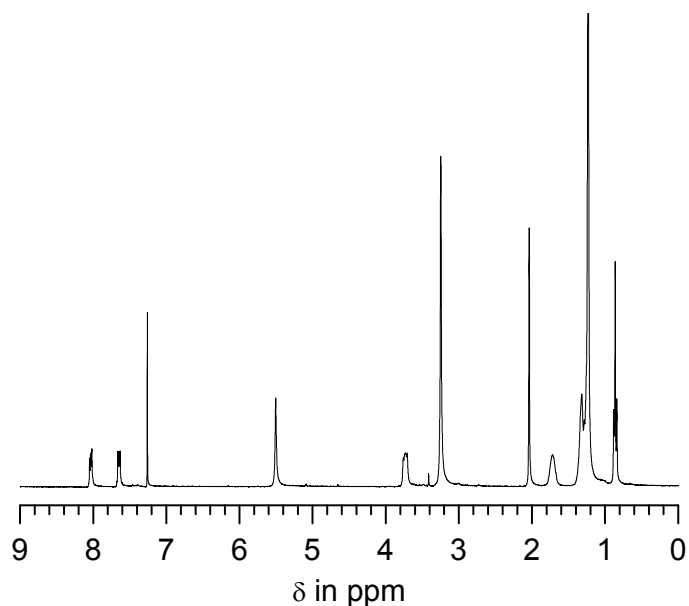
**Materials.**

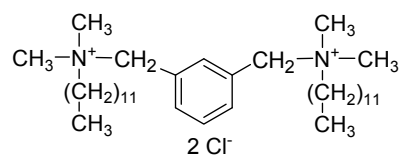
N,N-dimethylaminododecane (>97 %, $\rho=0.775$ g/ml), α,α' -dichloro-ortho-xylene 98 %, α,α' -dichloro-meta-xylene (98 %), α,α -dichloro-para-xylene (98 %), 2,3-dimethyl-2-butene (98 %) were used as received from Aldrich; 3-chloro-2-chloromethyl-1-propene (96 %) from Acros; 2,2'-dichloro-diethylether (puriss), trans-1,4-dichloro-2-butene (97 %) from Fluka. Solvents were analytical grade, or were distilled prior to use.

Synthesis of o-X-2. ($M_r = 601.87$ g/mol)

31.2 g (0.141 mol) of N,N-dimethylaminododecane and 10.02 g (0.056 mol) of α,α' -dichloro-o-xylene in 150 ml of ethanol are refluxed for 6 days. Then, the solvent is removed in vacuo. Addition of 200 ml of diethylether gives a gel-like precipitate that is kept in a freezer (at -18 °C) over 10 days. The white gel obtained is filtered off and dried. Purification by repeated dissolution in acetone and precipitation by diethylether gives a white hygroscopic powder which is freeze-dried. Yield: 46 % (15.5 g). The purity of the compound is checked by $^1\text{H-NMR}$.

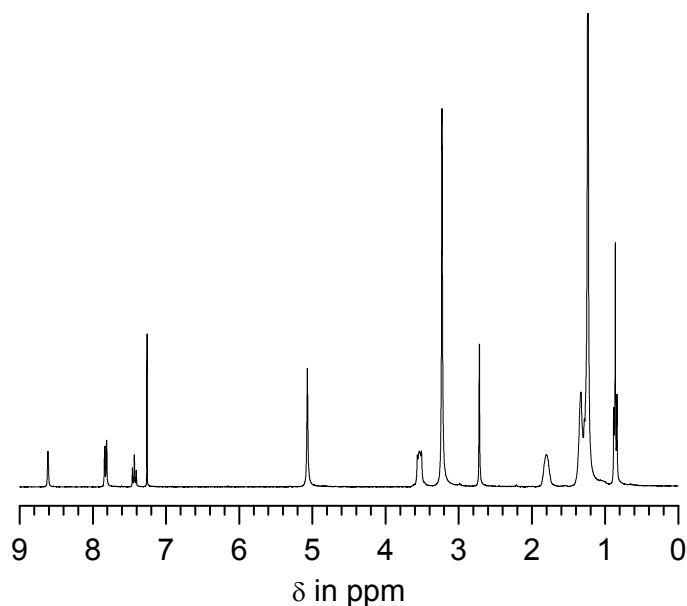
$^1\text{H-NMR}$ (300MHz, CDCl_3 , 128 scans, δ in ppm): 0.86 (t, 6H, CH_3 -); 1.15-1.40 (m, 36H, $-(\text{CH}_2)_9$ -); 1.72 (m, 4H, $-\text{CH}_2-\text{C}-\text{N}^+$); 3.25 (s, 12H, CH_3-N^+); 3.73 (m, 4H, $-\text{CH}_2-\text{N}^+$); 5.50 (s, 4H, $\text{N}^+-\text{CH}_2\text{-Aryl}$); 7.65, 8.02 (m, 2H+2H, CH_{aryl}).

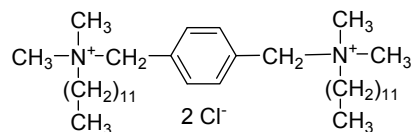


Synthesis of m-X-2. ($M_r = 601.87$ g/mol)

31.02 g (0.141 mol) of N,N-dimethylaminododecane and 10.02 g (0.056 mol) of α,α' -dichloro-m-xylene in 150 ml of ethanol are refluxed for 4 days. Then, most of the solvent is removed in vacuo, and 300 ml of acetone are added. The precipitate formed is filtered off, and crystallized thrice from acetonitrile. Yield: 62 % (20.9 g) of white hygroscopic solid, which is freeze-dried. The purity of the compound is checked by $^1\text{H-NMR}$

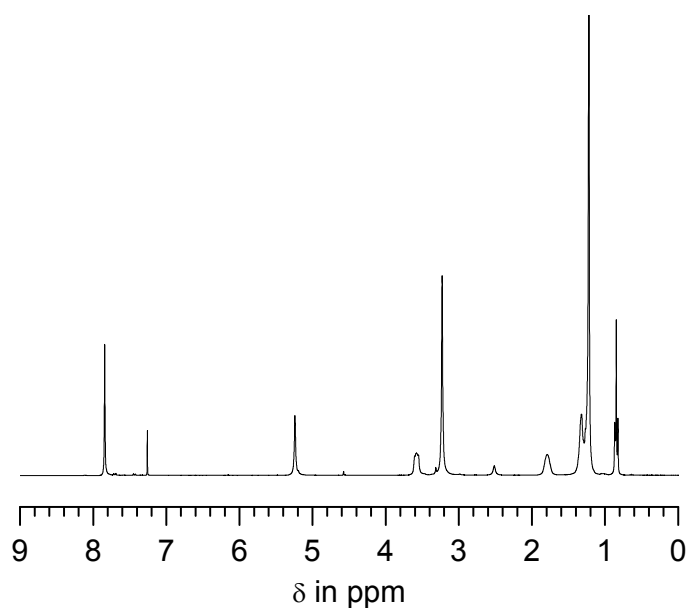
$^1\text{H-NMR}$ (300MHz, CDCl_3 , 128 scans, δ in ppm): 0.84 (t, 6H, CH_3 -); 1.15-1.40 (m, 36H, $-(\text{CH}_2)_9$ -); 1.78 (m, 4H, $-\text{CH}_2-\text{C}-\text{N}^+$); 3.20 (s, 12H, CH_3-N^+); 3.48 (m, 4H, $-\text{CH}_2-\text{N}^+$); 5.01 (s, 4H, $\text{N}^+-\text{CH}_2-\text{Aryl}$); 7.42 (m, 1H, CH_{aryl} in meta); 7.74 (d, 2H, CH_{aryl} in ortho); 8.45 (s, 1H, CH_{aryl} in ortho).

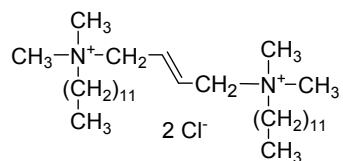


Synthesis of p-X-2. ($M_r = 601.87$ g/mol)

75 ml (56.3g, 0.264 mol) of N,N- dimethylaminododecane and 21.88 g (0.122 mol) of α,α' - dichloro-p-xylene in 300 ml of ethanol are refluxed for 4 days. Then, most of the solvent is removed in vacuo, and 200 ml of acetone are added. The precipitate formed is filtered off, and crystallized repeatedly from acetonitrile. Yield: 63.2 g (86%) of white hygroscopic solid.

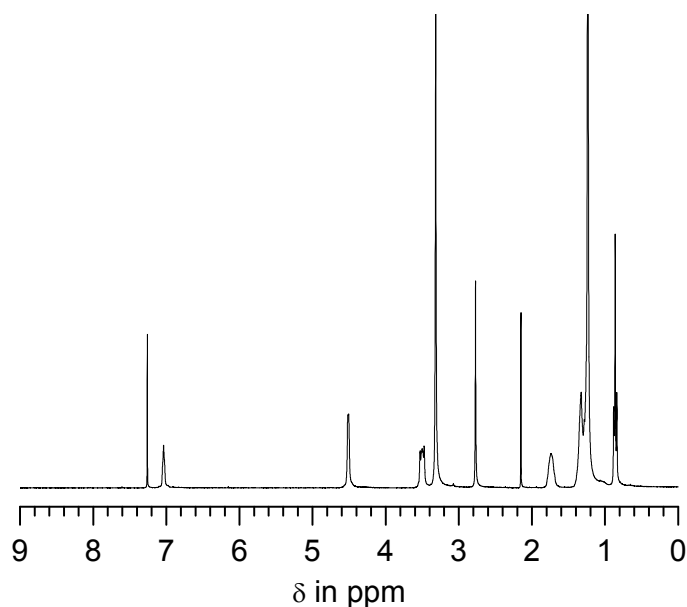
$^1\text{H-NMR}$ (300MHz, CDCl_3 , 128 scans, δ in ppm): 0.85 (t, 6H, CH_3 -); 1.15-1.40 (m, 36H, $-(\text{CH}_2)_9$ -) ; 1.79 (m, 4H, $-\text{CH}_2-\text{C}-\text{N}^+$) ; 3.23 (s, 12H, CH_3-N^+) ; 3.58 (m, 4H, $-\text{CH}_2-\text{N}^+$) ; 5.24 (s, 4H, $\text{N}^+-\text{CH}_2-\text{Aryl}$) ; 7.84 (s, 4H, CH_{aryl}).

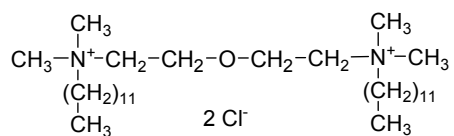


Synthesis of t-B-2. ($M_r = 551.81$ g/mol)

8.05 g (0.060 mol) of trans-1,4-dichloro-2-butene in 67 ml of acetonitrile are added dropwise under stirring to 40.3 g (0.183 mol) of N,N-dimethyldodecylamine at 105 °C. The mixture is refluxed for 3 days, then cooled to room temperature. 500 ml of acetone are added to the brown paste obtained and the precipitate formed is filtered off and washed with acetone. The precipitate is purified by repeated dissolution in ethanol and precipitation by acetone. A white hygroscopic powder is obtained and subsequently freeze-dried. Yield: 66 % (22 g). The purity is checked by $^1\text{H-NMR}$.

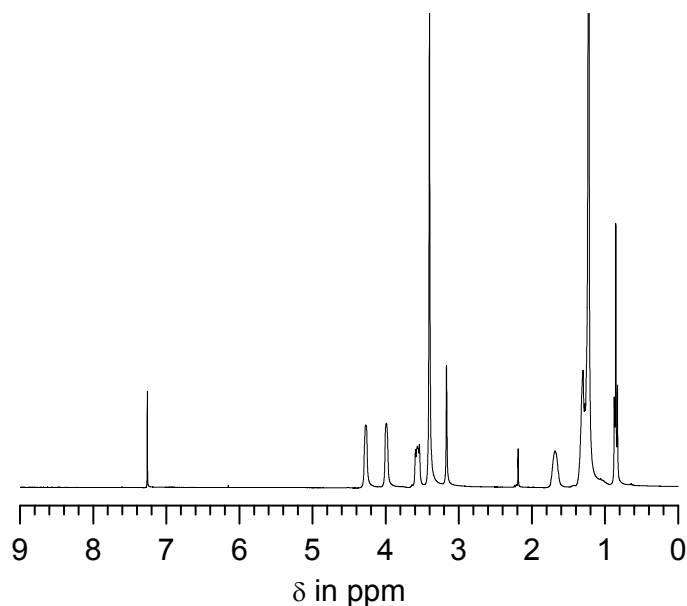
$^1\text{H-NMR}$ (300MHz, CDCl_3 , 128 scans, δ in ppm): 0.86 (t, 6H, CH_3 -); 1.15-1.40 (m, 36H, $-(\text{CH}_2)_9$ -); 1.74 (m, 4H, $-\text{CH}_2-\text{C}-\text{N}^+$); 3.32 (s, 12H, CH_3-N^+); 3.53 (m, 4H, $-\text{CH}_2-\text{N}^+$); 4.51 (m, 4H, $=\text{C}-\text{CH}_2-\text{N}^+$); 7.04 (m, 2H, $-\text{CH}=\text{}$).

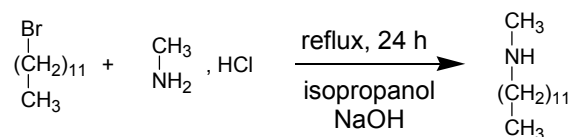


Synthesis of EO-2. ($M_r = 569.82$ g/mol)

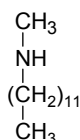
86.03 g (0.391 mol) of N,N-dimethylaminododecane and 25.62 g (0.179 mol) of 2,2'-dichloro-diethylether in 250 ml of ethanol were refluxed for 4 days. After evaporating most of the solvent, the product is precipitated by adding 900 ml of acetone. The crude product is recovered by filtration, and crystallized thrice from acetonitrile. Yield: 52 % (52.9 g) white hygroscopic solid. The purity of the compound is checked by $^1\text{H-NMR}$.

$^1\text{H-NMR}$ (300MHz, CDCl_3 , 128 scans, δ in ppm): 0.85 (t, 6H, CH_3 -); 1.15-1.40 (m, 36H, $-(\text{CH}_2)_9$ -); 1.69 (m, 4H, $-\text{CH}_2-\text{C}-\text{N}^+$); 3.42 (s, 12H, CH_3-N^+); 3.57 (m, 4H, $-\text{CH}_2-\text{N}^+$); 3.99 (m, 4H, $-\text{O}-\text{C}-\text{CH}_2-\text{N}^+$); 4.28 (m, 4H, $-\text{CH}_2-\text{O}$ -).



APPENDIX 2: Synthesis of N-methyldodecylamine**Materials.**

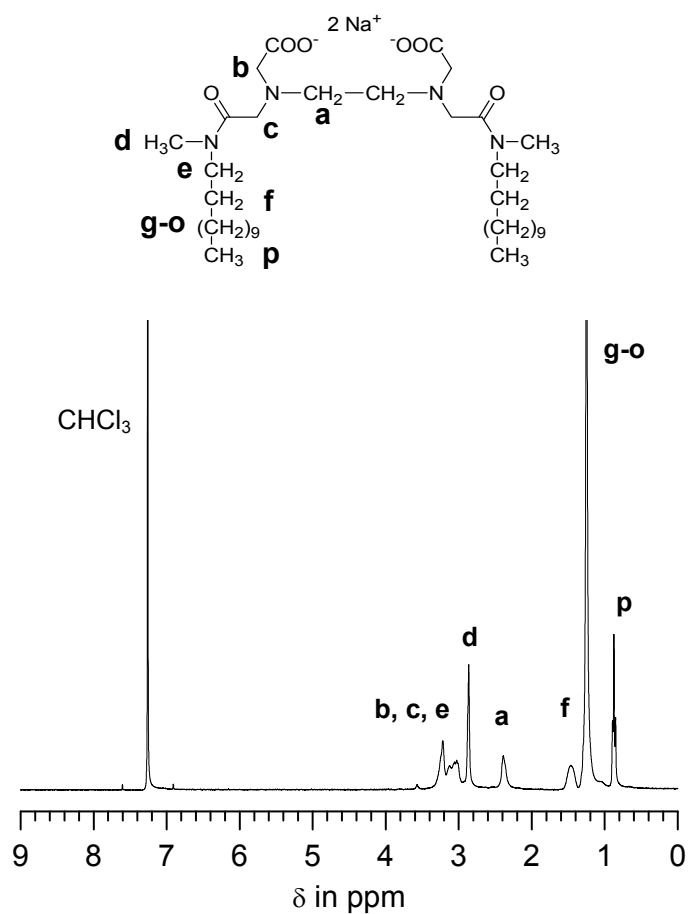
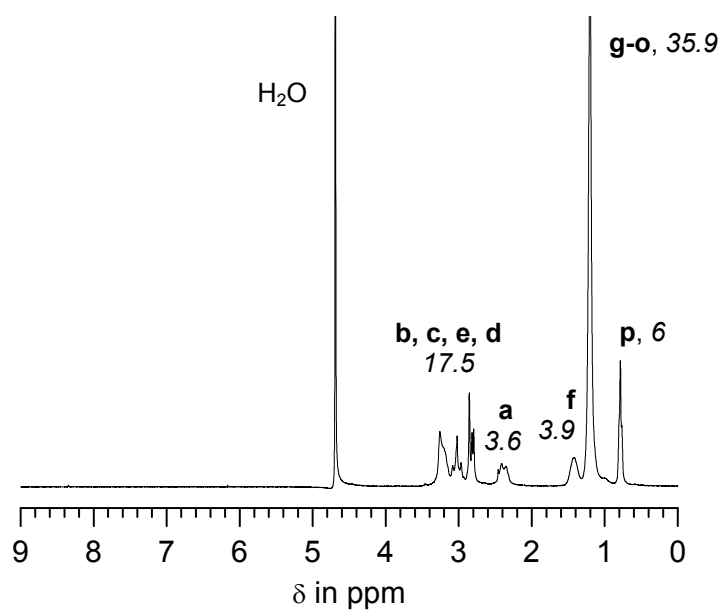
1-bromododecane (97 %) and methylamine hydrochlorid (98 %) were used as received from Fluka. Sodium hydroxide (99 %) was purchased from Riedel-de-Haen. Solvents were analytical grade, or were distilled prior to use.

Synthesis of N-methyldodecylamine.

1-Bromododecane (50.0 g, 0.584 mol) in 50 mL of isopropanol is added to a solution of methylamine hydrochloride (150 g, 2.18 mol) and NaOH (45.0 g, 1.11 mol) in 250 mL of isopropanol. The mixture is refluxed for 24 h. After evaporation of the solvent, 600 mL of 5M aq NaOH are added. The phase containing the N-methyldodecylamine is separated from the water phase by decantation. The water phase is extracted six times with portions of 100 mL of CH₂Cl₂, the organic phases are combined, dried over MgSO₄, and distilled at 0.25 mbar pressure, to yield the product (45.9 g, 38 %) as colorless oil. C₁₃H₂₉N, M_r = 199.38.

- ¹H-NMR (200 MHz, CDCl₃, δ in ppm): 0.85 (t, 3H, CH₃-); 1.22-1.29 (m, 18H, -(CH₂)₉-); 1.44 (t, 2H, -CH₂-C-N); 2.39 (s, 3H, CH₃-N); 2.52 (t, 2H, -CH₂-N).
- ¹³C-NMR (50 MHz, CDCl₃, δ in ppm): 14.0 (C-CH₃-); 22.6 (CH₃-C-CH₂-; -CH₂-C-N); 27.3 (-C-CH₂-C-N); 29.30, 29.51, 29.57 (-(CH₂)₆-); 31.9 (CH₃-C-CH₂-); 36.1 (C-CH₃-N); 51.9 (-CH₂-N).
- Mass spectroscopy (APCI, +): signal at = 200.3 (m/z) [M+H]⁺

APPENDIX 3: Characterization of dimer EDTA

Figure A3-1: $^1\text{H-NMR}$ spectrum (300 MHz) of Dimer EDTA (after neutralization) in CDCl_3 .Figure A3-2: $^1\text{H-NMR}$ spectrum (300 MHz) of Dimer EDTA (after neutralization, at pH 11) in D_2O . Values in *italics* give the integral of the corresponding signal group.

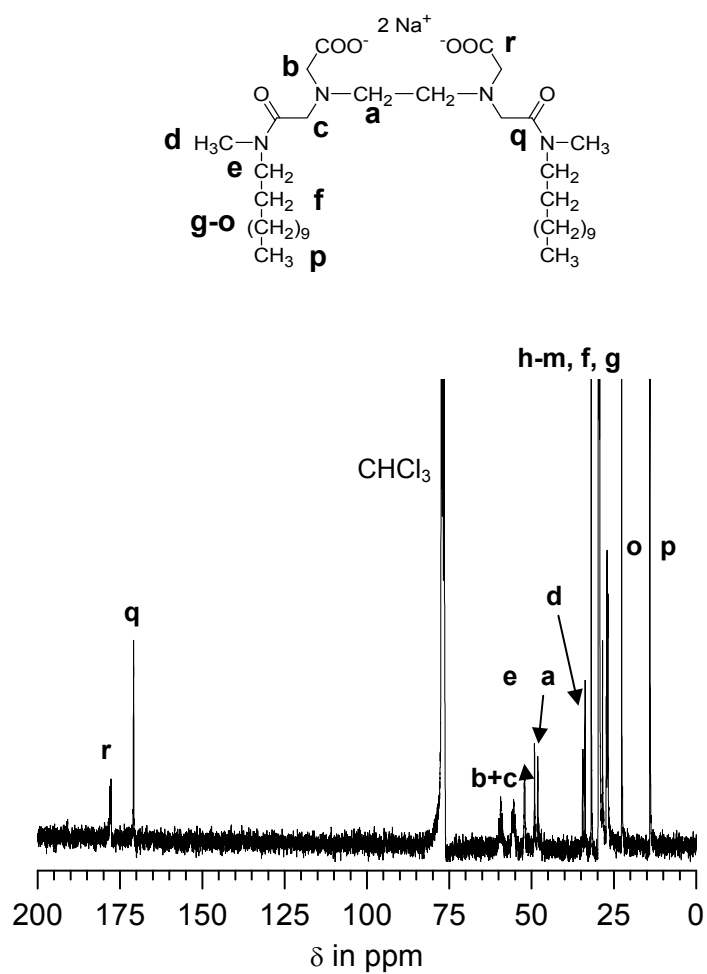


Figure A3-3: ¹³C-NMR spectrum (75 MHz) of Dimer EDTA (after neutralization) in CDCl₃, with hypothetical attributions.

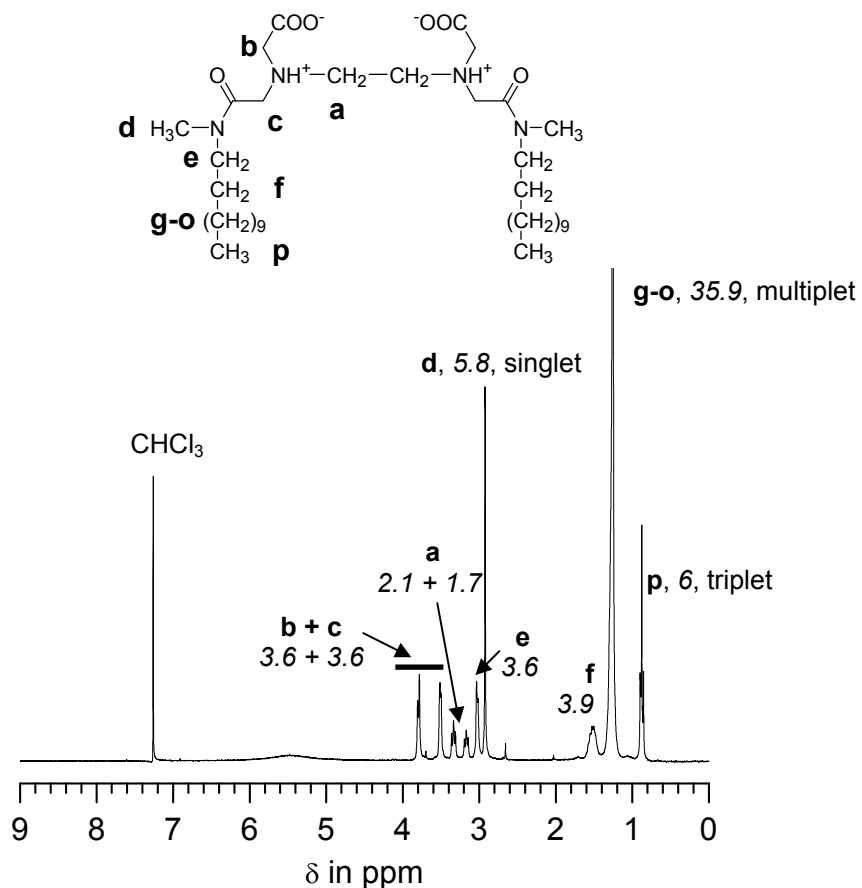


Figure A3-4: ¹H-NMR spectrum (300 MHz) of Dimer EDTA (before neutralization) in CDCl₃. Values in *italics* give the integral of the corresponding signal group.

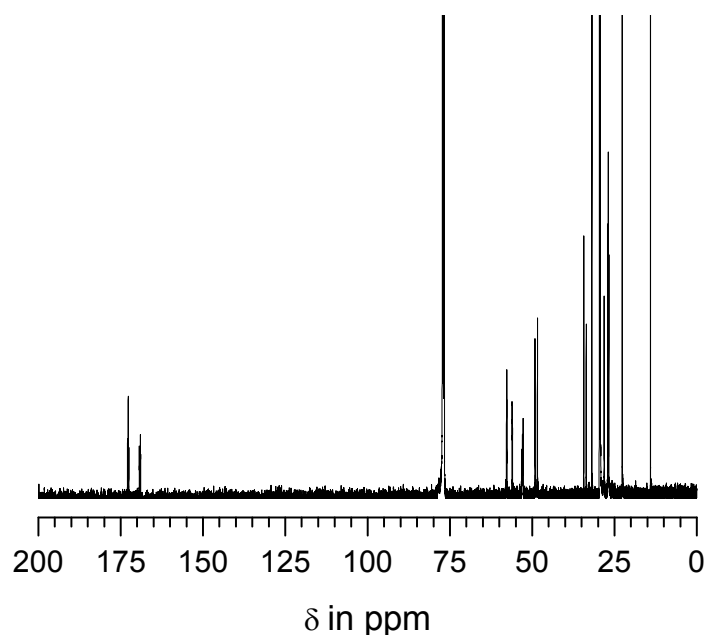


Figure A3-5: ¹³C-NMR spectrum (125 MHz) of Dimer EDTA (before neutralization) in CDCl₃.

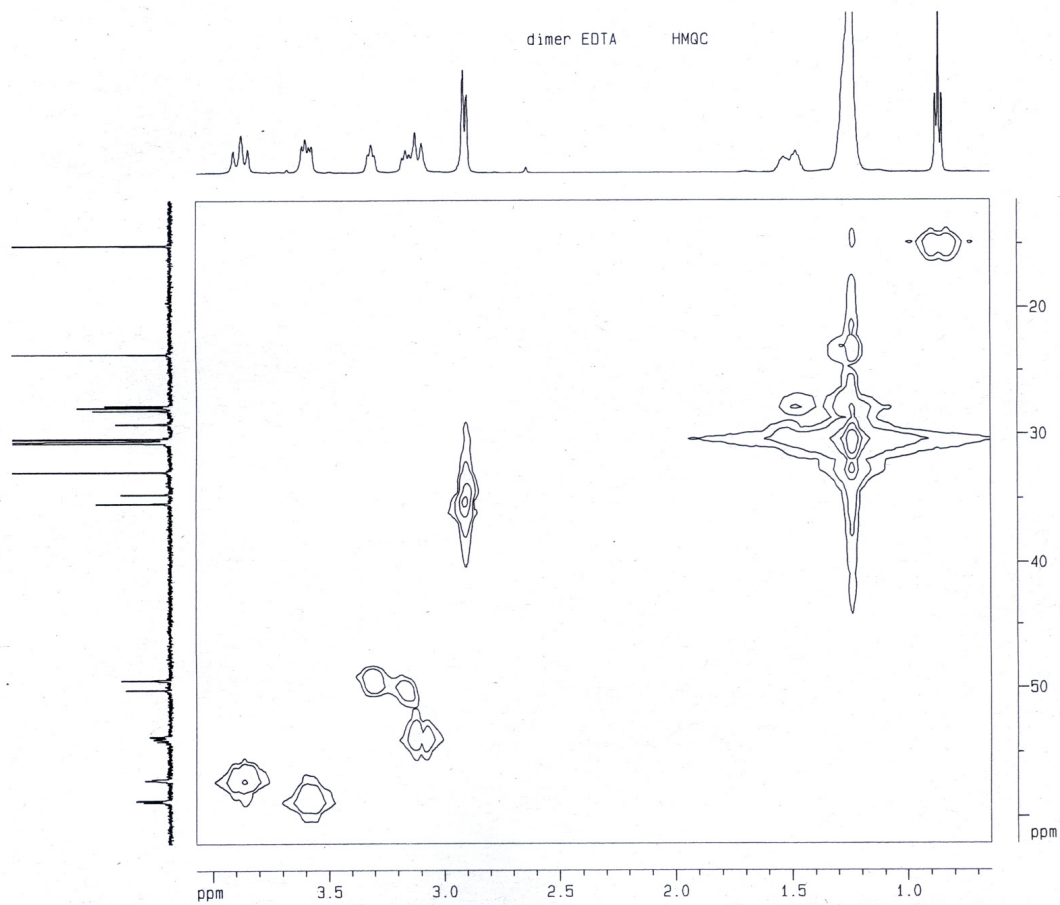


Figure A3-6: 2D-NMR spectrum (500 MHz) of Dimer EDTA (before neutralization) in CDCl₃.

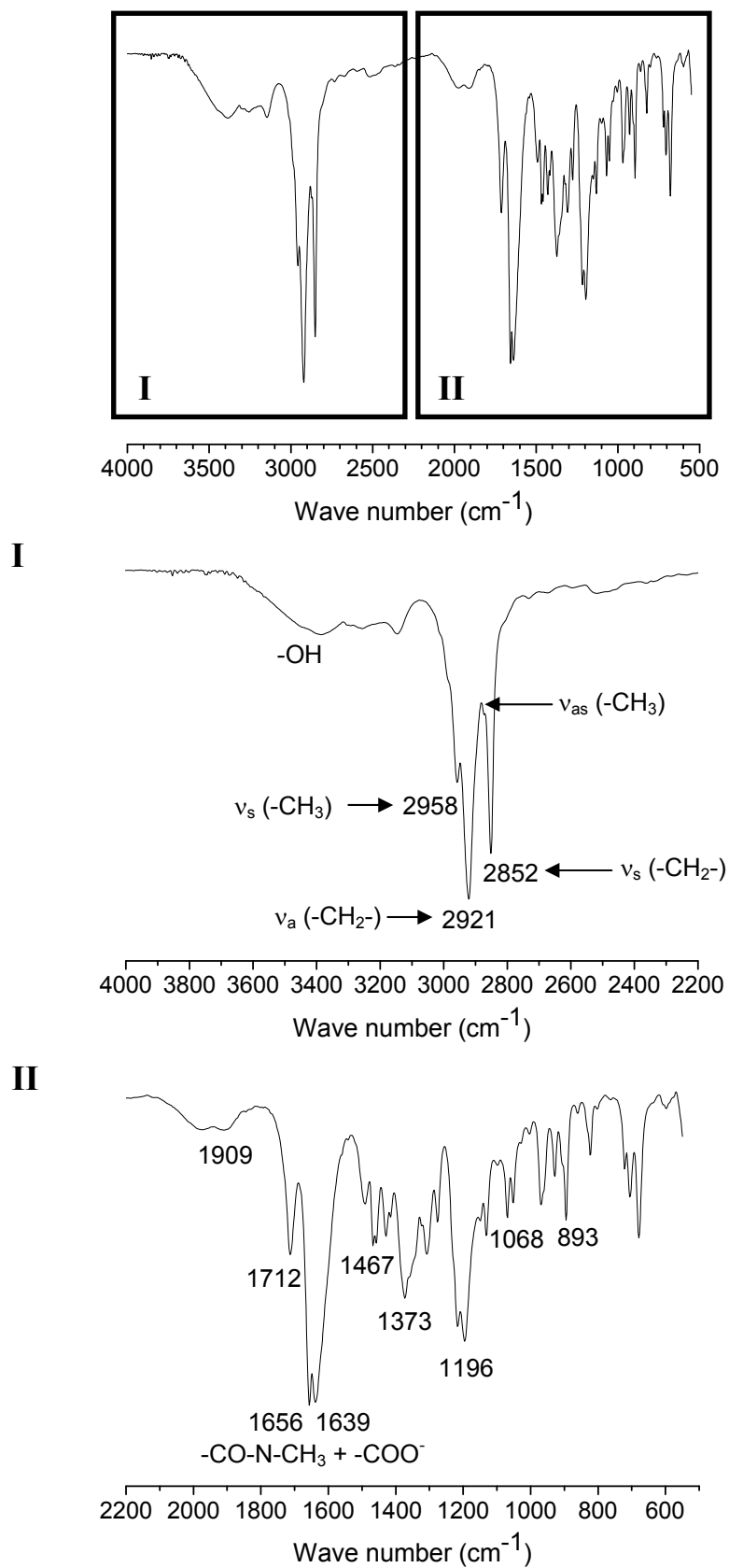


Figure A3-7: FT-IR spectrum of Dimer EDTA (before neutralization) and attribution of characteristic bands.

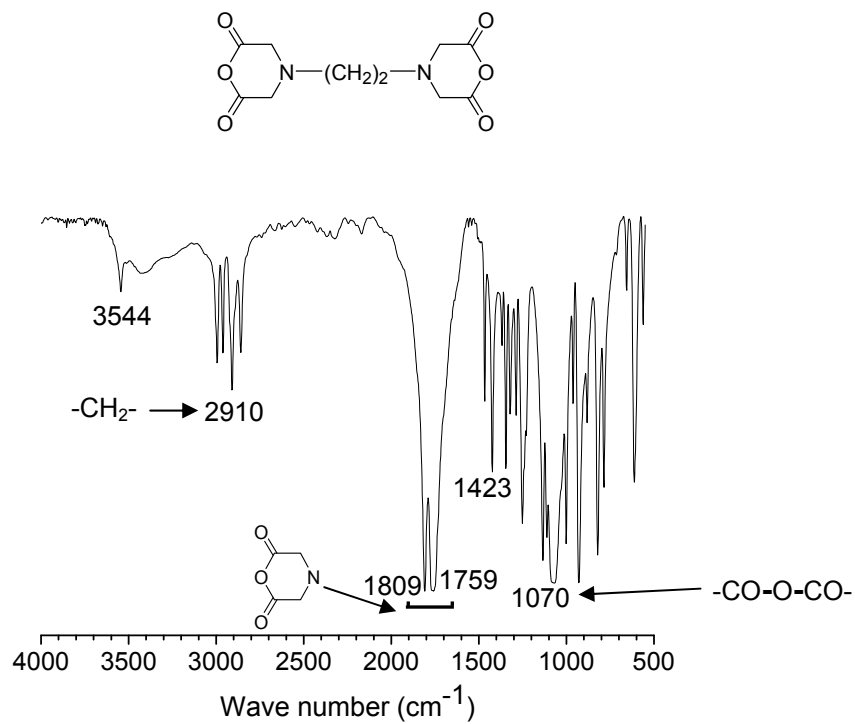


Figure A3-8: FT-IR spectrum of reactant EDTA anhydride and attribution of characteristic bands, for comparison.

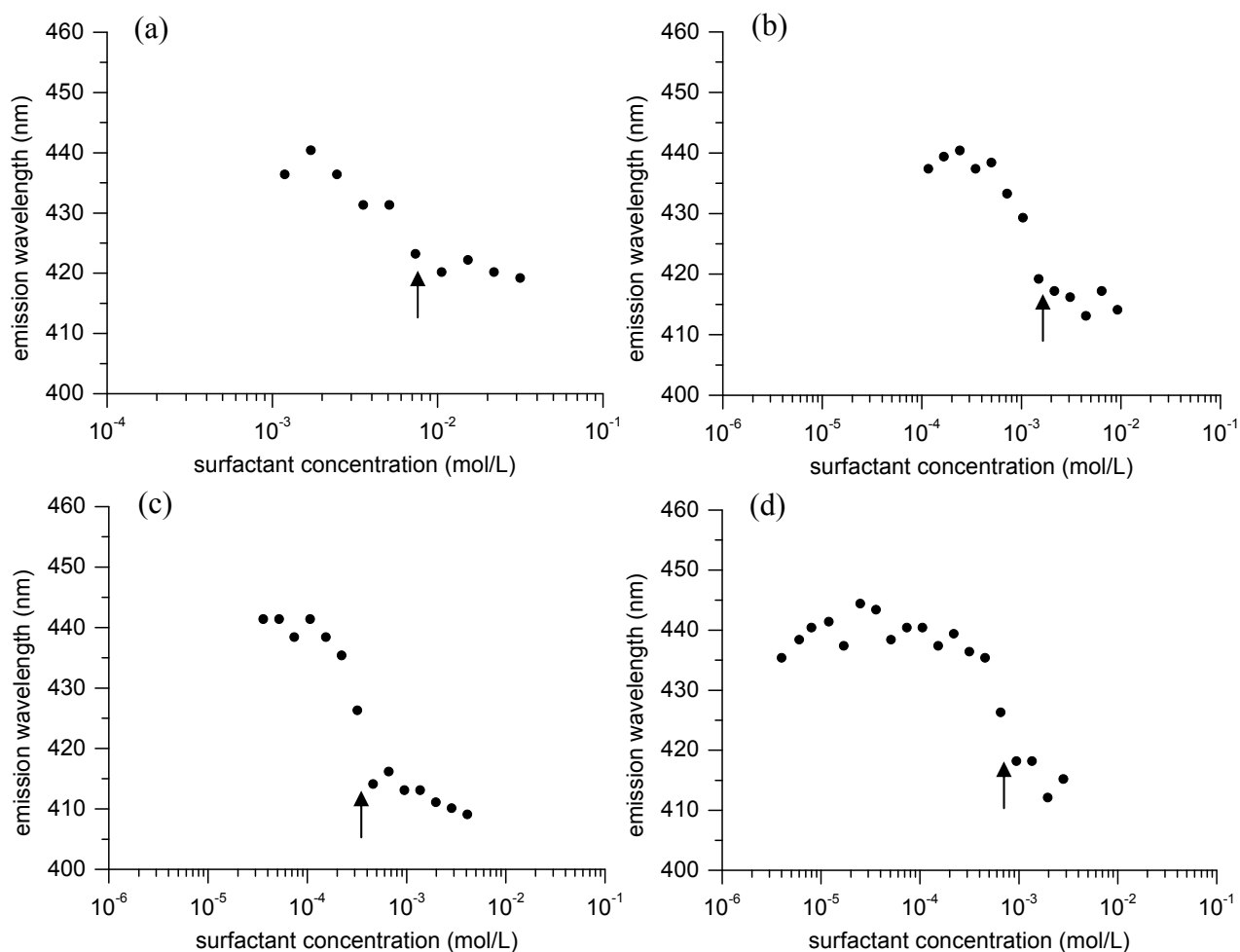
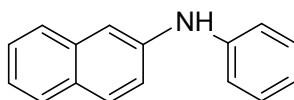
APPENDIX 4: Determination of CMC via solubilization of 2-AN

Figure A4-1: Examples of curves illustrating the shift of the wavelength of emission maximum of 2-AN vs. surfactant concentration, for the series of cationic surfactant oligomers with *p*-xylylene spacer. (a) surfactant “monomer” **BDDAC**; (b) dimer **p-X-2**; (c) trimer **p-X-3**; (d) tetramer **p-X-4**. Measurements performed by *M. Arotçaréna and A. Baudoult* (U.C.L.). The arrows indicate the CMC.

Reminder: Chemical structure of the dye 2-anilinonaphthalene (2-AN) or 2-*N*-phenylnaphthylamine



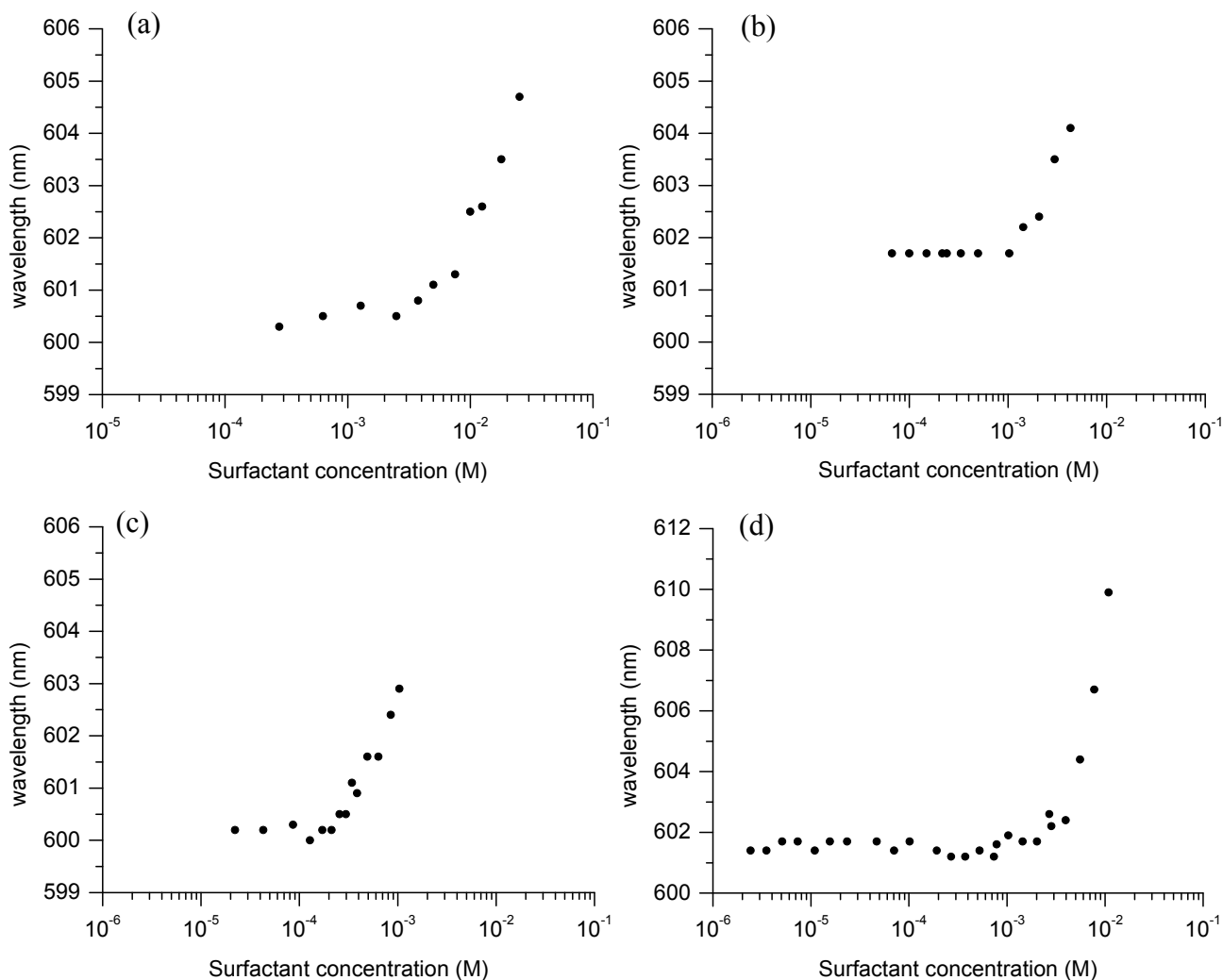
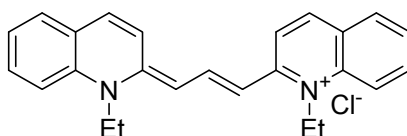
APPENDIX 5: Determination of CMC via solubilization of pinacyanol

Figure A5-1: Graphs representing the wavelength of absorbance maximum of pinacyanol chloride vs. surfactant concentration, for the reference cationic surfactant **BDDAC** and the cationic surfactant oligomers with *p*-xylylene spacer. (a) surfactant monomer **BDDAC**; (b) dimer **p-X-2** (according to *M. Arotçaréna*); (c) trimer **p-X-3**; (d) tetramer **p-X-4**.

CMCs are determined by extrapolation of the surfactant concentration at which the discontinuity in the wavelength of the absorbance maximum of pinacyanol vs. surfactant concentration is observed.

Reminder: Chemical structure of the dye pinacyanol chloride (1,1'-diethyl-2,2'-carbocyanine chloride also called quinaldine blue)



APPENDIX 6: Supporting information for TRFQ experiments

Table A6-1: Parameters for fluorescence decay of 9,10 dimethylantracene in micellar solutions in the presence of 1-*n*-dodecylpyridinium chloride as quencher, according to equation 5.9-1, and calculated aggregation numbers there from according to equation 5.9-2.

Note that the quencher concentration was chosen so that $0.3 < R < 1$.

Surfactant	C (moles of dodecyl chains / L)	R ([Quencher] /[micelles]) fitted from decay curves	fluorescence lifetime of probe in micellar environment τ_0 (ns)	Rate constant for intramolecular quenching $10^{-7} k_q$ (s^{-1})	N_{agg} (dodecyl chains per micelle core)	$10^{-7} N_{agg} k_q$ (s^{-1})
SDS	0.095	1.086	15.76	4.93	64.1	316
DTAC	0.104	0.985	16.09	5.10	34.3	174
BDDAC	0.110	0.783	16.78	4.00	27.3	109
i-B-2	0.106	0.928	16.32	3.82	32.2	123
t-B-2	0.104	0.912	16.36	3.98	31.0	123.4
EO-2	0.108	1.117	16.29	3.81	31.4	119.6
o-X-2	0.109	0.705	16.04	4.52	25.4	114.8
m-X-2	0.109	0.628	17.16	4.58	22.6	103.5
p-X-2	0.109	0.586	16.29	5.78	21.0	121.4
t-B-3	0.038	0.605	16.45	4.27	15.0	64.1
m-X-3	0.105	0.462	17.05	6.46	16.2	104.7
p-X-3	0.105	0.298	17.61	5.87	10.5	61.6
t-B-4	0.048	0.473	16.33	4.93	15.2	74.9
p-X-4	0.034	0.499	17.25	6.77	14.0	94.8

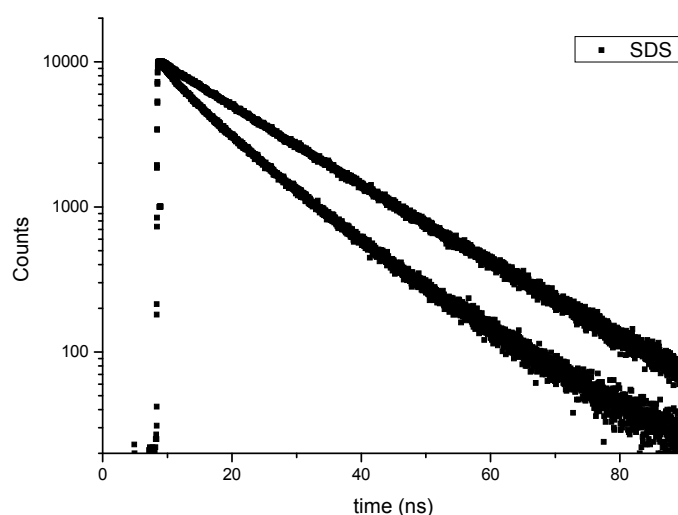


Figure A6-1: Decay curves of 9,10 dimethylantracene in a micellar solution of **SDS** (95 mmol/L) without quencher (upper curve) and with quencher 1-*n*-dodecylpyridinium chloride (lower curve).

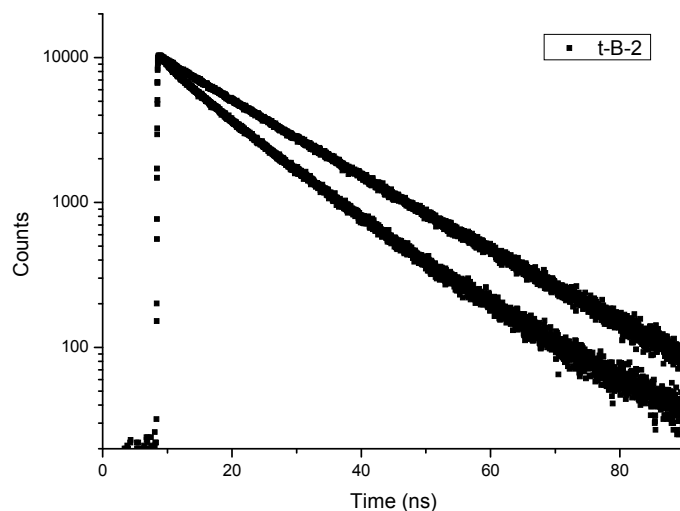


Figure A6-2: decay curves of 9,10 dimethylanthracene in a micellar solution of **t-B-2** (104 mmol/L) without quencher (upper curve) and with quencher 1-*n*-dodecylpyridinium chloride (lower curve).

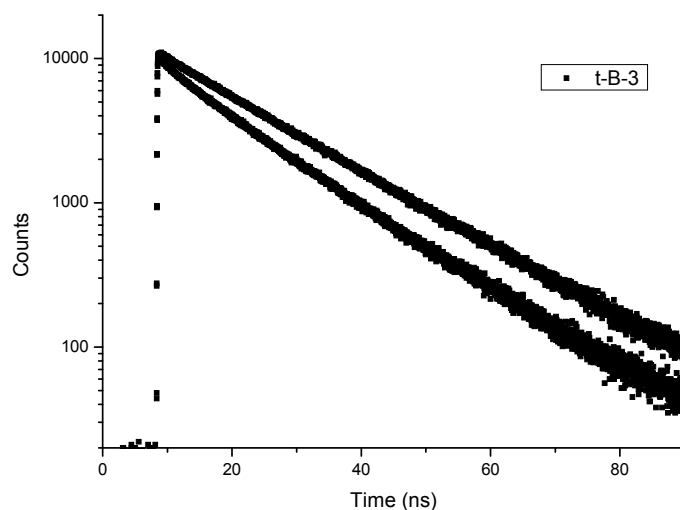


Figure A6-3: decay curves of 9,10 dimethylanthracene in a micellar solution of **t-B-3** (38 mmol/L) without quencher (upper curve) and with quencher 1-*n*-dodecylpyridinium chloride (lower curve).

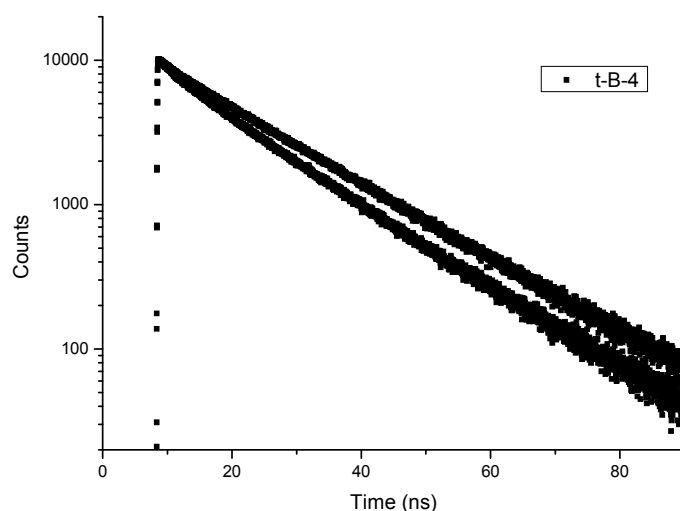
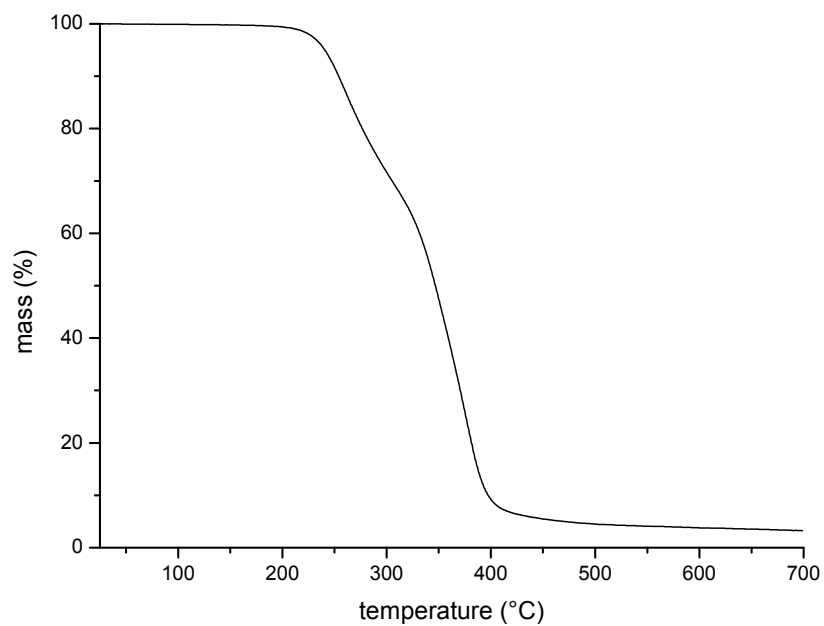
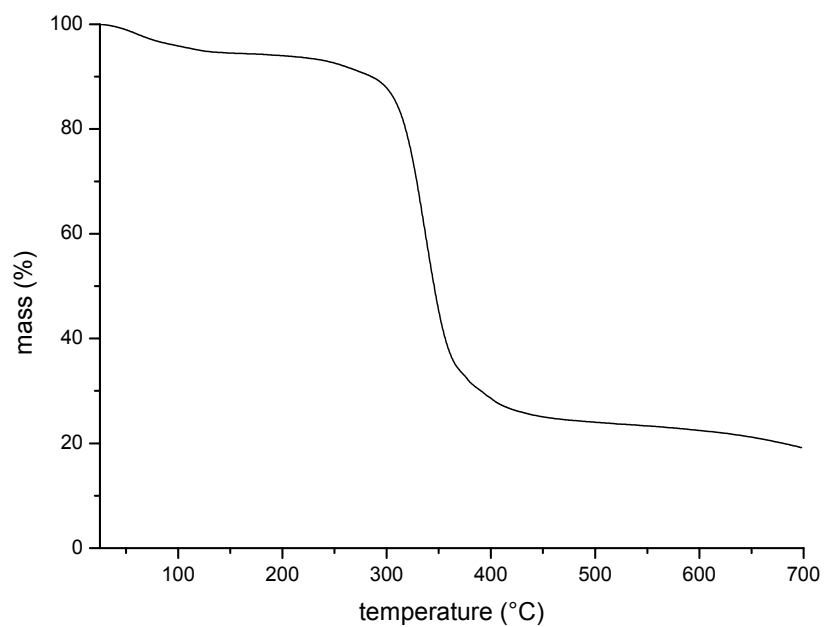


Figure A6-4: decay curves of 9,10 dimethylanthracene in a micellar solution of **t-B-4** (48 mmol/L) without quencher (upper curve) and with quencher 1-*n*-dodecylpyridinium chloride (lower curve).

APPENDIX 7: Thermal analysesFigure A7-1: Thermogravimetric analysis (TGA) of **dimer EDTA** (acidic form).Figure A7-2: Thermogravimetric analysis (TGA) of anionic **dimer EDTA**.

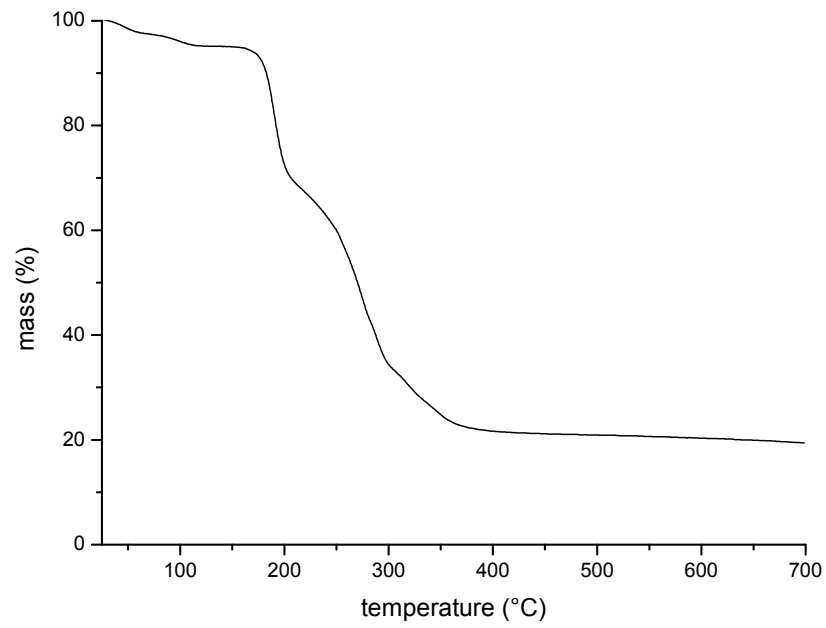


Figure A7-3: Thermogravimetric analysis (TGA) of **EO-2 MoO₄**.

APPENDIX 8: List of Tables

Table 1.1-1 Geometrical relations for spherical, cylindrical, and bilayer aggregates ^a	p.17
Table 1.1-2 Relationships between the shape of surfactant monomer and preferred aggregate morphology. [68]	p.18
Table 1.2-1: Comparison of typical properties of gemini surfactants vs. standard surfactants (all comparisons on equal amounts in weight).	p.28
Table 3.1-1: Surface activity and micellization data of gemini surfactants and corresponding “monomers”. Surface tension curves of dimeric surfactants made by K. Lunkenheimer.	p.53
Table 3.1-2: Surface activity and micellization data of studied oligomeric surfactants	p.58
Table 3.1-3: ¹ H-NMR data of dimeric surfactants (except p-X-2) at 0.03 wt% (below the CMC, value in upper row) and 1 wt% (above the CMC, value in lower row) in D ₂ O.	p.64
Table 3.1-4: Aggregation numbers of the studied series of oligomeric surfactants, expressed in number of dodecyl chains forming the micelles. The reproducibility of the experiment on the N _{agg} is ± 0.5. CMC values were taken from Tables 3.1-1 and 3.1-2 [1-2], except for SDS which was taken from reference [12].	p.69
Table 3.2-1: Surface activity and micellization data of surfactant dimer based on EDTA and reference carboxylic type surfactant “monomer” (sodium laurate). Data for cationic dimer t-B-2 are also listed for comparison (see 3.1.2.a).	p.79
Table 3.2-2: Solubilization capacity of solutions of monomeric and dimeric surfactants in D ₂ O for <i>para</i> -xylene, as determined by ¹ H NMR (surfactant concentration: 1 wt %). Values calculated per alkyl chains are rounding ones (one decimal).	p.83
Table 4.1-1: Surface activity and micellization data of cationic surfactant monomers and dimers and of their mixtures with sodium salicylate. The total molar mass for the mixtures corresponds to the sum of the molar masses of the chloride surfactant and of one or two equivalents of sodium salicylate.	p.96
Table 4.1-2: Rheological data for EO-2(salicylate)₂ and t-B-2(salicylate)₂ at a concentration of 0.5 % wt, measured by rotation (η_0) and oscillation experiments (G_0 , τ) at 35 °C. Values into brackets are the viscosity obtained from oscillation experiments (extrapolation of the complex viscosity at low frequency).	p.101
Table 4.1-3: Surface activity and micellization data of cationic surfactant dimer EO-2 and its mixtures with various organic salts, determined by tensiometry. Values for o-X-2 and one of its mixtures are also listed. (cf. corresponding abbreviations in Fig. 4.1-12).	p.106
Table 5.5-1: Volumes of HCl (1M) and corresponding numbers of moles, added between each equivalent point.	p.132
Table A6-1: Parameters for fluorescence decay of 9,10 dimethylantracene in micellar solutions in the presence of 1- <i>n</i> -dodecylpyridinium chloride as quencher, according to equation 5.9-1, and calculated aggregation numbers there from according to equation 5.9-2. Note that the quencher concentration was chosen so that 0.3 < R < 1.	p.XVII

APPENDIX 9: List of Figures

- Figure 1.1-1: common schematic design of a low-molar mass surfactant molecule. p.3
- Figure 1.1-2: examples of surfactants having a dodecyl chain and various head groups. (a) sodium dodecyl sulfate (SDS); (b) sodium dodecanoate; (c) dimethyldodecylammonium bromide; (d) dodecylpyridinium bromide; (e) N,N'-dimethyl-N-(3-sulfopropyl)-dodecylammonium (dodecyl sulfobetaine); (f) N,N'-dimethyl-N-(carboxymethyl)-dodecylammonium; (g) hexaethylene glycol mono-*n*-dodecyl ether (C₁₂E₆ or trade name Brij 30); (h) dodecylamine oxide. p.4
- Figure 1.1-3: examples of surfactants with various hydrophobic moieties. (a) dodecyl hydrocarbon chain; (b) perfluorinated chain (sodium perfluorooctanoate); (c) partially fluorinated chain (perfluorooctylbutane trimethylammonium bromide from [10]); (d) silicon-based chain (cationic siloxane surfactant from [11]); (e) sodium cholate (From [13]). p.4
- Figure 1.1-4: several designs of low molar-mass amphiphiles and corresponding examples. (a) Ascorbic acid based standard surfactant [14]; (b) double-headed pyridinium surfactant (left) [15] and ethylene glycol based surfactant (right); (c) double-chain surfactant: didecyl dimethylammonium bromide; (d) other double chain surfactants: sodium bis(2-ethylhexyl) sulfosuccinate – trade name Aerosol OT – (left) [16] and lecithin (right) [17]; (e) gemini surfactant (see 1.2.2.b): non-ionic dihexyl glucamide [18]; (f) Bola-surfactant [19]; (g) Shamrock surfactant [20]; (h) two-headed surfactant, alkyldiphenyloxide disulfonate salts (trade name: Dowfax surfactants) [21]. p.5
- Figure 1.1-5: (a) A molecule within the bulk liquid interacts in all directions with other surrounding molecules. (b) A molecule at the surface only experiences attractive interactions with molecules from the liquid interior. p.6
- Figure 1.1-6: scheme representing water molecules at the interface liquid-air. p.7
- Figure 1.1-7: Equilibrium between surfactants in the monolayer and in the bulk, at low surfactant concentration in aqueous solution. p.7
- Figure 1.1-8: Schematic representation of the concentration dependence of some physical properties of surfactant solutions [29]. p.9
- Figure 1.1-9: Scheme of a spherical micelle of surfactants in aqueous solution. p.9
- Figure 1.1-10: Schematic representation of the equilibrium in a surfactant solution above the CMC p.10
- Figure 1.1-11: Schematic phase diagram for an ionic surfactant solution. T_K is the Krafft point. p.14
- Figure 1.1-12: Idealized representation of various micellar morphologies [22]. p.15
- Figure 1.1-13: Mechanisms for the two relaxation times τ_1 and τ_2 for a surfactant solution above CMC. From reference [61]. p.16
- Figure 1.1-14: Illustration of the parameters v_0 , l_0 and a , involved in the calculation of the packing parameter P of a surfactant. p.17
- Figure 1.1-15: Common surfactant liquid crystalline phases. p.20

- Figure 1.2-1: Scheme of different types of polymeric surfactants: a) ionene-type, b) polysoap, c) hyperbranched, d) block copolymer, e) graft copolymer, and f) dendrimer. p.21
- Figure 1.2-2: Different architectures of well-defined surfactant oligomers. Variables: hydrophilic head, hydrophobic tail; Additional factors: degree of oligomerization, topology of oligomers, position of anchoring point. p.22
- Figure 1.2-3: Examples of surfactant oligomers: (a) and (b) star-like trimeric surfactants from [81] and [87], respectively; (c), (d) and (e) calixarene-based cyclic surfactant oligomers from [88], [85] and [89], respectively; (f) macrocyclic sugar-based surfactant from [84]; (g) anionic tetrameric surfactant with multiple-ring spacer from [90]. p.23
- Figure 1.2-4: Scheme of the dimerization of “monomeric” surfactant (I) via the end of the hydrophobic chain (= “bola” amphiphile) (II), or via the hydrophilic group (= “Gemini” amphiphile) (III). p.24
- Figure 1.2-5: Examples of Bola-amphiphiles: (a) amphoteric one with phosphocholine headgroups, from [98]; (b) and (c) cationic ones, from [97] and [19], respectively. p.25
- Figure 1.2-6: Design of “gemini” surfactants. p.25
- Figure 1.2-7: Examples of gemini surfactants [100-104]. p.26
- Figure 1.2-8: schematic representation of the distribution of distances between head groups in micelles of a conventional surfactant (a) and of a dimeric surfactant (b). Taken from [105]. p.26
- Figure 1.2-9: Examples of linear higher surfactant oligomers of the “head-type”: (a) trimeric surfactant “12-3-12-3-12” [111-116]; (b) tetrameric surfactant (from spermine) “12-3-12-4-12-3-12” [117]. p.27
- Figure 1.3-1: Oligomeric intermediates between monomeric and polymeric surfactants. p.30
- Figure 2.1-1: Structures of oligomeric surfactant with various spacer groups (n = degree of oligomerization). p.37
- Figure 2.1-2: Scheme of reaction to synthesize the dimeric surfactants. p.39
- Figure 2.1-3: Synthetic routes to trimeric and tetrameric surfactants (with R = spacer group). Routes applied by R. Rakotoaly [1]. p.40
- Figure 2.2-1: Examples of anionic dimeric surfactants from the literature: (a) [27]; (b) [38]; (c) [39]; (d) [41]; (e) [42]; (f) [45]; (g) [47]; (h) [51]; (i) [50]. p.42
- Figure 2.2-2: Examples of cleavable anionic dimeric surfactants. Thermally cleavable: (a) sulfonate “inisurf” [44]; (b) amphipathic 1,2 diazene [55]. Chemically cleavable: (c) cysteine-derived gemini [56]; (d) double-bond containing dimer [58]. p.43
- Figure 2.2-3: Scheme for the synthesis of the dimeric surfactant based on EDTA. p.44
- Figure 2.2-4: Trans-cis conformer equilibrium for one tertiary amide of dimer EDTA. p.46
- Figure 2.2-5: Titration curve by addition of HCl (0.1 M) to dimer EDTA previously neutralized with a known excess of NaOH (black curve) and its derivative (red curve) giving the equivalent points ($E_0 - E_2$). The dotted line indicates a visual change in the aspect of the solution (from transparent to turbid). p.48

- Figure 2.2-6: Hypothetical transitions occurring during the titration of anionic dimer with HCl. p.48
- Figure 3.1-1: Surface tension vs. concentration curves of studied surfactants: (+) = **BDDAC**; I: (Δ) = **i-B-2**, (∇) = **t-B-2**, (o) = **EO-2**; II: (\blacktriangle) = **o-X-2**, (\blacktriangledown) = **m-X-2**, (\bullet) = **p-X-2**. Measurements of surfactant dimers performed by K. Lunkenheimer (MPI-KG, Golm) [1]. Vertical and horizontal lines are a guide for the eyes, respectively positioning CMC- and σ_{cmc} -values of reference surfactants: **DTAC** (dashes); **BDDAC** (dots). p.54
- Figure 3.1-2: Surface tension vs. concentration isotherms of oligomeric surfactants: (\square) = reference **BDDAC**; I: series with *trans*-butenylene spacer: (\ast) = **t-B-2**, (o) = **t-B-3**, (\bullet) = **t-B-4**; II: series with *m*-xylylene spacer: (+) = **m-X-2**, (Δ) = **m-X-3**, (\blacktriangle) = **m-X-4**; III: series with *p*-xylylene spacer: (x) = **p-X-2**, (∇) = **p-X-3**, (\blacktriangledown) = **p-X-4**. Figure 3.1-3: Evolution of the critical micellar concentration: CMC decreases with the degree of oligomerization. (o) = *trans*-butenylene spacer; (+) = *m*-xylylene spacer; (x) = *p*-xylylene spacer. p.57
- Figure 3.1-3: Evolution of the critical micellar concentration: CMC decreases with the degree of oligomerization. (o) = *trans*-butenylene spacer; (+) = *m*-xylylene spacer; (x) = *p*-xylylene spacer. p.60
- Figure 3.1-4: Selected parts of the $^1\text{H-NMR}$ spectra of dimeric surfactants in D_2O , at 0.03 wt% (below the CMC, upper graphs), and at 1 wt% (above the CMC, lower graphs). (a) = **EO-2**, (b) = **i-B-2**, (c) = **t-B-2**. p.65
- Figure 3.1-5: Selected parts of the $^1\text{H-NMR}$ spectra of dimeric surfactants in D_2O , at 0.03 wt% (below the CMC, upper graphs), and 1 wt% (above the CMC, lower graphs). (a) = **m-X-2**, (b) = **o-X-2**. p.65
- Figure 3.1-6: Excitation spectrum of 9,10 dimethylantracene (0.02 mmol/L) solubilized in a micellar solution of **BDDAC** (30 mmol/L) without quencher [solid line] and with quencher (1.2 mmol/L) [dotted line], taken at 430 nm. p.68
- Figure 3.1-7: Example of decay curves for a micellar solution of **DTAC** (70 mmol/L) without quencher (upper curve) and with quencher (lower curve). p.70
- Figure 3.1-8: Micelle aggregation number N_{agg} as function of dodecyl chain concentration. (O) = **DTAC**, (\blacktriangle) = **t-B-2**, (X) = **EO-2**, (\bullet) = **BDDAC**, (Δ) = **p-X-2**. p.71
- Figure 3.1-9: Calculated maximum length of the spacers involved in the oligomeric surfactant series. p.72
- Figure 3.1-10: Micelle aggregation number N_{agg} as function of the spacer length for the sets of isomeric gemini surfactants, at a dodecyl chain concentration of ca. 0.1 M. (\bullet) = butenylene spacer groups, (O) = diethylether spacer, (Δ) = xylylene spacer groups. Dotted lines are a guide for the eyes. p.73
- Figure 3.1-11: Partial ternary phase diagrams (in weight) for the system surfactant/water/toluene-pentanol (1:1 v/v); (a): **DTAC**, **EO-2**, **i-B-2**, **t-B-2**; (b): **i-B-2**, **o-X-2**, **m-X-2**, **p-X-2**. The delimited areas correspond to the L_2 phases (or W/O microemulsions). p.76
- Figure 3.2-1: Surface tension vs. concentration curves of surfactant **dimer EDTA** at neutral pH (o) and pH = 12 (\bullet). Vertical and horizontal lines are a guide for the eyes, positioning CMC- and σ_{cmc} -values respectively of reference surfactants: **SL** at pH = 10 (-----) and **t-B-2** (--). p.79

- Figure 3.2-2: Evolution of the absorbance of the enol form of benzoylactone at 315 nm in aqueous solution (0.001 wt %) with increasing concentration of surfactant dimer EDTA. p.81
- Figure 3.2-3: Turbidimetric titration of aqueous surfactant solutions (25 mL; 2 g/L) with calcium chloride ($[\text{CaCl}_2] = 0.5 \text{ g/L}$) at 30 °C, pH = 7. (O) = sodium laurate, (●) = dimer EDTA. p.85
- Figure 4.1-1: Schematic representation of the binding of organic anions at the micellar interface of cationic surfactants. p.91
- Figure 4.1-2: Surface tension curves of cationic dimer **EO-2 (2Cl)** (∇) and of cationic dimer **EO-2 (MoO₄²⁻)** (!). Vertical and horizontal dashed lines show CMC and σ_{cmc} -value of analog **EO-2 (2Br)** (From ref. [80]), respectively. p.93
- Figure 4.1-3: Surface tension curves of dimer **EO-2** and its mixture with sodium salicylate (1:2 molar ratio): (+) **EO-2**; (●) **EO-2(salicylate)₂**. Dashed lines are a guide for the eyes. p.95
- Figure 4.1-4: Conductivity measurement for a mixture of monomer **DTAC** with sodium salicylate (1:1 molar ratio). Dashed lines are a guide for the eyes. CMC corresponds to the break point in the curve. p.95
- Figure 4.1-5: Relative viscosity of mixtures of monomer DTAC, dimers EO-2, t-B-2, m-X-2 and sodium salicylate as a function of mixture concentration: (○) DTAC(sal), (!) EO-2(sal)₂, (7) t-B-2(sal)₂, (●) m-X-2(sal)₂. In the experimental conditions, shear rate $\dot{\gamma}$ is superior to 100 s⁻¹. p.97
- Figure 4.1-6: Shear viscosity η vs. shear rate $\dot{\gamma}$, for **EO-2(salicylate)₂** (0.8 % wt), at 25 °C. p.98
- Figure 4.1-7: Frequency sweep experiment showing G' (●), G'' (o) for EO-2(sal)₂ (0.8 wt %) at a shear stress of 1 Pa, at 25 °C. The dashed red lines correspond to the fitting of the curves with the Maxwell model presented in the experimental part. p.98
- Figure 4.1-8: Zero-shear viscosity η_0 vs. concentration for the mixture **EO-2(sal)₂** at 25 °C. Points (o) are zero-viscosity values which are less accurate, since plateaus in the viscosity curves were hardly found for the system below 0.5 % wt in the measurement range. The dotted line is a guide for the eyes. p.99
- Figure 4.1-9: Relaxation time τ (∇) and plateau modulus G_0 (!) vs. concentration, for the mixture EO-2(sal)₂ at 25 °C. Dotted lines are a guide for the eyes. The inset shows the fitting of G_0 vs. concentration with a power law. p.100
- Figure 4.1-10: Linear, branched and saturated network of wormlike micelles. From ref. [94]. p.101
- Figure 4.1-11: Shear viscosity η vs. shear rate $\dot{\gamma}$, at 25 °C, for mixtures: (○) **EO-2(sal)₂** 0.5 % wt; (●) **EO-2(sal)₂** 1.0 % wt; (8) **CTAC(sal)** 0.5 % wt; (7) **CTAC(sal)** 1.0 % wt. p.103
- Figure 4.1-12: Examples of organic salts tested as additives to cationic dimeric surfactants. Abbreviations are in bold style. p.104
- Figure 4.1-13: Scheme of the hypothesized orientation of naphthoate anions on the micellar surface of cationic surfactants: (a) **6,2 HNC**; (b) **3,2 HNC**. The latter anion induces precipitation. p.105

- Figure 4.1-14: Surface tension curves of dimeric surfactants **EO-2** and **o-X-2** mixed with organic salt naphthalene dicarboxylate (**NDC**): (●) **EO-2 (NDC)**; (o) **o-X-2 (NDC)**. Vertical and horizontal lines are a guide for the eyes, respectively positioning CMC- and σ_{cmc} -values of pure dimeric surfactants: **EO-2** (dashes); **o-X-2** (dots). p.108
- Figure 4.1-15: Relative viscosity vs. concentration: (!) EO-2(salicylate)₂, (8) EO-2(6,2 HNC)₂, (∇) EO-2(tosylate)₂, (●) EO-2. In the experimental conditions, shear rate $\dot{\gamma}$ is superior to 100 s⁻¹. Dashed lines are a guide to the eyes. p.109
- Figure 4.1-16: Shear viscosity η vs. shear rate $\dot{\gamma}$, for o-X-2(benzoate)₂ 2 % wt (●), t-B-2(benzoate)₂ 2 % wt (7), t-B-2(cinnamate)₂ 1 % wt (!) and EO-2(vinylbenzoate)₂ 0.5 % wt (X), at 25 °C. p.109
- Figure 4.1-17: Relative viscosity of mixtures of monomer CTAC, dimer o-X-2 with sodium benzoate as a function of mixture concentration: (7) CTAC(benz), (●) o-X-2(benz)₂. In the experimental conditions, shear rate $\dot{\gamma}$ is superior to 100 s⁻¹. Dashed lines are a guide to the eyes. p.110
- Figure 4.1-18: Relative viscosity of mixtures of surfactant dimers and sodium acetylsalicylate vs. mixture concentration: (!) i-B-2(acsal)₂, (∇) t-B-2(acsal)₂, (B) EO-2(acsal)₂, (○) o-X-2(acsal)₂, (●) m-X-2(acsal)₂. In the experimental conditions, shear rate $\dot{\gamma}$ is superior to 100 s⁻¹. Dashed lines are a guide to the eyes. p.111
- Figure 4.1-19: Effect of added equimolar amounts of sodium 4-vinylbenzoate "4-VB" on the association of dimeric surfactant EO-2 in water; as studied by DLS showing the volume repartition vs. hydrodynamic diameter: a) (----) = pure EO-2; b) (—) = EO-2(4-VB) before polymerization (1 wt %); c) (⋯) = EO-2 (4-VB) at 1 day after polymerization (1 wt %); d) (-⋅) = EO-(4-VB) at 1 week after polymerization (1 wt %). p.113
- Figure 4.1-20: Effect of added equimolar amounts of sodium 4-vinylbenzoate "4-VB" on the association of dimeric surfactant EO-2 in D₂O; followed by ¹H-NMR: (a) pure EO-2; (b) pure 4-VB; (c) EO-2(4-VB) before polymerization (1 wt%); (d) EO-2(4-VB) after polymerization (1 wt%). Signal of solvent at 4.698 ppm. p.114
- Figure 4.1-21: ¹H-NMR spectra of 4-vinylbenzoate "4-VB" (a) before polymerization, and (b) after attempted polymerization in D₂O (concentration 13.5 mM). Signal of solvent at 4.698 ppm. p.115
- Figure 4.1-22: Effect of added amounts of sodium 4-vinylbenzoate "4-VB" on the association of dimeric surfactant EO-2 in water; as studied by DLS showing the volume repartition vs. hydrodynamic diameter: a) (----) = pure EO-2; b) (—) = EO-2(4-VB) mixture with molar ratio 1:1.5 before polymerization (0.5 wt %); c) (⋯) = EO-2 (4-VB) mixture with molar ratio 1:1.5 after polymerization (0.5 wt %). p.116
- Figure 4.1-23: Examples of organic salts tested as additives to the anionic dimeric surfactant. p.117
- Figure 4.2-1: Cryo-SEM micrograph of a mixture of SDS / EO-2 (80 / 20 in weight), 0.8 g/L in water, revealing the presence of small vesicular aggregates. p.119
- Figure 4.2-2: DLS measurements of pure surfactants and mixtures of oppositely charged surfactants in water, showing the volume repartition vs. hydrodynamic diameter: a) (—) = pure EO-2 (4 g/L); b) (—) = pure SDS (4 g/L); c) (—) = SDS / DTAC (80/20 w/w, 10 g/L); d) (—) = SDS / DTAC (80/20 w/w, 1 g/L, measured just after dilution); e) (—) = SDS / EO-2 (80/20 w/w, 0.8 g/L). p.120

- Figure 4.2-3: Shear viscosity η vs. shear rate $\dot{\gamma}$, for Dimer EDTA / EO-2 (molar ratio 2:1; 2 % wt), at 25 °C. p.122
- Figure 5.8-1: Chemical structure of dye pinacyanol chloride (quinaldine blue); 1,1'-diethyl-2,2'-carbocyanine chloride. p.136
- Figure 5.8-2: Chemical structure of dye 2-anilinonaphthalene (2-*N*-phenylnaphthylamine). p.136
- Figure 5.9-1: Chemical structure of (a) 9,10 dimethylantracene, (b) pyrene and (c) 1-n-dodecylpyridinium chloride. p.138
- Figure 5.12-1: Keto-enol tautomerism of benzoylacetone: left = ketone form; right = enol form. p.141
- Figure 5.12-2: UV-vis spectra of 0.001 wt % aqueous solution of benzoylacetone after adding 0.002 g/L (\square), 0.030 g/L (\square), 0.06 g/L (\square), 0.120 g/L (\square), 0.15 g/L (\square) dimer EDTA. Keto band at 250 nm decreases with increasing surfactant concentration whereas enol band at 315 nm increases. Presence of an isosbestic point at $\lambda = 280$ nm (cross point between the curves), indicating an equilibrium between two species in solution. p.142
- Figure 5.13-1: Example of $^1\text{H-NMR}$ spectrum (128 scans, 300 MHz) obtained for the solubilization study of p-xylene in micellar solution of SDS in D_2O (10 g/L). Values in italic corresponds to the integrals of the signal. p.144
- Figure 5.15-1: Scheme of the synthesis route towards EO-2 (MoO_4). p.145
- Figure 5.17-1: Concentration dependence of the conductivity for DTAB solutions in water at 25°C. Graph taken from ref. [54]. p.148
- Figure 5.19-1: Schematic mechanical model of a Maxwell-Material, with a spring and a dashpot. p.151
- Figure 5.19-2: A typical stress sweep experiment showing G' (\bullet), G'' (\circ) as a function of the amplitude of oscillatory shear stress, for **EO-2(salicylate) $_2$** (0.6 wt %) at a frequency of 1 Hz, at 25 °C. The vertical dashed line represents the critical stress, marking the end of the linear viscoelastic region. p.154
- Figure 5.19-3: A typical frequency sweep experiment showing G' (\bullet), G'' (\circ) and η^* (\blacksquare), for **EO-2(salicylate) $_2$** (0.6 wt %) at a shear stress of 0.1 Pa, at 25 °C. The dashed red lines correspond to the fitting of the curves with the Maxwell model. p.154
- Figure 5.19-4: A typical flow curve showing the shear stress σ (\bullet) and the shear viscosity η (\circ) vs. the shear rate $\dot{\gamma}$, for **EO-2(salicylate) $_2$** (0.6 wt %), at 25 °C. Lines are a guide for the eyes. The dashed red line corresponds to the fitting of the viscosity curve with the Giesekus model [73-81]. p.155
- Figure A3-1: $^1\text{H-NMR}$ spectrum (300 MHz) of Dimer EDTA (after neutralization) in CDCl_3 . p.IX
- Figure A3-2: $^1\text{H-NMR}$ spectrum (300 MHz) of Dimer EDTA (after neutralization, at pH 11) in D_2O . Values in italic give the integral of the corresponding signal group. p.IX
- Figure A3-3: $^{13}\text{C-NMR}$ spectrum (75 MHz) of Dimer EDTA (after neutralization) in CDCl_3 . p.X
- Figure A3-4: $^1\text{H-NMR}$ spectrum (300 MHz) of Dimer EDTA (before neutralization) in CDCl_3 . Values in italic give the integral of the corresponding signal group. p.XI

- Figure A3-5: ^{13}C -NMR spectrum (125 MHz) of Dimer EDTA (before neutralization) in CDCl_3 . p.XI
- Figure A3-6: 2D-NMR spectrum (500 MHz) of Dimer EDTA (before neutralization) in CDCl_3 . p.XII
- Figure A3-7: FT-IR spectrum of Dimer EDTA (before neutralization) and attribution of characteristic bands. p.XIII
- Figure A3-8: FT-IR spectrum of reactant EDTA anhydride and attribution of characteristic bands, for comparison. p.XIV
- Figure A4-1: Examples of curves illustrating the shift of the wavelength of emission maximum of 2-AN vs. surfactant concentration, for the series of cationic surfactant oligomers with *p*-xylylene spacer. (a) surfactant “monomer” **BDDAC**; (b) dimer **p-X-2**; (c) trimer **p-X-3**; (d) tetramer **p-X-4**. Measurements performed by *M. Arotçaréna and A. Baudoult* (U.C.L.). The arrows indicate the CMC. p.XV
- Figure A5-1: Graphs representing the wavelength of absorbance maximum of pinacyanol chloride vs. surfactant concentration, for the reference cationic surfactant **BDDAC** and the cationic surfactant oligomers with *p*-xylylene spacer. (a) surfactant monomer **BDDAC**; (b) dimer **p-X-2** (according to *M. Arotçaréna*); (c) trimer **p-X-3**; (d) tetramer **p-X-4**. p.XVI
- Figure A6-1: Decay curves of 9,10 dimethylantracene in a micellar solution of **SDS** (95 mmol/L) without quencher (upper curve) and with quencher 1-*n*-dodecylpyridinium chloride (lower curve). p.XVII
- Figure A6-2: decay curves of 9,10 dimethylantracene in a micellar solution of **t-B-2** (104 mmol/L) without quencher (upper curve) and with quencher 1-*n*-dodecylpyridinium chloride (lower curve). p.XVIII
- Figure A6-3: decay curves of 9,10 dimethylantracene in a micellar solution of **t-B-3** (38 mmol/L) without quencher (upper curve) and with quencher 1-*n*-dodecylpyridinium chloride (lower curve). p.XVIII
- Figure A6-4: decay curves of 9,10 dimethylantracene in a micellar solution of **t-B-4** (48 mmol/L) without quencher (upper curve) and with quencher 1-*n*-dodecylpyridinium chloride (lower curve). p.XVIII
- Figure A7-1: Thermogravimetric analysis (TGA) of **dimer EDTA** (acidic form). p.XIX
- Figure A7-2: Thermogravimetric analysis (TGA) of anionic **dimer EDTA**. p.XIX
- Figure A7-3: Thermogravimetric analysis (TGA) of **EO-2 MoO₄**. p.XX

APPENDIX 10: Communications concerning this thesis**Publications**

A. Laschewsky, K. Lunkenheimer, R. H. Rakotoaly, L. Wattebled, “Spacer Effects in Dimeric Cationic Surfactants”, *Colloid and Polymer Science* **2005**, 283, 469-479.

A. Laschewsky, L. Wattebled, M. Arotçaréna, J.-L. Habib-Jiwan, R. H. Rakotoaly, “Synthesis and Properties of Cationic Oligomeric Surfactants”, *Langmuir* **2005**, 21(16), 7170-7179.

L. Wattebled, A. Laschewsky, A. Moussa, J.-L. Habib-Jiwan, “Aggregation Numbers of Cationic Oligomeric Surfactants: a Time-Resolved Fluorescence Quenching Study”, *Langmuir* **2006**, 22 (6), 2551-2557.

A. Laschewsky, L. Wattebled, “Book Review: Karsa, D. R. ed; *Surfactants in Polymers, Coatings, Inks and Adhesives* (Applied Surfactant Series Vol. 1), Blackwell Publishing Ltd, Boca Raton, 2003”, *Tenside Surfactants Detergents* **2006**, 3, 155.

L. Wattebled, C. Note, A. Laschewsky, “Structure – property relationships of “gemini” surfactants and synergism with hydrotropes”, *Proceedings 53. SEPAWA Kongress* (Würzburg) **2006**, 73-87.

L. Wattebled, C. Note, A. Laschewsky, “Structure – property relationships of gemini surfactants and synergism with hydrotropes”, *Tenside Surfactants Detergents* **2007**, accepted for publication.

Oral presentations

L. Wattebled, A. Laschewsky, “Kationische Dimere Tenside”, Vortragsveranstaltung SEPAWA Landesgruppe Ost, in IAP, 21–22.04.2005, Potsdam, Germany.

L. Wattebled, A. Laschewsky, “Oligomeric Surfactants as Novel Type of Amphiphiles: Structure – Properties Relationships and Modification by Additives”, 3. Zsigmondy Colloquium (German Colloid Society), 6–7.04.2006, Technische Universität Berlin, Germany.

L. Wattebled, C. Note, A. Laschewsky, “Structure – Property Relationships of “Gemini” Surfactants and Synergism with Hydrotropes”, 53rd SEPAWA Congress with European Detergents Conference, 11–13.10.2006, Würzburg, Germany.

Posters

A. Laschewsky, R. Rakotoaly, L. Wattebled, “Oligomeric surfactants as novel type of amphiphiles”, 6th World Surfactants Congress CESIO 2004, 20–23.06.2004, Berlin (Germany).

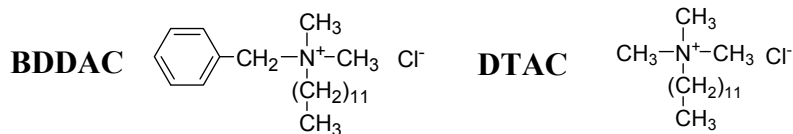
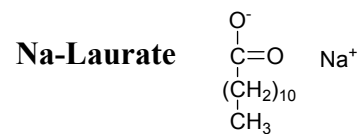
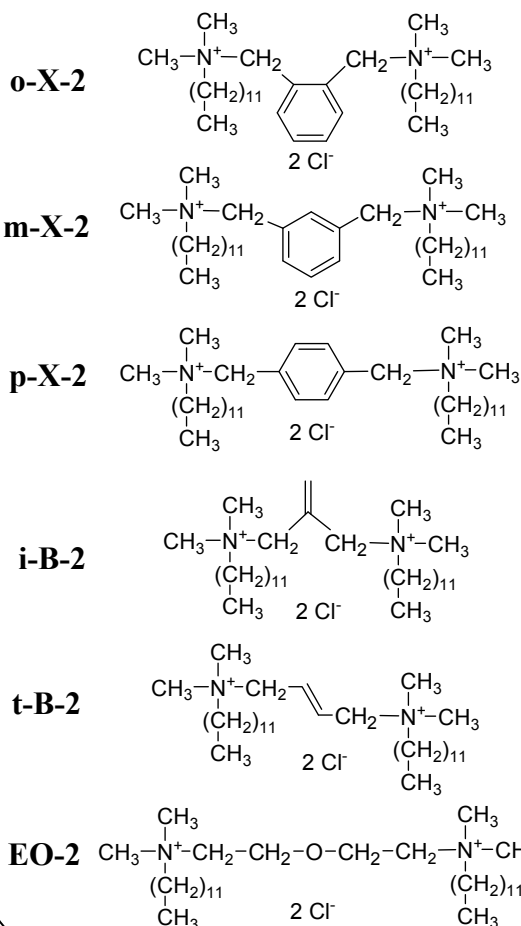
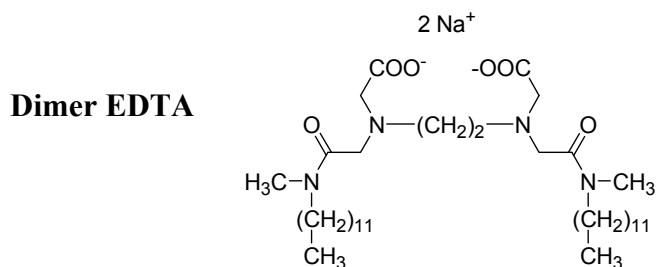
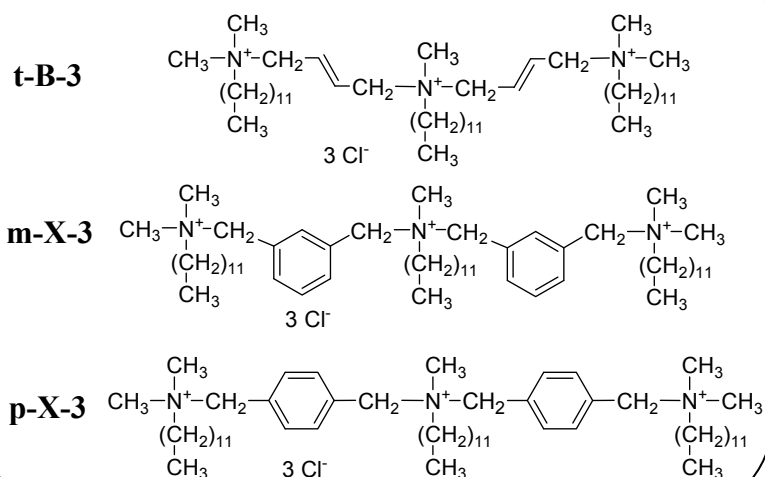
L. Wattebled, A. Laschewsky, K. Lunkenheimer, R. Rakotoaly, “Properties of new cationic oligomeric surfactants”, Tag der Chemie 2004 (Berliner Universitäten und Universität Potsdam, Verband der Chemische Industrie), 7.07.2004, Potsdam-Golm (Germany).

L. Wattebled, A. Laschewsky, K. Lunkenheimer, R. Rakotoaly, “Synthesis and properties of new cationic oligomeric surfactants”, Polydays 2004 (Biannual International Meeting on Polymers), 4–6.10.2004, Potsdam (Germany).

L. Wattebled, A. Laschewsky, “Novel Cationic Oligomeric Amphiphiles: Surface Activity, Aggregation Behaviour and Complexation with Organic Counterions”, Formula IV: Frontiers in Formulation Science (RSC & SFC), 4–7.07.2005, King’s College London (England).

L. Wattebled, A. Laschewsky, “Relations Structure - Propriétés chez les Tensio-Actifs Oligomères et Synergie avec Divers Additifs”, Club Emulsion 2006, 18–19.09.2006, Strasbourg (France).

APPENDIX 11: Surfactants studied in this work

Cationic monomersAnionic monomerCationic dimersAnionic dimerCationic trimersCationic tetramers